UNIVERSITY OF GENOA
DEPARTMENT OF CHEMISTRY AND INDUSTRIAL CHEMISTRY

DOCTORATE SCHOOL OF
CHEMICAL AND MATERIALS SCIENCES AND TECHNOLOGIES

CURRICULUM
CHEMICAL SCIENCES AND TECHNOLOGIES

NEW NAVAL FILLERS FOR INDUSTRIAL APPLICATIONS IN THE YACHTING

Supervisor:
Prof. Silvia Vicini
University of Genoa

Co-Supervisor
Dr. Rico Ricotti, Ph. D.
Boero Bartolomeo S.p.A.

PhD Student:
Silvia Vita

Academic year 2019-2020

"Niente nella vita va temuto,
dev'essere solamente compreso.
Ora è tempo di comprendere di più,
così possiamo temere di meno."

Marie Curie

Ai Miei Genitori

INDEX

ABSTRACT

In the Italian economy, the yachting field has a remarkable importance, indeed Italy is among the leading boat manufacturers both in Europe and in the world.

The coatings for external surface of ships play a fundamental role, because they have to resist to aggressive environment and to thermal stresses respecting the Safety of Life at Sea (*S.O.L.A.S.)* rules and maintaining all the aesthetic properties typical of a luxury product as: brightness, light reflection and their durability over time.

To respond to these demands the multi-coat systems are essential. They are protective systems based on the overlap of different layers with different thicknesses and aim, where the fundamental layer, from the mechanical point of view, is represented by the filler, a composite material with the first aim to fill the surface imperfections.

The two-component fillers have been extensively studied in the present research project and they consist of one A component (based on epoxy resin) and one B component (the curing agent, based on polyamide); once mixed in opportune ratios they form the filler to apply. Being composite materials, in the two matrices are present several extenders, such as hollow glass microspheres, alumina-silicate spheres, carbonates and some additives (dispersants, rheological modifiers and anti-foam agents). The production of two components is carried out with a dissolver equipped with cowles and butterfly that permit the dispersion of extenders and additives in the matrix.

In these composites several critical aspects are present and they are related both to the stability of the materials in the can (with respect to their rheology) and to the applied products (including the applications conditions, the mechanical properties and thermal stresses).

This project was carried out in collaboration with Boero Bartolomeo SpA, one of the oldest paint factories in Europe, leader in Italy in paint building sector and leader in world for the yachting field, and for this reason, it was not possible to publish some details of the research work, due to confidentiality agreements.

Targets of this research project are: the transition from empirical, typical of paint industry, to scientific knowledge in the formulation methodology, the optimisation of existing formulations and the development of a new filler for North European market, all this with particular attention to sustainability of the raw materials.

The thesis is divided into two sections: Section I (fundamentals) and Section II (experimental).

The first section reports the state of art on yacht coatings (Chapter 1) and on fillers (Chapter 2). In

this section, it is also present, in Chapter 3, a brief description of the techniques and instruments used.

Section II is the experimental part that consists of seven chapters, in which the results obtained and the work conclusions are reported.

Chapter 4 reports the characterisation of commercial fillers, performed with several techniques, and the study of their curing process. The characterisation of commercial fillers is essential to deepen the knowledge of these materials used as benchmark for the filler subsequently developed, for quality control and/or the investigation of anomalies, following in-field problems and for the setup of experimental methods useful in the development of new products.

Furthermore, the study of the curing process, performed with both techniques Infrared (IR) spectroscopy and Differential Scanning Calorimetry (DSC), allowed to evaluate how environmental conditions, such as temperature and humidity, influence the reaction evolution and to obtain further insight into the reaction mechanism.

Chapter 5 is focused on the study of extenders, the first part regards the characterisation, through infrared analysis and morphological characterisation, while the second part is on the rheological analysis of samples with increasing amounts of hollow glass microspheres (the most important ingredient of fillers). These characterisations are useful to quality control of incoming materials, avoiding so possible problems in the final product due to batches of altered raw materials. The results of the rheological analysis allowed to highlight the effect of microspheres on the rheological properties of single components, showing as high percentages of them had good effect on the rheological performance, allowing also the reduction of specific weight.

In Chapter 6, alternative and innovative extenders were studied. In particular, sustainable raw materials, such as wood fibres, that have low density and low cost, and more performing extenders, from the rheological point of view, as polymeric hollow microspheres were considered.

These extenders were tested replacing other standard extenders as alumina-silicate spheres or hollow glass microspheres, in both A and B components.

Coating tests, rheological and mechanical analyses and morphological characterisation were carried out. Generally, from these tests both the two innovative extenders performed really good in the A component, besides, the substitution of hollow glass microspheres with wood fibres permitted to save time, especially at the production site, since their dispersion in the matrix required the substitution of cowles with butterfly. On the other hand, in the B components, the wood fibres allowed to improve the sustainability, but they have an unsatisfactory rheology and so they have to be further tested, for instances, with different rheological modifiers. The hollow polymeric microspheres, even if they permitted to improve remarkably the rheology, they had scarce mechanical properties, and so they

have to be combined with other extenders which increase the mechanical performances. Nevertheless, these formulations allowed the company to investigate new raw materials permitting it to explore new areas of research and, besides, they can be considered the trailhead to use them in the future.

In Chapter 7 and in Chapter 8 the study of additives is presented, dispersants and rheological modifiers respectively. In the first one, rheological, mechanical analyses and morphological characterisation on samples with different dispersing agents are reported. The results highlight better performances for some dispersants respect others including the one traditionally used (soy lecithin) in coating formulations.

Chapter 8 is a first attempt to treat the rheological data with statistical methods, combining the univariate (analysis of variance, ANOVA) and the multivariate (Principal component analysis, PCA, after a low-level data fusion) techniques. Several rheological modifiers were tested on the A and B components and a rheological characterisation over time were performed. The two statistical approaches agree and highlight that the additives have no particular influence on A component, while they have a remarkable influence on the B components, showing also a scale of performance, due to the interaction matrix-additive.

Chapter 9 is focused on the development of a new commercial filler for the North European market, in which the filler is extruded with gear pumps at high operating pressures. After the optimisation of compression resistance and of the rheological behaviour of the A and B formulations, several characterisations in both laboratory and in-field were performed. The results highlight some innovative characteristics of the new filler, such as the better rheological behaviour of the B component, the ability to bear well some variations in the mixing ratio (up to 20%), the possibility to extrude the filler at lower pressures than competitors and so on. Therefore, the filler obtained appears a really good product that responds to North European market demands.

Concluding, the work performed in these three years, from a scientific point of view, permitted:

1) to deepen the knowledge of these materials, with the direct observation in laboratory and not only in-field, therefore transforming traditional and empirical know-how, into scientific knowledge;
2) to carry out a systematic study of the raw materials, from extenders to the additives, characterising them and observing their effects both on the single components and on the cross-linked product;
3) to better know the mechanism and time involved in the curing process, through the study of process by spectroscopic and calorimetric analysis in different environmental conditions (humidity and temperature);

4) to treat rheological data with advanced statistical analysis such as multivariate analysis that is not common in literature;

From an industrial point of view, the work permitted:

1) the better knowledge of the raw materials used, which is translated into the possibility of having increasingly performing trials;
2) the investigation of new raw materials such as wood fibers or polymeric microspheres, further introducing the company in the sustainable sector;
3) the development of A and B components for a filler that meets the requirements of a specific market, obtaining a product that shows also better characteristics than the commercial ones.

INDEX OF FIGURES

INDEX OF TABLES

INTRODUCTION

Today shipping lives an unusual expansion caused by a growing demand for services, especially from emerging countries such as China and India. This sector is a crucial market for the Italian economy; indeed, Italy has a prominent place among world boat manufacturers and is ranked second (after Holland) in the European framework [1 - 3].

Among the nautical market, yachts and superyachts play a primary role in the Italian economy. Our country is recognised as one of the most important yacht producers in the entire world. For instance, in 2016 a 35-million-euro project was launched to make Genoa the third reception centre for large yachts (Figure 1), above 30m of length, in Europe [4, 5].

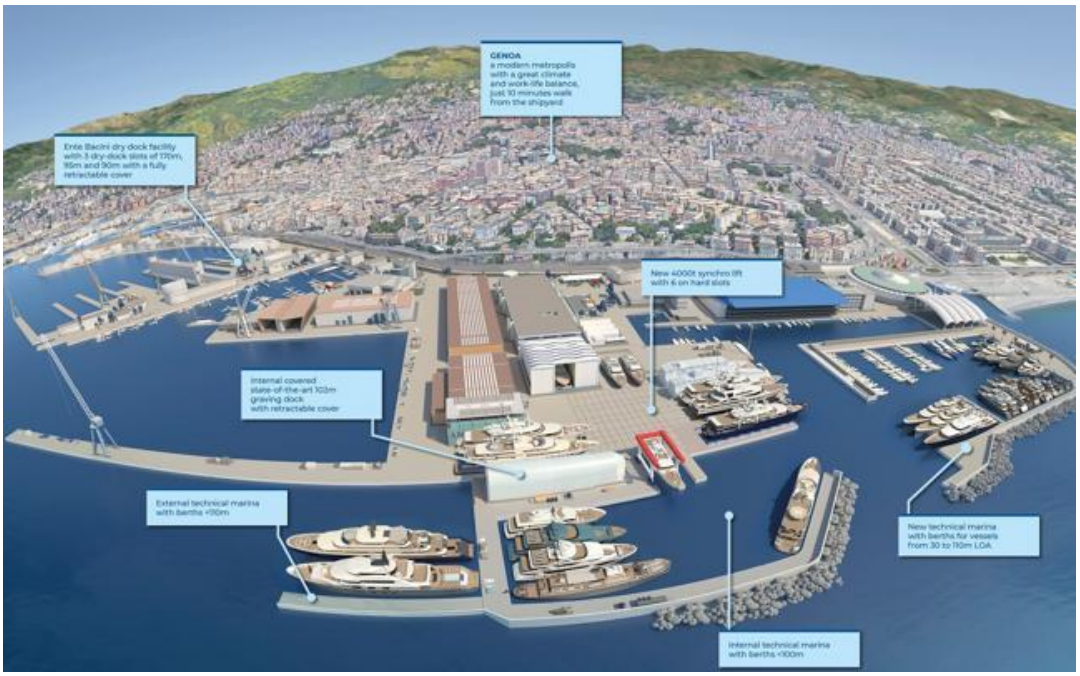

Figure 1: the reception centre for yacht project

In this sector, special coatings systems for ships external surfaces, which are the most exposed to aggressive environments, such as seawater and marine atmosphere, mechanical stresses and thermal variations, have a fundamental role. Furthermore, these coatings have to provide all the aesthetic properties typical of a luxury product as: brightness, light reflection and their durability over time. Such coatings systems have also to respect the Safety of Life at Sea (*S.O.L.A.S.*) rules that require cycles of surface preparation, painting, finishing and tests/final inspection that satisfy the requirement of 15 years of durability, with a lesser maintenance. It is therefore clear the need of the industry to invest in the search for appropriate materials to be used in the protection of naval surfaces to maintain

high levels of quality in the panorama of world production and to meet the increasingly stringent industry regulations [6 - 8].

In the current state of available technology, two-component epoxy or polyurethane systems are the products that provide excellent performances for long periods. Obviously, this is true only if the coatings are applied on surfaces carefully prepared through a sandblasting of high quality, with a steel preparation that provides the removal of all the imperfections and with quality controls before and after the application of multi-coat systems.

The difficulties of painting ships arise from the limited opportunities to apply the paint under ideal conditions. Paints as supplied must therefore be sufficiently "robust" to enable them to be applied under adverse conditions, for example, with poor surface preparation, where a perfect surface cannot be reach, or with severe ambient conditions, since in a shipyard it is difficult to control temperature and humidity.

The yacht structure could be divided in two parts as a function of waterline (Figure 2). The part above the waterline consists of superstructure and part of hull: usually they are referred as the topsides. The part under the waterline consists of the bigger part of hull, wheel, propellers and so on.

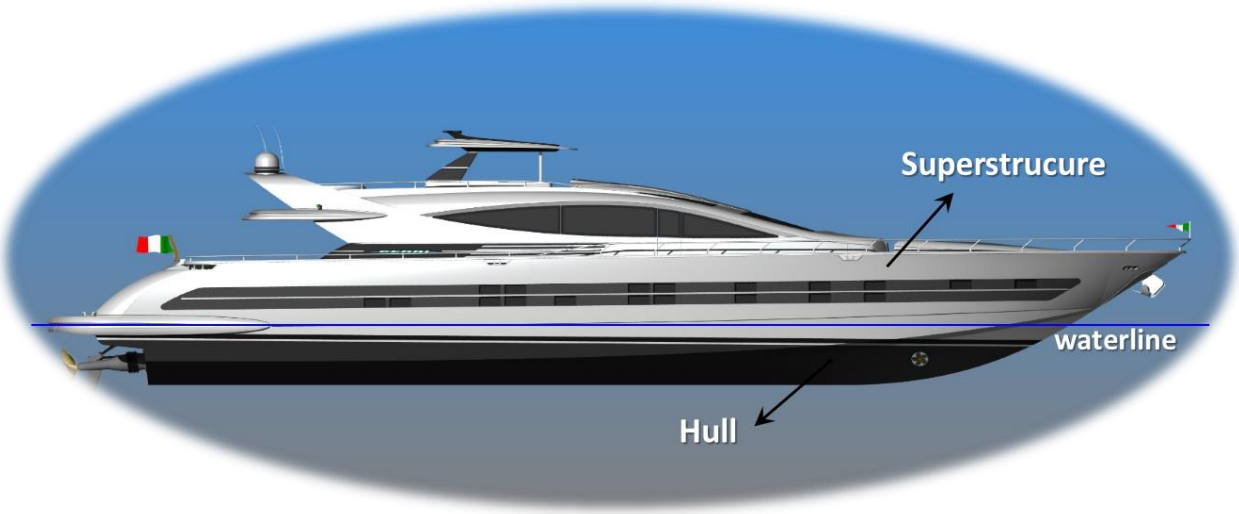

Figure 2: the yacht structure

It is well known that it is difficult, if not impossible, to meet all the requirements by the use of a single coat of paint. Indeed, the requirements of a typical paint system are many: colour, sheen (gloss), smoothness (or texture), adhesion to substrate, specific mechanical and physical properties, chemical resistance, corrosion protection, and the all-embracing term "durability". For this reason, different multi-coat systems are necessary and they will be different for each substrate (wood, fiberglass, aluminium and steel, to mention the most important). The multi-coat systems, also called painting

systems, are based on the overlap of different layers with different thicknesses, nature and aim. They result in the best system to protect the yacht external surface [7 - 9].

Consequently, the multi-coat systems are different depending on the part of the yacht considered and if it is above or below the waterline.

The typical layout for the part under the waterline is composed by a primer and a topcoat (with antifouling properties [10 - 12]).

The typical layout for the part above the waterline is more complex, it consists in a primer, two layers of undercoat, two layers of filler and a completely different topcoat.

All the used paint layers must meet specific requirements: anti-corrosion, aesthetic appearance, durability and so forth. These properties will be described in detail in the first chapter of this thesis.

Among the various coating layers used, epoxy fillers have been subject of particular attention, in recent years, by designers, builders and applicators. The main reason is the fact that these materials, in the past equated with a normal paint, are today seen almost on a par with a building material. On a boat, therefore, it is possible to find steel, aluminium, fiberglass, filler and so on. In addition, from the point of view of material consumption, fillers constitute the most part of the coatings system (high thicknesses for wide areas).

Considering these premises, in the present thesis, the fillers have been considered. Their main functions are to level and to prepare the surface for the subsequent layer of paint, in addition they have mechanical properties necessary to follow the substrate deformations and to protect and insulate it from the thermal shock [8, 13].

To better understand the importance of mechanical properties, consider that typically, a thickness of 1 cm of filler is applied on surfaces; sometimes more than 2 cm are used. In addition, in the last years or decades, speaking about Italy or North Europe respectively, shipyards are moving from a manual application to a robotic application. Consequently, the main properties of new fillers have to meet these new conditions of use.

Unfortunately, the producers have poor knowledge of the characteristics of these products and their development is focused on empirical, more than to scientific, considerations following the historical recipes.

The main critical aspects connected to these products are related both to the stability of the materials in the can (with respect to their rheology) and to the applied products (including the applications conditions, the mechanical properties and thermal stresses).

Targets of this project are therefore:

- ✓ a transition, from an industrial point of view, from very empirical knowledge to a more scientific and systematic know-how;
- ✓ the optimization of existing fillers through the systematic study of additives and extenders in the commercial formulations;
- ✓ the development of new product with specific properties for the North European market;
- ✓ a particular attention to the eco-friendly materials as requested from the market.

Since the thesis is carried out in collaboration with Boero Bartolomeo SpA, it was not possible to publish some details of the research work, due to confidentiality agreements.

Boero Bartolomeo SpA, founded in 1831 in Genoa, is an industrial holding company that formulates produces and distributes paints for the Architectural and Deco, Yachting, and Marine sectors. Boero Bartolomeo Spa is presented in the Building (Architectural and Deco) sector with brands Boero, Attiva, Rover and in the Yachting with Boero YachtCoatings, Attiva Marine and Veneziani Yachting.

This industry is one of the oldest paint factories in Europe, leader in Italy in paint building sector and leader in world for the yachting sector.

SECTION I: FUNDAMENTALS

CHAPTER 1: YACHTING PROTECTIVE ORGANIC COATINGS

The most commonly used organic coating is a paint. When applied for corrosion protection, paints are referred to as coatings. Indeed, the industrial coatings are primarily used for protection against potentially adverse environmental conditions, with the focus on durability. Coatings are typically thin layers, applied to a substrate.

They can be organic or inorganic, but for the specific study of this thesis just organic coatings are considered. Organic coatings are often composite materials, composed of more than one phase; the matrix, or binder, is typically an organic polymer and holds other components.

The term coating is used to describe both the material (liquid) that is applied to a substrate and the resultant "dry" film. Therefore, a liquid coating is a product that is applied to a substrate in the form of a continuous or discontinuous film by different application methods. A solid coating is a product physically dried (i.e. by evaporation) or chemically dried, as for the fillers by curing (cross-linking) [9, 10, 14, 15].

Modern chemically resistant paints, called high-duty or high-performance systems, are applied with fewer coats than conventional systems; nevertheless, high thickness is obtained and so called "high-build" paints. Thanks to their special composition, these paints can be applied to vertical surfaces in thick coats without sagging. When this property is due to a high extender amount, they are called "highly filled" paints [7, 13].

1.1 COATINGS STRUCTURE

A structure like a large ship offers a wide range of exposure conditions, giving rise to a complexity and diversity of corrosive and aesthetic situations that need to be solved.

Figure 2 shows the two basic painting systems of the ship: multi-layers above waterline and multi-layers under waterline for a metal substrate.

In the first case, there are six different layers on the substrate: a) primer, b) filler, c) finishing filler, d) undercoat High Built (*H.B.*) e) undercoat, f) topcoat. The multi-layer on metal substrate under waterline is characterised by two layers: a) primer and g) antifouling paint.

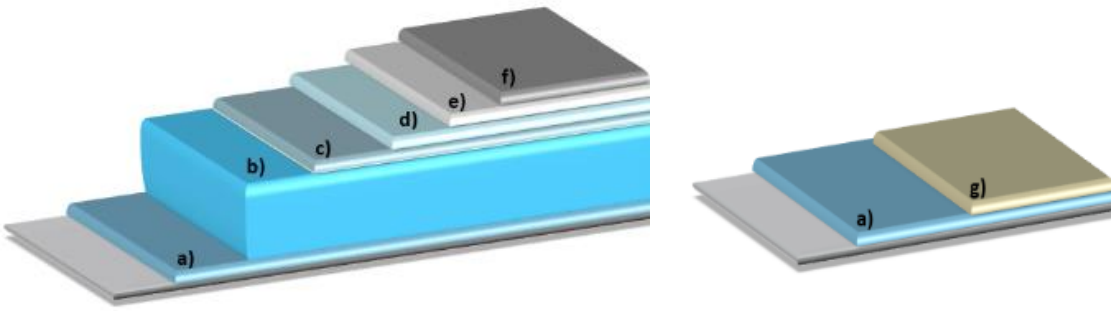

Figure 3: multi-layers system on metal substrate above waterline (left) and under waterline (right)

PRIMERS AND UNDERCOAT

Primers are the first layers applied on the substrate and their main properties are to improve the adhesion of the subsequent layers to the substrate. Primers can have a corrosion-inhibition effect, in this case most of them contain anti-corrosive pigments such as zinc powder, zinc phosphate and so on.

Undercoats are specially formulated to uniform the underlying layer and accept the topcoat, increasing grip on the surface. They can help to give a more attractive appearance to the finished paint.

Undercoats High Build are applied to obtain the total film thickness of the system. Usually, the thicker is the coating, the longer is the life. Undercoat are specially designed to enhance the overall protection and, when highly pigmented with suitable extenders, decrease permeability to oxygen and water, generating a protective barrier and isolating the underlying layers [9, 15].

FILLER AND FINISHING FILLER

The fillers are two-component epoxy composite materials and they have different aims: improve the surface finishing, prepare it for the next painting treatments, protect and insulate from thermal and mechanical shock.

At the filler are requested:

1. low density, to not increase significantly the weight of the vessel;
2. ease of mixing, in order to obtain a uniform material with little effort;
3. thixotropic behaviour to avoid sagging;
4. ease of sanding, to yield handy the works of painting;
5. elasticity, to follow the deformation of the metallic substrate;

The finishing fillers, as the undercoat, are specially formulated to make the filler more uniform and thus saturate most of the porosities of the prevoius layer (fillers).

TOPCOATS AND ANTIFOULING

The main requirements for these layers are appearance and durability. "Appearance" for topcoats is generally defined in terms of smoothness and uniformity of gloss, colour and pattern, if metallic pigments are used. These layers are usually formulated to impart high gloss.

Other properties important, in the selection of suitable topcoats, are mechanical properties and their durability on outdoor exposure. If the topcoats are used for pedestrian floors the slip resistance is also an important feature.

Antifouling paints are essential to protect any structure immersed in the seawater from fouling attack. They contain biocides, such as cuprous oxide or organometallic compounds that repel fouling organisms, both plants (flora) and animals (fauna), when released in a controlled way into the seawater.

For ships, the adverse effects caused by this biological settlement are well known: (a) high frictional resistance, due to the generated roughness, (b) high fuel consumption (c) increased emissions of harmful compounds, (d) increased of the frequency of dry-docking operations, (e) deterioration of the coating and, (f) introduction of species into environment where they were not naturally present [7, 16].

1.2 ORGANIC COATINGS COMPOSITION

Generally, organic coatings are complex mixtures of chemical substances that can be grouped into four basic categories: (1) *binders*, (2) *volatile components*, (3) *pigments and extenders*, and (4) *additives*.

- *BINDERS:* the matrix of the coating, the continuous polymeric phase in which all the components may be distributed. They are the main constituent of physical barrier that the coating provides in the protection of substrate. The type of binder largely extent determines properties such as adhesion, elasticity, gloss and chemical resistance to weathering, water, and so on. Many binders for paints are based on drying oils, synthetic (as epoxy) or natural (as rosin) resins, or combinations of these.

- *VOLATILE COMPONENTS:* usually solvents are included in a large majority of coatings. They have the function of reducing the viscosity of the binders and improving homogeneous mixing. Furthermore, the reduced viscosity allows to apply the coating in a thin, smooth and continuous film. Solvent makes the coating fluid enough for use, and evaporates during and after application.

  All solid components should be homogeneously distributed in the liquid phase. This requires a high compatibility between solvent and components, and the presence of repulsive forces between components themselves to avoid clustering. After the application, the interaction solvent-binder should decrease to enable the solvent to evaporate from the film in order to achieve optimum application. Correct material selection for coating formulation often is an extremely complicated operation, where practical experience is needed.

- *PIGMENT AND EXTENDERS:* the first are powders that are used decoratively as colorant or functionally as anticorrosion pigments.

  Extenders are also powders, but their main function is to impart structural consistency to materials, enabling application of thick coats through the incorporation of low cost materials (chalk, wood dust, carbonates…) and so make the paint cheaper. They may also be used to improve coating properties such as impact and abrasion resistance, water permeability and density lowering.

- *ADDITIVES:* it is referred to a large group of components with very specific properties; typically, they are added to paint in very small quantities. The function of the different additives may be very various. Some examples are dispersants, rheology modifiers, anti-foam agents, UV-absorbers, fire-retarding agents, anti-sagging agents and so forth [7, 9, 10, 17, 18].

1.3 SURFACE PREPARATION

Adequate surface preparation is essential to realize a long-lasting painting system: the surface must be clean, to avoid poor coatings adhesion or corrosion phenomena, and it must have a definite roughness degree, to improve the mechanical adhesion between substrate and coatings.

In the surface preparation, there are two operations: 1) “mechanical cleaning” used to remove rust, oxide, impurities, mill-scale, welding defects and 2) “hand cleaning” used to remove visible and not visible contaminants (dust, general dirt, oil, residual metal powders and so on).

Among mechanical cleaning there are different methods: sand-blasting, sanding or grinding, used as

a function of the substrate. In case of steel (the most common substrate) sand-blasting is used, in which small particles of abrasives are shoot on the substrate at high speed in order to remove contaminants and create roughness.

This roughening is called anchor pattern or "profile roughness" and it is essentially a peaks and valleys pattern on the steel surface. This pattern has to be carefully controlled according to the coating system being applied. If the peaks are too high, they will be above the coating and will be sites of initiation of rust and corrosion. A rule of thumb for surface profile is that it should be approximately one-third of the required coating system thickness up to a coating thickness of 0.3 mm.

Different parameters influence the results of sand-blasting such as sizes, materials (metallic or not), speed of particles and so forth.

The cleaning can be performed with: a) water, b) solvent, c) degreaser, and d) compressed air.

If water is used, this must be soft (4-12°F) with pH between 6.5 and 8. Different pressures can be used, in order to remove oil and well adherent contaminants; after the cleaning, the substrate must be well dried to avoid corrosion phenomena;

The cleaning with solvent can be carried out with a cloth, spray or immersing the substrate in the solvent. Particular attention must be pay to safety and to the Lower Explosive Limit (*LEL*), the solvent concentration has to stay under the flammability limit of the solvent itself.

In the case of cleaning with degreaser, usually, a spray method is employed and the contaminants are emulsified. Thereafter a washing is necessary to remove the degreaser residual.

For dust and residual not well adherent to the substrate the cleaning with compressed air is the more useful method.

In Figure 4, some examples of defects due to an incorrect surface preparation are reported.

Figure 4: defect examples: poor adhesion (left), blistering (center) and fish eye (right)

1.4 COATINGS APPLICATION

There are several methods available for applying a coating layer to the surfaces. The choice of the application method depends on many factors: whether the material to be applied is solid, liquid or powder; whether coated films should be thick or thin, or if it is clear, metallic or wrinkled, and so on. The nature and the shape of the surface are also important. For example, flat surfaces may require a different method than the contoured ones. The more common application techniques and equipment are described below [7, 8, 10, 13].

BRUSHING

It is one of the oldest method used for the application of coatings. The method is rather simple and its success depends on the quality of the brushes and the rheological properties of the coatings. The quality of brushes is related to shape, length and nature of the bristles.

Brushing is an effective method, particularly used during primers application to lay the paint into pores and surface irregularities, or when painting small surfaces (as in spot repairs), or when painting places inaccessible to spraying or where for safety reasons spraying is prohibited.

Some brushing disadvantages are linked to the fact that it does not produce a very uniform film thickness and that is a slow method [7, 13].

ROLLING

Rollers are used on large, flat areas that do not require the surface smoothness or uniformity achievable by spraying. This method is more or less five times faster than brushing.

The nap (fibre length) of a roller normally varies from 6.4 to 19 mm. A longer nap holds more paint but does not give a smooth finish; therefore, it is used on rough surfaces. Rollers with extra-long naps (32 mm) are used for chain-link fencing [8, 10, 13].

SPRAY PAINTING

This method is faster than the others and suitable for large surface that require excellent uniformity.

To apply by spraying, a special gun must be used and it can be for conventional air spraying or airless spraying. In the first case the paint is forced by compressed air from a feed cup to the spray gun, while in the airless spraying the paint is brought at high pressure by means of a pump and forced through a narrow orifice in which it is atomized.

The airless spraying has some advantages respect conventional spraying:

1) significantly higher production rates which makes faster spraying possible;
2) paints can be generally sprayed at a somewhat higher viscosity, resulting in higher dry film thicknesses;
3) the loss of solvents and thinners by evaporation in airless spraying is much lower than in air spraying. This allows the use of more volatile solvents, with less risk of sagging.

However, airless also has some disadvantages compared to conventional spraying:

1) the high production rate which makes it unsuitable for spraying small objects;
2) spray tips must be regularly checked and replaced if necessary since the spray orifices are narrow, they become worn out in prolonged use, particularly when paints contain hard pigments or extenders;
3) the jet of paint has such a high speed that it can easily pierce the operator skin;
4) special cares are required to avoid excessive build-up of paint that causes solvent entrapment, pinholes, runs, sags and wrinkles (Figure 5) [7, 8].

Figure 5: pinholes (left) and wrinkles (right) defects

FILLER APPLICATIONS

The application of the filler, unlike the methods just mentioned, occurs with spatulas and trowels. In this case, it is necessary to compress the filler in order to de-aerate it if air bubbles are present (incorporated in the mixing) and distribute it as evenly as possible, avoiding to leave smears that would complicate the sanding. Generally, it is necessary to wait 24 hours before sanding and applying the next layer.

CHAPTER 2: FILLERS

The two-component epoxy fillers are "high-build" paints, composite materials, which consist of the A component with epoxy matrix, and B component with polyamide matrix, that is the curing agent (or hardener). As dispersed phase, there are different extenders such as: hollow glass microspheres, alumina-silicate spheres, carbonates, talc, and fumed silica. In addition, there are various additives: dispersants, rheology modifiers and anti-foam agents.

The A and B components once mixed together in opportune ratio form the product to be applied, i.e. they cross-link, forming infusible, insoluble and rigid products.

The degree of cure has a high impact on the physical, mechanical and chemical properties of epoxy systems. Hardener type and concentration, temperature and humidity of the application environment affect the curing process of epoxy resins (see 2.1.4 "Properties of cross-linked polymers").

The filler needs some specific properties: rheological, mechanical and thermal. The rheological properties are essential in order to have:

1. an ease of mixing, indeed the filler high thickness (~ 2 cm) and the wide yacht surface require mixing of considerable materials volume,
2. thixotropy, that is essential in order to avoid sagging effect during or just after the application.

The mechanical properties of fillers are fundamental to ensure the painting systems integrity, because they must be able to withstand the deformations suffered by the structure. In fact, the hull undergoes different stresses and deformations depending on:

- ✓ the point where it is located (bulb, rudder, keel, topsides or superstructure),
- ✓ the specific condition to which it is subjected (stationary or sailing)
- ✓ the material of construction (aluminium, steel, wood or glass-reinforced plastic).

Thermal properties are strictly related to the application conditions and are influenced by the glass transition of materials [6, 19].

The mechanical, physical, and thermal properties can be tailored with the addition of inert extenders as glass microspheres and silica.

The critical aspects of the nautical filler can be grouped in two broad categories:

- related to the rheology of single component:
  - ✓ viscous behaviour when subjected to stress and thixotropic behaviour;
  - ✓ material stability in the can;

- related to the cross-linked product:
  - ✓ filler application conditions: the environmental conditions, such as temperature, humidity and the variable thicknesses of the material play a fundamental role for the good application of the coating;
  - ✓ glass transition temperature (T_g) acceptable in the usage temperature range and compatible with the possible thermal stresses;
  - ✓ thermal stresses: since the boats can undergo considerable temperature changes, for example on summer days the temperatures can reach peaks of 80 °C on dark-coloured hulls and on winter days the temperatures are well below zero, the filler must withstand both conditions;
  - ✓ mechanical properties once applied, including the elasticity to adapt to the deformations of the substrate;
  - ✓ the possible recycling of these materials (currently there are strong difficulties in their recycling).

All these aspects should be addressed in an economically acceptable and sustainable context.

In order to have a visual feedback on the good mixing of the two-components, epoxy matrix component has a very low percentage (<1%) of colouring pigment (based on copper phthalocyanine blue or green and on orthonitroaniline orange), as visible in Figure 6.

The epoxy fillers belong to high solids solvent-borne, in which the percentage of solvent is low (<6% in both components).

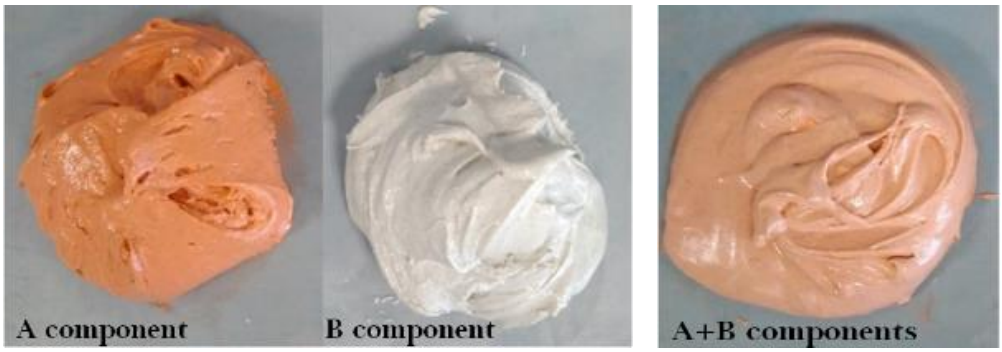

Figure 6: A component (left), B component (centre) and mixing of two components (rights)

2.1 MATRIX

The term resin is used to refer to polymer matrix. Most of the common resins are liquids are room temperature, although they can be powder materials that will be subsequently heated and then formed or shaped.

A continuous film is formed either by physical curing, chemical curing or a combination of the two [7, 15, 20].

2.1.1 EPOXY RESINS

Epoxy resins as thermosetting polymers, were introduced commercially in the USA in the late 1940s. They have gained wide acceptance in protective coatings and electrical and structural applications because of their exceptional combination of properties such as toughness, adhesion, chemical resistance and superior electrical properties. The largest use is for surface coatings, which account for about 50% of current epoxy resin output. Further applications include laminated circuit boards, carbon fibre composites, electronic component encapsulations and adhesives.

Most epoxy coatings used in shipbuilding are the “high-duty” and chemical resistant two-component type. They dry by chemical reaction of epoxy resin with an added hardener (polyamine or polyamide) [7, 8].

There are two main categories of epoxy resins, namely the glycidyl epoxy, and non-glycidyl epoxy resins. The first are further classified as glycidyl-ether, glycidyl-ester and glycidyl-amine. The non-glycidyl epoxies are either aliphatic or cycloaliphatic epoxy resins.

Glycidyl-ether epoxies such as diglycidyl ether of bisphenol A (*DGEBA*) is among the most commonly used epoxies. DGEBA oligomers typically contain a certain amount of hydroxyl groups that play an important catalytic role in the curing process. All of them have at least two oxirane functional groups, so they can lead to the 3D network. The nature and functionality of the epoxy monomer will determine its reactivity as well as the properties and performance of the final material. The bond between the aromatic ring and the oxygen (ether) in DGEBA has a strong electron-withdrawing effect that makes the oxirane group highly reactive towards nucleophilic compounds (like amines and polyamides) [8, 9, 21].

At the present time, 80-90% of commercial epoxy resins are prepared by the reaction of 2,2-bis(4'-hydroxyphenyl)propane (bisphenol A) and epichlorhydrin.

Bisphenol A is so called since it is formed from phenol and acetone (Figure 7):

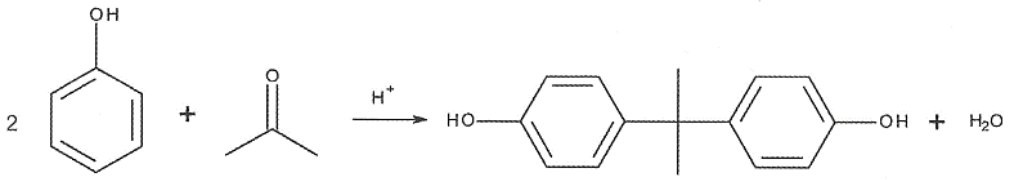

Figure 7: formation of bisphenol A

Although the reaction theoretically requires the molar ratio of reactants to be 2:1, an improved yield of bisphenol A is obtained if additional phenol is present, so the optimum molar ratio is 4:1. In a typical process, the phenol and acetone are mixed and warmed to 50°C. Hydrogen chloride (catalyst) is passed into the mixture for about 8 hours, when the temperature is kept below 70°C to suppress the formation of isomeric products. Bisphenol A precipitated is filtered off and washed with toluene to remove unreacted phenol (which is recovered). The product is then recrystallized from aqueous ethanol [17, 20].

The formation of bisphenol A is reported in Figure 8:

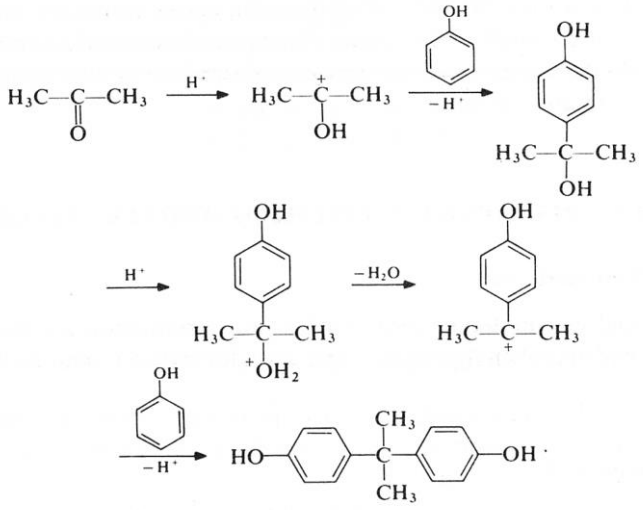

Figure 8: mechanism of bisphenol A formation

RESIN PREPARATION

Both the preparation of liquid and solid resins are briefly described. In a typical process for the liquid epoxy resin preparation, a mixture of bisphenol A and epichlorohydrin (about 1:4 molar) is heated to about 60°C with stirring. Solid sodium hydroxide (2 moles per mole bisphenol A) is added slowly at such a rate that the reaction mixture remains neutral. The reaction is exothermic and cooling is applied to keep the temperature at 60°C. Excess of epichlorohydrin is then removed by distillation under

reduced pressure. The residue consists of epoxy resin mixed with sodium chloride. The latter is filtered off, toluene having been added to the mixture in order to facilitate filtration. The toluene is removed by distillation under reduced pressure and then the resin is heated at 150°C/0.6 kPa to remove traces of volatile matter. This last step is important since the presence of volatiles may lead to bubble formation when the resin is subsequently used. Finally, the resin is filtered by through a fine filter.

In the solid epoxy resins preparation, the above process is slightly modified. A mixture of bisphenol A and epichlorohydrin is heated to 100°C and aqueous sodium hydroxide is added slowly with vigorous stirring. The molar ratio of reactants used depends on the resin molecular weight required. When reaction is complete the is stopped and a ‘taffy' (which is an emulsion of about 30% water in resin) rises to the top of the reaction mixture. The lower brine layer is removed; the resinous layer is coagulated and washed with hot water. The resin is heated at 150°C under reduced pressure to remove water, clarified by passage through a filter and then allowed to solidify. Solvent can be added at the washing stageshing and filtration, but then it is very difficult to remove all its traces. Alternatively, solid epoxy resins may be prepared by two step-processes in which a pre-formed liquid resin is heated with bisphenol A in the presence of a basic catalyst to effect chain extension. This method avoids the difficulty of washing sodium chloride from highly viscous material.

When epichlorohydrin reacts with a difunctional phenol such as bisphenol A the lead to linear polymers. In order to obtain polymers to be commercially useful as epoxy resins it is necessary that they are terminated by epoxy groups (through which they may be subsequently cross-linked). This is achieved by carrying out the polymerization with a molar excess of epichlorohydrin [17, 22].

The formation of the epoxy resin is illustrated by the scheme in Figure 9.

The value of *n* is determined by the molar ratio of the reactants; when this ratio approaches unity the molecular weight of the product is higher [18, 20, 21].

The most important parameter in epoxy resins is the content of epoxy groups, because they react with the curing agent and so they determine the amount of this agent to be used. Epoxies are typically cured with stoichiometric or near-stoichiometric quantities of curing agent to achieve maximum physical properties. There are several methods to express this content, but the most common is the epoxide equivalent weight (*EEW*). This parameter indicates how many grams of epoxy resin contain 1 mole of epoxy groups (oxirane rings). Thus, a high epoxy equivalent mass indicates a low content of epoxy groups.

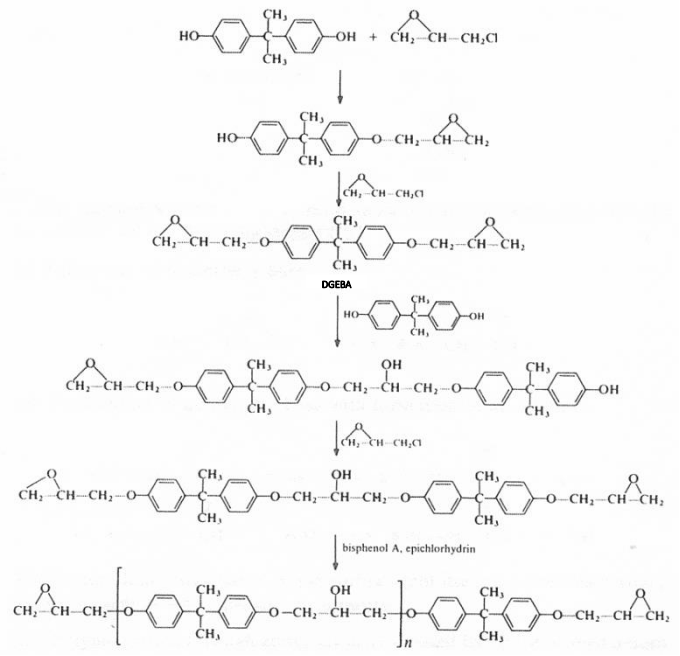

Figure 9: epoxy resins formation

Approximation for epoxy resins based on bisphenol A is EEW ≈ (resin molar mass) / 2 [17, 20, 21]. To determine the EEW there are several methods, but the most important involve reaction of hydrogen halides with epoxy group according the reaction reported below:

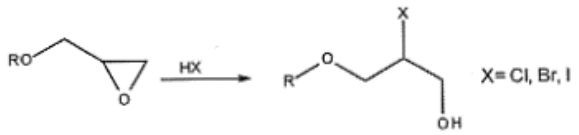

Figure 10: reaction between epoxides and hydrogen halides

2.1.2 CURING AGENTS

The bisphenol A epichlorohydrin resins produced by the methods described above cannot be cross-linked at a reasonable rate by heat alone; even the heating at 200°C has little effect. In order to convert the resins into highly cross-linked, three-dimensional network, it is necessary to add a curing agent. The cure kinetic and the glass transition temperature of cross-linked system are dependent on the hardener molecular structure. The choice of resin and hardeners depends on: 1) the application, 2) the process selected, and 3) the properties desired. The stoichiometry of the epoxy-hardener system also affects the properties of the cross-linked material.

A wide variety of curing agent for epoxy resins is available such as amines, anhydrides, polyamides and so on. Examples of tertiary amines include benzyldimethylamine (*BDMA*), 2-(dimethylaminomethyl)phenol (*DMAMP*), 2,4,6-tris(dimethylaminomethyl)phenol (*TDMAMP*), triethanolamine and N-n-butylimidazole (Figure 11)

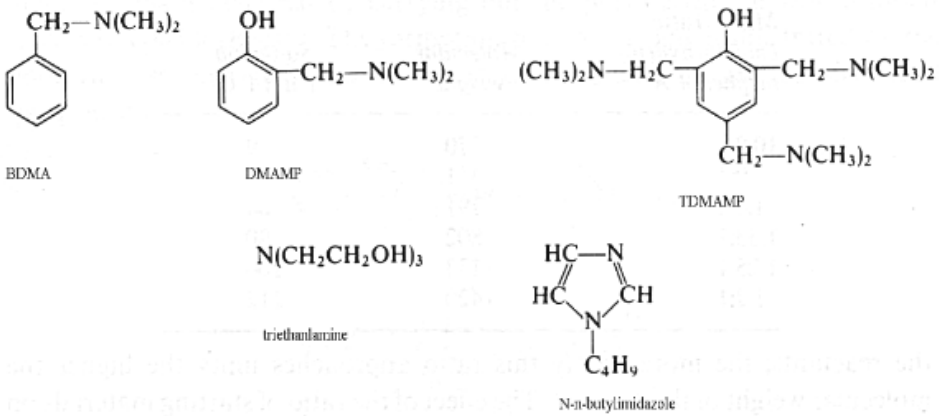

Figure 11: tertiary amines

Regarding polyfunctional amines, both aliphatic and aromatic compounds having at least three active hydrogen atoms in primary and/or secondary amine groups are widely used as curing agents for epoxy resins. Examples of such polyfunctional amines are diethylenetriamine (*DTA*), triethylenetetramine (*TET*), m-phenyleledіamine (*MPD*), 4,4'-diaminodiphenylmethane (*DDM*) and 4,4'-diaminodiphenylsulphone (*DDS*), reported in Figure 12.

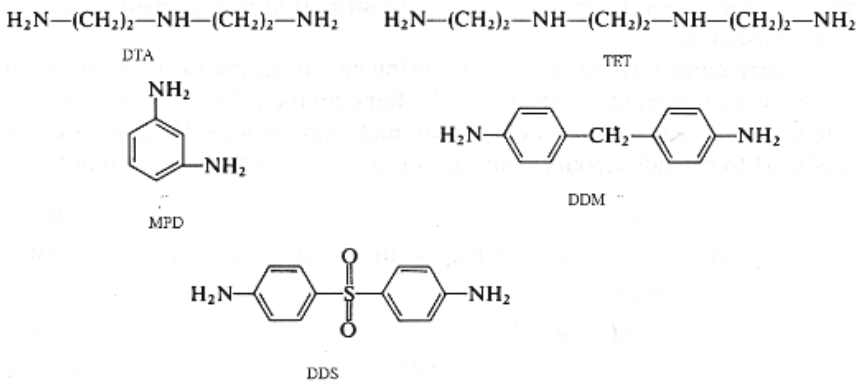

Figure 12: polyfunctional amines

Examples of acid anhydrides are: maleic anhydride (MA), dodecenylsuccinic anhydride (DDSA), hexahydrophtalic anhydride (HPA) and phtalic anhydride (PA), reported in Figure 13. The reaction between epoxy resin and anhydrides is complex: several different reactions are involved [17, 18, 21].

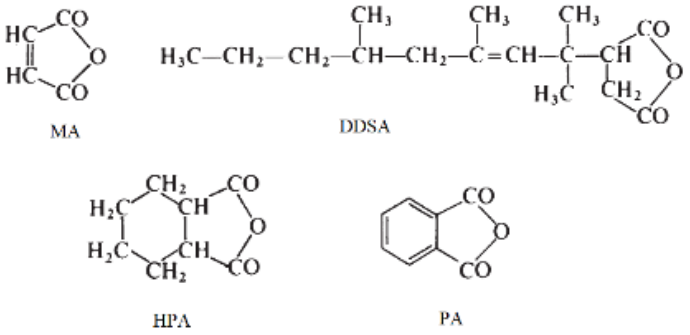

Figure 13: acid anhydrides

POLYAMIDES

Polyamide resins were commercialized in the late 1950s to use with epoxy resins in the wide variety of applications: the manufacture of two-component adhesives and high-performance coatings for machinery, equipment and marine applications. The early commercial epoxy/amine coatings contained aliphatic amines, primarily diethylenetriamine, which had several negative features, such as critical mix ratios and toxicity. The introduction of liquid polyamide resins allowed the coatings manufacturer to produce high-performance coatings characterised by convenient mix ratios, such as 1:1 or 2:1, with very low toxicity.

The presence of the long fatty chains gives coatings with much better flexibility as well as better wetting and adhesion than those obtained with the earlier aliphatic amine cured systems [15].

Polyamide resins are polycondensation products of difunctional fatty acids and polyfunctional amines. In a typical commercial example, 1 mole of dimeric acid is reacted with 2 moles of diethylenetriamine. During the condensation reaction, 2 moles of water are evolved. As the reaction proceeds, side reaction occurs and an additional water mole evolves from a secondary reaction. One of the primary amine groups reacts with the dimer acid to form an amide linkage. The ethylene chain next to the amide function and the secondary amine nitrogen are incorporated into a five-membered ring (imidazoline ring). This condensation reaction eliminates an active hydrogen to yield a tertiary amine group. The degree of cyclization is controlled to yield a product with specific useful properties, such as improved solubility and compatibility and longer pot life. Similar reactions occur at the other carboxylic acid group of the dimer. If 50 % of the diethylenetriamine present in the polyamide is cyclized to imidazoline, 3 moles of water are evolved.

The most important parameters that characterise an amine curing agent are: the amine value, the hydrogen equivalent weight, and the viscosity. The active hydrogen equivalent weight is used to calculate the amount of polyamide resin required to react with a given amount of an epoxy resin of known epoxide equivalent weight. The ratio of these values, known as the stoichiometric mix ratio,

is most often only a starting point. By varying the mix ratio of the polyamide resin to the epoxy resin, certain properties of the cured coating are enhanced (and others are sacrificed) to obtain specific application properties [15, 23, 24]. In Figure 14 an example of polyamide structure is reported.

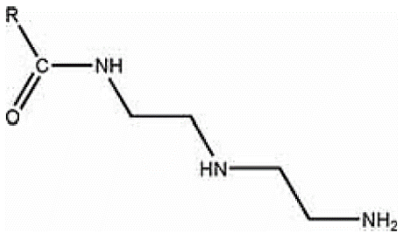

Figure 14: polyamide structure

MECHANISM OF CURING IN EPOXY/POLYAMIDE SYSTEMS

Polyamide resins react with epoxy resins in several stages to form a complex insoluble cross-linked matrix. The initial reaction is between the terminal primary amine groups of the polyamide resin and the oxirane ring of the epoxy resin (Figure 15).

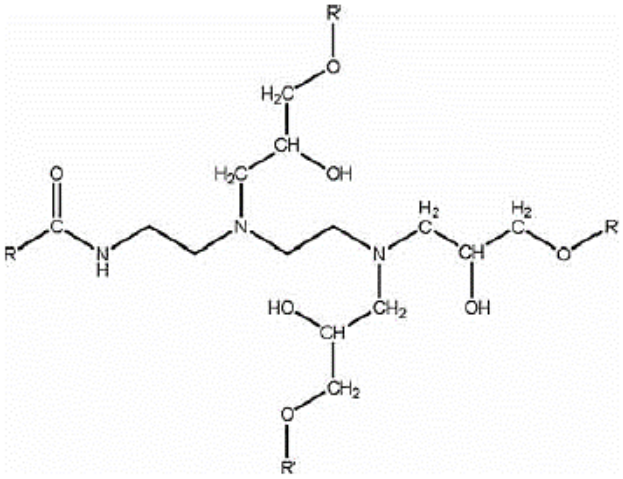

Figure 15: polyamide reaction with epoxy resin

The active hydrogen opens the ring and the oligomers join end to end. The reaction of the oxirane ring and active hydrogen also occurs at the secondary amine sites in the polyamide resin.

A secondary reaction, moreover, occurs between pendant hydroxyl groups in the epoxy resin molecule and other oxirane rings present. [23 - 26].

2.1.3 STUDY OF CURING PROCESS

As already mentioned, curing agent type and concentration, environment temperature and humidity during application affect the curing process of epoxy resins.

The degree of cure has a high impact on the physical, mechanical and chemical properties of epoxy systems. Since the curing process of an epoxy thermoset resins is thermally activated and temperature dependent, the thermal analysis is the most common method to monitor this process. Indeed, the differential scanning calorimetry (*DSC*) has been widely used as a method to determine cure kinetics of thermoset resins, with the analysis of glass transition temperature (*Tg*) and enthalpy of reaction (ΔH_r) variation. On the other hand, infrared spectroscopy (Near-Infrared and Mid- Infrared) turned out to be well suited for analysing the degree of cure for epoxy systems and the reaction at molecular level, directly by analysing structural changes. Although the IR spectra are very complex, showing a number of overlapped bands, it is possible to identify several spectroscopic features whose detection and changes shall be considered diagnostic of the curing process.

Generally, for the two-component epoxy filler, the glass transition is more sensitive to the cross-linking degree, the humidity has an important influence at low temperature of applications (below 10°C) [22, 27 - 31].

2.1.4 PROPERTIES OF CROSS-LINKED POLYMERS

Since the characteristic group in epoxy resins largely disappears upon cross-linking, it is difficult to make simple generalizations relating structure to properties.

The cross-linked polymers properties depend on:

- ✓ the curing agent (type and concentration),
- ✓ the applications conditions (temperature and humidity)
- ✓ the extenders (type and shape)

The cure of epoxy resins involves slight molecular reorientation and no evolution of volatile by-products: shrinkage is low and the cured products are relatively strain-free, resulting usually tough. The main skeletons of the resins themselves are rather stable structures with good heat resistance but the overall stability of the cured products is very dependent on the nature of the cross-links present. In Figure 16 is reported an example of cured filler.

Figure 16: commercial cured filler example

The electrical insulating properties of epoxies are very good although the presence of polar hydroxyl and ether groups results in comparatively high dielectric constant and power factor. These polar groups also lead to outstanding adhesion to many surfaces.

Being cross-linked, the epoxies are swollen by liquids of similar solubility parameter (e.g. chlorinated hydrocarbons and alcohols). Resistance to acids and alkalis is largely determined by the curing agent used; ether links (formed by the use of hardeners) are stable toward most inorganic and organic acids and alkalis whereas ester links (produced by anhydrides) are sensitive to strong alkalis and inorganic acids.

The C-N bond (formed by amines) is generally stable toward inorganic acids and alkalis but not organic acids [17, 20].

2.2 EXTENDERS

Extenders are mainly used to reduce the raw material cost of the coatings formulation increasing the volume and improving coating performance (e.g. lower density or abrasion resistance). Most are white or near-white inorganic minerals, with a coarser particle size (from sub-micrometre to a few tens of micrometres) and lower oil absorption, i.e. the binder demand (see 3.2.1 “Oil adsorption”) than pigments.

A secondary task can be to fill the coatings spatially with skeletal material and therefore to influence the mechanical properties in a particular direction, depending on the relevant function of the paint film [13, 18, 32].

Usually they are commercial product and their chemical composition is not disclosed.

2.2.1 MICROSPHERES

The glass microspheres are hollow spheres with diameters in the micrometric range (<120μm) and their composition is soda-lime-borosilicate glass.

These extenders have some advantages:

- a very low density
- a very low surface area and therefore a low oil absorption, which results in a lesser resin demand from extenders
- a gas inside, which permits:
    1. low thermal conductivity, so that coating shows a very good effect on heat insulation;
    2. good contractility resistance to hot and cold, thus enhancing the flexibility of coating, greatly reducing the cracking and peeling of the coating due to thermal expansion and contraction.

They have good effect on the formulation: the coatings rheology is improved because of their spherical shape, glass microspheres behave like tiny ball bearings, flowing within a liquid polymer much better than common other extenders. A benefit is the ability to form highly-filled composites.

The hollow glass microspheres also have a good effect on the cross-linked product, since the vitrified surface can improve the chemical corrosion resistance.

When these extenders are mixed with epoxy resin it is obtained a material extremely tenacious, slightly elastic and difficult to break, with good hardness and with very low density.

The hollow glass microspheres are available in a wide range of densities and crush strength.

2.2.2 ALUMINA-SILICATE SPHERES

These extenders are hollow spheres, belonged to cenospheres materials. They are primarily used to reduce the weight of plastics, rubbers, resins, cement, and so on, but also impart further benefits in many situations.

The glass ceramic microspheres have variable size from 100-400μm. The particles are formed during high-temperature combustion of pulverized coal. Qualitative characteristics of alumina-silicate spheres are directly dependent on the characteristics of the ash waste produced by a power station.

The chemical composition is silicon oxide SiO_2 (50-60%), aluminium oxide Al_2O_3 (34-42%), iron oxide Fe_2O_3 (1.0-10%), calcium oxide CaO (1.5- 4.5%), potassium oxide K_2O (2.0-4.5%) and other oxides typically less than 1.0%. Inside the spheres there are N_2 (30%) and CO_2 (70%) gasses.

Similar to hollow glass spheres, the alumina-silicate spheres, having a spherical shape, exhibit:

- low surface area;
- low oil absorption;

- good flow characteristics, improving the coatings rheology.

2.2.3 CARBONATES

Calcium carbonates are used traditionally as inexpensive extender materials. They have interesting properties such as: high whiteness and low oil absorption, easy dispersibility and low abrasiveness, good anti-corrosion and rheological properties.

Calcium carbonates are differentiated by physical properties, such as particle size, brightness, oil absorption and so on. Fine-particle-size products have an average particle size from less than 1 to about 5μm. Ground carbonates have low oil absorption, which correlates with a low resin demand in coatings [15, 18].

Related to the particle size distribution and to the fineness, the coatings opacity is varied.

2.2.4 TALC

Talc (soapstone) is a hydrated magnesium aluminium silicate with the chemical formula $3MgO{\cdot}4SiO_2{\cdot}H_2O$. Key properties of this extender include colour, particle size, water solubility, and oil absorption. Its lamellar, hydrophobic and chemical inert structure makes it to a perfect extender for the coatings industry. Indeed, talc increases coverage and weather resistance of the products, creating a barrier effect, which limits the penetration of water and corrosive agents into paints and coatings. These properties lead to a reduction in bubble formation, corrosion and peeling.

Talc is used in many different types of coatings as interior and exterior trade sales paints, primers, traffic paints, and industrial coatings. Some grades are available with an average particle size of 1–3μm, but most are around 5–15μm. Oil absorption depends on particle shape and size, but, in general, it is similar to carbonates.

2.2.5 FUMED SILICA

Silica is a general term describing products with the chemical formula SiO_2 and both natural and synthetic are available. The most used in paint and coatings are crystalline, microcrystalline, diatomaceous, precipitated and fumed.

Fumed silica is a white, fluffy powder composed of submicron-sized amorphous silica spheres arranged in branching chains of varying lengths. The extremely small particles result in a large

specific surface area and so high oil absorption. The surface area of fumed silica is almost entirely external, due to its roughness, and is not derived from any porosity.

The fumed silica can be reinforcement extender in composite materials and produces a considerable improvement in their mechanical properties, such as tensile strength, elongation at break and tear resistance. It also helps to control the influence of temperature on mechanical properties and it can be used as rheology modifiers.

2.3 ADDITIVES

Additives belong to a wide and diffuse category of key components in a coating formulation. They are present in a small percentage in the formulation, usually less than 5%, but their influence is very significant. Coating additives are utilized to give characteristic properties to the main components, i.e. the matrix, pigment and/or extender and solvent (if presents). In Figure 17 is reported a scheme of additives and other coating component interactions.

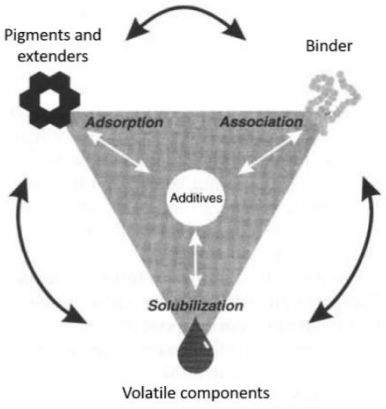

Figure 17: interaction between additives and the other coating-materials [33]

Additive function is generally specific, but some additives are multi-purpose. In recent years, multi-purpose additives have been developed, thus allowing the use of fewer additives in many formulations. Sometimes more additives are necessary to obtain a desired property because they work in a synergic way.

Also for these raw materials, it is difficult to know the specific chemical composition because they are commercial products and this can make general recommendations difficult. Moreover, this lack of structural knowledge means that additive substitutions cannot be made based on fundamental structural chemistry [33, 34].

In the filler formulations, such already mentioned, the additives employed are dispersants, rheology modifiers and anti-foam agents.

2.3.1 DISPERSANTS

A dispersant is an additive that increases the stability of a powder suspension (pigments and/or extenders) in a liquid medium. Thus, the dispersant must be able to wet totally the particles and interact with the dispersing medium.

The powder-dispersing step is one of the most important, the most difficult and time/energy consuming part of the paint manufacturing process. This is due to the difference in surface tension between the liquids (polymers and solvents) and the solids (pigments and extenders).

Pigments and extenders are often received as agglomerates and then are grinded by incorporating the powder into the vehicle during paint manufacture. During the grinding, the agglomerates are dissociated into a dispersion of particles. In the process, dispersants are used to prevent their re-association. The dispersants are adsorbed onto the particles and hinder close approach of particles by charge repulsion effects (ionic dispersants, generally having low molecular weight) or by steric effects (non-ionic dispersants, generally having high molecular weight).

These agents are compounds consisting in two well-defined parts: oil soluble (hydrofobic) one, generally with aliphatic or aromatic hydrocarbon residue, and water soluble (hydrophilic) one. The hydrophilic group, the "head", could be ionic or non-ionic and it allows to classify the dispersant into two categories: ionic and non-ionic. In the first case, the stabilisation mechanism is based on ionic repulsion: the charged molecules adsorbed on the particle surface, impart a charge, forming the Helmholtz electric layer; the charged layer, around the particle, creates electrostatic repulsive forces to hinder aggregation. The ionic dispersant can be anionic (negatively charged polar "head"), cationic (positively charged polar "head") or Zwitterionic (Figure 18).

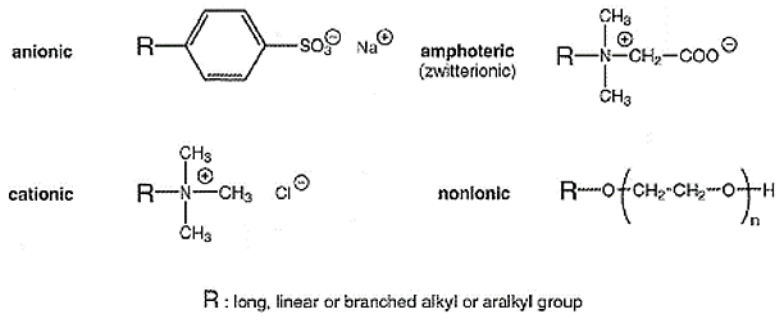

Figure 18: dispersants classification according to the charge on the hydrophilic group

If the dispersing agents have a non-ionic "head", the stabilisation mechanism is based on steric hindrance; these dispersants have pendant anchoring groups which adsorb onto the particles surface by hydrogen bonding, dipole-dipole interactions or Van der Waals forces. The long chain part of the dispersant is large enough to cause steric stabilization and to prevent the approaching of particles to each others [15, 34 - 36].

Examples of dispersants are: phosphates, sulfonates, polyphosphates, polyoxyethylene derivatives, alkyl trimethyl ammonium chloride and lecithin.

2.3.2 RHEOLOGICAL MODIFIERS

Rheology modifiers are chemicals that alter the deformation and flow characteristics of matter when it is under the influence of stress, generally are often used in coatings to alter viscosity at low and/or high shear rates. A basic understanding of coatings rheology is essential to the development of acceptable flow properties. Indeed, the coating rheology determines many of the properties such as in-can appearance, anti-settling of powders, colour stability, application performance (thixotropic behaviour), brush or roller loading, brush drag, flow, levelling and film build.

The required rheology profile for a coating formulation may vary dramatically during its lifetime, starting from the manufacturing process, through transportation and storage, and finally during application processes. This profile can be associated with different shear rates and rheological demands (Figure 19).

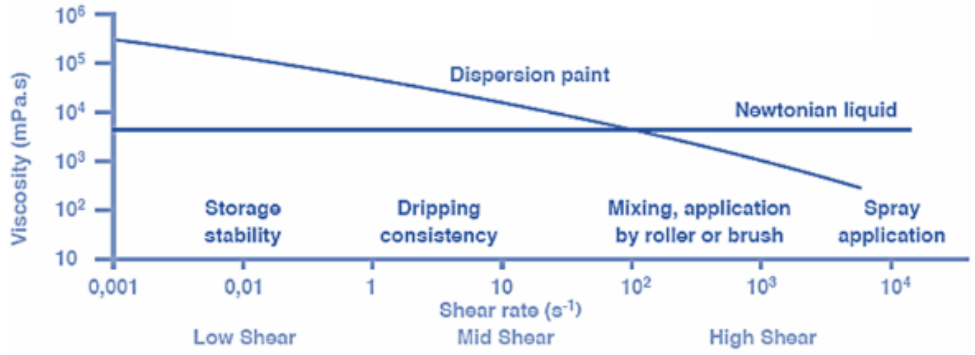

Figure 19: different shear rates and rheological demands for coatings systems

Viscosity curves are often used to characterise the rheological behaviour of coating systems. Three are the main viscosity profiles used to describe the fluids rheological behaviour: 1) shear thinning (pseudoplastic), 2) Newtonian (shear has no effect on viscosity) and 3) shear thickening (dilatant).

Pseudoplasticity systems recover quickly after shear is removed and it is often referred to as thixotropy. The longer this material is sheared the lower is the viscosity, until a minimum value is

reached. This behaviour is due to a structure loss in coating system. This loss in viscosity is usually temporary and time-dependent in a true thixotropic system (time-depending behaviour). The system will rebuild to its original state given enough time (minutes to hours).

Viscosity is constant at all shear rates for a Newtonian fluid; this flow behaviour is typical of water, solvents and oils. Dilatant flow shows a viscosity increasing as the shear rate is increased and is characterised by solutions of PVC (polyvinyl chloride) in solvent or plasticizer.

Because each profile has advantages and disadvantages, quite often combinations of rheological additives are used to optimize final coating properties.

These additives can be inorganic or organic; inorganic additives are supplied as powders and are attapulgite clays, bentonite clays, organoclays, treated and untreated synthetic silica and so on. Particles surface is often modified with organic treatments to make it hydrophilic or hydrophobic as a function of the matrix.

Organic additives are: natural raw materials (based on cellulosic polysaccharides) and some synthetic materials (such as polyacrylates or polyurethanes).

The synthetic products can be dived into non-associative, associative and other solvent-based rheology modifiers (Figure 20).

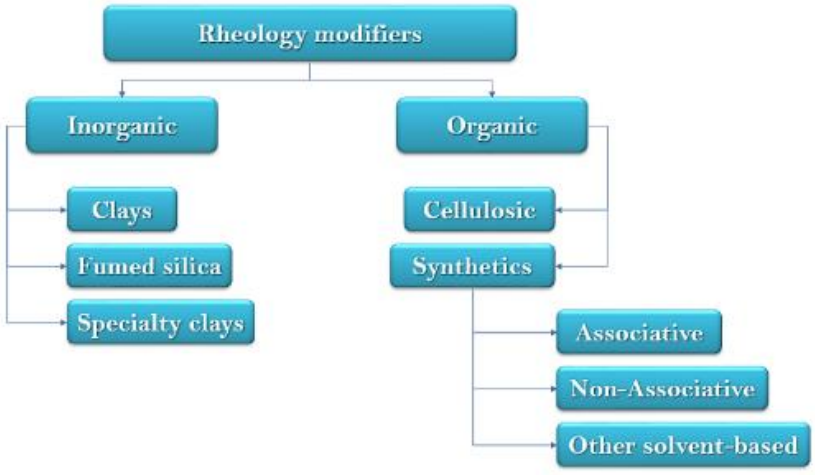

Figure 20: overview and classification of major rheology modifiers

The associative and non-associative additives are for water-borne system, while the last rheology modifiers are for solvent-borne systems

Organoclays, hydrogenated castor oils, fumed silica or polyamides commonly are used [15, 33, 34].

2.3.3 ANTI-FOAM AGENTS

Foam is created when air is introduced into paint during manufacturing or application. Foaming is highly almost undesirable, it reduces manufacturing efficiency and causes film defects. Thus, it is necessary the use of foam control agents-surface-active additives that prevent, reduce, or eliminate foaming during manufacturing and application. If the additives prevent the foam formation they are called anti-foam, while if the additives destabilized the foam already formed, they are called defoamer.

Various products are used as foam control agents, including fatty acid esters, metallic soaps, mineral oils, waxes, silicon oils, and siloxanes and so on. [15, 33, 37].

CHAPTER 3: TECHNIQUES

In this chapter the techinques the instruments and the measurement conditions are briefly explain to give an overview of the methods used in the thesis. To a deeeper knowledge of these methods compared to the informations here reported see the references.

3.1 COMPONENTS DISPERSION AND CROSS-LINKING PROCESS

The extenders and additives dispersion in the matrix was carried out with a dissolver Dispermat LC30 220V (Dispermat® VMA-Getzmann, GmbH). The dispersion of additives and the majority of extenders was performed with a cowles, but for hollow glass microspheres it is necessary to use a butterfly to prevent them from breaking (see Figure 21). The mixture temperature, speed and time during the dispersion were controlled.

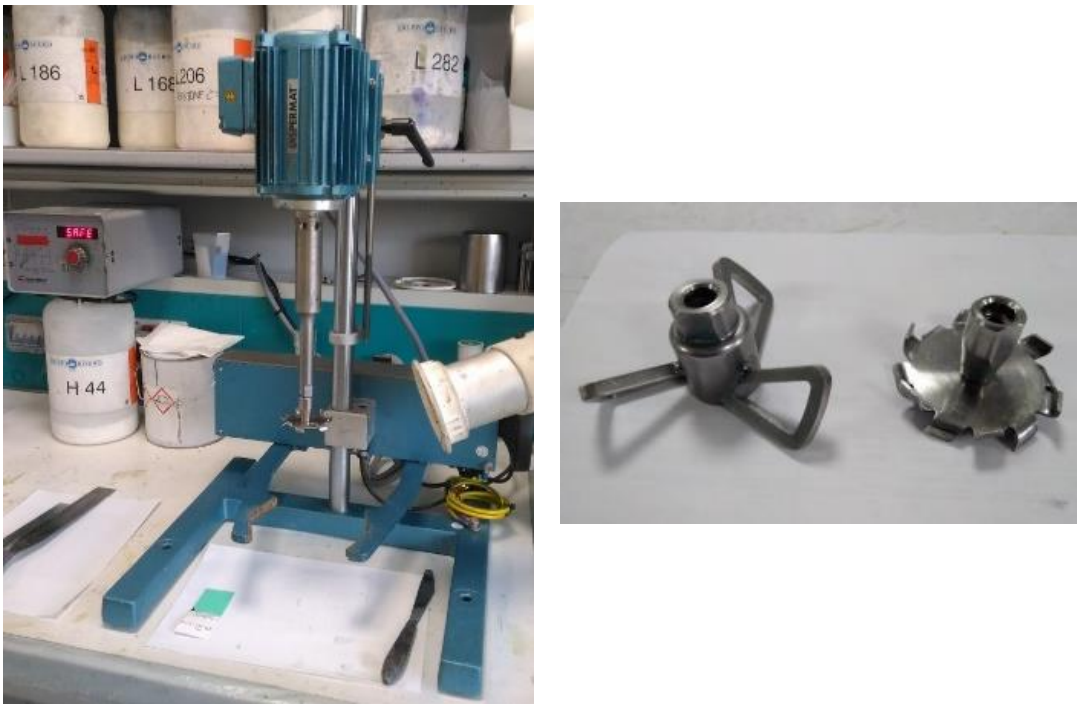

Figure 21: Dispermat LC30 220V equipped with cowles (left); butterfly and cowles (right)

To obtain a cross-linked product, the A and B components were mixed togheter in volume ratio 1:1. Then, for the laboratory samples, the mixture were placed quickly in opportune mold as a function of the tests to perfom and left to cross-link for one week at room temperature.

For the application in field, after the A and B components were mixed togheter, they are directly applied on the yacht surface.

3.2 COATING TESTS

Many tests are traditionally used in coatings industry by formulators. For instance, oil adsorption is an extenders characterisation, specific weight is tested on the single component instead pot life, hardness test and sagging test are used to characterise the cross-linked product. All of these tests are regulated by international standards (ASTM, ISO and so on). Note that in the coating and painting filed, the visual aspect to spatula, after its immersion in the can, is a traditional method that a formulators use. It is an empirical and subjective method, based on the experience of each formulator.

3.2.1 OIL ADSORPTION

The oil adsorption of powder (pigment and/or extender) is a practical measure of the surface area. It gives indirect information about shape/surface type (morphology) of particles.

The oil absorption value (OA) is obtained using linseed oil (of specified quality, with acid number about 2.8 mg KOH/g). The oil and an amount of powder are slowly worked with a spatula on a glass plate. When just enough oil has been added, a powder paste is formed (Figure 22).

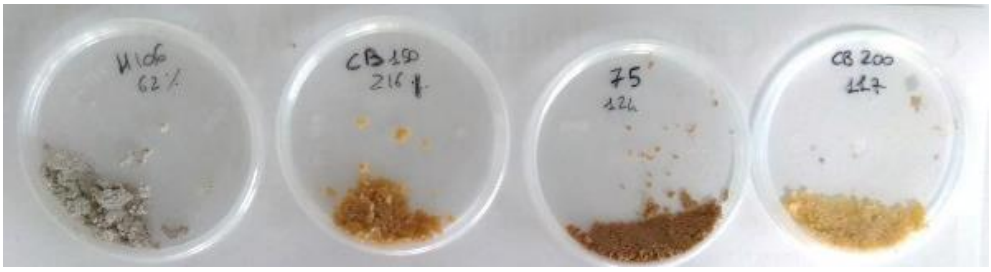

Figure 22: visual aspect of extenders with linsed oil

The value of OA is calculated as following (1), according ISO 787/5:

$$OA = \frac{g_{linsed\ oil}}{100 g_{extenders}} \quad (1)$$

The higher is the oil absorption value of the pigment/extender the higher is the material's surface area and so more resin will be required to bind it [15].

Generally, the formulators use the total adsorption value that is the sum of each extenders oil adsorption value related to its percentage in the formulation and it is expressed as percentage.

3.2.2 SPECIFIC WEIGHT

The density in the coatings context is commonly called specific weight. Normally, the coatings matrix and solvents have a specific weight of about 1 g/cm^3, whereas pigments and extenders are heavy and some of them (for example, copper or zinc compounds) have a specific weight higher than 5 g/cm^3. For this reason, products that have a high content of pigments and extenders (such as antifouling) will have high specific weight. Fillers, in particular, being applied with high thicknesses are formulated with density lower than 0.85 g/cm^3. Thus, hollow glass microspheres and alumina-silicate spheres are essential extenders. Specific weight, such as pot life and other important filler characteristics are reported in their technical data sheets (*TDS*).

To measure the specific weight a pycnometer, also called specific gravity cup, is used (Figure 23). It is made by aluminium or stainless steel, with a volume of 50 ml or 100 ml; the measurement is carried out at 20°C according to UNI EN ISO 2811-1.

Figure 23: specific gravity cup with comercial filler

3.2.3 POT LIFE

Once both components have been mixed, the application time is limited; this time restriction is called pot-life. The pot-life is the period during which the mixed system can be applied without any problems. After the pot-life time has elapsed, the mixture hardens and it is no longer applicable. Any attempt to dilute it is useless, and even harmful, as it would alter a chemical reaction that has already begun [15]. For filler, pot life is an important data that is reported in technical data sheets of products, referring to 200 g of product mixed at 20°C, according to ISO 10364. Typical pot-life for filler is around 1h, but it depends on the product type (for instance fast fillers have a pot-life of 30 min).

3.2.4 HARDNESS TEST

Hardness can be defined as a material's resistance to permanent indentation. The term can be applied also to deformation from scratching, cutting or bending.

There is a large variety of methods used for determining the substance hardness, such as Brinell, Rockwell, Shore and so on. For the polymers, hardness is generally measured using a Shore scale durometer. This manual instrument, in particular, measures the penetration resistance of material by a spring penetrator (or indenter) with pre-calibrated force. The penetrator can be in the shape of a truncated cone (Shore A scale) or a cone with a rounded tip (Shore D scale), as in Figure 24.

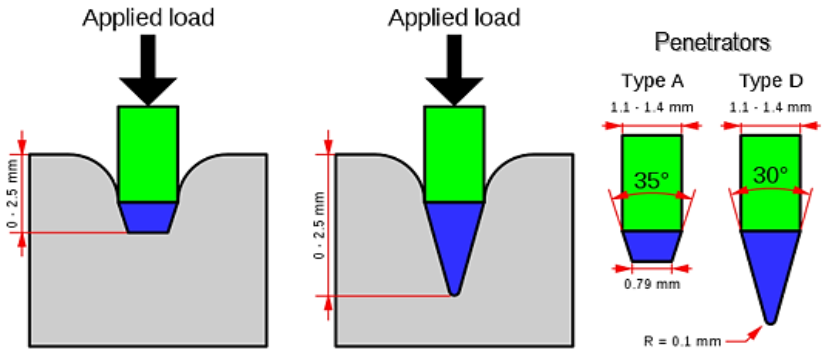

Figure 24: diagram of a durometer with different penetrators used for Shores A and D scales

The A scale is for soft materials, while the D scale is for hard ones.

For the filler measures is used Shore D durometer and, in general, this measure is reported in relation to the cross-linking time. The measurements reported are instantaneous and after 15s and they are in agreement to ASTM D-2240 and/or ISO R.868.

3.2.5 SAGGING TEST

When coatings are applied on tilted or vertical surfaces, the coatings material can flow downward (under the influence of gravity) and this effect is called sagging.

Therefore, it is necessary to perform sagging test; after mixing A and B components, the coating is applied on a metallic substrate, with a filler sagging tester, having variable thickness: 2 cm, 1 cm or 0.5 cm (Figure 25).

The metallic substrate is then held vertically and the filler is left to harden. During the cross-linking process, it is observed the eventual sagging of the product (Figure 25). This test is according to ASTM D4400.

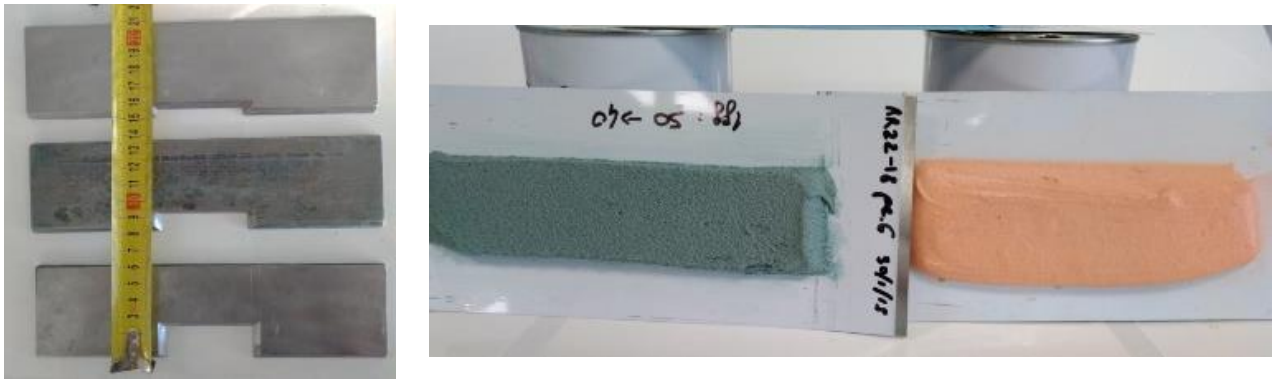

Figure 25: three filler sagging testers (left) and sagging tests of two samples (right)

3.3 INFRARED SPECTROSCOPY ANALYSIS

The IR radiation (12800-10 cm^{-1}) interaction with matter involves a variation of the molecule dipole moment following transitions between adjacent levels of vibrational energy, granted by the selection rules (IR – active molecules vibrations). These molecular vibrations can be partially broken down in simpler vibrations, such as stretching, which lead to oscillations of the bond length values around the equilibrium position and bending vibrations, which lead to oscillations of the bond angles values around the equilibrium one. Then there are complex molecular vibrations that cannot be divided into simpler ones.

Absorptions corresponding to stretching vibrations appear in any area of the spectrum (from 4000 to 400cm^{-1}), while those referred to bending and complex molecular vibrations only at wave numbers lower than 1450cm^{-1} (area of "*fingerprint*"). The interpretation of spectrum absorption peaks allows the recognition of specific bonds and therefore of functional groups.

IR can be subdivided into three regions: near-IR, mid-IR and far-IR. Specific wavenumber regions associated with these regions along with their fundamental applications are summary in Table 1.

Region	Wavelength [μm]	Wavenumber [cm^{-1}]	Main applications
Near – IR	0.78 – 2.5	12800 – 4000	Quantitative determination of solid, liquid and gaseous samples
Mid – IR	2.5 – 50	4000 – 200	Qualitative determination of complex solids, liquids and gaseous mixtures (especially organic molecules)
Far – IR	50 – 1000	200 – 10	Qualitative determination of organic and organometallic species

Table 1: wavenumber regions associated with the three IR regions along with their fundamental applications

Currently, most of the instruments for infrared spectrometry are Fourier transform with a single beam (*FTIR*).

Fourier transform infrared spectroscopy is a technique used to obtain an infrared spectrum of absorption or emission of a solid, liquid or gas. An FTIR spectrometer simultaneously collects high spectral resolution data over a wide spectral range, thanks to the Michelson interferometer that separates wavelengths not over space, but over time. This confers a significant advantage over a dispersive spectrometer, which measures intensity over a narrow range of wavelengths at a time.

The goal of any absorption spectroscopy (FTIR, UV-VIS, and so on) is to measure how a sample absorbs light at each wavelength. The most straightforward way to do this, the "dispersive spectroscopy" technique, is to send a monochromatic light beam to sample, measure how much of the light is absorbed, and repeat for each different wavelength.

Fourier transform spectroscopy is a less intuitive way to obtain the same information. Rather than shining a monochromatic beam of light at the sample, this technique shines a beam containing many frequencies of light at once, and measures how much of that beam is absorbed by the sample. Next, the beam is modified to contain a different combination of frequencies, giving a second data point. This process is repeated many times. Afterwards, a computer takes all these data and works backwards to infer what the absorption is at each wavelength. [38 - 41].

In this thesis, infrared spectroscopy (near-IR and mid-IR) was used to:

1. characterise the raw materials, A and B single components, cross-linked filler,
2. analyse the degree of cure for epoxy systems directly by analysing structural changes,
3. study the mixing ratio of the two single components.

The mixing ratio knowledge is essential for the fillers application control, indeed the mixing ratio is strictly connected to the mechanical properties and to the glass transition temperatures [29, 30]. The applicators in the shipyards generally mix the A and B components "by eye", considering the pails volumes. Therefore, it is necessary to identify a method that allows to quickly characterise the mixing ratio of the filler already applied as for the quality control. One possibility is the creation of a calibration line obtained from IR spectra of different known mixing ratios (see 9.3.2 "Infrared spectroscopy analysis").

For in-situ monitoring processes such as curing, phase separation or even ageing, the interpretation of the spectra and the assignment of the bands are critical.

Mid-infrared spectroscopy has been widely used for characterisation of organic compounds and plenty of reliable information and spectra libraries can easily be found. Both qualitative and quantitative information can be obtained by this technique, although its use in epoxy systems is quite

restricted because of the position and intensity of the oxirane ring absorptions.

Near-IR is more useful for epoxies. Near-IR spectrum covers the overtones of the strong vibrations in mid-IR and combination bands. In this range, fewer overlapped bands are observed so it has been used by several authors for monitoring the curing reaction. The intensity of the bands in this region is much lower than in the mid-range, allowing the use of thicker and undiluted samples to get good quality data.

IR spectra are collected with three different instruments: 1) FT Thermofisher Spectrometer (Thermo Fischer Scientific, USA) with OMNIC series software, 2) JASCO instrument with JASCO acquisition software both used at Department of Civil, Chemical and Environmental Engineering (University of Genoa) and 3) Spectrum One FT-IR Spectrometer (Perkin Elmer, USA) with Spectrum version 5.3 software, used at R&D centre "Riccardo Cavalleroni" (Boero Bartolomeo S.p.A).

With the first spectrometer a transmission method was used to acquire the spectra, using a KBr support (mid-IR); with the second instrument near-IR was studied with a Diffuse Reflectance accessory and a simple metal container was used to place sample; with the Spectrum One FT-IR Spectrometer (in mid-IR), attenuated total reflectance (ATR) method was used. With all the instruments, a blank spectrum was registered and then it was subtracted to the sample spectrum.

TYPICAL MID-IR SIGNALS OF A COMPONENT

There are two characteristic absorptions of the oxirane ring (A component matrix) in the range between 4000cm^{-1} and 400cm^{-1}. The first one, at 915cm^{-1}, is attributed to the C-O deformation of the oxirane group, even if in some works this band does not correspond exclusively to this deformation but also to some other unknown process [29, 30, 42]. The other band is located at 3050 cm^{-1} and is attributed to the C-H stretching of the methylene group of the epoxy ring. This band is not very useful since its intensity is low and it is also very close to the strong O-H absorptions;

Summarising the principal bands of A component are:

1. in the range 3100-3000cm^{-1}, the aromatic C-H stretching bands;
2. C-H stretching of alkyl chain, centred between 3000- 2800cm^{-1};
3. the broad band at 3500cm^{-1} assigned to O-H stretching of hydroxyl groups/ revealing the presence of dimers or high molecular weight species;
4. between 1650-1450cm^{-1} is the C-C stretching modes of aromatic rings.

TYPICAL MID-IR SIGNALS OF B COMPONENT

In the polyamide matrix, typical of filler B component, the main absorptions, in the mid-range, are stretching and deformation of NH bonds:

(1) at 3300-3500cm^{-1} (N-H stretching mode) and at 1650-1500cm^{-1} (C=O stretching band and CN/CNH vibrational mode);

(2) slightly lower than 3000cm^{-1} the C-H stretching bands of alkyl chains [29, 30].

3.4 THERMAL ANALYSIS

Since the curing process of an epoxy resin is thermally activated and temperature dependent, the thermal analysis is the most common method to monitor this process. In general, thermal analyses (*TA*) measure the material response when it is heated or cooled (or, in some cases, held isothermally). Their aim is to establish a relation between temperature and physical properties of materials.

The main techniques are: differential scanning calorimetry (*DSC*), thermogravimetric analysis (*TGA*), thermomechanical analysis (*TMA*), dynamic mechanical analysis (*DMA*).

In particular, the differential scanning calorimetry and thermogravimetric analysis has been widely used to characterise the materials. The first is used to determine cure kinetics of thermoset resins, with the analysis of glass transition temperature (*Tg*) and enthalpy of reaction (ΔH_r) variation; the second is used to determine the degradation temperature of the material [27, 29, 30, 43 - 47].

3.4.1 THERMOGRAVIMETRIC ANALYSIS (TGA)

The thermogravimetric analyser (*TGA*) or thermobalance is used to measure the sample mass as a function of a variation of temperature or time (at temperature constant). The analysis is carried out by heating rate, gas atmosphere, flow rate, crucible type. A TGA is composed of a sample pan put on a precision balance in a furnace. The sample mass is monitored during the experiment. A gas, inert or reactive, flows over the sample. It is possible to couple mass spectrometers, FT-IR spectrometers and/or GC-MS (gas chromatograph-mass spectrometers) with the TGA, in order to analyse the gas that can be developed from the sample during the analysis. Generally, it is used in the research & development to obtain knowledge about the materials composition and the thermal stability [19, 46].

A Mettler-Toledo thermal gravimetric analyser (TGA/DSC 1 Star^{e} System), reported in Figure 26a), was used. The measurements were performed on cross-linked products with a profile set from 30 to

700°C in nitrogen atmosphere (gas flow of 80 ml/min), and in the range from 700 to 900°C in oxygen atmosphere (gas flow of 80 ml/min), at heating rate of 10°C/min.

3.4.2 DIFFERENTIAL SCANNING CALORIMETRY (DSC)

The differential scanning calorimetry *(DSC)* is a thermoanalytical technique used to measure the temperature and the heat flow associated to the transition that could happen into a material at the variation of time or temperature in a controlled environment.

With DSC it can be obtained qualitative and quantitative information related to physical or chemical change in the material, such as melting, crystallisation, glass transition and thermal history in general. In particular, endothermic and exothermic processes and variation of thermal capacity are measured.

The sample is placed into a furnace with a standard reference, which generally is an empty sample holder in a controlled atmosphere, usually nitrogen, in order to avoid oxidation processes. With the use of thermocouples, resistances and refrigerate units, a variation in the temperature is imposed to both the sample and the reference. In the system are also present sensors to evaluate the differences in the thermal resistance, heat capacity and heating rate for both the sample and the reference, that allow a correct evaluation of the difference in temperature and thus in the heat flow, between them [19, 46, 47].

A Mettler-Toledo differential scanning calorimeter (Model DSC 1 Star^e System), reported in Figure 26b), was used. The measurements were performed only on cross-linked products with a profile set from −10°C to 160°C, at heating rate of 10°C/min. To study the curing process the measurements were performed with a profile set from −100°C to 280°C, at heating rate of 20°C/min.

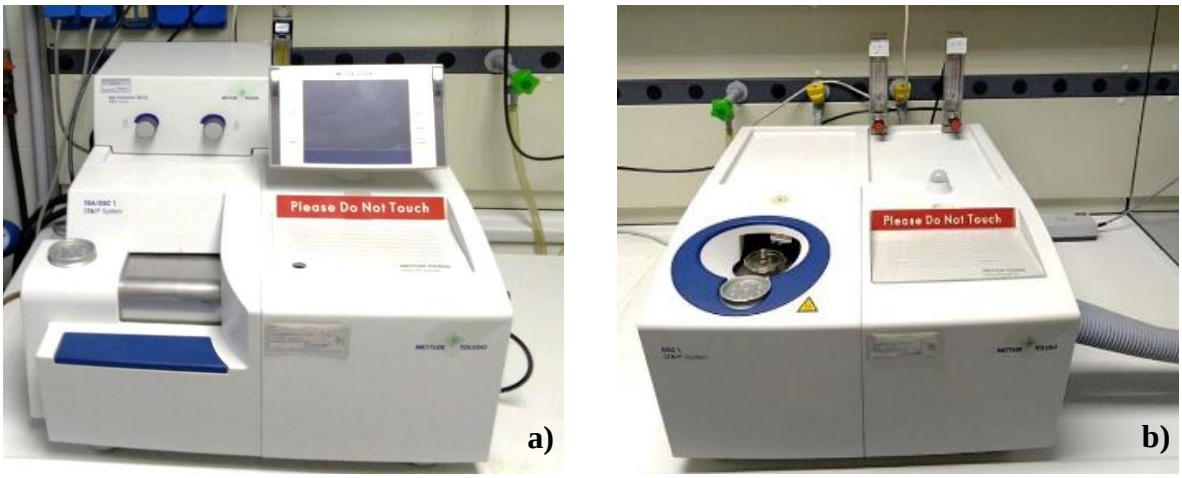

Figure 26: a) TGA/DSC 1 Star^e System (Mettler-Toledo), b) Model DSC 1 Star^e System (Mettler-Toledo)

3.5 RHEOLOGICAL ANALYSIS

The importance of understanding coatings rheology is paramount to the successful utilization of such products to a degree matched by few other areas. Experienced formulators say that more than half the cost of new product development is consumed in “getting the rheology right" [10, 13, 15].

The material viscosity is one of the properties that can be obtained from rheological measurements; however, viscosity is not a discrete measurement and depends on the conditions of measurement (e.g. shear rate). This is particularly significant for materials such as paints since are often exposed to a variety of different shear rates (Figure 27) and hence may result in different apparent viscosities.

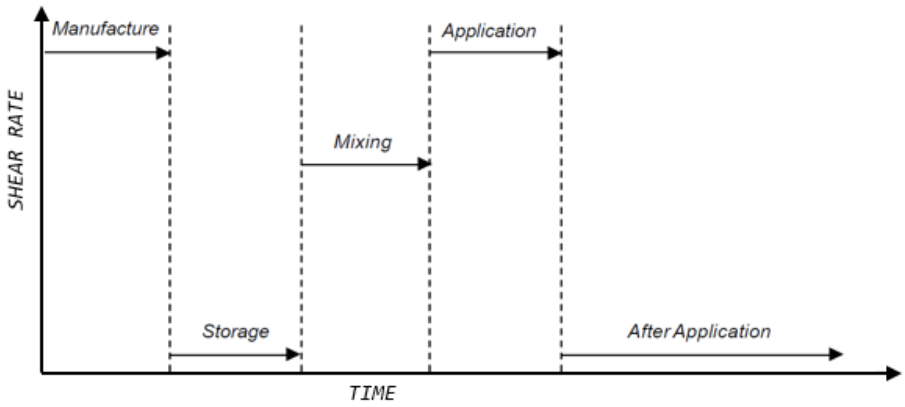

Figure 27: shear rate profile over the lifespan of a coating

Rheology is the science of deformation and flow. All forms of shear behaviour can be viewed between two extremes: the ideal viscous liquids flow and the ideal elastic solids deformation. Ideal fluids, such as liquids and gases, deform irreversibly; the energy required for the deformation is dissipated within the fluid (as heat) and cannot be recovered by simply removing the applied stress.

On the contrary, ideal solids only deform elastically: when the stress is removed they return to their initial state and the deformation energy is fully recovered.

The real materials behaviour, such as coatings, is based on the combination of both ideal viscous liquids and ideal elastic solids, which results in the so called viscoelastic materials.

The rheological measurements allow to evaluate the material viscoelastic proprieties, such as the viscosity and viscoelastic moduli (i.e. elastic modulus G’ and loss modulus G’’). Today, they can be determined by several different types of measurement, the mainly are rotational and oscillatory.

One of the simplest and most used theoretical representation to describe the rheological response of a material is considering it confined between two parallel plates (Figure 28); whereas the bottom plate is fixed and the upper one is able to slip.

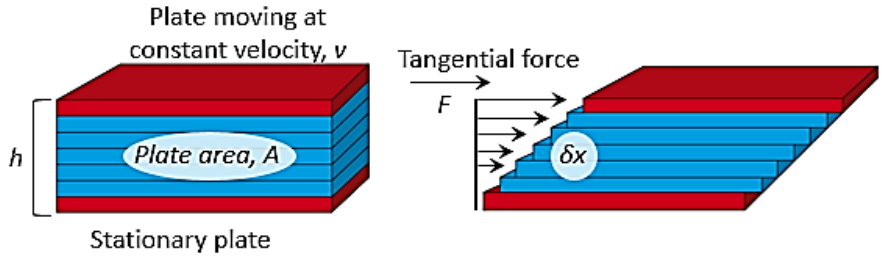

Figure 28: schematic representation of parallel plate

When subjected to a tangential force F (N), the upper plate, posed at a fixed distance h (m) from the bottom plate and with a certain surface area A (m^2) slips in one direction at a certain speed v (m/s), creating/inducing a in laminar flow of the thin materials layers between the two plates. The resulting velocity depends on the internal friction (resistance) between the layers and tends to zero close to the lower plate.

This simple model, allow to obtain the fundamental parameters involved into a rheological measurement. In particular, the shear stress, τ (2), the shear strain, γ (3) and the shear rate $\dot{\gamma}$ (4) can be defined as following:

$$\tau = \frac{F}{A} \tag{2}$$

$$\gamma = \frac{x}{h} \tag{3}$$

where x is the displacement of the upper plate.

The shear stress is expressed in Pascal (Pa), instead the shear strain is dimensionless (or more often expressed as strain percentage).

However, in rheological studies, the speed at which a deformation is applied has a fundamental role; thus instead of the shear strain is better to use the cinematic parameters, shear rate, expressed in s^{-1}:

$$\dot{\gamma} = \frac{1}{h}\frac{\delta x}{dt} = \frac{\delta \gamma}{\delta t} \tag{4}$$

From the concept of shear stress and shear rate, above mentioned, the viscosity ($Pa \cdot s$) can be defined as the ratio between the shear stress over the shear rate (Newton – Stockes law):

$$\eta = \frac{\tau}{\dot{\gamma}} \tag{5}$$

It is easy to image that the higher the viscosity the higher is the force necessary to force the flowing of a material. Moreover, from this law it is possible to appreciate the linear correlation between the stress and the shear rate; it means that, at a fixed temperature, the graphical representation of the shear stress versus the shear rate (flow curve) is a straight line and the viscosity does not depend on the applied shear rate (Newtonian fluid). Despite this behaviour is the simplest rheological response, it allows to describe with high accuracy many different systems (e.g. polymer solutions and polymer melts).

However, when the correlation between the shear stress and the shear rate is non-linear the fluid is a non-Newtonian or complex fluid; in this case the viscosity is not constant, but is a function of the shear rate.

The non-Newtonian behaviour can be generally classified into three main categories of time-dependent viscosity profiles already mentioned (see 2.3.1 “Rheological modifiers”): shear thinning (pseudoplastic), shear thickening, and Bingham fluids (yield stress). Despite the last one is similar to the shear thinning behaviour, it is characterised by the presence of a yield point, corresponding to the load at which the material starts to flow (Figure 29).

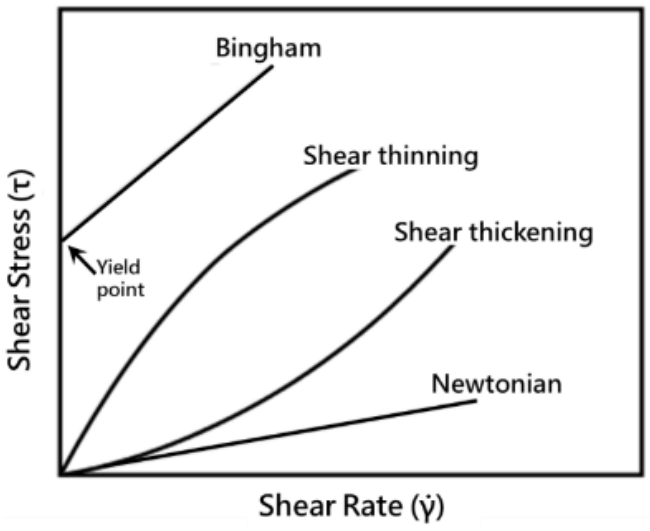

Figure 29: viscosity curves of different rheological behaviour

In order to have a deeper knowledge of materials rheological properties, tests in oscillatory mode are also required. In this kind of measurements, the material undergoes to an oscillatory stress applied by

a sinusoidal displacement of the movable pan of the geometry used in the test. The material is thus deformed following a sinusoidal law:

$$\gamma = \gamma_0 sin(\omega t) \quad (6)$$

where γ_0 is the applied maximum deformation and ω is the frequency of the oscillation.

Due to the periodic deformation action, the material returns a tangential stress (σ) which can be expressed as reported in (7) once the system has reached a stationary condition.

Since the applied deformation and the recollected stress have the same frequency, but out of phase, φ is defined as the phase between the two. For viscoelastic materials, the tangential stress can be defined as the sum of its two components, the viscous and the elastic one, as expressed in (8).

$$\sigma = \sigma_0 sin(\omega t + \varphi) \quad (7)$$

$$\sigma = \sigma_0 \cos\varphi \sin(\omega t) + \sigma_0 sen\, \varphi \cos(\omega t) \quad (8)$$

By dividing for the maximum deformation (γ_0), (8) can be rewritten as following:

$$\frac{\sigma}{\gamma_0} = G' sin(\omega t) + G'' \cos(\omega t) \quad (9)$$

The two parameters introduced, *G'* and *G''*, have the dimension of a modulus and are the storage and the loss modulus, respectively; G' represents the elastic (conservative) contribution to the deformation and G'' the viscous (dissipative) contribution.

The complex sum of the elastic and viscous components of the material is the so-called complex shear modulus *G** (10) and it describes the entire viscoelastic behaviour of the material.

$$G^* = G' + iG'' \quad (10)$$

Another important parameter, which can be defined, is the loss factor (*tanδ*), sometimes called damping factor. It can be defined as the ratio of the two components of the viscoelastic behaviour (10). For the ideally elastic behaviour δ is 0°, while for the ideally viscous behaviour is 90° [48 - 52].

$$\tan \delta = \frac{G''}{G'} \tag{11}$$

All rheological measurements were performed with Anton Paar MCR 102 rheometer (Anton Paar, GmbH, Germany) in combination with a Peltier temperature control unit, equipped with 25 mm diameter parallel plate geometry (PP25), as shown in Figure 30. All measurements were performed with a gap distance of 1 mm. The data were collected and analysed using RheoCompass s1.19 software.

Figure 30: rheometer Anton Paar MCR 102

3.5.1 VISCOSITY TEST

The fluid viscous behaviour is generally reported with a viscosity curve in a double logarithmic scale (viscosity *vs.* shear rate) instead of a flow curve (shear stress *vs.* shear rate), due to the easier interpretation of the data.

Another important rheological parameter is the zero-shear viscosity, i.e. the viscosity extrapolated at zero-shear. In literature, many models (such as Carreau, Carreau-Yasuda, Cross…) allow to take into account the viscosity variation as a function of the shear rate and to extrapolate the zero-shear rate viscosity. In this thesis, the viscosity curves were modelled with Carreau equation, as reported below:

$$\frac{\eta - \eta_\infty}{\eta_0 - \eta_\infty} = \frac{1}{[1 + (K\dot{\gamma})^2]^{m/2}} \quad (12)$$

where η is the viscosity, η_0 and η_∞ are the zero and infinite shear viscosity, $\dot{\gamma}$ is the shear rate, K is the relaxation time and m is a flow behaviour index [51 - 54].

In this thesis, viscosity tests were carried out in order to obtain information about the coatings behaviour over a wide range of shear rates (or shear stresses).

The viscosity curves were acquired at 25°C, with a shear rate ($\dot{\gamma}$) between 0.01s^{-1} and 10s^{-1}, collecting 25 points.

3.5.2 RECOVERY TEST

Recovery tests can be applied to simulate the deconstruction and reformation of the coatings network structure; indeed, after their application, coatings should regenerate their structure (recovery process) in the desired time. This recovery capacity is an important property to consider and it is, usually, defined as thixotropy, which is the time-dependent viscosity variation under application of a certain shear.

Thixotropy is related to the time-dependent microstructural rearrangements occurring in a shear thinning fluid subsequently to the application of a step variation in the applied shear (Figure 31).

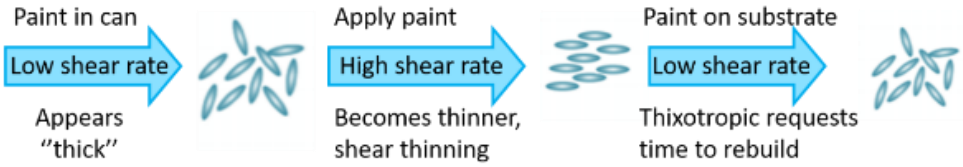

Figure 31: microstructural variations occurring in a dispersion of irregularly shaped particles in response to variable shear

A good practical example of a thixotropic material is represented by coatings. They should be thick in the can when stored for long periods to prevent separation, whereas they should be easily workable showing a strong shear thinning behaviour when applied. Most often, their structure does not rebuild instantaneously on ceasing stirring, but they take a certain time.

Strictly connected to thixotropy are the levelling and sagging phenomena once the coatings are applied to the substrate; indeed, they must have a low enough viscosity at the application shear rate to be homogeneously distributed with a roller or a brush (levelling), but should recover their viscosity in a controlled manner to avoid sagging once applied.

The best way to evaluate and quantify thixotropy is by using a three steps shear test (Figure 32).

A low shear rate is applied until a steady viscosity value is attained (first step) in order to evaluate the structure at rest, thus emulating the coating state in the can. The shear rate is then increased (second step) to a value ideally corresponding to the shear rate of interest with the aim to evaluate the coatings behaviour in the structural deconstruction phase, simulating the application process (e.g. brushing or spatula application). Finally, the shear rate is dropped back to the initial low value (third step) to allow the structural reformation over time, simulating the coatings behaviour after application [50 - 52, 55].

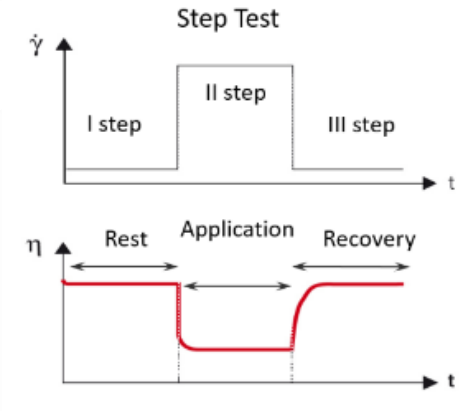

Figure 32: step test profile with three intervals

Speaking about a generic coating, the recovery process time should be not too slow to prevent sagging, Figure 33a, and not too fast to allow for good levelling, Figure 33b.

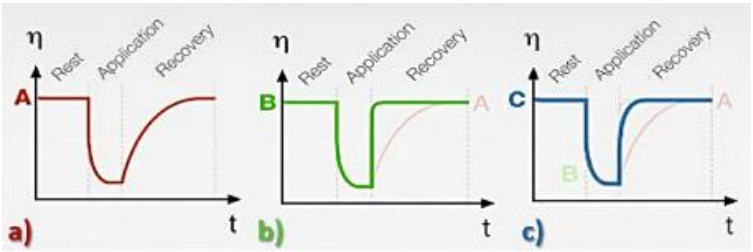

Figure 33: evaluation of the structural regeneration: a) sagging, b) levelling trouble and c) the desired coatings

In the case of fillers, a good levelling is not required and consequently the faster is the recovery the higher is the applicable thickness.

To compare the thixotropic behaviour of the samples, for the first time, new indices were used: the recovery percentage after 30s from the starting of the third interval (12) and the total recovery percentage (13)

$$Rec_{30s}\ (\%) = \frac{\eta_i}{\eta_{30s}} \cdot 100 \quad (13)$$

where η_i is initial viscosity, while η_{30s} is the viscosity after 30s from the starting of the third interval. Total recovery percentage was calculated by the ratio between η_i and the final viscosity (η_f) in the third interval:

$$Rec_{tot}\ (\%) = \frac{\eta_i}{\eta_f} \cdot 100 \quad (14)$$

The recovery curves were acquired at 25°C, in three steps: 1) fixed $\dot{\gamma}$ at $0.01s^{-1}$ with 5 points measured every 100s; 2) fixed $\dot{\gamma}$ at $5s^{-1}$ with 100 points measured every 0.1s; 3) fixed $\dot{\gamma}$ at $0.01s^{-1}$ with 500 points measured every 0.1s, until 800s, and subsequently 4 points measured every 25s. A total of 609 points were collected.

3.5.3 AMPLITUDE SWEEP TEST

Oscillatory tests have important advantages being able to: characterise both the viscous and the elastic response of the material behaviour, so that the complete viscoelastic behaviour can be described. On the contrary, rotational tests only provide insights into the viscous response of the materials and do not give any information about its elastic behaviour.

Performing oscillatory measurements on a rotational rheometer is the most common approach to investigate material linear viscoelastic properties, which are related to the intact microstructure under small stresses. In this case, it is of extremely importance to perform such measurements in the linear viscoelastic region, *LVER*, where the viscoelastic moduli do not depend on the applied stress or strain. In the LVER, the applied stress is insufficient to cause the structural breakdown and consequently the microstructural properties are measured. This region can be determined by an amplitude sweep test, observing the point at which the structure begins to yield [50 - 52, 56, 57]; this corresponds to the point at which G' and G" become stress or strain dependent. In amplitude sweep tests, the frequency is fixed whereas the deformation amplitude is varied.

The storage and loss modulus curves were acquired at 25°C, with a variable amplitude between 0.001% and 10%, and at a constant frequency of 1Hz, collecting 25 points.

3.6 MECHANICAL ANALYSIS

Among the several filler requirements, mechanical properties represent a fundamental aspect taking into account that the perfect shape of the boat must be maintained and that the fillers must withstand the deformations associated with both thermal variations, mechanical stresses and wave motion (see "Chapter 2: Fillers"). Therefore, mechanical characterisation of fillers it is clearly necessary. Torsional oscillatory tests, belonging to the dynamic mechanical thermoanalysis (*DMTA*), tensile tests, three-point bending tests and compression were carried out.

3.6.1 DYNAMIC MECHANICAL THERMOANALYSIS (DMTA)

Dynamic mechanical thermoanalysis is a characterisation technique that measures the mechanical properties of materials under periodic stress as a function of the frequency, the deformation amplitude and the temperature. Despite this type of analysis can be performed in torsion, tensile, bending or compression mode, torsional tests were used in this thesis.

Both the frequency and the amplitude are kept at a constant value, so that constant dynamic-mechanical shear conditions are pre-set. The temperature is varied in a specific range at a fixed heating/cooling rate and the rheological parameters (storage modulus, loss modulus and loss factor) are determined.

Despite the dynamic mechanical thermo analysis mainly supplies information about transition, it also allows the characterisation of bulk properties directly affecting the material performance [51, 52, 58].

Compared to the uniaxial tensile tests carried out in this thesis, DTMA provided a continuous value of sample moduli as a function of the temperature, thus giving a better understanding of the temperature dependence of the tested materials.

Dynamic-mechanical measurements were performed with Anton Paar MCR 301 rheometer (Anton Paar, GmbH, Germany) in combination with a climatic chamber, CTD 450, using a SRF 12 geometry (Figure 34). The data were collected and analysed using RheoCompass s1.19 software.

The measurements were carried out on specimens with the following sizes: thickness of 5 mm, width of 10 mm and length of 40 mm.

The LVER was determined through amplitude sweep tests performed at 25°C, with variable amplitude, between 0.0001% and 0.1%, and at a constant frequency of 1Hz, collecting 31 points.

The curves were acquired with a fixed amplitude, as a function of sample LVER, with a fixed frequency of 1Hz and with the normal force set at -1N. The measurements were carried out in the temperature range between 10 and 70°C, collecting 31 points.

Figure 34: rheometer Anton Paar MCR 301 with SRF 12 geometry and filler sample

3.6.2 UNIAXIAL TESTS

Mechanical properties are commonly obtained through tensile test, three-point bending test and compression test, in which the force is in one direction, the so-called uniaxial tests. Different commercial machines for mechanical characterisation exist, in this thesis, universal testing machines are used and they allow to stretch (tensile), bend (flexural), squash (compression) a sample until it breaks.

The mechanical strength can be classified, in terms of the direction in which strain is induced and second, in terms of the speed at which the force is applied.

The tensile test, three-point bending test and compression test were carried out with the dynamometers Instron 3365 (Instron, Norwood, MA), used at R&D centre "Riccardo Cavalleroni" (Boero Bartolomeo S.p.A), and Instron 5566 (Instron, Norwood, MA) equipped with a climatic chamber (Figure 35) used at Research Institutes of Sweden (RISE). All measurements were performed on the cross-linked products.

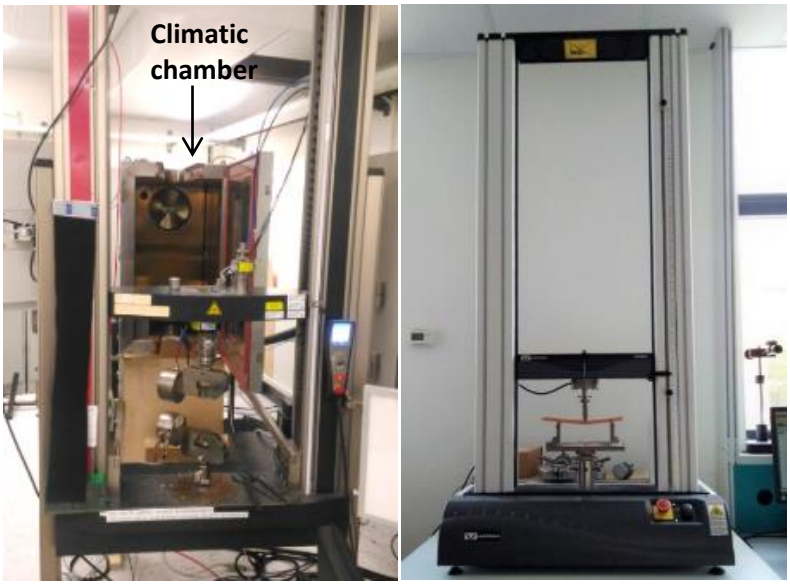

Figure 35: universal testing machines; Instron 5566 equipped with a climatic chamber (left) and Instron 3365 with a sample (right)

TENSILE TEST

Tensile strength, as well as elastic modulus, are important parameters of engineering materials used in structures and mechanical devices.

Tensile tests measure the force required to break a specimen and the extent to which the specimen elongates before the breaking point. Tensile tests produce a stress-strain diagram, which is used to determine tensile modulus. Since the physical properties of materials vary depend on the temperature, it is useful to make the tests at different temperatures in order to evaluate the behaviour of the sample in different conditions of use. Specimens, with a specific shape, "dog bone" (see Figure 36), are placed between the grips of the machine and pulled until failure [15]. The test speed is determined by the ASTM D638.

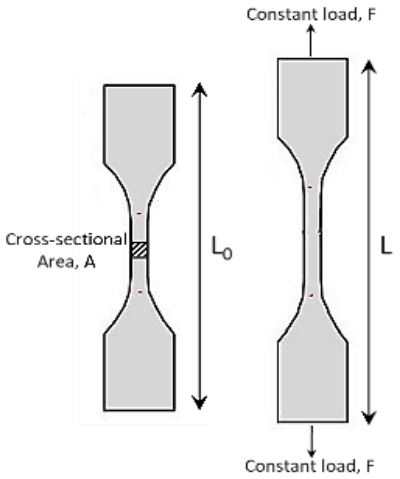

Figure 36:"dog bone" before (left) and after (right) tensile test

THREE-POINT BENDING TEST

This test measures the force required to bend a specimen under 3-points loading conditions (see Figure 37).

The data are often used to select materials that will support loads without flexing. Flexural modulus is used as an indication of a material stiffness when flexed. Similarly, to the tensile test, it is useful to test the specimens at different temperature to emulate the environmental conditions. In this case, the specimen is parallelepiped.

Most commonly, the specimen is placed on a support and the load is applied to the centre producing three-point bending with an imposed rate. The parameters for this test are the support span and the speed of the loading. These parameters are based on the specimen thickness, and are defined by ASTM D790-03.

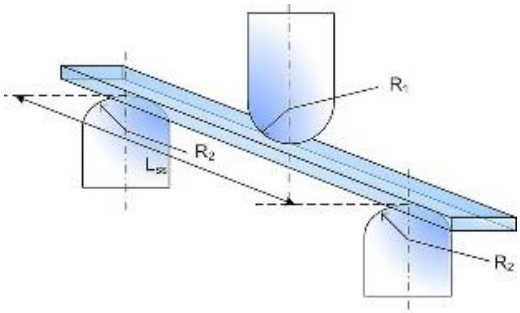

Figure 37: scheme of three-point bending test

COMPRESSION TESTS

The compressive strength is calculated as the stress required to break or deform the specimen to a given percentage of its height. Compressive strength data may be useful in specifications for distinguishing the behaviour of the material under applied crushing loads, and are typically conducted by applying compressive pressure to a test specimen (usually with cuboid or cylindrical geometry, Figure 38). Such tests are performed according to ASTM D695 and/or ISO 604.

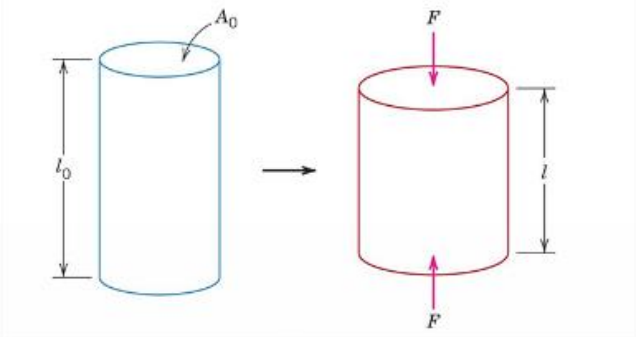

Figure 38: sample before (left) and after (right) compression test

From the test, a stress-strain diagram was obtained and elastic limit, proportional limit, yield point, yield strength, and compressive strength were calculated.

3.7 MORPHOLOGICAL CHARACTERISATION

Scanning electron microscopy, *SEM*, is a technique based on the interaction between a specimen and an accelerated electrons beam. SEM is made up by an electron column, where the electron beam is accelerated, focalised and scanned on the sample. To generate the electrons, called "primary electrons", exist two main methodologies: the field emission or thermionic effect. If the electrons are generated by field emission, the source is usually a wire of a tungsten (W) single crystal fashioned into a sharp point and welded with hairpin. If the "primary electrons" are thermionically generated, the source, generally, is a tungsten filament. In to the column there are collimators and magnetic lenses used to accelerate and direct the beam on the sample. To obtain images, the electron beam is focalised into a fine probe, which is scanned across the surface of the specimen with the help of scanning coils.

Each point on the sample, hit by the accelerated primary electrons, emits a signal in the form of electromagnetic radiation. The beam goes down into the specimen and the interaction volume is a function of the energy of the beam itself (see Figure 39).

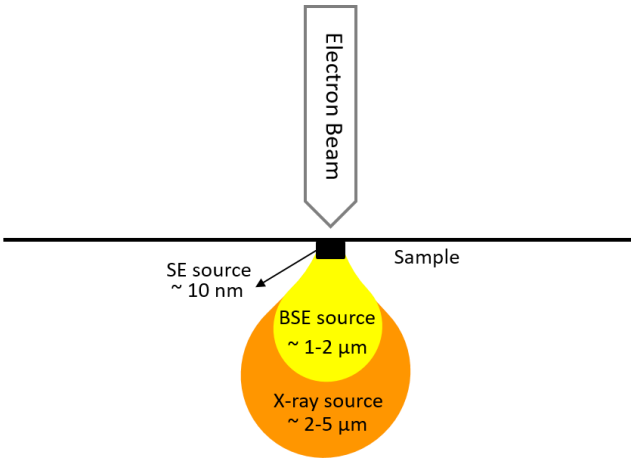

Figure 39: different signals and their interaction volume of the interaction zone

The principal signals are:

- ✓ Secondary electrons (*SE*): are produced by anelastic scattering between the primary electrons and the valence electrons of the sample atoms. These low energy electrons (< 50 eV) are

ejected from their orbitals and detected. Only the secondary electrons generated at the sample top surface (1-10 nm depth) are emitted outside. Therefore, topological information can be obtained.

- ✓ Back-scattered electrons (*BSE*): are high energy electrons back scattered out of the sample by elastic interactions of the primary beam with specimen atoms. Because heavy elements (high atomic number) backscatter electrons stronger than light elements, they appear brighter in the image. Thus, back-scattered electrons are used to generate images with contrast between areas with different chemical compositions ("composition contrast"). The number of phases in the sample is identified with this signal.
- ✓ X-ray: are generated as a result of the inelastic scattering interactions core vacancies. To fill these vacancies, electrons from higher energy levels fall down emitting typical X-rays. The X-rays are characteristic for each element and can be used for qualitative and quantitative analysis, discriminating them based on their energy, by means of an Energy Dispersive X-ray Spectroscopy (*EDXS)* probe.

These signals are collected by specific detectors, amplified and displayed on a computer [59, 60].

In this thesis, scanning electron microscopy was used to evaluate the powder raw materials and filler morphology, in particular to evaluate the adhesion between matrix and extenders.

The analyses were carried out with two different instruments both equipped with an Oxford INCA energy-dispersive X-ray microanalysis (EDX): 1) Zeiss Supra 40VP scanning electron microscope, SEM, (Carl Zeiss, AG, Germany), used at RISE, on extenders and on cross-linked samples and 2) Zeiss Supra 40 field emission scanning electron microscope, used at Department of chemistry and industrial chemistry (University of Genoa) only on cross-linked samples. With the first one some samples were thinly coated with gold and palladium (0,150 kÅ Au/Pd) using physical vapour deposition (Precision Etching Coating System, Model 682, Gatan Inc.) to obtain good conductivity. The cross-linked products were broken and analysed along the sample section.

Other samples (powders) were analysed in Low Vacuum mode (LVSEM) and so they were not coated. With the second SEM samples were thinly sputter-coated with carbon using a Polaron E5100 sputter coater.

Manual image analysis was carried out on digitalised SEM images, using the image analysis open source software ImageJ 1.51 to measure of particles size, distance between matrix and extenders and so on.

3.8 UNIVARIATE AND MULTIVARIATE ANALYSES

3.8.1 UNIVARIATE ANALYSIS

Univariate analysis is a well-known technique, in this paragraph only some basic concepts are reported, useful for understanding the results reported in the experimental part.

The analysis of variance (*ANOVA*) is a statistical data analysis technique that allows verifying if the means of two or more populations are significantly different. To do this, it is used the null hypothesis (H_0): it asserts all the means of different groups are equal to each other and the differences, if present, are due to the case. From the mathematical point of view, if μ is the groups mean and k is the number of groups, H_0 is:

$$H_0: \mu_1 = \mu_2 = \ldots = \mu_k \tag{15}$$

If H_0 is not correct, then exist at least one mean different from the others. This hypothesis is called alternative hypothesis (H_1) and mathematically can be defined as following:

$$H_1: \mu_j \neq \mu_i = \ldots = \mu_k \tag{16}$$

where μ_j and μ_i are the means of the groups j and i respectively ($i,j = 1, 2\ldots, k$). To validate or reject H_0, a Fisher test (*F test*), or analysis of one-factor variance, must be performed. It consists in the ratio between the variance among the groups and the variance within the groups and it follows the Fisher distribution. Mathematically it can be expressed as:

$$F = \frac{\frac{SSB}{df-1}}{\frac{SSW}{N-df}} \tag{17}$$

where *SSB* (Sum of Squared Between) is the sum of variance between the means of different groups and *SSW* (Sum of Squared Within) is the sum of variance within the means of different groups. *df-1* are the degrees of freedom related to SSB and *N-df* are the degrees of freedom related to SSW, with *N* as number of observation.

The null hypothesis is rejected when F is major of an F critical value (F_c) tabulated and related to degrees of freedom (*df*) and the significance level (α).

The significance level is the probability of rejecting the null hypothesis when it is true. For example, a significance level of 0.05 indicates a 5% risk of concluding that a difference exists when there is no actual difference. Lower significance levels indicate that stronger evidences are needed before rejecting the null hypothesis.

A p-value is the probability to obtain the effect observed in your sample, or larger, if the null hypothesis is true for the populations. P-values are calculated based on sample data and under the assumption that the null hypothesis is true. Lower p-values indicate greater evidence against the null hypothesis.

In other words, to accept or reject H_0 it is necessary to compare the obtained p-value with the significance level chosen. If the p-value is less than the significance level, the null hypothesis can be rejected and it is possible to conclude that the effect is statistically significant.

Once the null hypothesis is rejected, it is necessary to perform the post hoc test. These tests allow identifying which are the different means, verifying the equality of all possible comparisons in pairs. In each comparison, it is possible to consider the Bonferroni's inequality [61, 62]. It considers a critical reference value related to a fraction (equal to total number of comparison necessary) of significance level. Using the 5% error rate from example, two tests would yield an error rate of 0.025 or (0.05/2) while four tests would have an error rate of 0.0125 or (0.05/4).

The software used to perform the univariate analysis was Excel 2013.

3.8.2 MULTIVARIATE ANALYSIS

According to the International Chemometrics Society, chemometrics is “the chemical discipline that uses mathematical and statistical methods to design or select optimal procedures and experiments and to provide maximum chemical information by analysing chemical data”.

As a matter of fact, chemometric tools are multidisciplinary and can be used for different purposes such as: in the design of experiments; in selection and optimization of analytical conditions; in quality control of series of measurements; and in data processing, including sample correction and compression, calibration, pattern recognition and classification.

The main objectives of chemometrics are the optimization of analytical chemistry methods through the technique of experimental design and the extraction of maximum useful information from a set of multivariate data. In this case, one of the main strategy is the exploration of data through Principal

Component Analysis (*PCA*). Principal component analysis (PCA) is a statistical procedure that uses an orthogonal transformation to convert a set of observations of possibly correlated variables into a set of values of linearly uncorrelated variables called principal components. The number of principal components is less than or equal to the number of original variables.

In particular, in this thesis PCA is used to evaluate the rheological data from a statistical point of view. A single rheological measure is formed by more data (for instances, more viscosities measured at different shear rate). These data are not independent between them, but are rather a correlated dataset. The PCA is useful to simplify this correlated multidimensional dataset to a new uncorrelated dataset.

Mathematically, a multivariate dataset can be represented as a matrix *X*, with dimension $O_{(rows)}xV_{(column)}$. The rows represent the samples (objects) and the columns the variables, so the matrix can be written as $X_{o,v}$ (with *o* varies between 1 and O and *v* between 1 and V). The principal components ($s_{o,p}$) are calculated as linear combination of the original variables as follows:

$$s_{o,1} = x_{o,1} \cdot l_{1,1} + x_{o,2} \cdot l_{2,1} + x_{o,3} \cdot l_{3,1} + \ldots + x_{o,v} \cdot l_{v,1} = x_{o,v} \cdot l_{v,1} \quad (18)$$

$$s_{o,2} = x_{o,1} \cdot l_{1,2} + x_{o,2} \cdot l_{2,2} + x_{o,3} \cdot l_{3,2} + \ldots + x_{o,v} \cdot l_{v,2} = x_{o,v} \cdot l_{v,2} \quad (19)$$

$$S_{O,1} = X_{O,V} \cdot l_{V,1} \qquad S_{O,2} = X_{O,V} \cdot l_{V,2} \quad (20)$$

where only the first two principal component were considered.

$S_{O,1}$ e $S_{O,2}$ are two new vectors resulting from the product of the original data ($X_{O,V}$) and the relative coefficients $l_{V,1}$, $l_{V,2}$.

For all *PCs* (Principal Components)

$$S_{O,P} = X_{O,V} \cdot L_{V,P} \quad (21)$$

where $S_{O,P}$ is called scores matrix and $L_{V,P}$ is called loadings matrix.

The PCs can be considered projections of the original data matrix, ***X*,** onto the scores, *S.*

Before running PCA, typically data are first pre-processed to normalize their mean and variance. The data mean is set to zero with a “mean-centred” operation and each coordinate is rescaled to have unit

variance. This operation ensures that different attributes are all treated on the same "scale". The combination of the two process is called "Autoscaling" or "unit variance scaling".

Scores are expressed in the same unit of the original data when data are mean-centred, while they are dimensionless when data are autoscaled. Scores can assume any value but their mean is equal to zero. Loadings are dimensionless and normalized; therefore they can assume values from -1 to 1.

From a geometric point of view, understanding the transformation of the original variables into the main components is easier. Considering the two-dimensional space, the PCA is a rotation process of the original variables (V_1 and V_2) in order to identify new directions (PC_1 and PC_2) that show the maximum variance; these new directions are the principal components as shown in Figure 40.

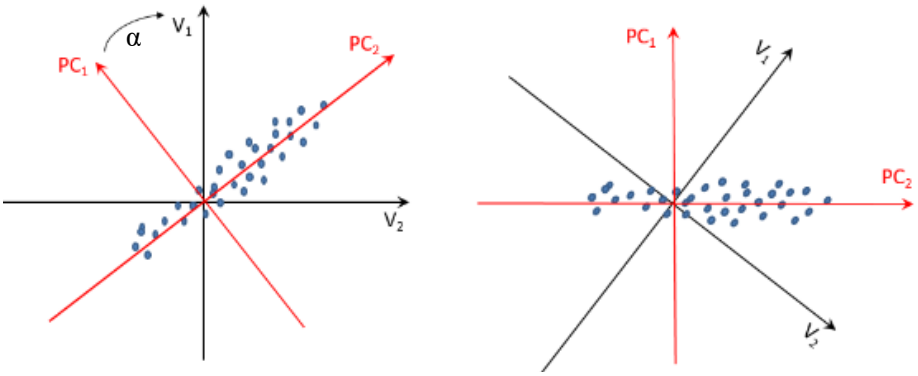

Figure 40: orthogonal transformation to convert the original variables (V_1 and V_2) into principal components

They are ranked by decreasing variance: the variable with greater variance is projected on the first axis (PC_1 – the first principal component), the second on the second axis (PC_2 – the second principal component), orthogonal to the previous one, with null covariance with PC_1, and so on. The reduction of the complexity occurs only by analyzing the main ones between the new variables [63, 64].

The scores are the coordinates in the new variables and the loadings are the cosine of the angle (α, see Figure 40) necessary to position the new axes (PC_1 and PC_2).

Interpretation of the results of a PCA is usually carried out by visualization of the component scores and loadings plots.

The score plot allows evaluating the behaviour of the data in the new orthogonal space defined by the principal components highlighting similarities and differences among samples. The aim is to identify outliers, trends and groupings or the occurrence of particular regularities and distributions among samples.

The loading plot, instead, allows understanding the importance of each original variable in constructing the components and the type of correlation (positive or negative) between all of them.

The loading plot could be drawn as a scatter plot, in which the axes are the new components, or as a line plot, in which loadings are plotted against the original variables (continuous variables, e.g. wavelengths). When variables are in the same area of the plot, they are positively correlated; vice versa, variables located in opposite quarters are negatively correlated. The evaluation is limited to the components considered in the plot and is more significant if the explained variance of the component is relevant.

In some cases, PCA was used after low-level data fusion. With this method signals coming from rheological tests are simply concatenated sample-wise into a single matrix that has as many rows as samples analysed (for instance for eight samples triplicated, 24 rows) and as many columns as variables (viscosity tests, recovery tests and amplitude sweep tests data points) measured. Since multivariate analysis is scale dependent, data from single techniques are usually pre-processed in order to compensating for the different measuring scales and variability of each technique, to prevent one block (recovery test with 609 variables) from being dominant on the others (viscosity curves and amplitude sweep test with 25 variables). In this sense, each data block is weighted separately by a modified column autoscaling (block-scaling), in which each variable is normalized by subtracting the average value of the corresponding column and by dividing by the product between the standard deviation of the column and the square root of the number of variables of the block.

Fisher Weight (FW) [65] has been used in some analysis to compare the degree of separation within a group of data. It was calculated for pairs of data groups (*m* and *n*). The Fisher weight is defined, for a variable *j*, as the ratio between inter-group sample variance and the mean of intra-group sample variances, rearrangeable as:

$$FW_{j,m,n} = \frac{\left(\overline{x}_{m,j} - \overline{x}_{n,j}\right)^2}{\frac{\sum_{k=1}^{N_m}\left(x_{k,m,j} - \overline{x}_{m,j}\right)^2}{N_m} + \frac{\sum_{k=1}^{N_n}\left(x_{k,n,j} - \overline{x}_{n,j}\right)^2}{N_n}} \tag{22}$$

in which N_m and N_n represent the number of data points in groups *m* and *n*, respectively.

In this way, not only the distance between the centroids of the two groups are considered, but also the dispersion within each group. FW values lower than 1 generally indicate poor separation between two data groups, while the higher the FW, the better the differentiation. In the present study, this approach was applied for comparing differences between pairs of groups based on scores of PC1.

The software used to perform the multivariate analysis were two: a) R-based software CAT (Chemometric Agile Tool) and b) PLS Toolbox 8.7 by Eigenvector Research, Inc. for Matlab (version 2017b).

SECTION II: EXPERIMENTAL

CHAPTER 4: CHARACTERISATION OF COMMERCIAL FILLERS

In this chapter, two different commercial fillers, Filler_1 and Filler_2, are characterised with different techniques to understand their properties for subsequent research. The code Filler_1A means A component of Filler_1 and the same for the B component. The commercial Filler_1 and Filler_2 are different for three principal reasons: 1) the mixing ration of A and B components, 2) the different extenders and 3) the density.

Filler_1 contains hollow glass microspheres, Filler_2 has both alumina-silicate spheres and hollow glass microspheres, showing higher density than Filler_1.

The characterisation was carried out with different techniques: coatings tests, infrared spectroscopy, both on single components and on cross-linked product, thermal analysis, rheological analysis, mechanical analysis and morphological characterisation. Furthermore, a curing process study through IR and DSC analysis is described.

To perform the thermal and mechanical analyses on cross-linked product, A and B components of each filler were mixed together, in the correct ratio. For the morphological characterisation, instead, each component was mixed with a suitable amount of the matrix of other component and so, Filler_A was mixed just with polyamide resin and Filler_B was mixed with epoxy resin. This to better analyse the adhesion between matrix and extenders.

4.1 COATINGS TESTS

In Table 2, the specific weights of the two components of Filler_1 and of Filler_2 are reported. Both the components of Filler_1 exhibit values lower than Filler_2.

	Specific weight [g/cm^3]		**Specific weight** [g/cm^3]
Filler_1A	0.62	**Filler_2A**	0.70
Filler_1B	0.53	**Filler_2B**	0.72

Table 2: specific weights of commercial fillers

The pot life and the hardness test values (see 3.2 "Coating tests") of Filler_1 and Filler_2 are reported in Table 3. The pot life was measured at 20°C and the Shore D after one week from the mixing of A and B components.

The pot life is the same for both fillers, while the Shore D values are higher for the Filler_2 than for Filler_1. From the Shore D values, both fillers appear homogeneously cross-linked, in fact the instantaneous measure and the one after 15s are very similar (as reported in table). It is possible to observe how for low specific weights also the Shore D values are low. This could be related to the hollow glass microspheres content, indeed high amounts of this extender involve low specific weight and high porosity in the structure leading to low Shore D values.

	Pot Life [min]	**Shore D_{7days}**
Filler_1	60	55/50
Filler_2	60	61/60

Table 3: pot life and Shore D values of commercial fillers

4.2 INFRARED SPECTROSCOPY ANALYSIS

The composition of A and B components is very complex, such already mentioned (see "Chapter 2: Fillers") and so, the resulting IR spectra are very complex, showing overlapped bands. Nevertheless, in such complex matrix, several spectroscopic features are identified and their detection and changes shall be considered diagnostic of the curing process, as discussed in the following.

In Figure 41, mid-IR spectra of pure components A and B are reported in comparison with the cross-linked Filler_1. IR spectra of Filler_2 are not reported since similar to those of Filler_1.

The main bands detected in the spectrum of Filler_1A, are: =C-H stretching bands of aromatic rings in range 3100-3000cm^{-1}, whose corresponding ring vibrations fall in the 1650-1450cm^{-1} region; C-H stretching bands of alkyl chains, centered between 3000-2800 cm^{-1}; C-H deformation bands (1450-1250 cm^{-1}) and C-C/C-O stretching modes (1200-1000 cm^{-1}), strongly overlapped with bands due to the inorganic components.

The broad band at 3500cm^{-1} with a maximum at 3400cm^{-1} is assigned to O-H stretching of hydroxyl groups interacting through H-bonds [66]. The two typical absorption bands of the oxirane ring are observed as weak bands at 915cm^{-1}, due to the C-O-C deformation and at around 3060cm^{-1} due to the C-H stretching mode [26, 67, 68]. It is reported that the latter band can be used as a qualitative

indication of the presence of epoxy groups in low polymerization degree epoxy monomers [26]. However in Figure 41, this component extensively overlaps with the strong O-H absorptions and, mostly, with bands due to the =C-H stretching mode of the aromatic rings.

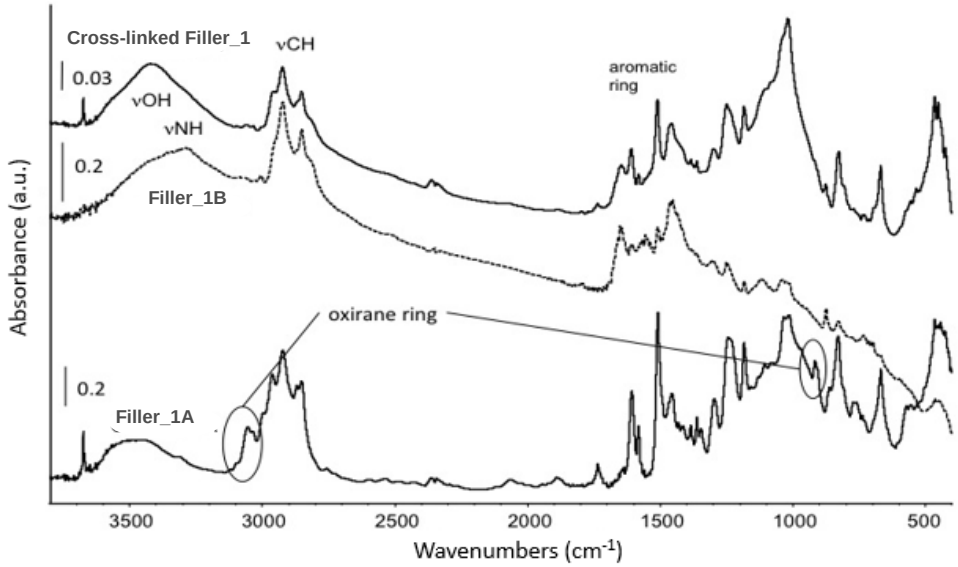

Figure 41: mid-IR spectra of A and B components and of the cross-linked Filler_1

For Filler_1B, in the high frequency spectral region (between 3000 and 2700cm^{-1}) C-H stretching bands of alkylic chains are observed. A weak absorption above 3000cm^{-1} is due to the presence of unsaturated compounds in the composition mixture. Typical bands assigned to NH groups are detected at 3300cm^{-1} (N-H stretching mode) and 3080cm^{-1} (Fermi resonance enhanced overtone) and at 1650-1500cm^{-1} are evident C=O stretching band and CN/CNH vibrational mode [66].

All these observations are in agreement with the typical IR signals of A and B components (see 3.3 "Infrared spectroscopy analysis")

The spectrum of cross-linked Filler_1 evidences some changes in spectral features:

- an increase in the intensity of the band around 3500cm^{-1}, typical of hydroxy groups, whose maximum moves to 3400 cm^{-1},
- a decrease of bands corresponding to amino groups, i.e. the weak absorption at 3300 cm^{-1} and
- a decrease of the bands due to the epoxy ring at 3050cm^{-1} and 915cm^{-1} (which completely disappeared).

4.2.1 STUDY OF CURING PROCESS

The different signals between single components spectra and cross-linked Filler_1 are due to the curing process, which involves these functional groups, i.e. ring-opening reactions of electrophilic epoxides with amino groups as nucleophilic agents. As already reported, in Chapter 2, the curing of an epoxy resin is described as a two steps reaction: the amino group from a primary amine reacts with the epoxide group to form a hydroxyl group and a secondary amine, spectroscopic reacts to form a tertiary amine and an additional hydroxyl group [26, 67]. The obtained data suggest that the same mechanism occurs, starting from an amide-containing component.

Therefore, the curing process can be monitored through changes in the intensity and shape of bands assigned to oxirane, amino groups or hydroxy groups which are diagnostic in the FTIR spectroscopic analysis of these materials. Actually, the complexity of the spectra in the range 1650-1300cm^{-1} as well as the superimposition of the NH stretching mode on the band due to OH stretching modes, limits the possibility to use NH vibrational modes. Therefore, it seems reasonable to follow preferentially the trend of bands related to epoxy rings and hydroxyl groups. Thus, the IR analysis were carried out immediately after the mixing of the two components and IR spectra are recorded at 25°C every 4s for 12h to monitor the evolution of such diagnostic bands.

Figure 42 reports some of the spectra recorded during the experiment.

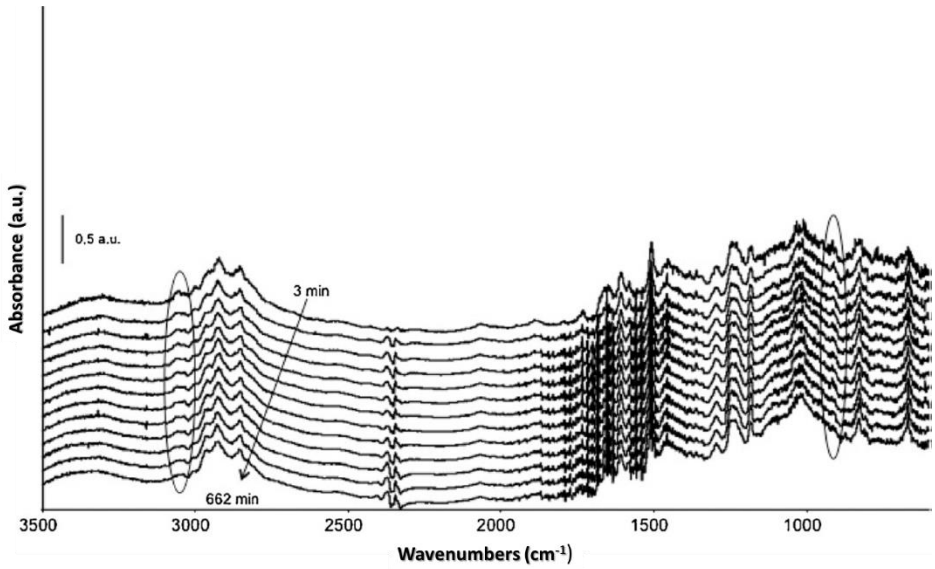

Figure 42: IR spectra of the mix A+B collected at different times

In spite of a general decrease in the signals intensities, the relative intensity of the band at 915cm^{-1} decreases even faster, whereas it is observed an increase in intensity and a change in the shape of the band centred is at 3400cm^{-1}, in agreement with the proposed reaction mechanism [67].

In addition, near-IR spectroscopy in Diffuse Reflectance method is often used to monitor the epoxy curing. The intensity of bands in this region (overtones and combination bands) is lower than that in the mid-IR region (fundamental bands) but the overall spectrum results to be simplified. In particular, the spectral region around 6500cm^{-1} shows well defined and characteristic signal of amino groups, both from amide and amine molecules, avoiding overlapping with other IR signals. The analysis of this region is reported by several authors to be useful in order to evaluate reaction kinetics and the degree of curing process in different conditions [68 - 73].

In Figure 43, Diffuse Reflectance spectra of A and B components and cross-linked Filler_1 are reported in the range 7500-4500cm^{-1}. Two strong absorptions are related to the oxirane group in A component: at 4535cm^{-1} (sharp and strong) are assigned to the combination band of the second overtone of the C–O stretching in the epoxy ring with the fundamental C–H stretching mode and at 6079cm^{-1} assigned to overtone of terminal CH_2 stretching mode, partially overlapped with overtones of CH and CH_2 stretching modes and of aromatic ring [68]. The former band, depending on the oxirane ring concentration, is used to determine the degree of cure in epoxy/amine resins, once normalized with the two aromatic ring combination bands around 4600cm^{-1} [70]. As previously reported, the envelop of band in the 5600-6000cm^{-1} range is mainly due to overtones of CH stretching modes, from alkyl chains and from aromatic rings. The band at 7195cm^{-1}, could be due to an overtone of hydroxy groups stretching modes, while the weaker band at 5240cm^{-1} are assigned to combination of asymmetric stretching and bending of O-H groups [26].

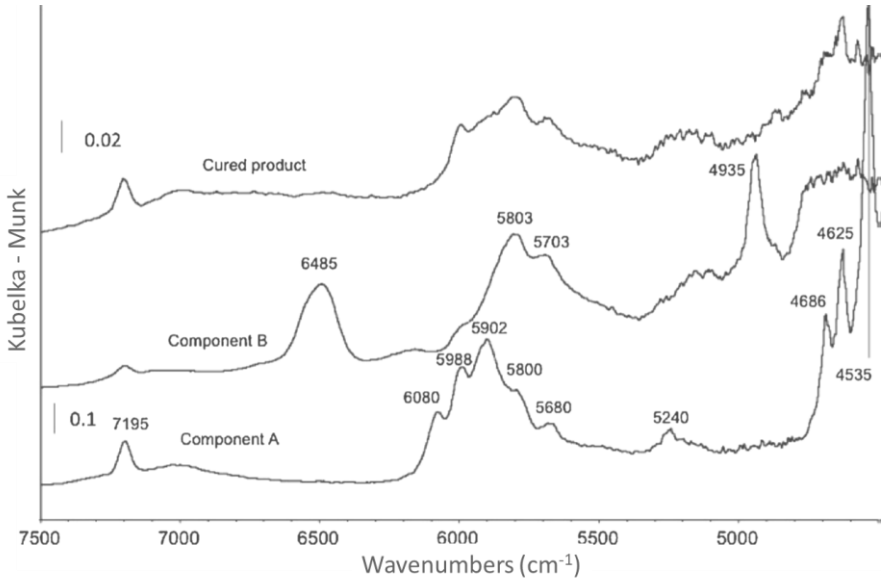

Figure 43: near-IR spectra of A and B components and of the cross-linked Filler_1

The spectrum of B component in the near-IR range shows the main band of amino group at 6495cm^{-1} strong and broad. This peak should correspond to the first overtone of N-H stretching in secondary amides [74]. On the other side, the detection of a band at 4935cm^{-1} could also suggest the presence of primary amino groups [72].

As expected, due to the curing reaction, the band at 6485cm^{-1} (oxirane, A component) disappears almost completely in the final product, as well as the band at 4530cm^{-1} (amino group, B component) in agreement with the results from mid-IR region. The formation of new OH groups is also confirmed by the broad absorption around 7000cm^{-1} tailing towards lower frequencies, assigned to OH overtones [75]

Several near-IR analyses, using the same diagnostic bands, were performed on samples with different A/B ratios, 1:1, 1.3:1, 2:1, 2.7:1 and 3.3:1, to evaluate the extent of the curing reaction. These spectra are reported in Figure 44.

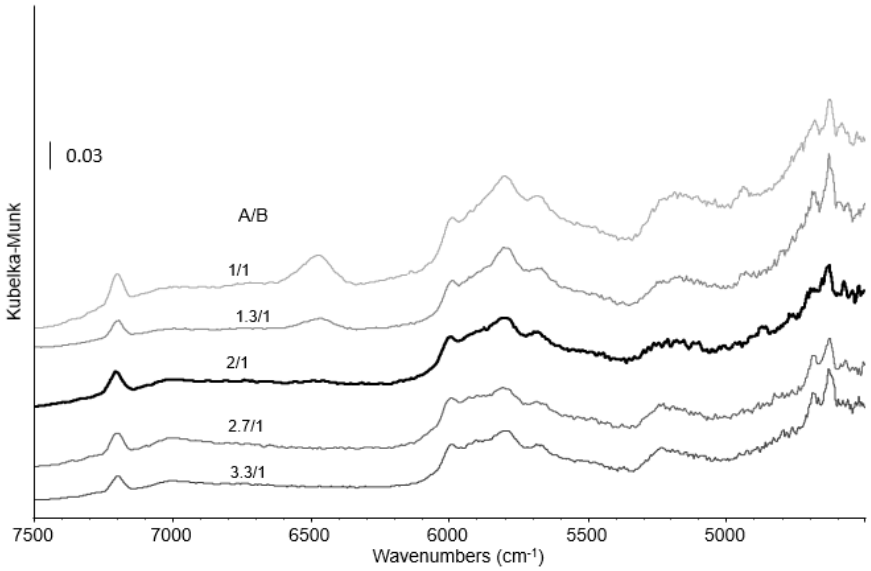

Figure 44: near-IR spectra of samples with different A/B ratio

A sample with the prevalence of a component over the other will have a spectrum that follows closely the characteristics of the most abundant component. For this reason, samples with low A/B ratio will have high absorbance values in bands related to amino groups, whereas samples with majority of component A are likely to have higher intensity in oxirane and hydroxyl group bands. Following literature suggestions [26, 73] it is chosen to analyse the intensity of the band representative of a reactive group (i.e. 6485cm^{-1}, amino group) normalized to a largely invariant component, to be selected in the alkyl region of the spectra. The invariant component can be represented by the CH groups (i.e. bands in the range 6100–5600cm^{-1}) whose presence is considered constant during the

process. Actually, CH groups are present in the spectra of both components, thus we selected two main maxima at 5703cm^{-1} and 5803cm^{-1} that are much more evident in B and that can be considered characteristic of this component. Therefore, the intensity ratio I6485/I5803 (as band height at the main maximum) is analysed in several samples with different B/A content. An almost linear trend of absorbance ratio I6485/ I5803 is detected in the final cured product as a function of B/A suggesting that this ratio could be taken as diagnostic of the component B consumption during the curing. The spectrum of the composition 2:1 (A/B) ratio, i.e. the best composition suggested by the producer, shows some very weak residual absorption in the region of NH signal, suggesting a not complete consumption of these groups. Indeed, the excess of the B component (below 2:1 A/B ratio) leads to an increase in the intensity of the NH signal, corresponding to an increasing fraction of unreacted NH groups. On the other side, even at the lowest contents of component B, bands characterizing the very reactive epoxy group in component A disappear almost completely. From these data it is suggested that the normalized NH signal can actually be chosen as diagnostic to evaluate the final cross-linked product even in such a very complex formulation.

4.3 THERMAL ANALYSIS

The two commercial fillers were analysed with both the thermogravimetric analysis and the differential scanning calorimetry to characterise them thermically. Furthermore, the last one was also used to study the curing process on Filler_1 over time.

4.3.1 THERMOGRAVIMETRIC ANALYSIS (TGA)

TGA was performed to determine the degradation temperature of the resin and the curves of Filler_1 and Filler_2 are reported respectively in Figure 45 and Figure 46.

Considering Filler_1 shows a first loss at around 150 °C, due to the loss of low molecular weight molecules present into the filler. Then the loss of material (58.13%wt) in the range 300–700 °C is due to real decomposition of the organic part of the resins, confirming their thermal resistance up to 350 °C. Moreover, at 700 °C, it is observed the switch from N_2 to O_2 atmosphere and the residue of 37.24% wt is ascribed to the inorganic extenders.

Filler_2 shows a first loss at around 100 °C, due to the loss of low molecular weight molecules contained into the filler. Then the loss of material (55.08%wt) in the range 300–700 °C is due to real decomposition of the organic part of the resins, confirming their thermal resistance up to 350 °C.

Moreover, at 700 °C, it is observed the switch from N_2 to O_2 atmosphere and the residue of 32.29% wt is ascribed to the inorganic extenders.

To summarise, the trend of TGA curves are really similar and the residual is comparable.

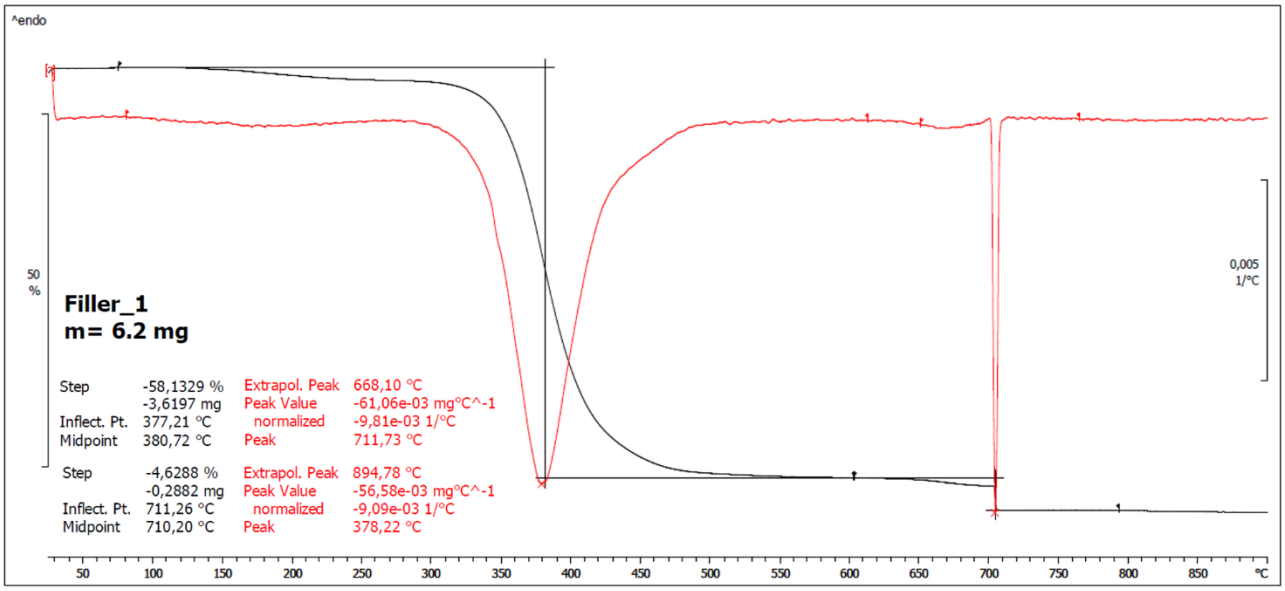

Figure 45: TGA curves of Filler_1

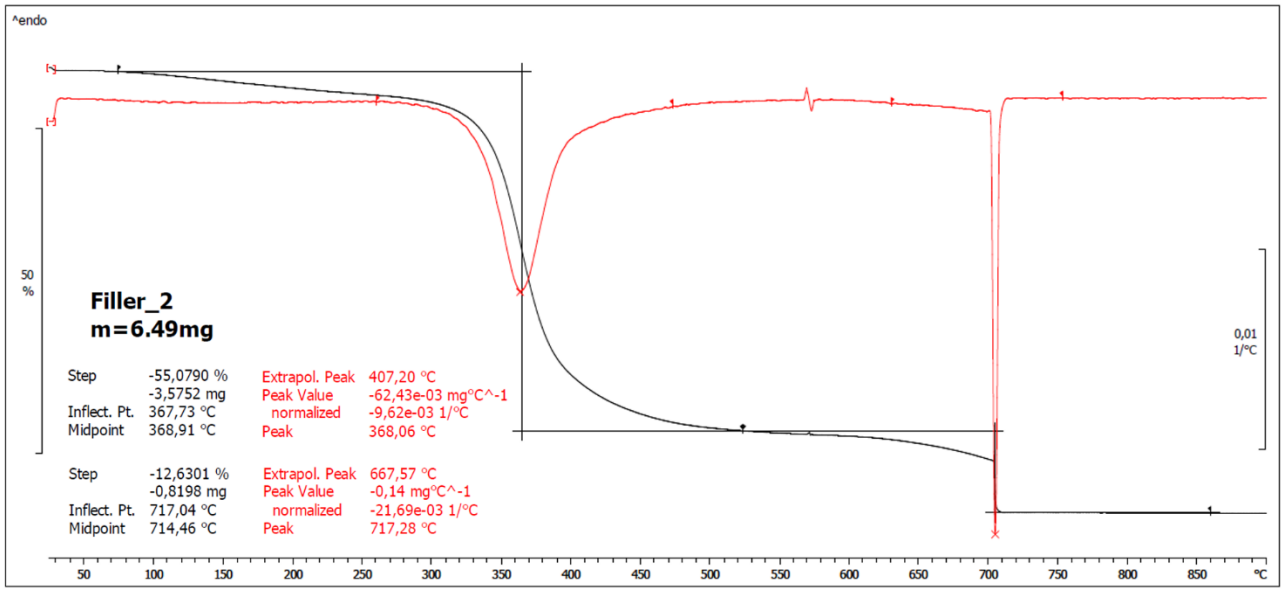

Figure 46: TGA curves of Filler_2

4.3.2 DIFFERENTIAL SCANNING CALORIMETRY (DSC)

The DSC curves, used to determine the temperature of glass transition (*Tg*), are reported in Figure 47, the trend of the two fillers is around the same.

The transition between glassy and rubbery state is not a single point, but a region and the Tg is considered the midpoint value of this transition region, as reported in ASTM E1356-98.

Tg of Filler_1, is at 43°C, while of Filler_2 is at 41°C. In both the fillers appear a residual enthalpy (i.e. the difference between the actual enthalpy and that ideal), and in Filler_1 appears a trace of enthalpy relaxation, in the range 55-65°C.

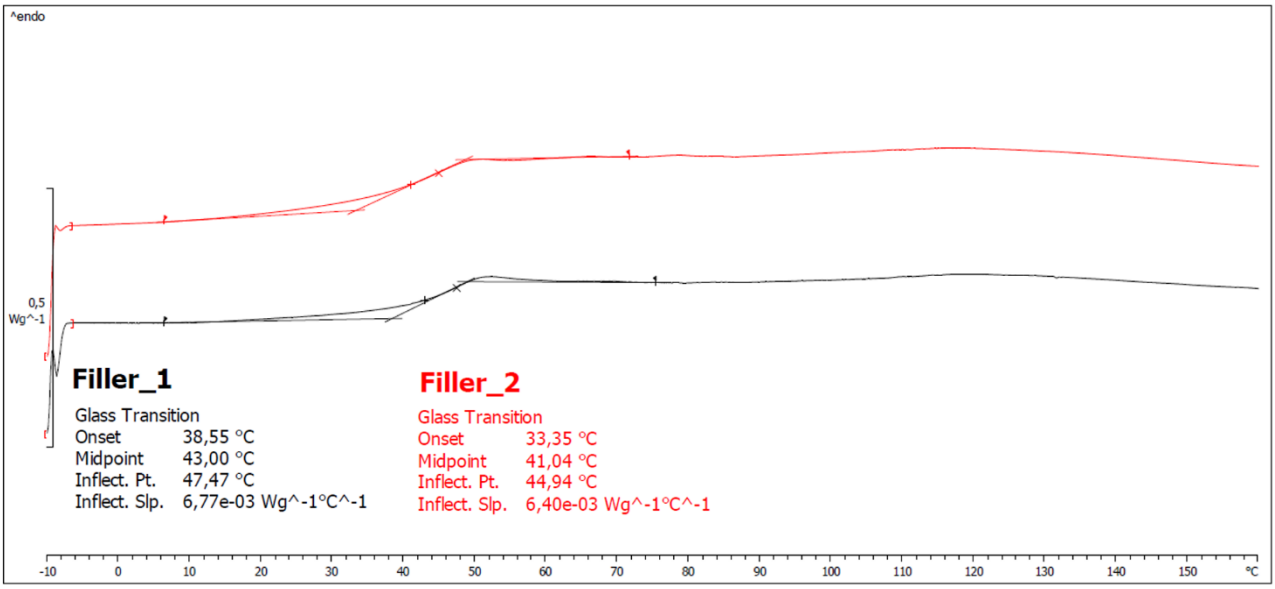

Figure 47: DSC curves of Filler_1 and Filler_2

STUDY OF CURING PROCESS

Such already mentioned in paragraph 2.1.3 "Study of curing process", the curing process can be influenced by several factors and it has a remarkable impact on the physical, mechanical and chemical properties of the cross-linked product. In particular, the fillers are applied in some environmental conditions and so, there is the necessity to study as the curing process is developed in these situations.

Therefore, the curing process of Filler_1 was studied as a function of time, temperature and humidity, to evaluate how these environmental parameters influence the reaction evolution and gain further insight into the reaction mechanism.

After the mixing of A and B components of Filler_1, the samples are left in an oven at the temperature of 80°C for different times: 2.5, 5, 7.5, 15, 20, 30, 40, 60, 240min. Once the samples reached the predetermined residence time in the oven, a quenching in liquid N_2 took place and then DSC measurements were carried out. By this procedure, it was possible to obtain characteristic curves of each sample at the different curing times.

In addition, in order to evaluate the cross-linking degree of the samples cured in different, temperature and humidity conditions, four experiments were carried out:

1. samples cross-linked at 25 °C and absolute humidity 1g/Kg or relative humidity (RH) 7%, (dry environment) for 24, 48, 72, 96 and 168h.
2. samples cross-linked at 25 °C and absolute humidity 6g/Kg or RH 30% for 24, 48, 72, 96 and 168h.
3. samples cross-linked at 10 °C and absolute humidity 1g/Kg or RH 7% (dry environment) for 24, 48, 72, 96, 168 and 336h.
4. samples cross-linked at 10 °C and absolute humidity 6g/Kg or RH 80% for 24, 48, 72, 96, 168 and 336h.

The parameter combinations were chosen based on the realistic application conditions: room temperature or low temperature in dry or wet atmosphere

The DSC plots of Filler_1 after different times of curing are reported in Figure 48. From these measures the glass transition temperature *(Tg)* and the enthalpies of reaction *(ΔH_r)* were obtained.

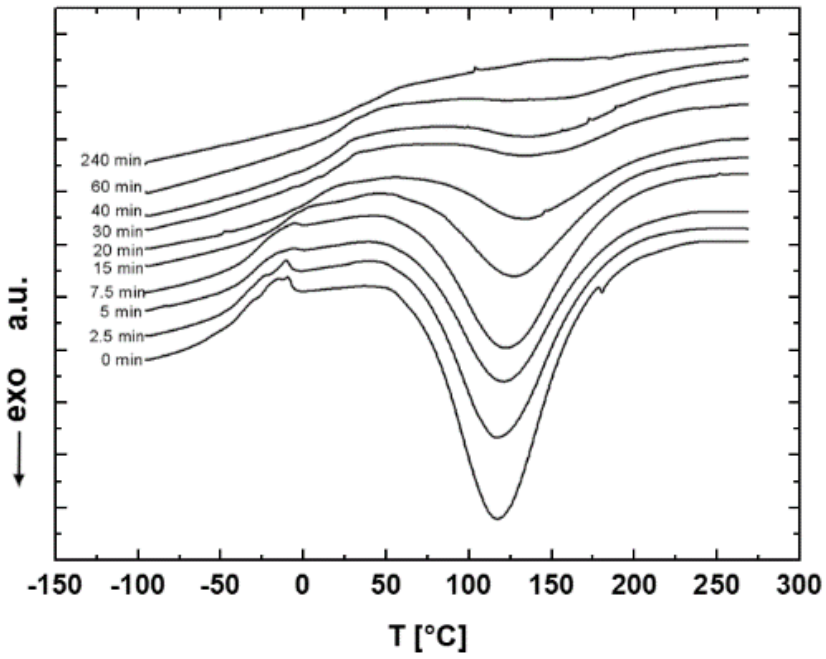

Figure 48: DSC curves of Filler_1 kept in oven at 80°C from 0 to 240min

By increasing the treatment time in the oven, the value of ΔH_r decreases and the Tg increase due to the increase of cross-linking in the thermosetting resins. Furthermore, the curing degree *(CD%)* is reported in Table 4 and it is evaluated through the variations in the enthalpy of reaction [76], using the equation:

$$CD\% = \left(\frac{(\Delta H_r - \Delta H_t)}{\Delta H_r}\right) \cdot 100 \quad (23)$$

where ΔH_r is the total enthalpy of reaction measured before the permanence in the oven and ΔH_t are the residual enthalpies of reaction after different residence times in the oven.

Time [min]	**Enthalpy of reaction** [J/g]	**Glass transition temperature** [°C]	**Curing degree [%]**
0	197.0	-37.5	0
2.5	152.5	-32.8	22.6
5	128.4	-29.8	34.8
7.5	125.2	-24.9	36.4
15	83.7	-9.8	57.5
20	51.0	7.3	74.1
30	25.2	25.0	87.2
40	26.4	22.9	86.6
60	12.8	30.4	93.5
240	0.9	40.3	99.5

Table 4: calorimetric data and curing evaluation at different times in oven at 80°C

Considering the Tg variations as a function of the curing degree it is possible to build up the scatter plot (Figure 49), in which it is also shown the Tg value of a 100% cross-linked sample (60°C).
As visible, the Tg is more sensitive to the CD variation in the final steps of reaction (> 90%), which is often the most critical part of the process due to the strong increase of the system viscosity. It can also be observed that the slope was around 5°C/CD% for cross-linking degree between 90 and 99%.
The calorimetric data (ΔH_r and Tg) of the experiments obtained in different environmental conditions are reported in Table 5 and Table 6. By using the equation (23), and therefore the enthalpy of reaction, the curing degree is calculated in function of time.

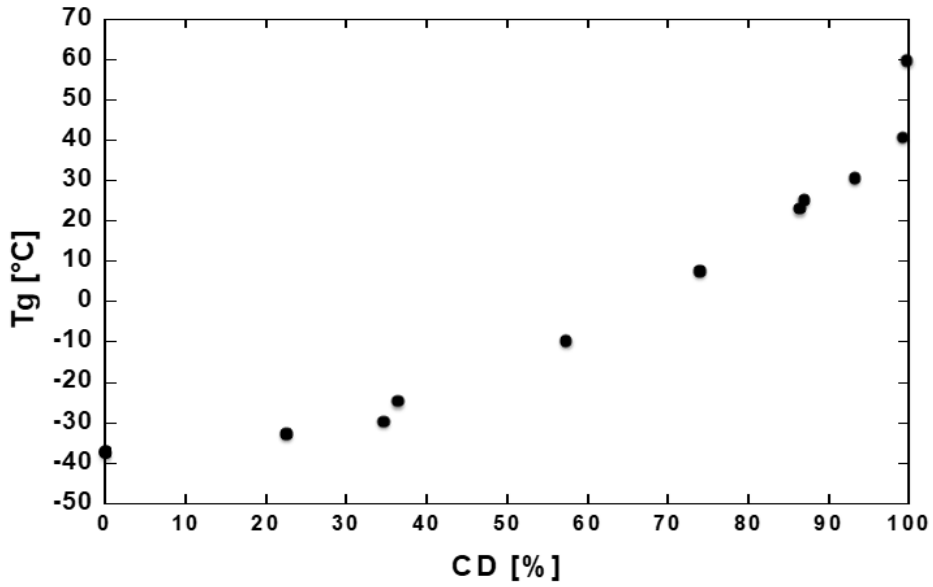

Figure 49: scatter plot of Tg in function of the curing degree (CD) of the filler undergone different curing time interval

	25 °C, RH 7%			25 °C, RH 30%		
Time [h]	**ΔH** [J/g]	**Tg** [°C]	**CD** [%]	**ΔH** [J/g]	**Tg** [°C]	**CD** [%]
0	197.0	-37.5	0	197.0	-37.5	0
24	10.9	36.7	94.4	7.6	36.5	95.9
48	10.2	42.8	94.9	5.4	40.7	97.5
72	5.4	43.9	97.5	1.4	42.3	99.5
96	2.4	44.1	99.0	3.9	45.1	98.0
168	0.7	47.9	99.5	1.2	47.9	99.5
336	-	-	-	-	-	-

Table 5: Tg and ΔH data obtained from the first two experiments at different environmental conditions

	10°C, RH 7%			10 °C, RH 30%		
Time [h]	**ΔH** [J/g]	**Tg** [°C]	**CD** [%]	**ΔH** [J/g]	**Tg** [°C]	**CD** [%]
0	197.0	-37.5	0	197.0	-37.5	0
24	68.2	-2.7	65.5	65.3	0.4	79
48	37.1	19.8	81.2	39.8	19.7	79.7
72	39.6	23.3	79.7	36.7	25.0	81.2
96	26.8	28.6	86.3	25.1	27.1	87.3
168	21.0	33.7	89.3	19.1	31.8	90.3
336	16.1	36.0	91.9	13.0	38.6	93.4

Table 6: Tg and ΔH data obtained from the last two experiments at different environmental conditions

As highlighted in the data, the samples cured at 25 °C reach the maximum curing degree in one week (168 h) independently of the humidity; on the contrary, the samples cured at lower temperature (10 °C), even after two weeks (336 h), do not reach the complete cross-linking.

In order to verify the reliability of the cross-linking degree evaluated from the enthalpies of reaction, the Tg values of the highest cured samples, i.e. samples after 96 h of curing and above, are plotted in Figure 50. For cross-linking degree between 93 and 99% at 10 °C and 25 °C, the curve has the best fit to the experimental points. It was also evident that the humidity did not influence the curing at 25 °C, while it had a slight effect at lower temperature (10 °C).

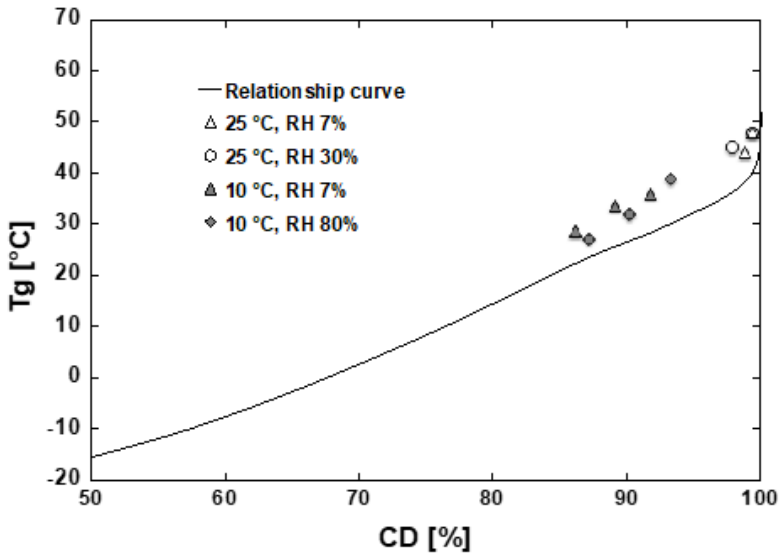

Figure 50: experimental curve with data of filler cross-linked in different environmental conditions

4.4 RHEOLOGICAL ANALYSIS

On both two components, the rheological analyses were performed both in rotatory mode, with viscosity test (see 3.5.1 "Viscosity test") recovery tests (see 3.5.2 "Recovery test"), and in oscillatory mode, with amplitude sweep tests (see 3.5.3 "Amplitude sweep test").

The measurements were carried out at two different times: 1) after one week (t_1) and 2) after one year (t_2) from the production. Time t_1 is representative for the first step of the supply chain (from manufacturer to shipyard), and t_2 is representative for the shelf-life of the product.

Triplicate measurements have been carried out on each sample.

In Table 7 are reported the means and the standard deviations of the rheological results of rotational tests: initial viscosity at shear rate $0.01s^{-1}$ ($\eta_{0.01\_F}$), the recovery percentage after 30s (Rec_{30s}) and the total recovery percentage (Rec_{tot}). Furthermore, in the same table are reported the means and the standard deviations of the rheological results of oscillatory tests: the distance between the moduli, at very low strain ($\gamma = 0.001\%$), indicated as G'-G'', its increment in percentage after one year respect to the measure performed at one week, indicated as $\Delta(G'\text{-}G'')$ and the end of Linear Viscoelastic Range (*LVER*), obtained from the software RheoCompass s1.19.

Filler	Times	$\eta_{0.001\_F}$ [kPa s]	Rec_{30s} [%]	Rec_{tot} [%]	G'-G'' [kPa]	Δ(G'-G'') [%]	LVER end [%]
Filler_1A	7days	16±2	97±7	96±3	58±6	-	0.001
	1year	19±1	74±4	73±3	100±15	72	0.001
Filler_2A	7days	15±1	53±5	92±6	25±2	-	0.005
	1year	25±1	55±3	85±4	31±2	24	0.005
Filler_1B	7days	11±1	82±2	73±4	54±8	-	0.003
	1year	16±1	66±3	59±2	98±14	82	0.003
Filler_2B	7days	12±2	56±3	50±1	12±1	-	0.005
	1year	20±2	44±5	45±1	20±1	67	0.005

Table 7: the rheological data of viscosity, recovery and amplitude sweep tests of commercial fillers

4.4.1 VISCOSITY TEST

Figure 51 reports the flow curves of both A and B components of commercial fillers.

As visible in Figure 51a and in Table 7, the Filler_1A appears more stable than Filler_2A, that exhibits a remarkable increase of viscosity. In addition, Filler_1A shows a stable slope, unlike Filler_2A.

Regarding the B components (Figure 51b), the trend is the same of A components.

Generally, the two commercial fillers appear quite stable over time and more or less comparable between them.

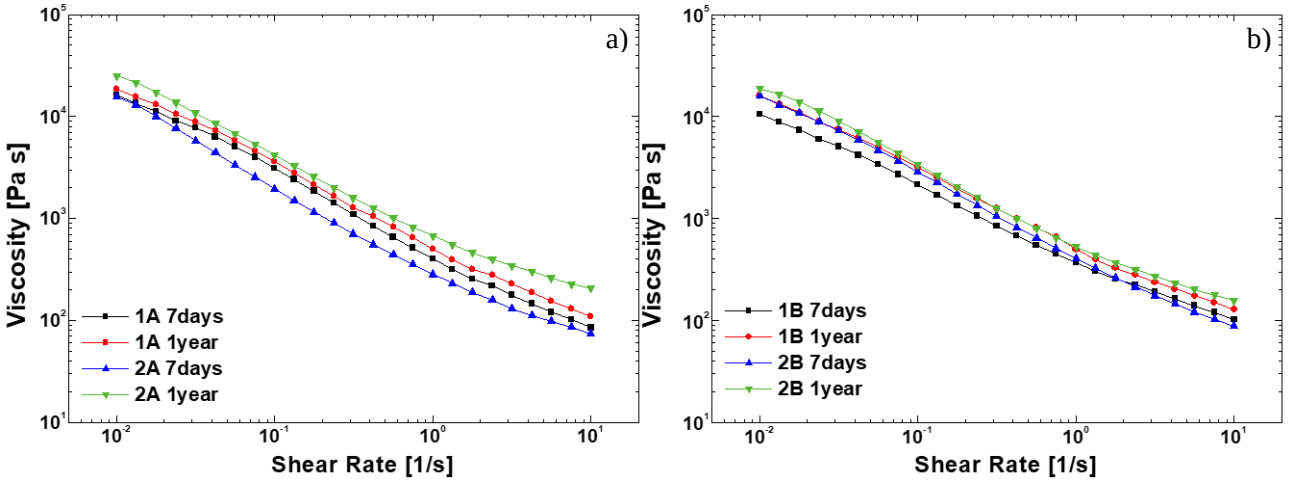

Figure 51: viscosity test of commercial fillers; A components (a) and B components (b)

4.4.2 RECOVERY TEST

Figure 52 reports the recovery test of commercial fillers of A component (Figure 52a) and of B component Figure 52b). Over time, all recoveries decrease, but there are some differences to highlight.

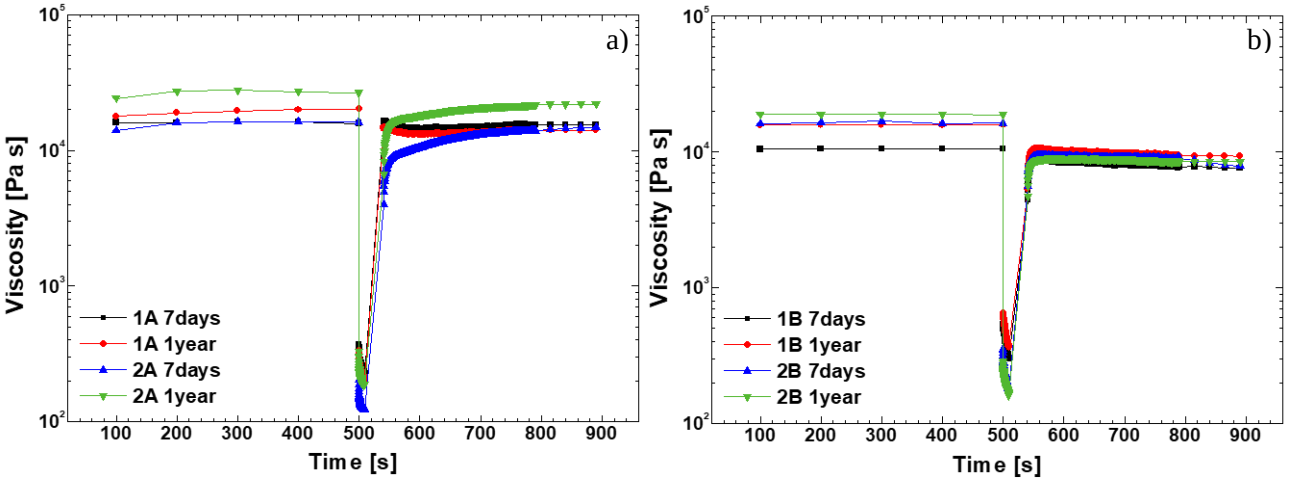

Figure 52: recovery test of commercial fillers; A components (a) and B components (b)

Considering the A components, unlike the flow curves, the recovery curves of Filler_1A and Filler_2A exhibit different trends and shapes. Indeed, as reported in Table 7, the Rec_{30s} and Rec_{tot} of Filler_1A are almost equal (at t_1 97 and 96, at t_2 74 and 73%), while for Filler_2A the Rec_{30s} (at t_1 53

and at t_2 55%) are lower than Rec_{tot} (at t_1 92 and at t_2 85%). Besides, the recoveries of Filler_1A are higher than Filler_2A, with the exception of Filler_2A (85%) at t_2 that is higher than Filler_1A (73%).

Considering the B components, the samples trend is very similar: the total recovery is lower than the recovery after 30s. Furthermore, the recoveries of Filler_1B are higher than in Filler_2B.

Filler_1 appears better then Filler_2 for the fillers rheological requirements, indeed, as already mentioned, the faster is the recovery the higher is the applicable thickness (see 3.5.2 "Recovery test").

4.4.3 AMPLITUDE SWEEP TEST

Figure 53 reports the amplitude sweep test of commercial fillers of A component (Figure 53a) and of B component Figure 53b).

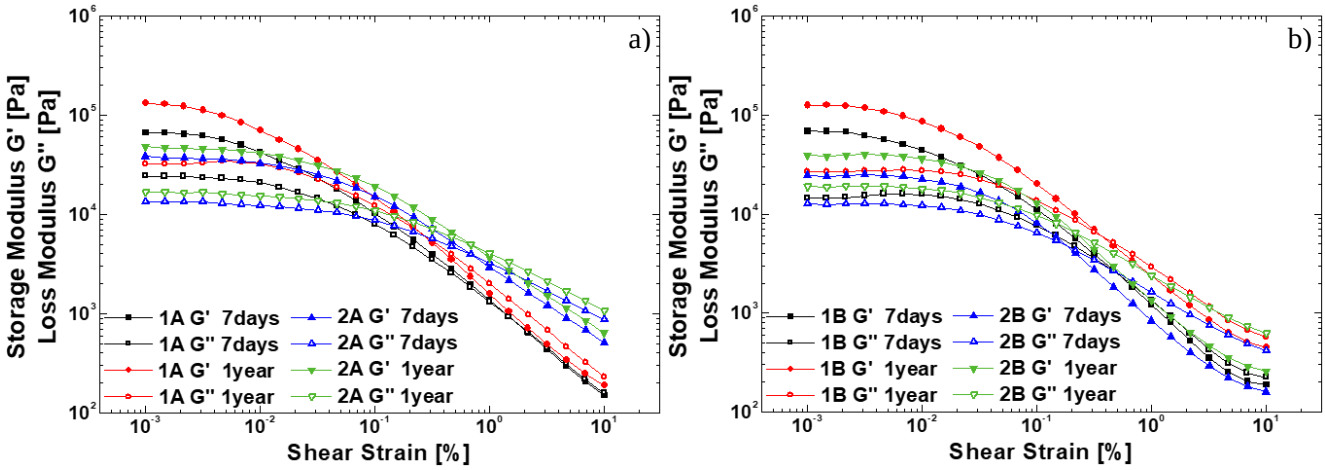

Figure 53: amplitude sweep test of commercial fillers; A components (a) and B components (b)

As visible from the amplitude sweep test and from the Table 7, all the samples exhibit a good separation between the moduli (over 10kPa), that increases over time. In both the components, the Filler_1 exhibits a higher separation than Filler_2.

Considering the A components, Filler_1A shows an increment in percentage of the distance between the moduli of 72%, while Filler_2A of 24%. The end of LVER, instead, is higher in Filler_2A (0.005%) than in Filler_1A (0.001%) and so Filler_2A can suffer shear strain higher without disrupting its internal structure. Over time, both fillers appear quite stable.

Considering the B components, the Filler_1B exhibits again higher separation between the moduli than the Filler_2B, and over time, the increase (82%) is higher than the Filler_2B (67%).

Finally, as for the A components, the Filler_2B has an end of LVER higher than Filler_1B.

In this case, Filler_2B appears more stable than Filler_1B.

Generally, Filler_2A is the most stable among all samples in amplitude, while the B components are comparable; the Filler_1 is the least stable. Furthermore, Filler_2 has a higher end of LVER than Filler_1.

4.5 MECHANICAL ANALYSIS

The mechanical analyses were performed on the cross-linked product, obtained mixing A and B components. To have a complete cross-link, the samples were measured after one week from the application.

4.5.1 DYNAMIC MECHANICAL THERMOANALYSIS (DMTA)

As for the rheological characterisation, three measurements for each sample were carried out and the results represent the mean values. The measurements were performed in torsional mode (see 3.6.1 "Dynamic mechanical thermoanalysis (DMTA)"), after the identification of LVER using an amplitude sweep tests, as reported in Figure 54.

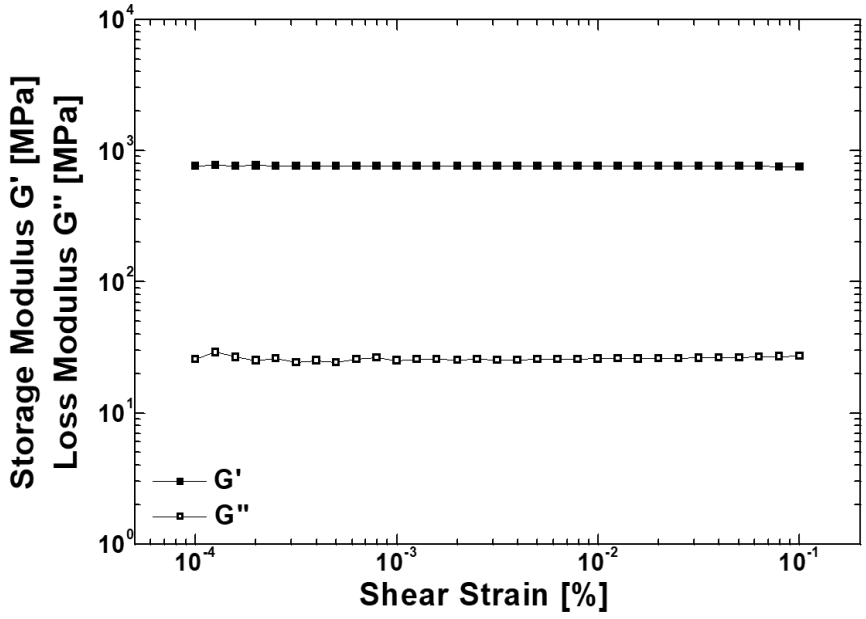

Figure 54: amplitude sweep DMTA in torsion of Filler_1

Identified the LVER, a heating ramp check was carried out in order to find the better conditions (not too fast to allow the material to heat homogeneously, not even too slowly to avoid long measurements times). The Filler_1 and the Filler_2 DMTA in torsion are reported in Figure 55.

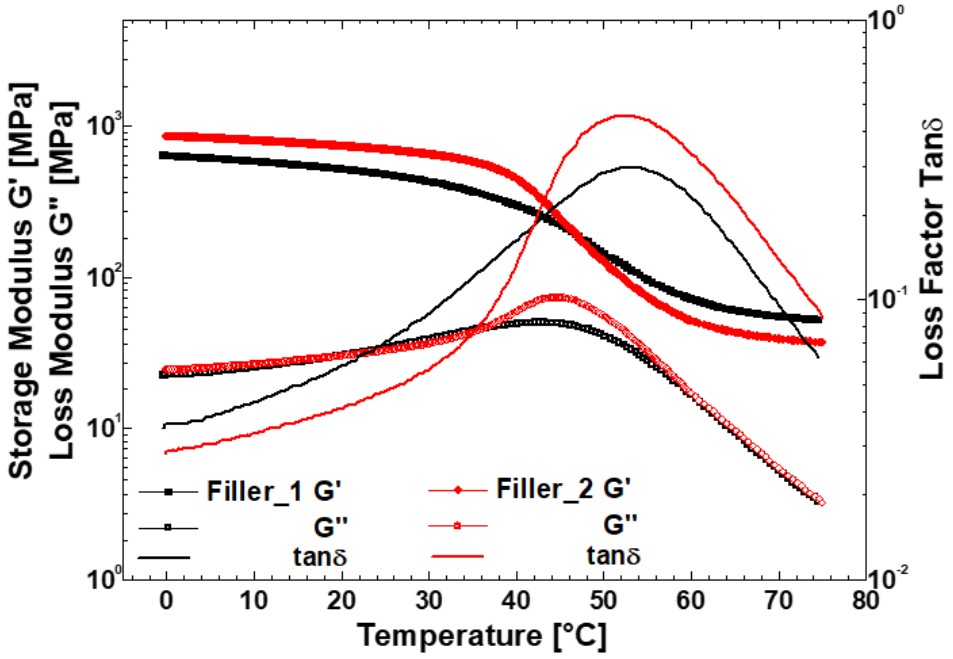

Figure 55: DMTA in torsion of commercial fillers

From the DMTA, the glass transition temperatures were obtained considering the loss factor peaks. The mean of the three measurements of Filler_1 are reported in Table 8 with the corresponding standard deviation; the same for the Filler_2.

The coefficient of thermal expansion, α, was also calculated from the DMTA data. The sample initial length, L_0, was measured at temperature T_0, heating the sample, its size varied and so the sample final length, L, was measured at temperature T. The sample length variation, ΔL, was the difference between L and L_0.

This coefficient was calculated as in (24):

$$\alpha = \frac{\Delta L}{L_0 \cdot \Delta T} \tag{24}$$

where ΔT was the difference between the two temperatures considered (T-T_0).

In particular, the ΔT selected were: 1)T_1, before glass transition temperature, in range 20-30°C, and 2) T_2, after glass transition temperature, in range 60-70°C. In Table 8 are reported the coefficient of expansion related to T_1 and T_2 respectively called α_1, α_2 and their increment in percentage ($\Delta\%$).

Knowing this coefficient is very important for the painting system performance, indeed various materials (i.e. polymeric based and metallic) are coupled and it is necessary that their coefficients are similar in order to avoid defects, such as detachment, when the temperature increases.

Not being the correct technique for the study of the coefficients of expansion, the reported values are only indicative, but they can still be used to have a preliminary comparison.

Filler	T_g [°C]	α_1 [$10^{-4} \cdot$ °C]	α_2 [$10^{-4} \cdot$ °C^{-1}]	$\Delta\alpha$ [%]
Filler_1	52.6±0.5	1.24	1.44	16.1
Filler_2	52.3±0.1	1.30	1.51	16.2

Table 8: commercial fillers glass transition temperatures and its coefficients of expansion

4.5.2 UNIAXIAL TESTS

All the uniaxial tests were performed on three different temperatures, 0, 20 and 30°C, in order to evaluate the mechanical properties varying the temperature. As for DMTA, three measurements for each sample were carried out and the results reported in tables are the means and the standard deviations values.

TENSILE TEST

The samples were in "dog bone" shape with the following sizes: thickness 0.8cm, width 2.0cm and length 15cm. In the Table 9, are reported the Young's modulus (MPa), E_t, the stress (MPa), σ_t, and the deformation (%), ε_t.

Filler	Temperature [°C]	E_t [MPa]	σ_t [MPa]	ε_t [%]
Filler_1	0	532 ± 89	8.4 ± 0.19	0.52 ± 0.01
	20	313 ± 32	6.87 ± 0.82	1.09 ± 0.41
	30	275 ± 69	5.61 ± 0.60	1.76 ± 0.26
Filler_2	0	761 ± 107	13.36 ± 0.93	1.05 ± 0.18
	20	510 ± 87	11.77 ± 0.89	1.87 ± 0.06
	30	160 ± 36	7.36 ± 0.34	3.48 ± 0.39

Table 9: tensile values of commercial fillers

In Figure 56, the stress (σ_t) is plotted against the deformation (ε_t). The influence of temperature is stronger in the Filler_2 than in the Filler_1. From an application point of view, Filler_1 appears the best.

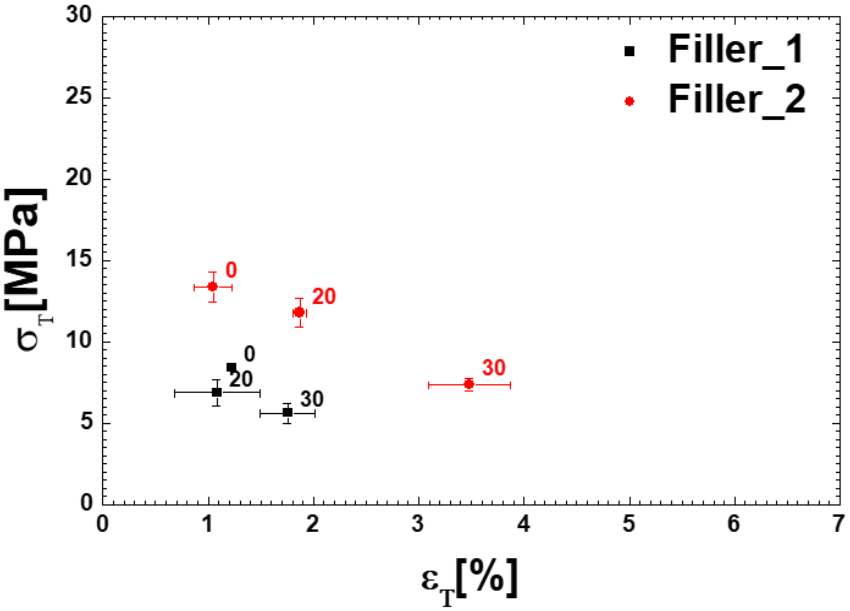

Figure 56: tensile results for commercial fillers

THREE-POINT BENDING TEST

The samples sizes were: thickness 0.8cm, width 2.0cm and length 20cm. In the Table 10, are reported the Young's modulus (MPa), E_b, the stress (MPa), σ_b, and the deformation (%), ε_b, and in Figure 57 the stress (σ_t) is plotted against the deformation (ε_t).

Filler	Temperature [°C]	E_t [MPa]	σ_t [MPa]	ε_t [%]
Filler_1	0	1153 ± 21	11.5 ± 0.5	1.08 ± 0.05
	20	835 ± 13	9.7 ± 0.1	1.43 ± 0.05
	30	444 ± 19	6.4 ± 0.3	2.34 ± 0.08
Filler_2	0	1657 ± 53	19.4 ± 0.9	1.30 ± 0.11
	20	843 ± 29	14.0 ± 0.7	2.81 ± 0.26
	30	290 ± 19	6.2 ± 0.5	5.75 ± 0.01

Table 10: three-point bending values of commercial fillers

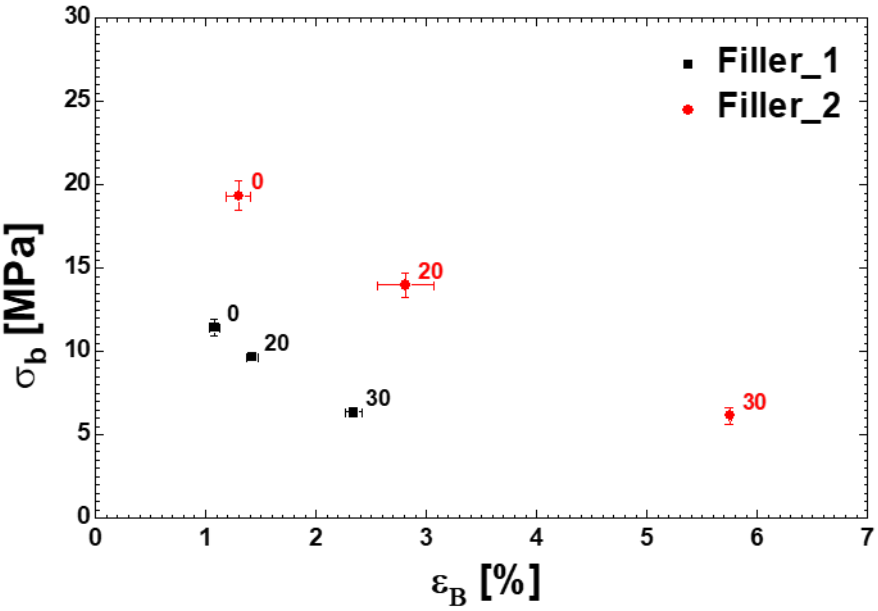

Figure 57: three-points bending test results of commercial fillers

Similarly, to the tensile test, Filler_1 shows a less dependence from the temperature than Filler_2. In addition, standard deviations are always very low, above all for Filler_1.

COMPRESSION TEST

The samples were in cylindrical shape with the following sizes: thickness 2.5cm and diameter 3.1cm. The averages and the standard deviations are shown in the Table 11, while in Figure 58 the stress (σ_t) is plotted against the deformation (ε_t).

Filler	Temperature [°C]	E_t [MPa]	σ_t [MPa]	ε_t [%]
Filler_1	0	722 ± 159	16.3 ± 0.1	3.57 ± 0.26
	20	514 ± 121	11.7 ± 0.3	3.15 ± 0.28
	30	376 ± 48	8.8 ± 0.3	2.94 ± 0.26
Filler_2	0	1002 ± 170	26.7 ± 1.7	3.59 ± 0.32
	20	929 ± 78	20.8 ± 0.3	2.95 ± 0.25
	30	556 ± 11	14.5 ± 0.6	2.71 ± 0.13

Table 11: compression values of commercial fillers

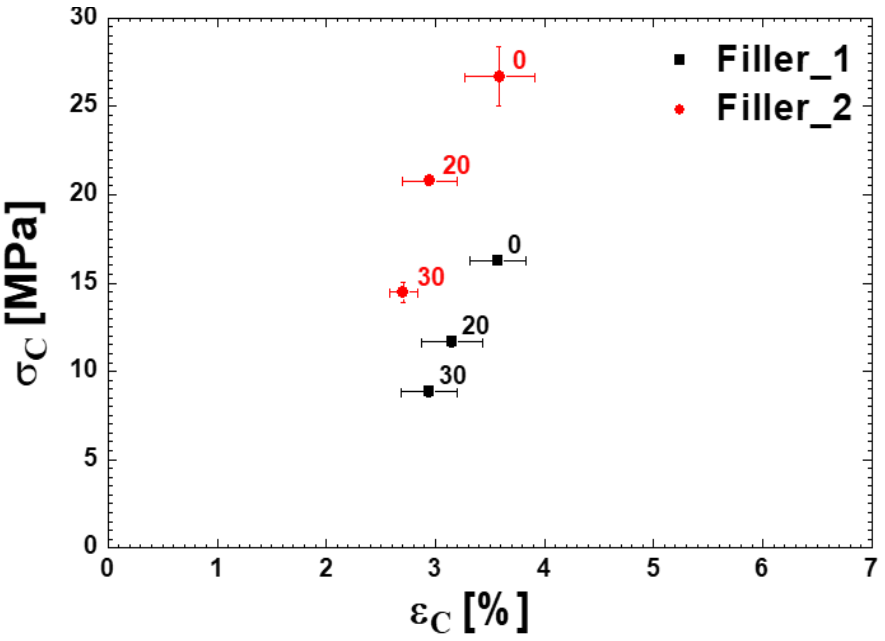

Figure 58: compression results of commercial fillers

According to the compression test, the two commercial fillers are not relevantly different.

Generally, from the uniaxial tests, the Filler_1 results the less influenced by temperature. The three-point bending test results indicate greater data reliability compared to tensile and compression tests.

4.6 MORPHOLOGICAL CHARACTERISATION

This analysis was performed to see the adhesion between matrix and extenders and to understand if extenders agglomerate.

SEM images and EDX spectra of Filler_1A are reported respectively in Figure 59 and Figure 60.

For Filler_1A (Figure 59) it is clearly visible the good adhesion between matrix and hollow glass microspheres, easily identifiable. The other extenders appear quite well dispersed. In Figure 60, the two EDX spectra show how hollow glass microspheres are mainly composed of silicon and oxygen and the matrix is fundamentally composed of carbon, calcium and oxygen. The presence of calcium indicates the presence of carbonates dispersed in the matrix.

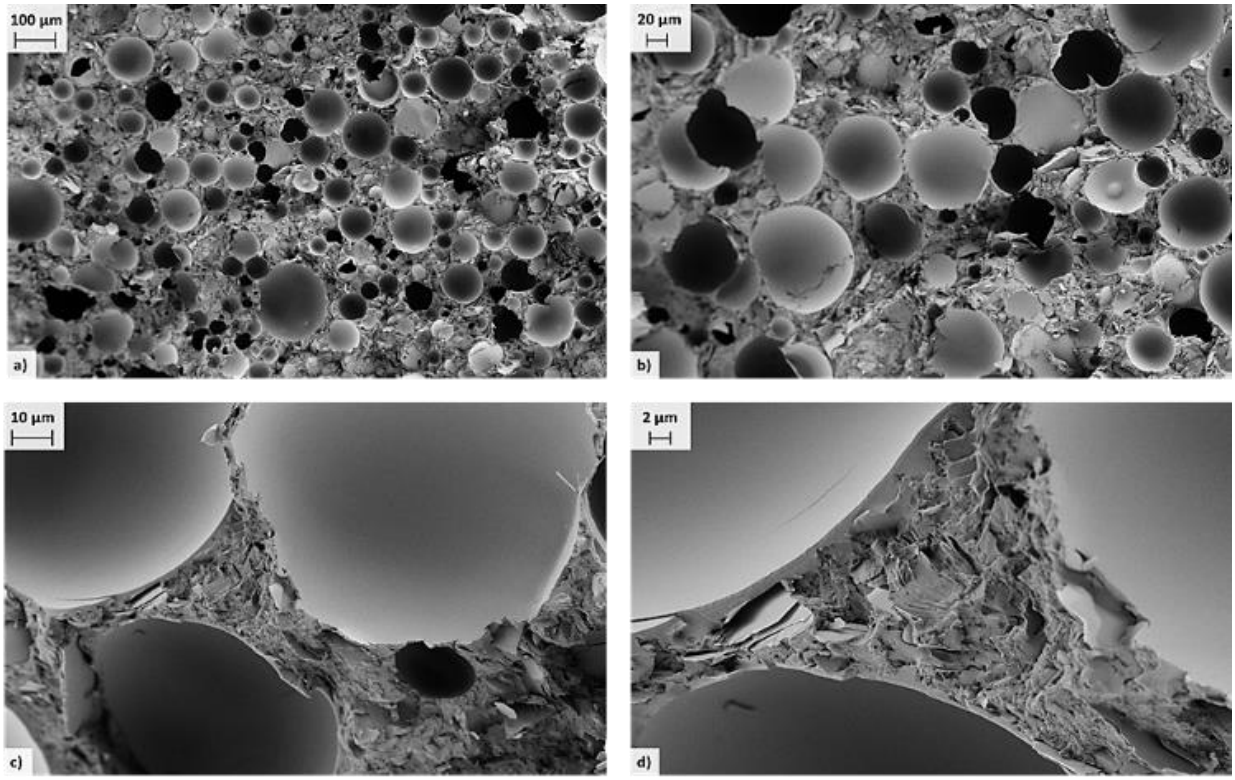

Figure 59: SEM images of Filler_1A

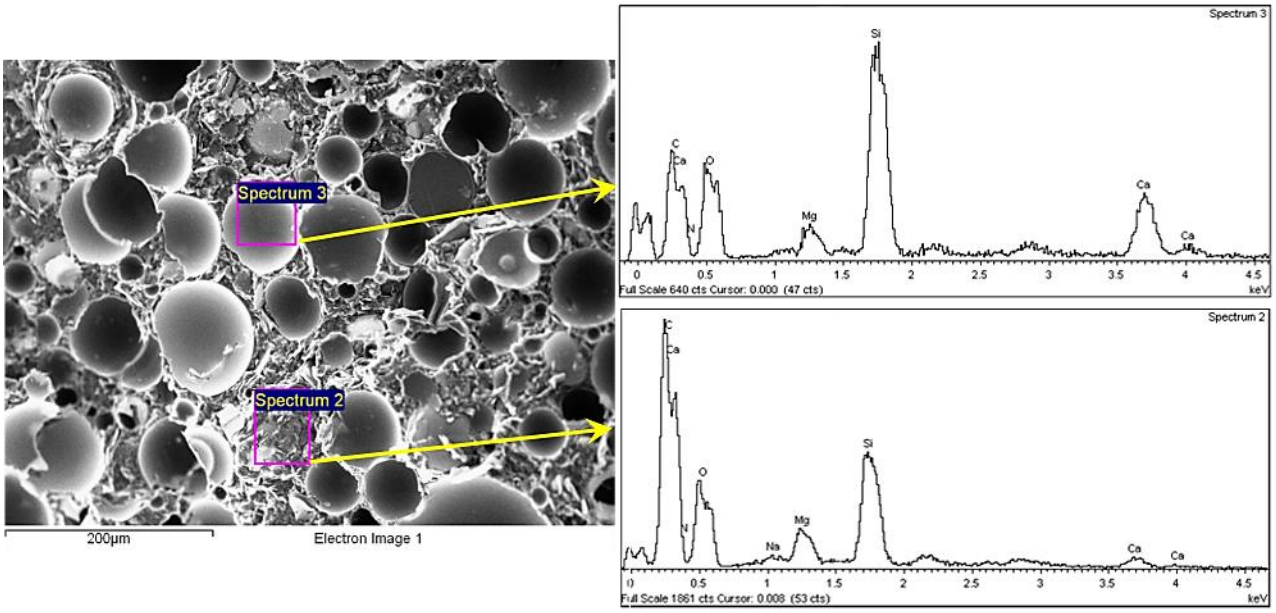

Figure 60: Fliler_1A SEM images (left) and EDX spectra of two sites

SEM images and EDX spectra of Filler_1B are reported respectively in Figure 61 and in Figure 62.

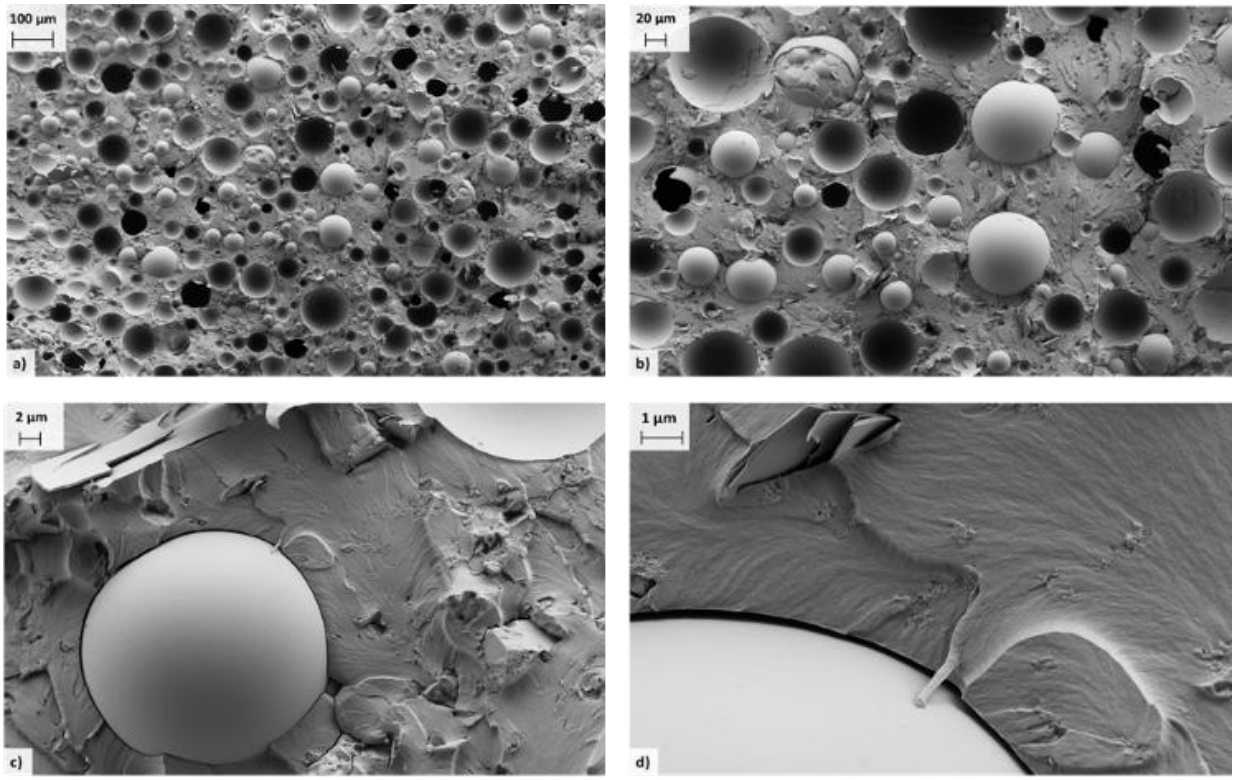

Figure 61: SEM images of Filler_1B

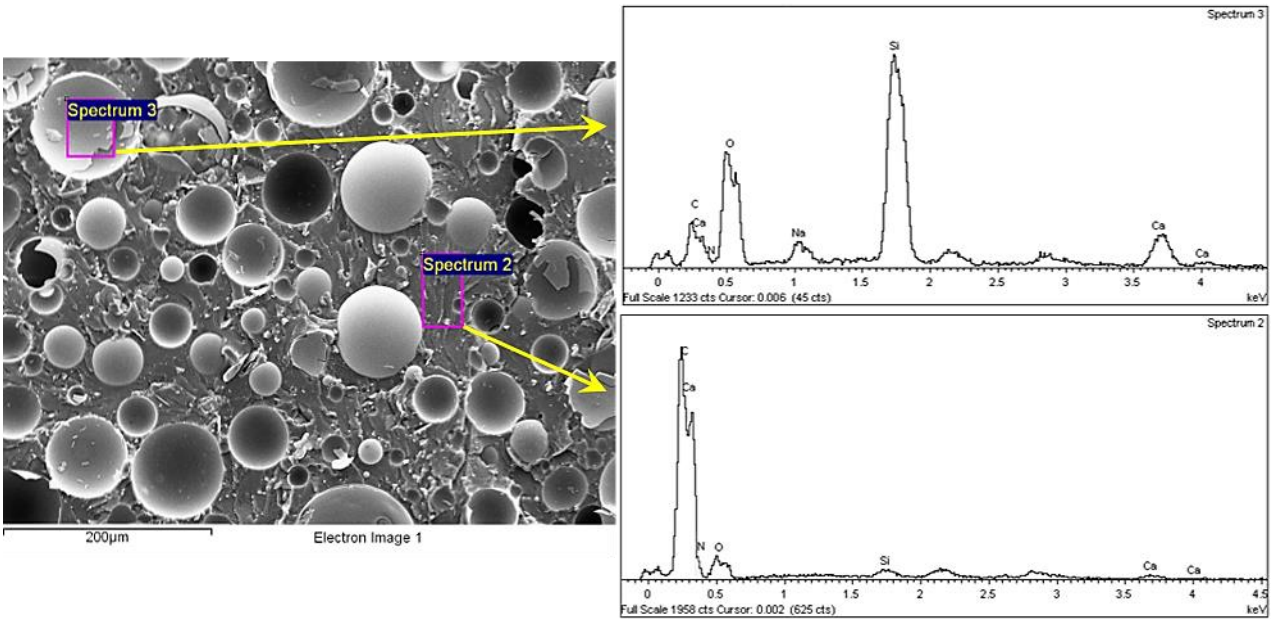

Figure 62: Filler_1B SEM images (left) and EDX spectra of two sites;

For Filler_1B (Figure 61), the adhesion is not really good, as is visible in c) and d) SEM images. Also here, the other extenders appear more or less dispersed. The same observations for Filler_1A component EDX spectra are applied to B component see Figure 62.

SEM images and EDX spectra of Filler_2A are reported respectively in Figure 63 and in Figure 64.

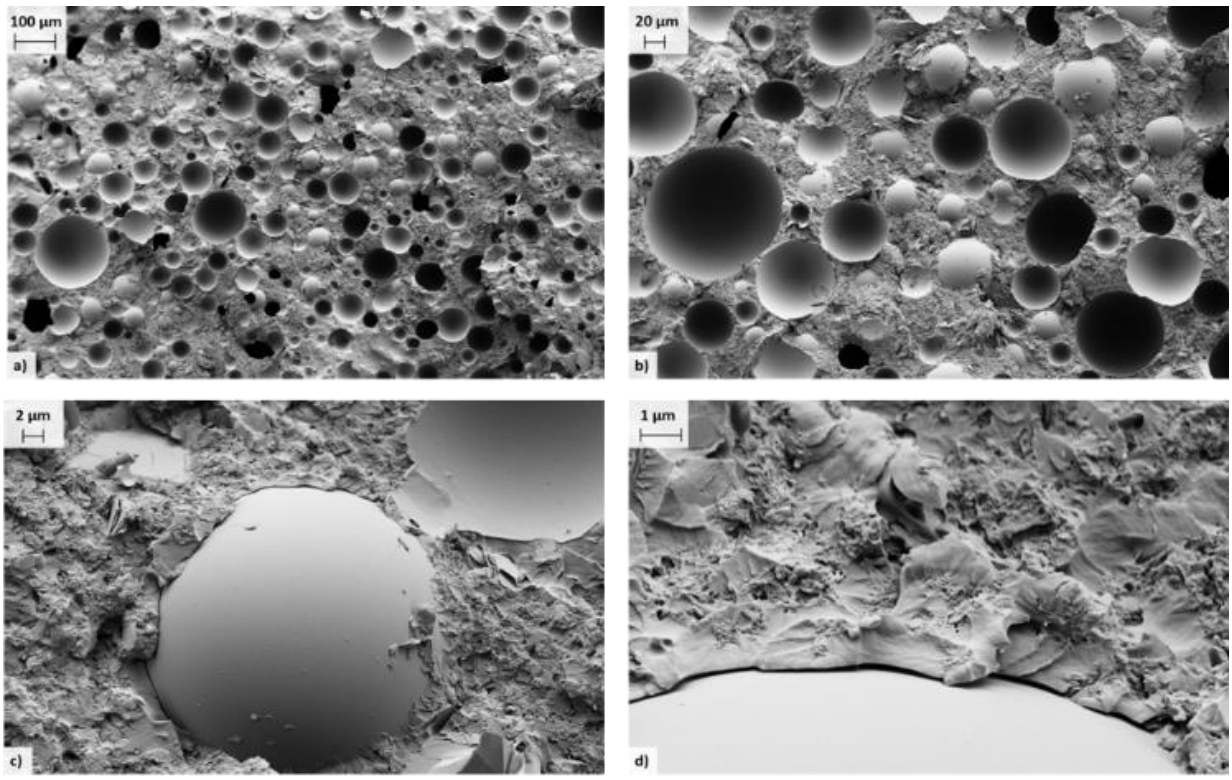

Figure 63: SEM images of Filler_2A

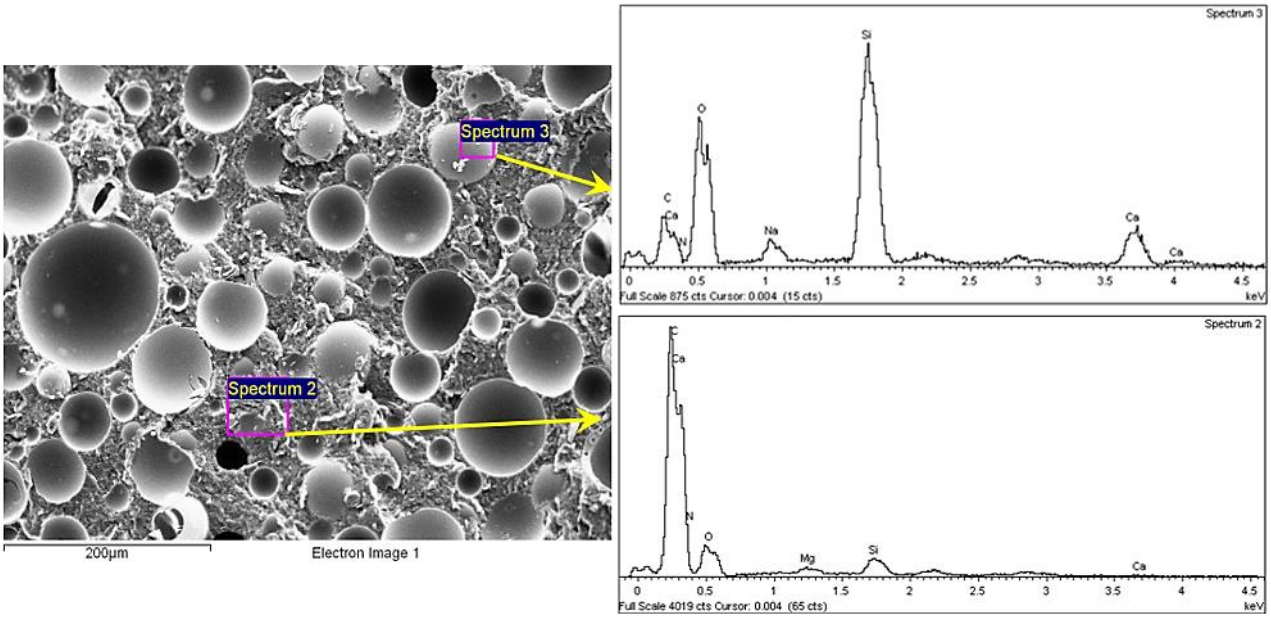

Figure 64: Filler_2A SEM images (left) and EDX spectra of two sites;

For Filler_2A (Figure 63), the incomplete adhesion between matrix and the hollow glass microspheres is visible. The other extenders appear quite well dispersed. In this filler, there are also

alumina-silicate spheres, but in the SEM images they are not visible. In Figure 64, the same observations for the EDX spectra, reported for Filler_1A, are applied to Filler_2A.

SEM images and EDX spectra of Filler_2B are reported respectively in Figure 65 and in Figure 66.

For Filler_2B (Figure 65), the adhesion between matrix and the hollow glass microspheres is better than the Filler_2A, confirmed also by the values reported in Table 12. The other extenders appear quite well dispersed. Here, the alumina-silicate spheres are highlighted by yellow arrows in Figure 65b), they appear as very porous powders. In Figure 66, the EDX spectra of three sites are reported: the first two are entirely analogous to the spectra already discussed, while the third shows how the alumina-silicate spheres are composed mainly by silicon, oxygen, aluminium, titanium and iron.

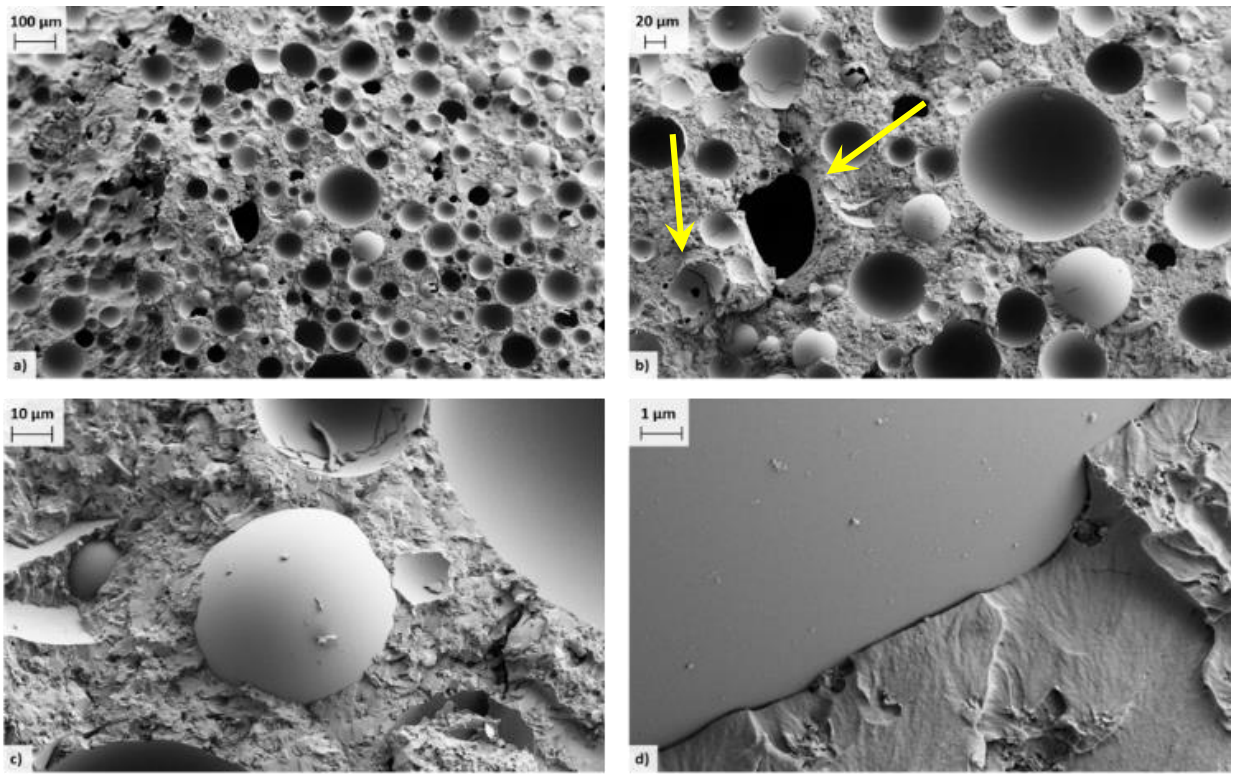

Figure 65: SEM images of Filler_2B

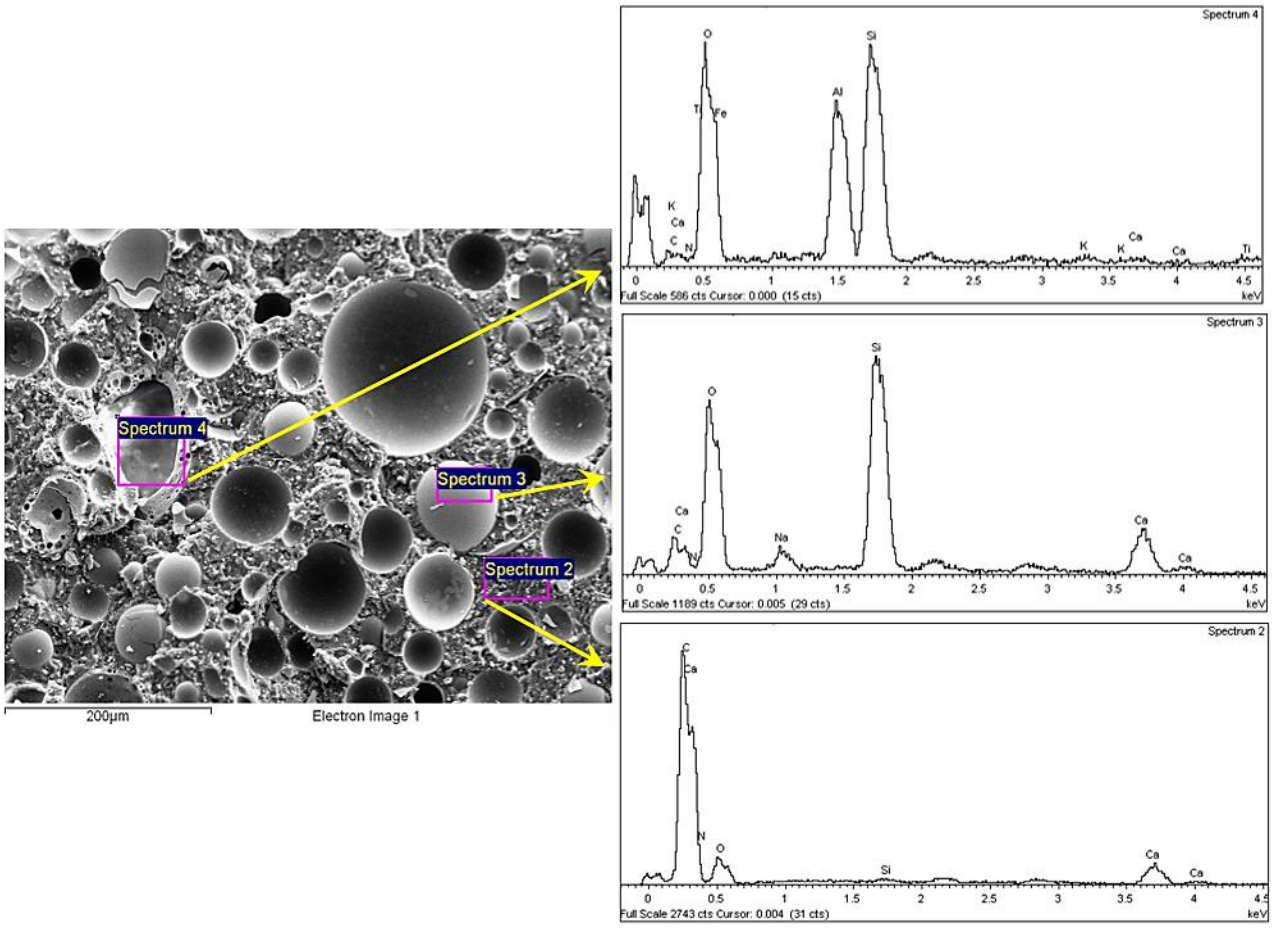

Figure 66: Filler_2B SEM images (left) and EDX spectra of three sites;

Furthermore, to obtain a quantitative analysis of samples, manual image analysis was carried out on digitalised SEM images, by using the image analysis open source software ImageJ 1.51 to measure: 1) the microspheres diameter, 2) the wall thickness and 3) the distance matrix-hollow glass microspheres. These values are reported in Table 12 and each value is a mean of fifty measures.

Filler	Microspheres diameter	Wall thickness	Matrix-microspheres distance
	[µm]		
Filler_1A	47.95 ± 12.5	0.416 ±0.080	~ 0
Filler_1B	43.64 ± 10.01	0.384 ± 0.049	0.249 ± 0.055
Filler_2A	46.81 ± 9.03	0.390 ± 0.50	0.162 ± 0.23
Filler_2B	40.01 ± 10.4	0.377 ± 0.43	0.100 ± 0.36

Table 12: morphological results of commercial fillers

The different adhesion between matrix and extenders, observed in the samples, is confirmed by the values reported in Table 12. Filler_1A exhibits the best adhesion of the matrix with the hollow glass microspheres, indeed the distance between them is not detected (~ 0μm)

4.7 CONCLUSIONS

The characterisation of two commercial filler was necessary in order to have a deeper knowledge of the products and to use them as benchmark for the product subsequently developed (see "Chapter 9: Development of a new filler"). Furthermore, it makes possible also a quality control and/or the investigation of anomalies, following in-field problems.

The study of curing, performed with both techniques IR spectroscopy and DSC, is necessary to evaluate how environmental conditions, such as temperature and humidity, influence the reaction evolution and gain further insight into the reaction mechanism.

More specifically FTIR spectroscopy allows to monitor the curing process at 25°C by following changes in intensity of some diagnostic bands detectable even in such a complex matrix. The analysis of the mid-IR region evidences the decreasing of the relative intensity of the band at 915cm^{-1} assigned to the oxirane ring and the increase in intensity of the broad band centred at 3400cm^{-1} (OH group) confirming the curing process based on the opening of the oxirane group and the nucleophilic addition from the amino group in the amide structure.

The analysis of near-IR spectra of component B also suggests that the normalised NH signal can be related to the extent of curing in the final product depending on the different A/B ratio.

Applying the DSC, the correlation between the glass transition temperature and/or the enthalpy of reaction with curing degree is used to evaluate the kinetic of the cross-linking process. The obtained cross-link degree ranges between 93 and 99 %, for 10°C and 25°C respectively. The samples cured at 25°C reach the maximum curing degree in one week independently of humidity; on the contrary, the samples cured at lower temperature, even after two weeks, do not reach the complete cross-linking. It is evident that the humidity does not influence the curing at 25°C, while it has a slight effect at lower temperature (10°C).

Considering the two commercial fillers, it is evident how for almost all characterisations they appear very similar. Indeed, their slight differences are identified in some rheological behaviours (in recovery and in amplitude sweep tests), in the uniaxial test, in which Filler_1 appears less influenced by

temperature than Filler_2, and finally in the morphological characterisation, where Filler_1A shows the best adhesion matrix and extenders.

CHAPTER 5: EXTENDERS STUDY

This chapter is focalised on the extenders commonly used in the market: two types of glass microspheres (GM), called GM_1 and GM_2, alumina-silicate spheres, carbonates, talc and fumed silica.

In Table 13 are reported the apparent densities, oil adsorption values and the crush resistances. The crush resistance is provided by the suppliers only for hollow glass microspheres and alumina-silicate spheres.

Extenders	Apparent Density [g/cm^3]	OA value [$g_{linseed\ oil}$/100g]	Crush resistance [Bar]
GM_1	0.095	271	21
GM_2	0.155	195	52
Alumina-silicate spheres	0.416	60	208
Carbonates	0.964	23	n.a.
Talc	0.849	40	n.a.
Fumed silica	0.062	320	n.a.

Table 13: apparent densities, oil adsorption values and crush resistances of extenders

The extenders were analysed with IR and morphologically with LVSEM (see 3.7 "Morphological characterisation") to have a deep knowledge of the raw materials.

Furthermore, the GM_1 microspheres were studied rheologically in ad hoc formulations to observe their effect on the rheological performance, over time. This extender was selected, since having low density it can be used in high percentage in the formulation of commercial fillers.

5.1 INFRARED SPECTROSCOPY ANALYSIS

5.1.1 MICROSPHERES

The types of hollow glass microspheres were used in different field of applications, indeed the GM_1 were employed in commercial fillers, while GM_2 were used in the new filler development (see "Chapter 9: Development of a new filler"). The employ of GM_1 in commercial filler was due to the lower density and cost respect GM_2. Compared to the other extenders, they have a lower density,

with the only exception of fumed silica; they show different oil absorption values and different crush resistance, as visible in Table 13.

GM_1 and GM_2 IR spectra are reported in Figure 67, in which a strong band around 1020cm^{-1} is visible. This signal is related to all forms of SiO_2 that show an intense band in range 1110-1080cm^{-1}, as reported in various database of FT-IR spectra [77]. From the IR spectra, the two types of microspheres exhibit the same composition.

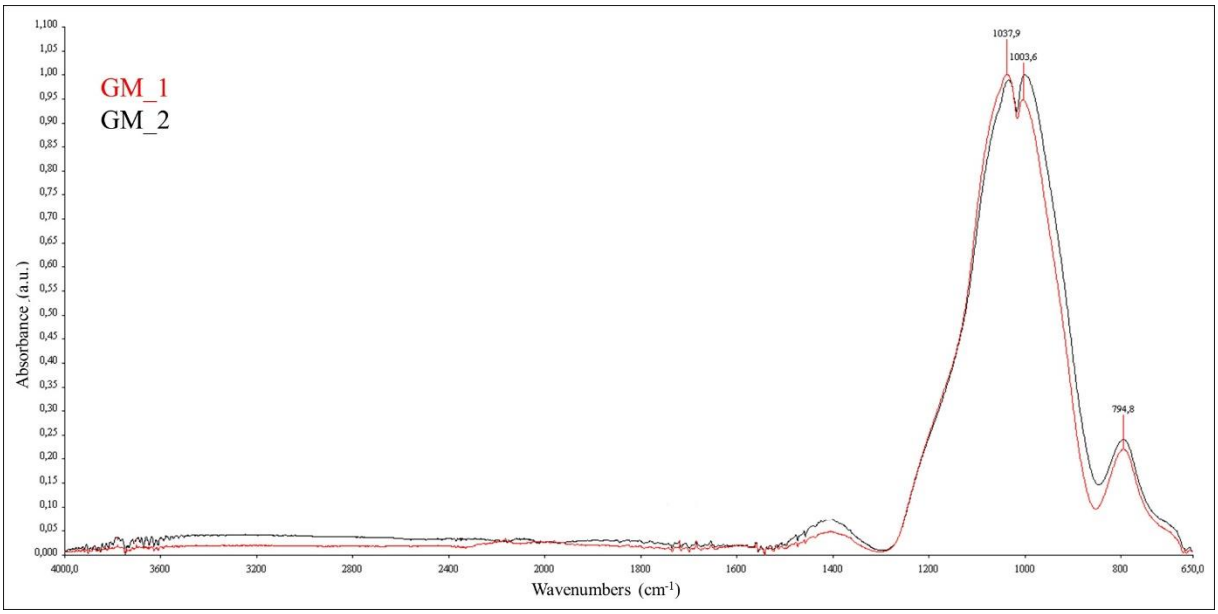

Figure 67: IR spectra of GM_1 and GM_2

5.1.2 ALUMINA-SILICATE SPHERES

For alumina-silicate spheres the apparent density, oil adsorption value and crush resistance are reported in Table 13. The apparent density is higher than that of microspheres and the oil adsorption value is quite low. The crush resistance (208 Bar) is much higher than microspheres resistance.

IR spectrum of alumina-silicate spheres used from the company is reported in Figure 68.

The main peak is at 1027cm^{-1} and it is related to the SiO_2. The other peaks can be associated to the different oxides present in the extender.

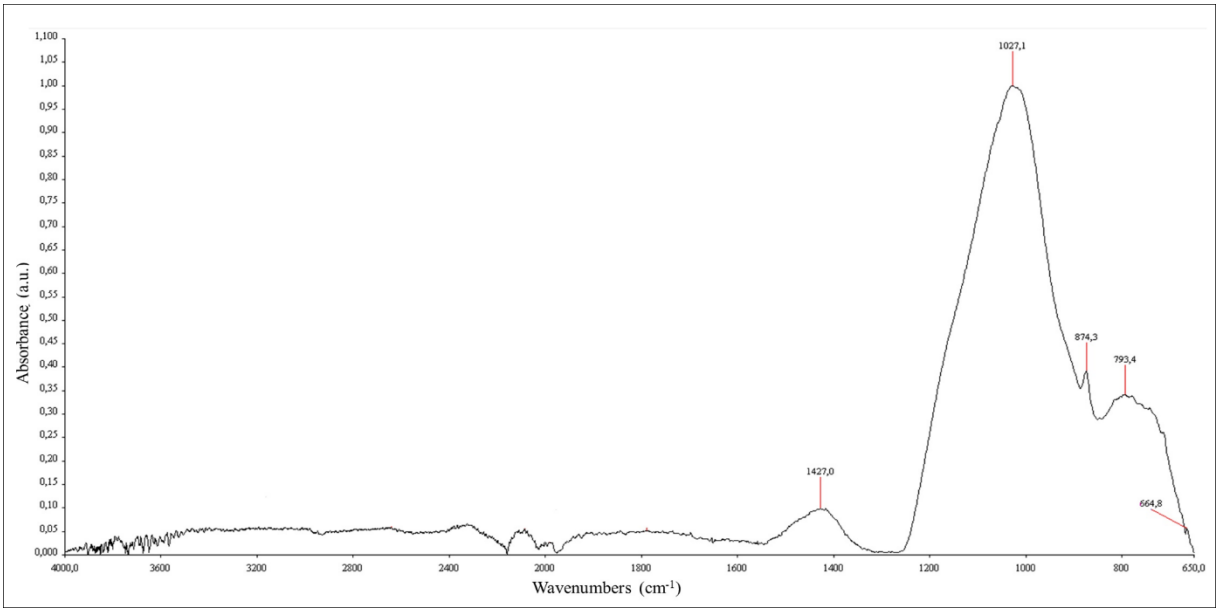

Figure 68: IR spectrum of alumina-silicate spheres

5.1.3 CARBONATES

The carbonates apparent density and the oil adsorption value are reported in Table 13. The apparent density is higher and the oil adsorption value is lower than other standard extenders.

IR spectrum of carbonates is reported in Figure 69.

The main peaks are at 1414, at 874 and 712cm^{-1}, in agreement with the carbonates signals as reported in various database of ATR and FT-IR [77].

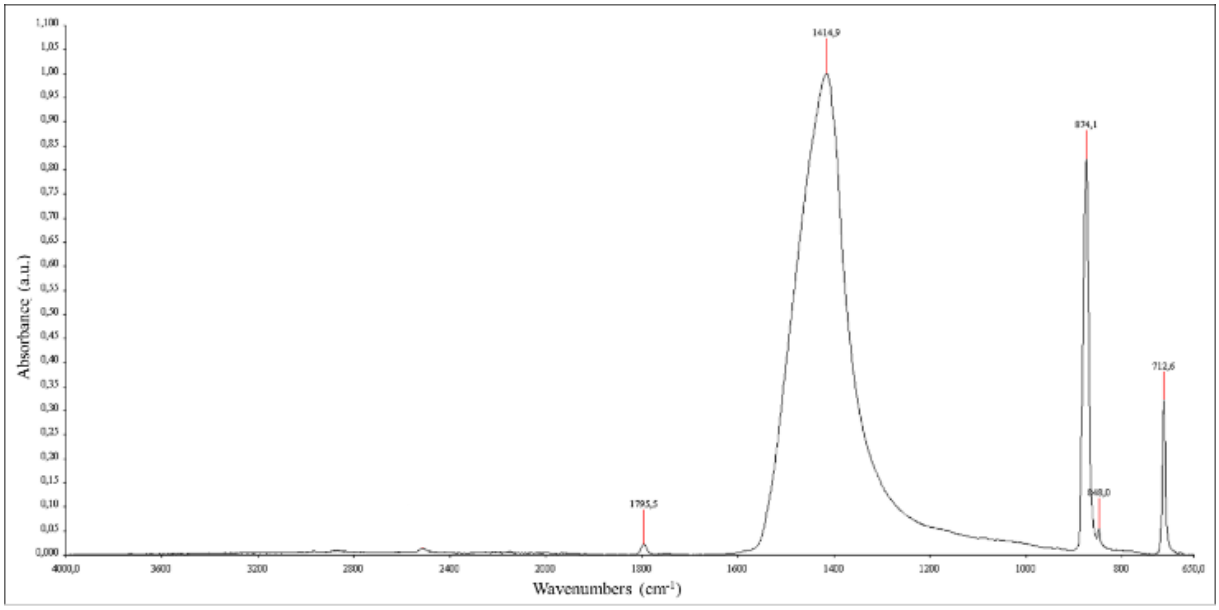

Figure 69: IR spectrum of carbonates

5.1.4 TALC

The talc apparent density and the oil adsorption value are reported in Table 13.

IR spectrum of talc is reported in Figure 70, in which the main peaks are visible at 987 and 663cm^{-1} and they are related to the talc powder as reported in database of FT-IR spectra [77].

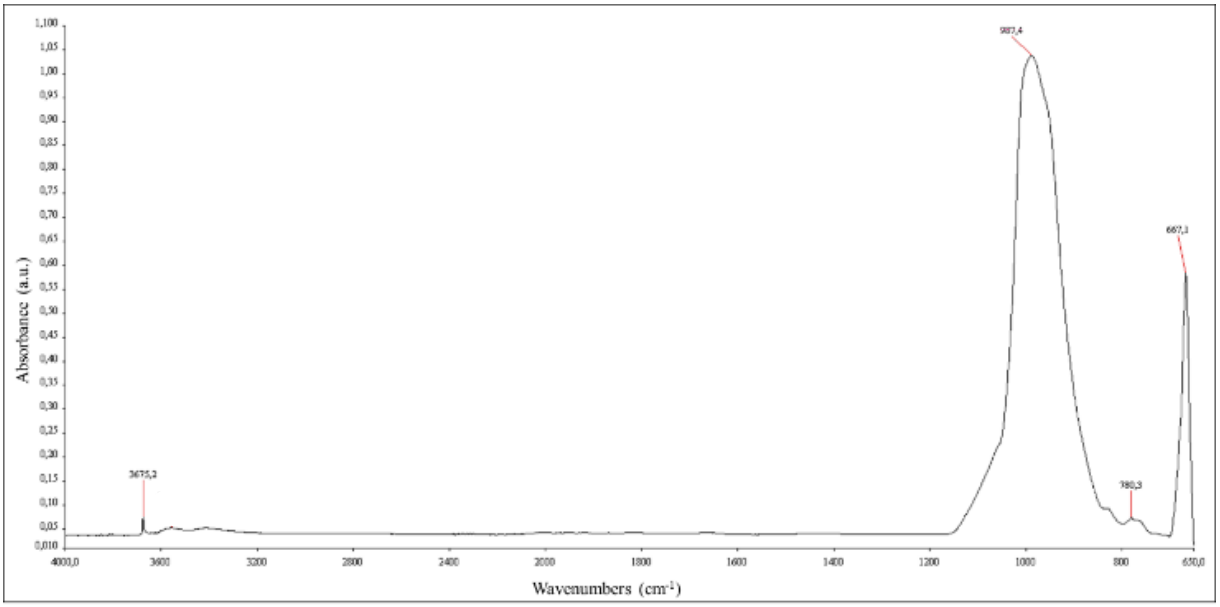

Figure 70: IR spectrum of talc

5.1.5 FUMED SILICA

The fumed silica apparent density and the oil adsorption value are reported in Table 13. The apparent density is lower and the oil adsorption value is higher, as expected, than other extenders.

IR spectrum of fumed silica is reported in Figure 71.

The peak at 1068cm^{-1} is related to all forms of SiO_2 that show on intense band in range 1110-1080 cm^{-1}. The other two peaks at 1220 and at 880-800cm^{-1} are related to the amorphous form of silica.

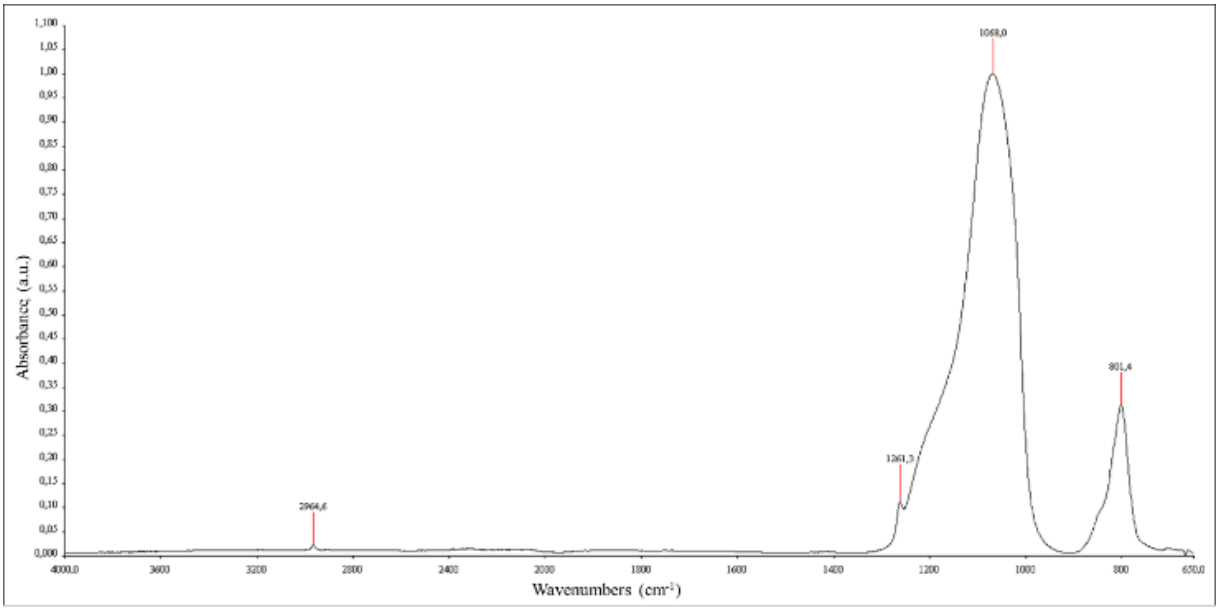

Figure 71: IR spectrum of fumed silica

5.2 MORPHOLOGICAL CHARACTERISATION

Microspheres, alumina-silicate spheres and carbonates, that represent the extenders used in greater quantities in formulations, were morphologically analysed also in cross-linked product, to investigate the matrix-extenders adhesion. Therefore, five samples were prepared each one with a single type of extender (GM_1, GM_2, alumina-silicate spheres…), dispersing them into epoxy resin and, subsequently, cross-linking with a suitable amount of polyamide.

5.2.1 MICROSPHERES

GM_1 and GM_2 SEM images are reported respectively in Figure 72 and Figure 73.

Many GM_1 microspheres are crushed, because they have a lower resistance than GM_2 and so the vacuum, due to LVSEM, caused their explosion.

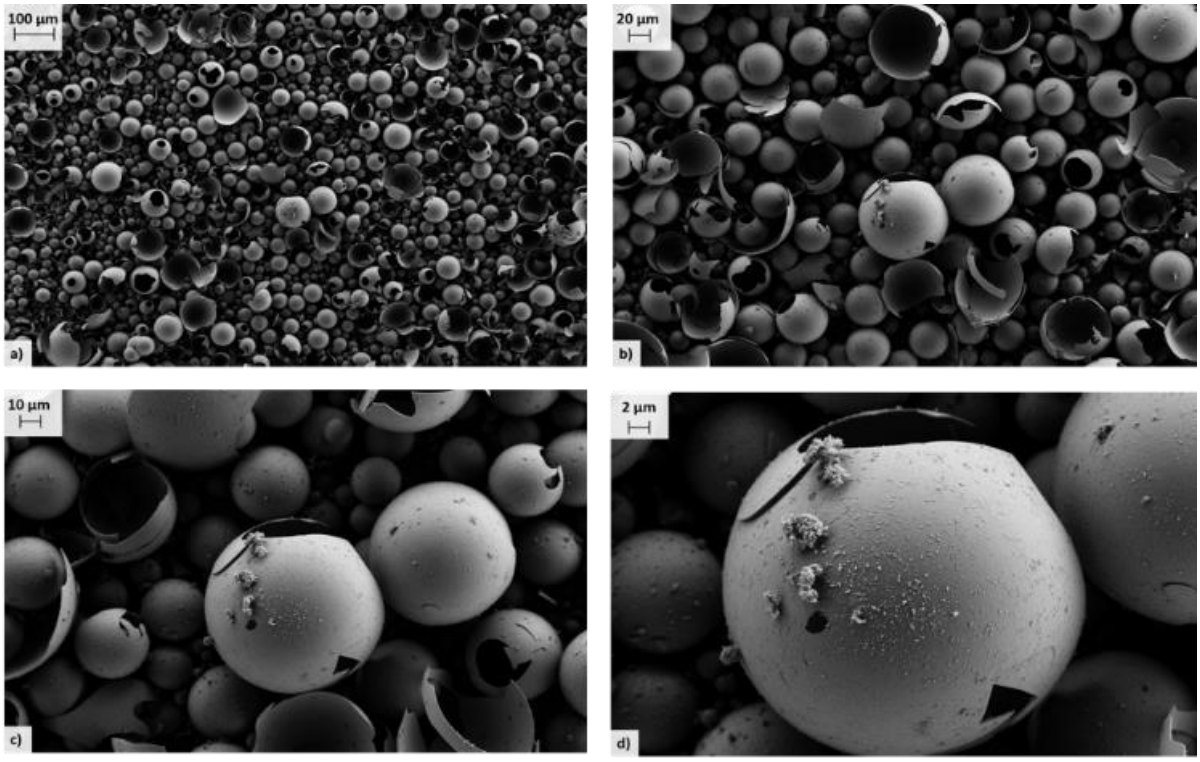

Figure 72: SEM images of GM_1 at different magnifications

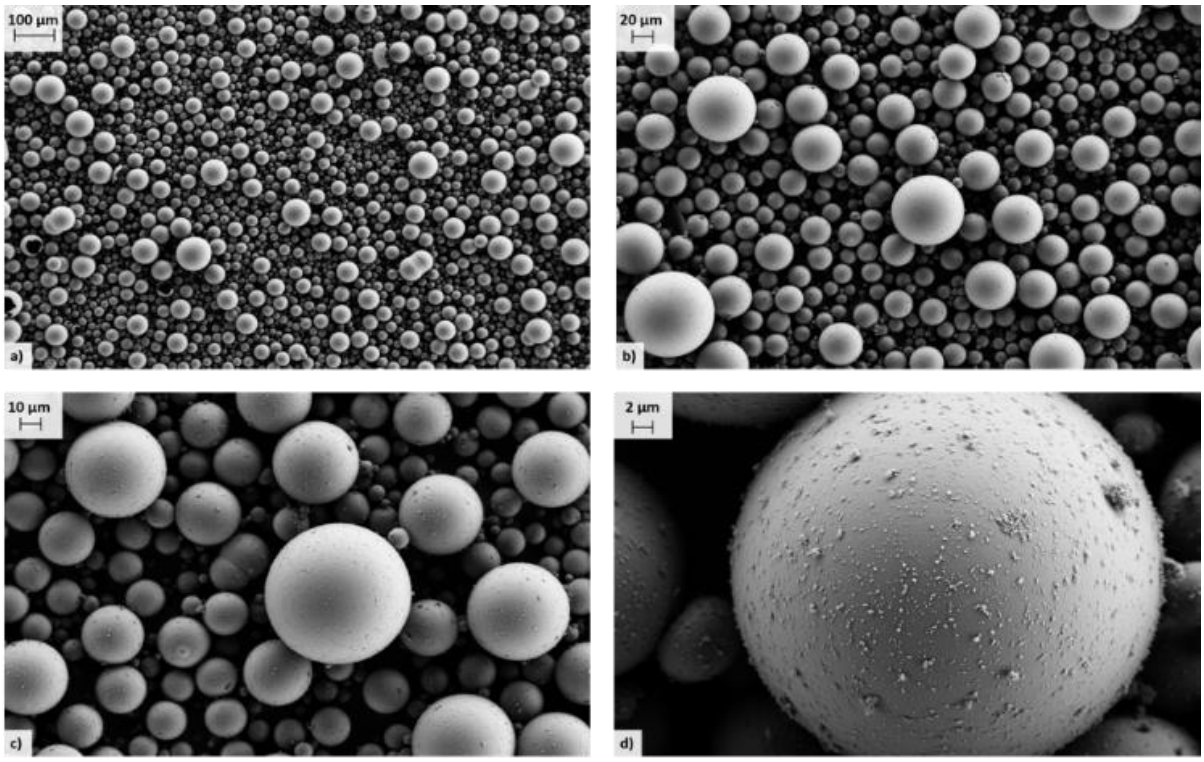

Figure 73: SEM images of GM_2 at different magnifications

SEM images of cross-linked products with GM_1 and GM_2 are reported respectively in Figure 74 and Figure 75.

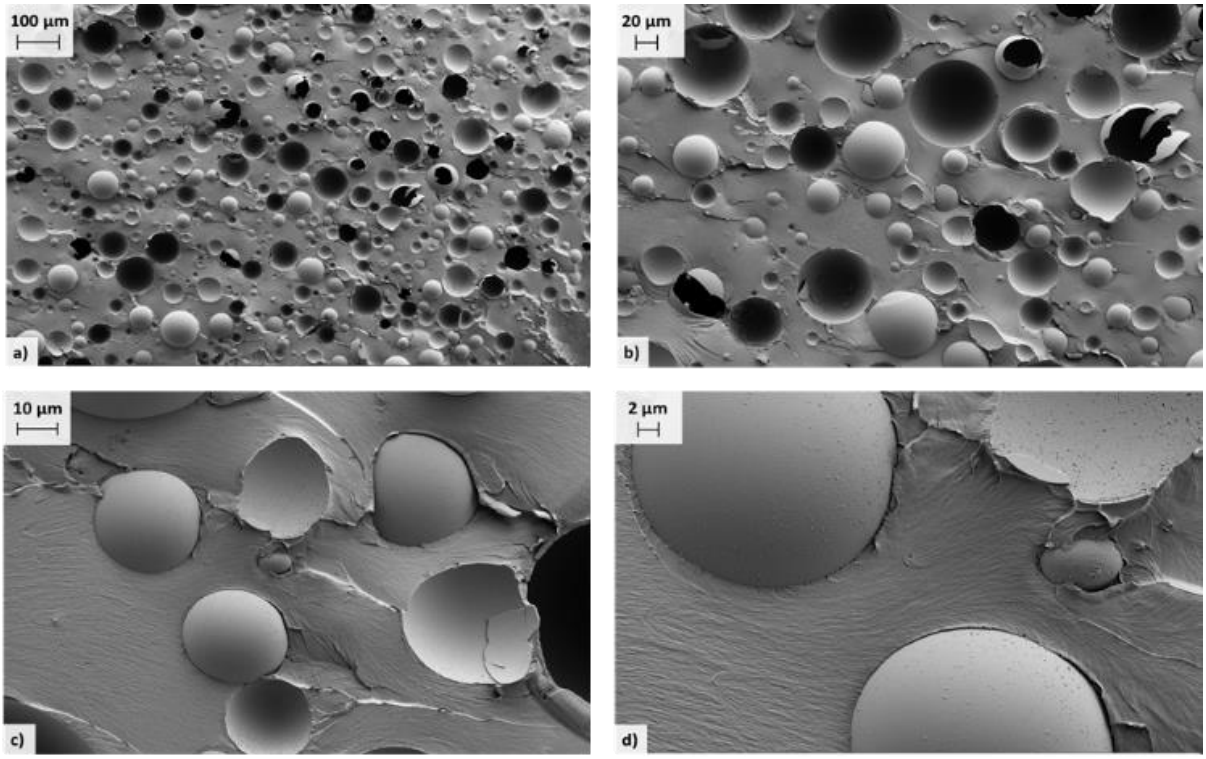

Figure 74: SEM images of cross-linked product with GM_1

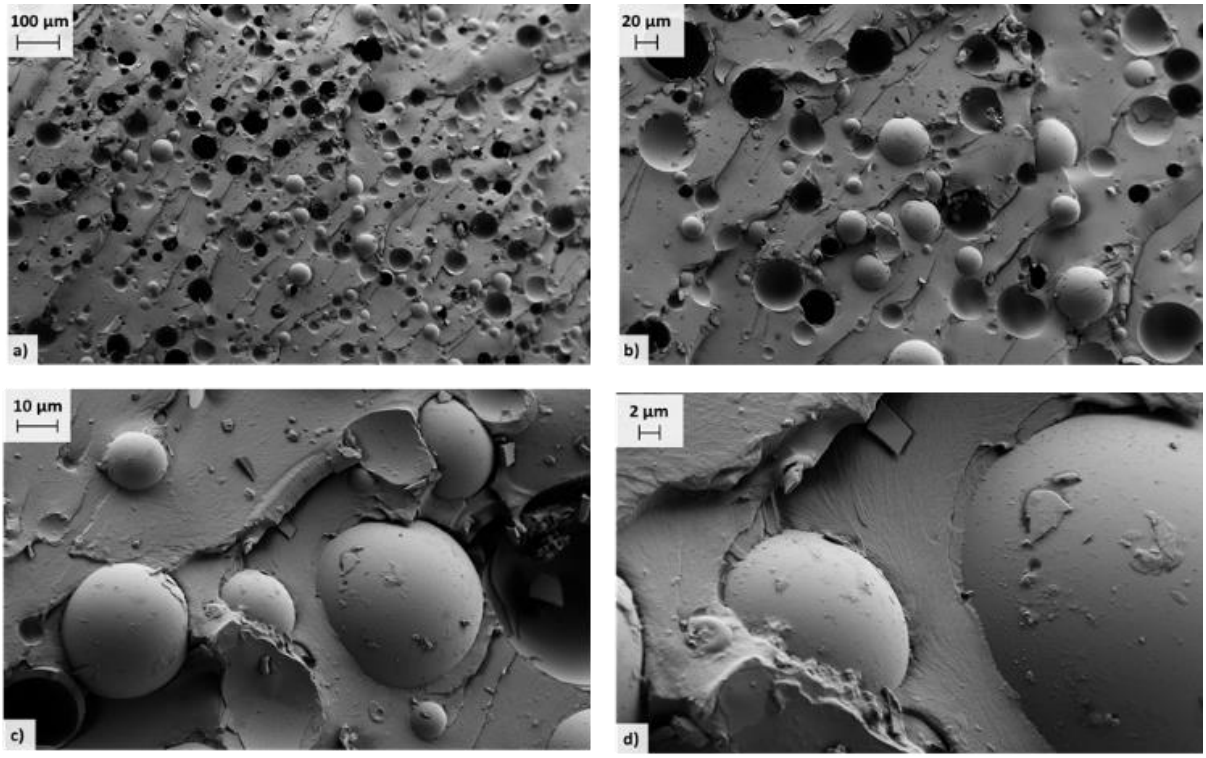

Figure 75: SEM images of cross-linked product with GM_2

Also in the cross-linked product, GM_1 exhibits a higher number of crushed microspheres than in cross-linked product with GM_2. From the SEM images the GM_1 cross-linked product exhibit gaps between matrix and microspheres surface, while in GM_2 gaps are not evident. Therefore, the GM_2 has a stronger matrix-extenders adhesion than GM_1.

The EDX spectra of cross-linked sample with GM_1 and with GM_2 are respectively reported in Figure 76 and in Figure 77. The spectra show the same composition for the two type of microspheres.

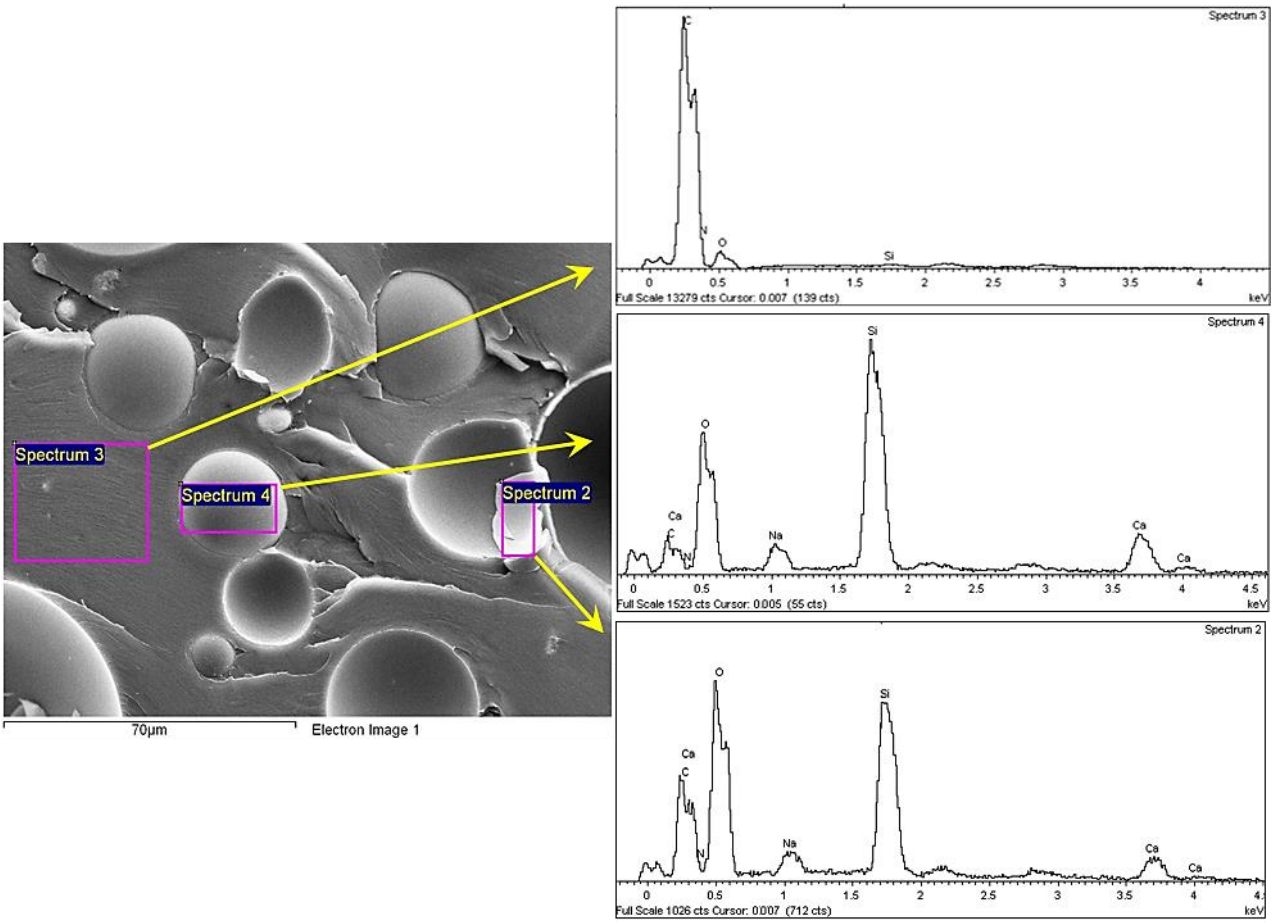

Figure 76: cross-linked product of GM_1: SEM images (left) and EDX spectra of three sites

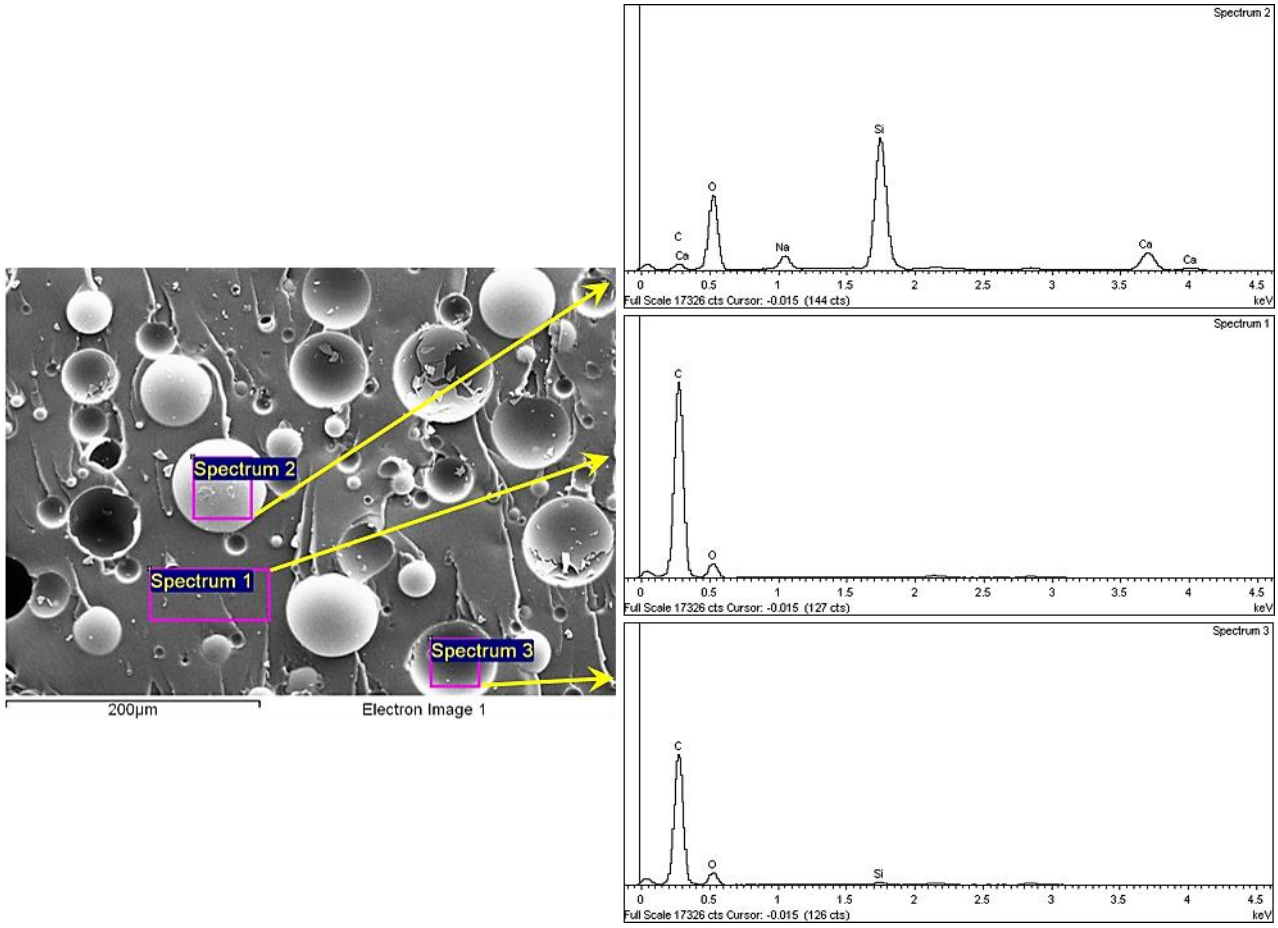

Figure 77: cross-linked product of GM_2: SEM images (left) and EDX spectra of three sites

5.2.2 ALUMINA-SILICATE SPHERES

SEM images of alumina-silicate spheres powders and of cross-linked product are reported respectively in Figure 78 and in Figure 78.

The alumina-silicate spheres, compared with GM_1 and GM_2, have a more irregular morphology, as visible in Figure 78, and are characterised by surface porosity, as already seen previously (see Chapter 4: Characterisation of commercial fillers).

The adhesion between matrix and alumina-silicate spheres appears really strong (see Figure 79).

It is also possible to observe as for particles with spherical shape only the extenders walls are porous and for the particles with irregular shape, as visible in Figure 79c) and d), the porosity is in the whole structure.

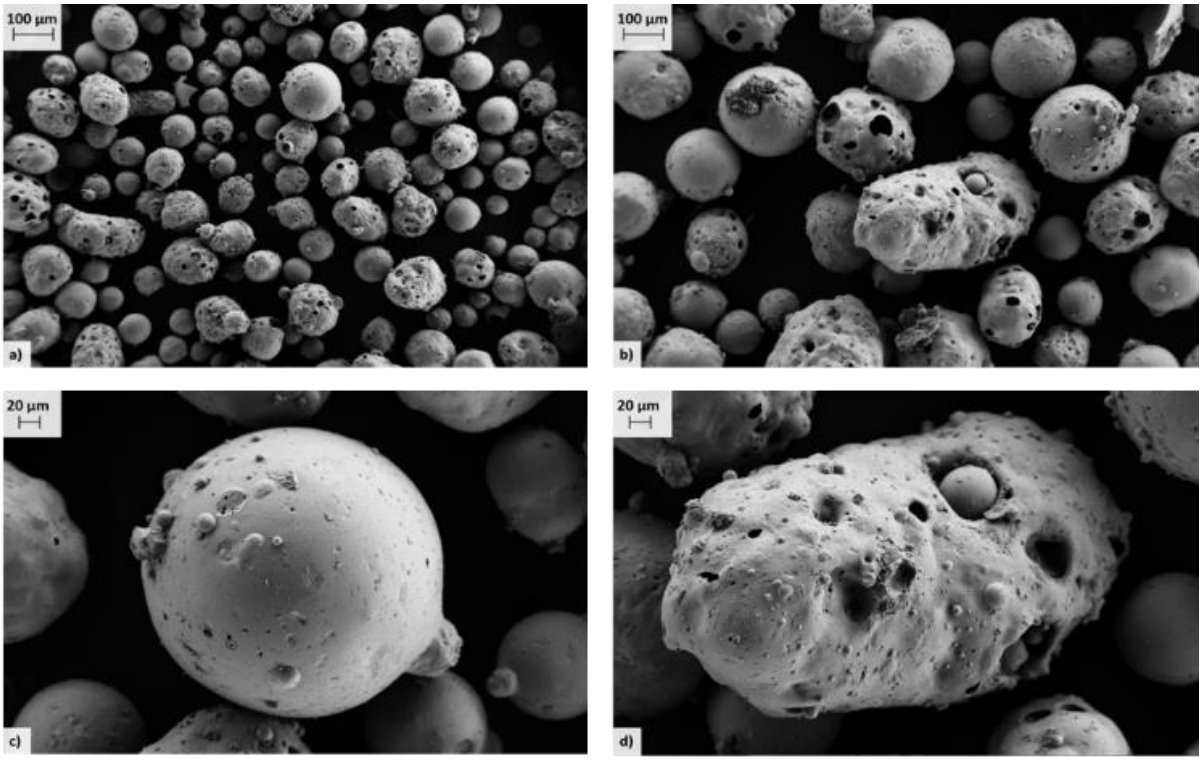

Figure 78: SEM images of alumina-silicate spheres at different magnifications

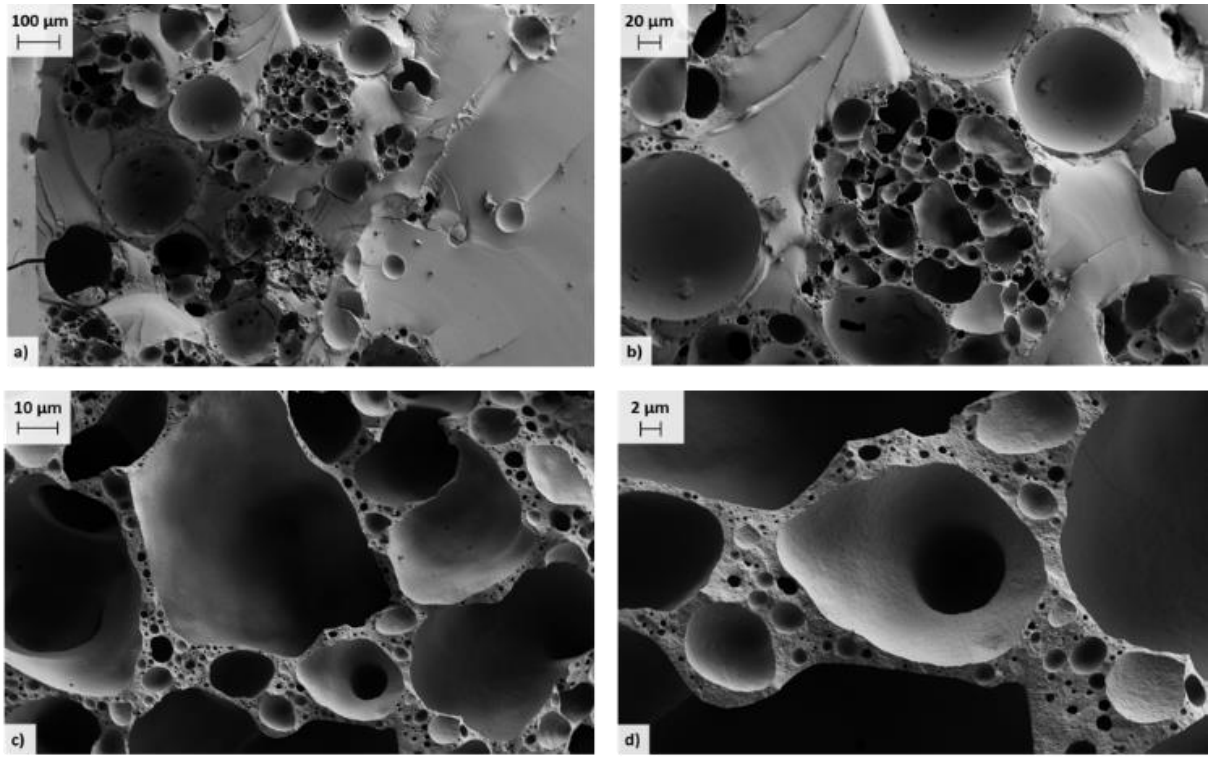

Figure 79: SEM images of cross-linked product with alumina-silicate spheres

The EDX spectra of cross-linked product with alumina-silicate spheres are reported in Figure 80. The spectra show the composition of three sites: the first and the third represent the extenders, the

second the matrix. Indeed, spectrum 4 exhibits high concentrations of Al, Si and O, as the spectrum 2, the spectrum 3 shows high concentrations of C and O.

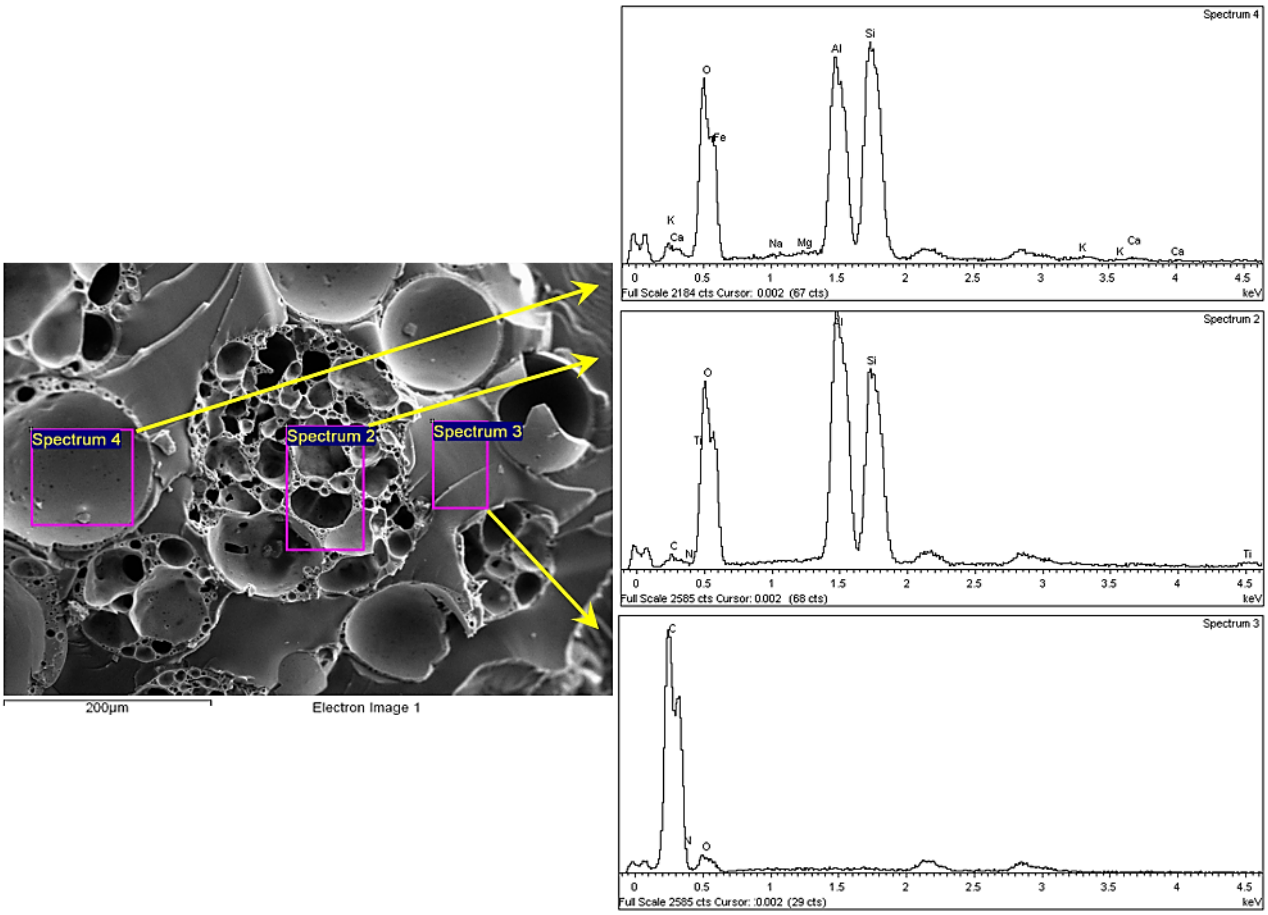

Figure 80: cross-linked product of alumina-silicate spheres: SEM images (left) and EDX spectra of three sites

5.2.3 CARBONATES

SEM images of carbonates powders and of cross-linked product are reported respectively in Figure 81 and Figure 82.

The shape is generally rounded and the size is quite variable. In the cross-linked product, these extenders appear dispersed. The morphology does not allow to identify the gaps between particles and matrix. In Figure 82a), it is also visible a contamination of sample with spherical particle, probably a hollow glass microsphere.

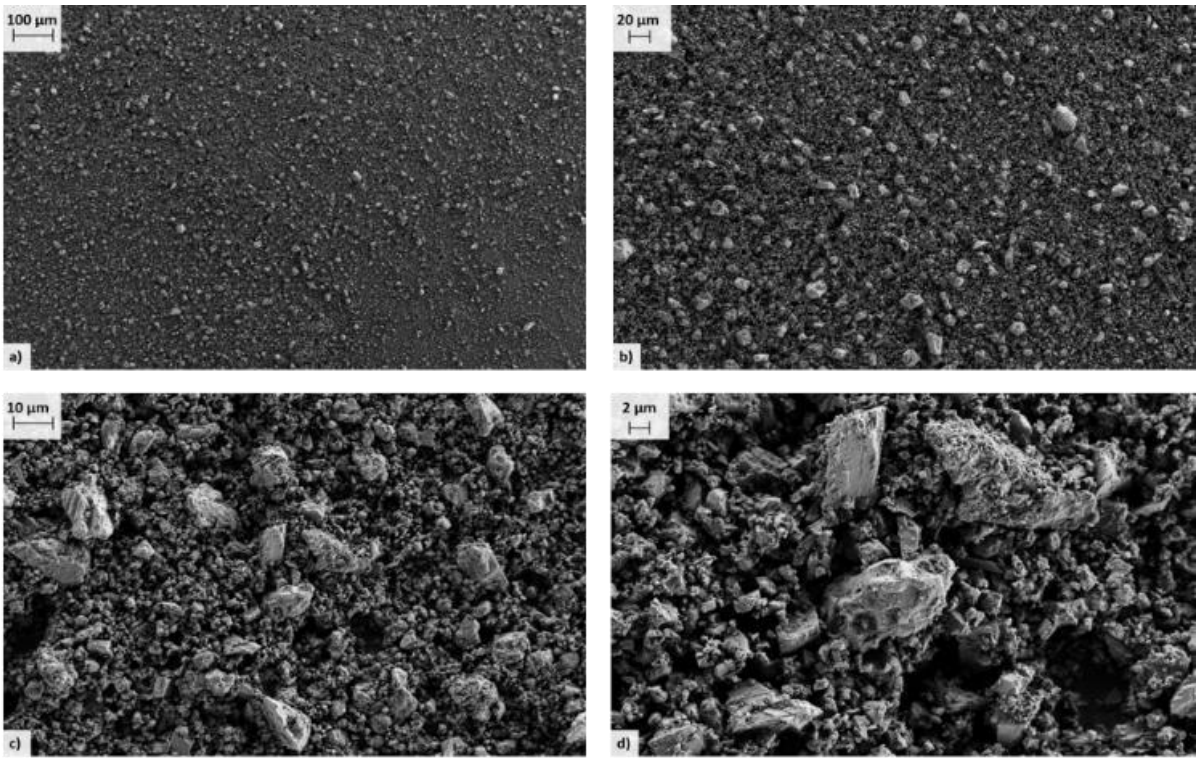

Figure 81: SEM images of carbonates at different magnifications

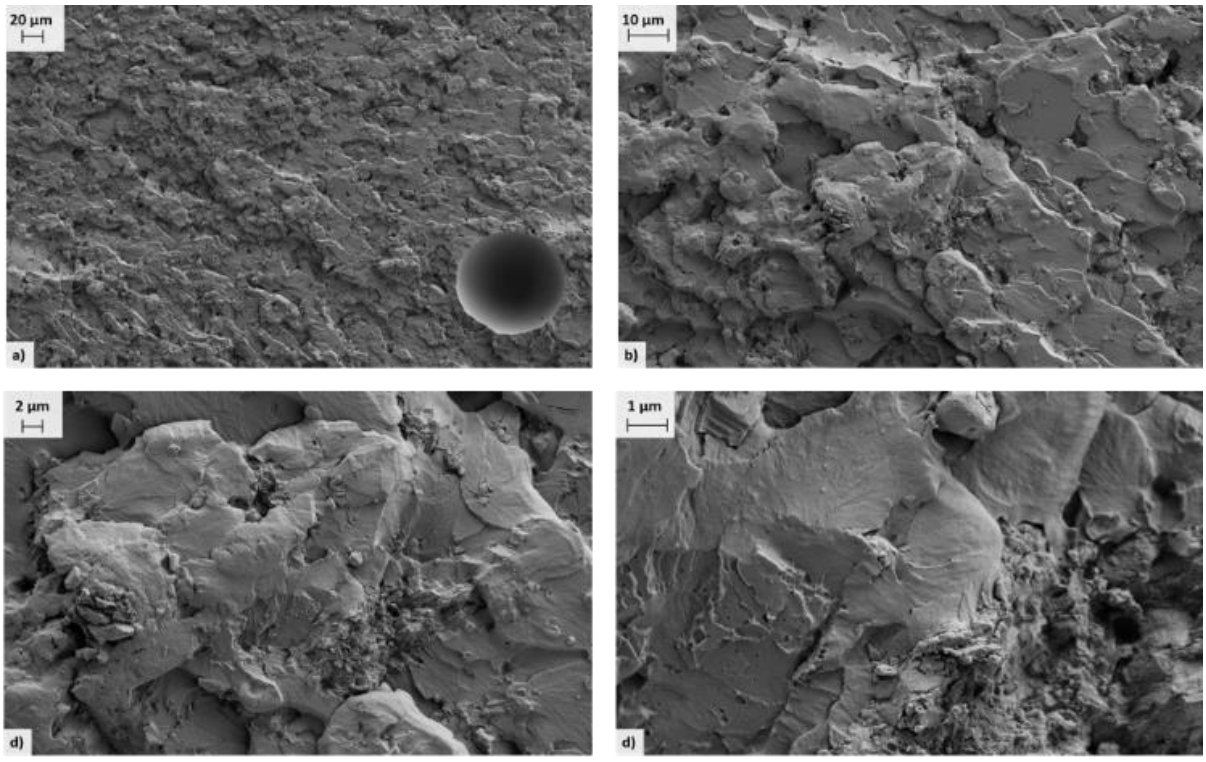

Figure 82: SEM images of cross-linked product with carbonates

The EDX spectra of cross-linked product with carbonates are reported in Figure 83. The two spectra show the same composition (C, Ca and O) and so, the carbonates appear quite dispersed.

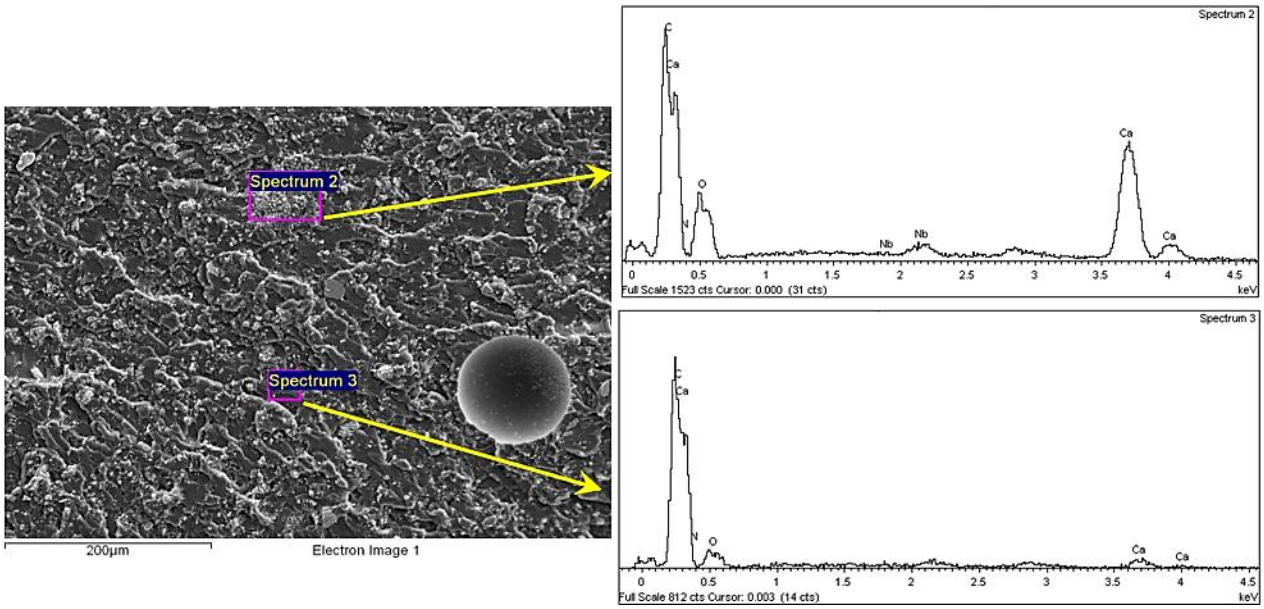

Figure 83: cross-linked product of carbonates: SEM images (left) and EDX spectra of three sites

5.2.4 TALC

SEM images of powders are reported in Figure 84.

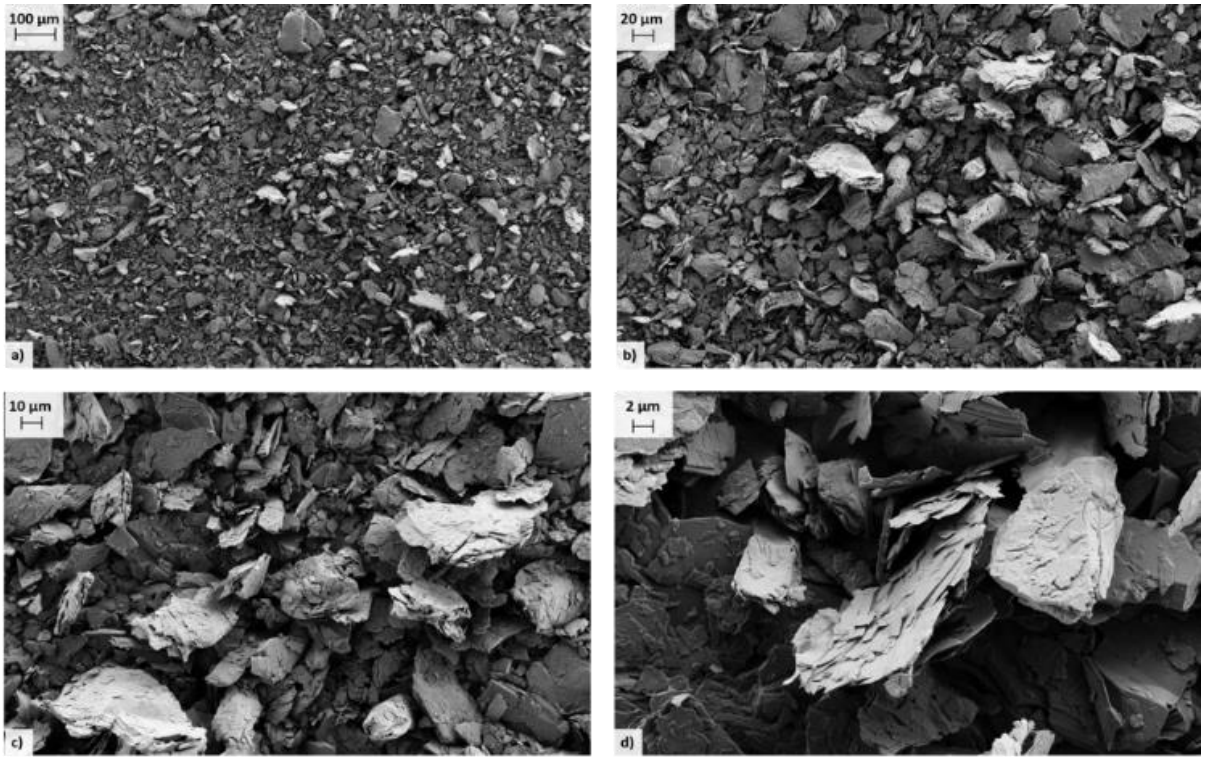

Figure 84: SEM images of talc at different magnifications

The particles appear in flakes and with sizes, similarly to carbonates, varying in a wide range.

5.2.5 *FUMED SILICA*

SEM images of fumed silica powders are reported in Figure 85. The particles appear really small and aggregated.

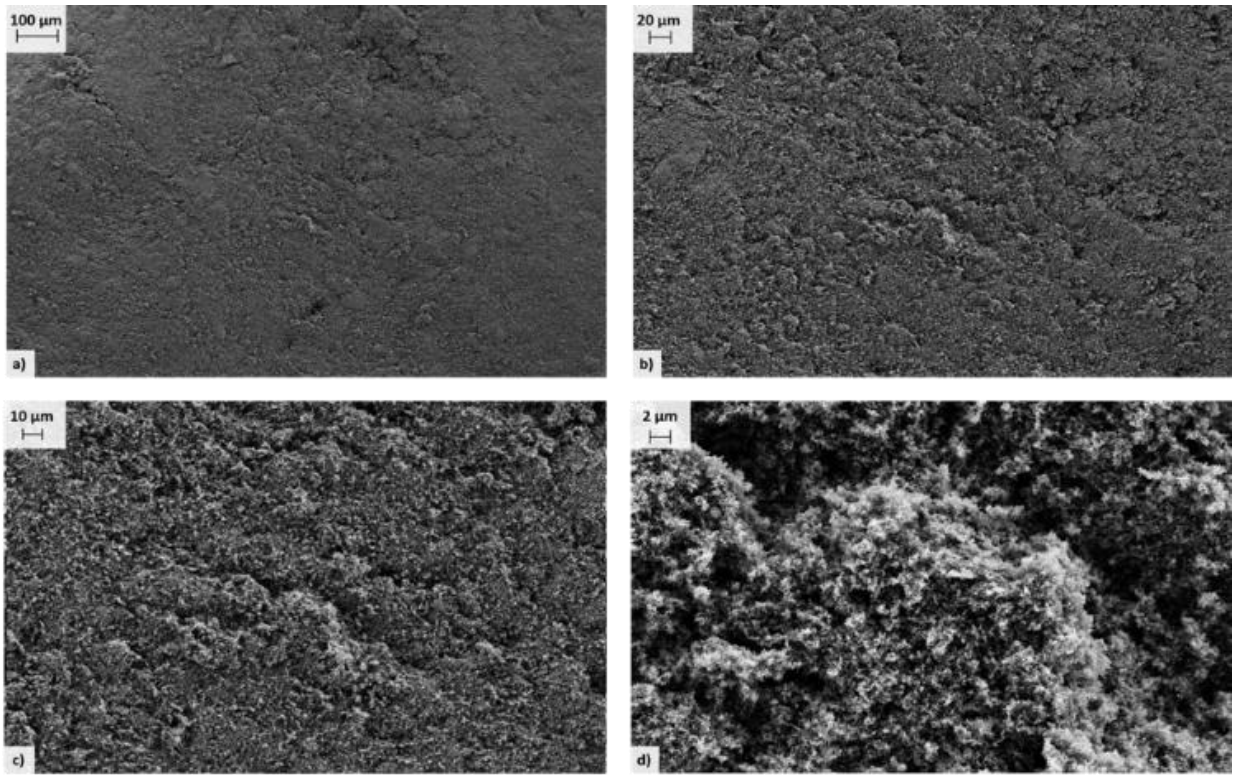

Figure 85: SEM images of fumed silica at different magnifications

Furthermore, to obtain a quantitative analysis of samples, manual image analysis was carried out on digitalised SEM images, by using the image analysis open source software ImageJ 1.51 to measure: 1) the microspheres diameter, 2) the wall thickness and 3) the distance matrix-hollow glass microspheres. These values are reported in Table 14 and each value is a mean of fifty measures.

It was impossible to measure the wall thickness and the distance between matrix-extenders for carbonates and talc.

Extenders	Size	Wall thickness	Distance matrix-extenders
	[µm]		
GM_1	40.1±2.5	0.400±0.053	0.295±0.091
GM_2	39.1±1.3	0.962±0.091	~ 0
Alumina-silicate spheres	167±84	14.8±5.5	~ 0
Carbonates	11.4±8.5	-	-
Talc	25.2±19.1	-	-

Table 14: morphological results of extenders

From the morphological results, reported in Table 14 the microspheres size is more or less the same for both types, but in GM_1 the wall thickness is almost half of GM_2 and indeed, the GM_2 have a greater crush resistance (see Table 13). Regarding the distance between matrix and microspheres surface, the values show the presence of gaps for sample with GM_1 (average value 0.295µm), while for the GM_2 microspheres the adhesion with the matrix is really strong, indeed the gaps are not detected (~0µm).

From the morphological results, the alumina-silicate spheres size is definitely higher than that of microspheres and the high standard deviation is related to the irregular morphology of the particles.

Considering the morphological results of carbonates and talc, the high standard deviation shows as the size of this extender varies in a quite wide range.

Concluding, the different adhesion between matrix and extenders, observed in the samples, is confirmed by the values of the quantitative analysis reported in Table 14.

5.3 RHEOLOGICAL STUDY

To study the effect of GM_1 on single components rheology ad hoc formulations were prepared, in which were added increasing rates of microspheres, replacing alumina-silicate spheres.

Five samples for A component and five for the B component were prepared and they are reported in Table 15 with the GM_1 and alumina-silicate percentages.

Samples	GM_1 Microspheres	Alumina-silicate spheres	Samples	GM_1 Microspheres	Alumina-silicate spheres
	[%]			[%]	
A_0	0.0	14.7	B_0	0.0	17.0
A_2	2.0	12.7	B_2	2.0	15.0
A_4	4.0	10.7	B_4	4.0	13.0
A_6	6.0	8.7	B_6	6.0	11.0
A_9	9.0	5.7	B_9	9.0	8.0

Table 15: samples with increasing rates of GM_1 in both components

The screening test was carried out using recovery test (see 3.5.2 "Recovery test"), since it is quite fast and with the use of the recovery percentage after 30s and the total recovery percentage (see 3.5.2 "Recovery test") it is possible to compare the thixotropic behaviour of different samples numerically. The recovery test was performed at two different times: after one week, t_1, and after six months, t_2, from the production to control its behaviour in time. Indeed, t_1 is representative for the first step of the supply chain (from manufacturer to shipyard), and t_2 is representative of the life-cycle of the product.

The recovery test of A component and of B component samples are reported respectively in Figure 86 and in Figure 87.

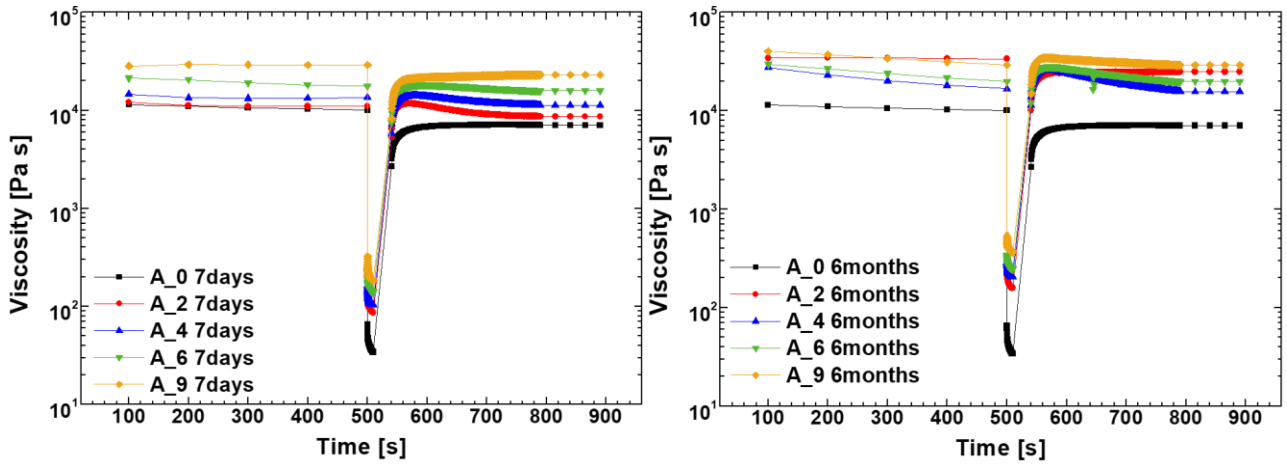

Figure 86: recovery test of A component samples with increasing rates of GM_1 after one week (a) and after six months (b) from the production

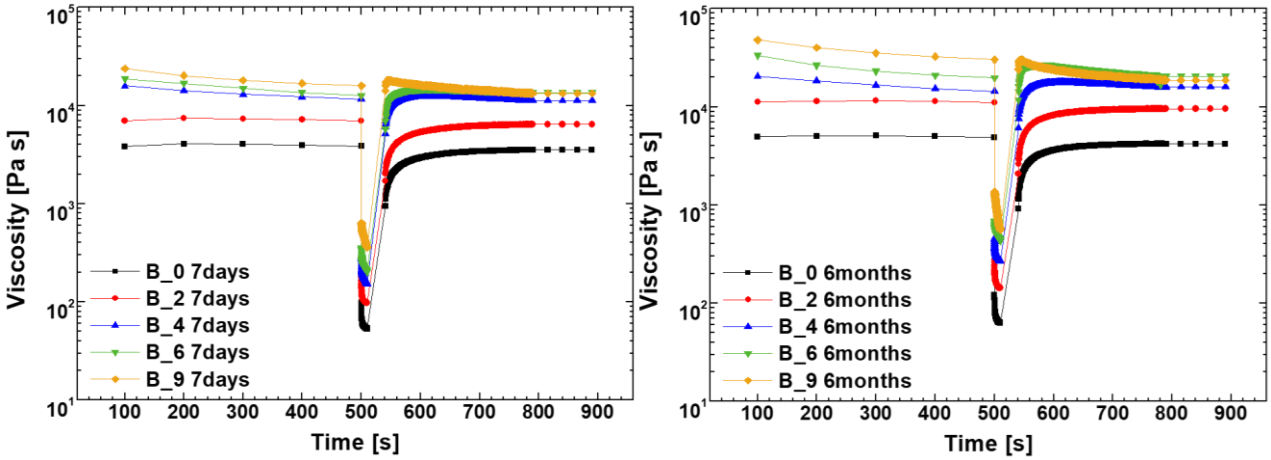

Figure 87: recovery test of B component samples with increasing rates of GM_1 after one week (a) and after six months (b) from the production

In Table 16, the recovery after 30s (Rec_{30s}) and the total recovery (Rec_{tot}) of A component samples are reported.

Samples	Times	Rec_{30s} [%]	Rec_{tot} [%]
A_0	7 days	49	66
	6 months	45	60
A_2	7 days	93	77
	6 months	57	72
A_4	7 days	88	83
	6 months	109	74
A_6	7 days	78	82
	6 months	101	81
A_9	7 days	62	79
	6 months	91	84

Table 16: recovery after 30s and total recovery of A component samples

Observing Figure 86a), A component samples measured after one week from the production, it is visible as increasing the percentage of GM_1, the viscosity increases, as expected. It is also found that, as soon as the high stress is stopped (between 500 and 600s), an elastic contribution is observed that decreases by increasing of the percentage of GM_1.

Indeed, observing the results reported in Table 16, the Rec_{30s} of A_2 is higher than other samples and it decreases as increases the GM_1 percentage.

The total recovery instead is more or less stable, as confirmed by the results listed in Table 16.

After six months, observing Figure 86b), the viscosity tends to increase a little bit for all samples. Moreover, the elastic contribution, as soon as the high stress is stopped (between 500 and 600s), tends to increase above all for samples A_4 and A_6, as visible from the Rec30s listed in Table 16. Instead, the total recoveries grow up increasing the GM_1 percentage.

In Table 17, the recovery after 30s (Rec_{30s}) and the total recovery (Rec_{tot}) of B component samples are reported.

Samples	Times	Rec_{30s} [%]	Rec_{tot} [%]
B_0	7 days	47	89
	6 months	45	84
B_2	7 days	45	92
	6 months	43	87
B_4	7 days	73	88
	6 months	79	83
B_6	7 days	77	88
	6 months	99	84
B_9	7 days	94	70
	6 months	78	51

Table 17: recovery after 30s and total recovery of B component samples

Observing Figure 87a), B component samples measured after one week from the production, it is visible as increasing the percentage of GM_1, the viscosity increases, as expected.

It is also found that, as soon as the high stress is stopped (between 500 and 600s), an elastic contribution is observed that grows by increasing of the percentage of GM_1. The total recovery, instead, has an opposite trend. These considerations are in agreement with the data listed in Table 17.

After six months, observing Figure 87b), the viscosity tends to increases a little bit for all samples, in particular, for samples with high percentage of GM_1. Moreover, the elastic contribution, as soon as the high stress is stopped (between 500 and 600s), tends to increase, above all for samples B_4 and B_6, as visible from the Rec_{30s} listed in Table 17. Conversely, the total recoveries decrease as increases the GM_1 percentage.

5.4 CONCLUSIONS

IR spectra of single components allow a better interpretation of the spectrum of the finished product, making possible also a quality control or the investigation of anomalies, following in-field problems.

Furthermore, the analyses of extenders were performed on:

1. Powders, to have a systematic characterisation, useful for the quality control of incoming materials. It is essential to monitor the raw materials to avoid eventual problems in the final product;
2. cross-linked products, to investigate the adhesion with the matrix, such in case of microspheres.

The study of rheological behaviour of samples with increasing rates of microspheres has permitted to know their effect on the two components. The results confirm that also relative high percentages of microspheres could be inserted in A and B formulations without loss of the rheological performances. The increasing of microspheres involves also in a further advantage: the lowering of specific weight.

CHAPTER 6: SUSTAINABLE & MORE PERFORMANT EXTENDERS

In this chapter, alternative extenders, based on wood fibres and on polymeric microspheres, are studied. These specific products were selected from the products available on the market. Wood fibres were chosen because they are more sustainable than other extenders, polymeric hollow microspheres, according to preliminary tests performed, are more performant, from the rheological point of view, than glass microspheres. Samples realised have been subjected to some coatings tests, rheological and mechanical analyses and morphological characterisation.

6.1 WOOD FIBRES

Recent trends, such as depletion of fossil resources and the increase of greenhouse gas emissions, have encouraged the development of new biodegradable materials produced from renewable sources. For this, natural fibre-reinforced/polymer composites have been developed to replace synthetic composites. The innovative step occurred in the '50s when natural fibres were combined with thermoplastics in various applications. The natural fibres as plant fibres and cellulose-based fibres are the most commonly used bio-extenders, which are available worldwide. Indeed, wood is made up of three of the most abundant natural polymers on Earth: cellulose, lignin and hemicellulose. They can be used for reinforcing various types of polymer matrices, such as thermoplastics or thermoset with potential applications as low-cost building materials, automotive components and others.

Main advantages of natural wood fibres are: renewable character, low cost and lightweight, in addition, they give to the composites stiffness and strength. However, there are some disadvantages such as the hydrophilic character of cellulose and their tendency to adsorb humidity, which is in contrast with most polymers (hydrophobic) [78 - 82].

The natural wood fibres tested were of two types and, for confidentiality agreements, they are called F1 and F2.

In Table 18 are reported the extenders parameters essential for the fillers formulation: apparent densities and oil adsorption values.

Fibres	Apparent Density [g/cm^3]	OA value [$g_{linseed\ oil}$/100g]
F1	0.60	54.0
F2	0.13	216

Table 18: apparent densities and oil adsorption values of natural fibres

6.1.1 NATURAL FIBRES: F1

This fibre was used in A component standard commercial, Filler_2A, in order to replace two standard extenders: alumina-silicate spheres and talc, having similar oil adsorption values, respectively 60 and 51g/100$g_{extenders}$.

In B component standard, Filler_2B, where talc was not present, only alumina-silicate spheres were replaced. An attempt has been done to replace also the hollow glass microspheres, because they are expensive and, during their production, a lot of energy was consumed. In addition, from the point of view of filler production, they require the substitution of cowles with butterfly, in dissolver, causing time loss.

Different formulations were tested and, in Table 19, the percentage of F1, the extenders replaced and total adsorption (see 3.2.1 “Oil adsorption”) of filler are reported.

Sample	F_1	Alumina-silicate spheres	Talc	Microspheres	Total adsorption
	[%]				
Filler_2A	-	5.7	3.5	9.0	39.2
A1_F1	3.5	5.7	-	9.0	39.2
A3_F1	9.2	-	-	9.0	38.7
Filler_2B	-	9.0	-	9.5	38.5
B2_F1	9.0	-	-	9.5	38.0
B4_F1	12.0	-	-	6.5	36.6

Table 19: extenders and total adsorption percentage of fillers with F1

COATINGS TESTS

The specific weight (*S.W.*) was measured at two different times: after one week from the production and after six months, in order to evaluate the stability of products. These values and the increase in

percentage (*Δ*) are reported in Table 20. Note that for the specific weight, there is not a possibility to carry out accelerated tests and therefore the tests continue for a long time (6 months, one year).

Sample	S.W.$_{7days}$ [g/cm^3]	S.W.$_{6months}$ [g/cm^3]	Δ [%]
Filler_2A	0.700	0.750	7.14
A1_F1	0.750	0.830	10.7
A3_F1	0.800	0.893	11.6
Filler_2B	0.720	0.795	10.4
B2_F1	0.743	0.826	11.2
B4_F1	0.882	0.998	13.1

Table 20: specific weight at two different times and their increment in percentage of F1 samples

The specific weight after six months increases for all samples and it increases as the F1 percentage increases. The increase of specific weight is a bit higher than in standards for both new A and B components. However, the specific weight of samples appear acceptable to use these formulation as filler for hull, with the exception of B4_F1, that has a specific weight too high, 0.882 g/cm^3 (see 3.2 “Coating tests”). The specific weight increase is related to the continuous matrix adsorption by the extenders: over time, the adsorption increases up to a saturation value.

The hardness test and the sagging test were performed on the cross-linked products, by mixing A1_F1 with B2_F1, to obtain sample A1+B2_F1, the same for samples A3_F1 and B4_F1.

Example of no sag is reported in Figure 88, for the sample A3+B4_F1. The two components have the highest specific weight among all the samples; nevertheless, it is evident that the cross-linked product does not sag.

Figure 88: sagging test of sample A3+B4_F1

The values of Shore D test, after 7 days from application, are reported in Table 21. As to the specific weight, also the Shore D values increase as the percentage of F1 increases. The samples appear

homogeneously cross-linked, in fact the instantaneous measures and the one after 15s reported in table are very similar.

Sample	Shore D_{7days}
Filler_2A+2B	61/60
A1+B2_F1	68/67
A3+B4_F1	71/69

Table 21: Shore D values of F1 cross-linked samples

RHEOLOGICAL ANALYSIS

Each sample was measured at different times: after one week, after thirty days and after six months form the production to control its behaviour in time. The rheological analyses were performed both in rotatory mode, with recovery tests (see 3.5.2 "Recovery test"), and in oscillatory mode, with amplitude sweep tests (see 3.5.3 "Amplitude sweep test").

A components

In Table 22 are reported the recovery percentage after 30s (Rec_{30s}), the total recovery percentage (Rec_{tot}), the distance between the moduli (G'-G'') its increment in percentage after one month and six months respect to the measure performed at one week, $\Delta(G'-G'')$, and the end of Linear Viscoelastic Range (*LVER*), obtained from RheoCompass s1.19.

Data of A component standard are reported in Table 22 to compare them with the new samples.

Sample	Times	Rec_{30s} [%]	Rec_{tot} [%]	G'-G'' [kPa]	Δ(G'-G'') [%]	LVER end [%]
Filler_2A	7 days	53	92	25	-	0.005
	6 months	57	85	27	8.00	0.005
A1_F1	7 days	209	82	26	-	0.020
	30 days	208	92	27	3.85	0.020
	6 months	217	100	30	15.4	0.010
A3_F1	7 days	260	103	22	-	0.020
	30 days	195	100	28	27.3	0.010
	6 months	158	99	31	40.9	0.010

Table 22: rheological data of recovery and amplitude sweep tests of A components

Sample A1_F1 recovery test and amplitude sweep test are reported in Figure 89.

It shows an excellent thixotropic behaviour: there is a remarkable elastic contribution, as soon as the high stress is stopped (between 500 and 600s). This thixotropic behaviour is better than in the standard, indeed as visible in Table 22, A1_F1 exhibits a higher Rec_{30s} (over 200%) respect to the standard (below 60%). This is valid for all measurements over time. It is also highlighted the Rec_{tot} increases over time.

In addition, the sample exhibits a good separation between the moduli (over 26 kPa), that increases more, over time, compared to the standard. Furthermore, the end of LVER is detectable at higher shear strain (0.01-0.02%) than that of standard (0.005%). At the end, the measurements show that A1_F1 is quite stable over time.

Consequently, from the rheological point of view, A1_F1 appears a very good A component: it is applicable at a greater thickness (high Rec_{30s} and Rec_{tot}), it can suffer shear strain higher without disrupting its internal structure and its storage stability is really good.

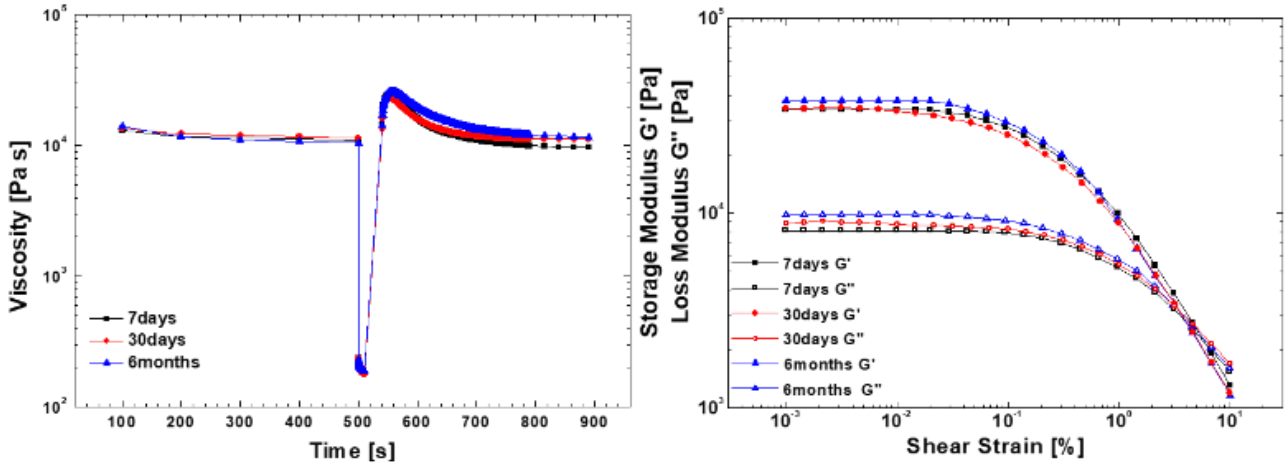

Figure 89: recovery test (left) and amplitude sweep test (right) of sample A1_F1

Sample A3_F1 recovery test and amplitude sweep test are reported in Figure 90.

The same considerations for A1_F1 can be made for A3_F1, indeed both samples have trends comparable. However, in A3_F1 the viscosity increases a bit during the time and so the Rec_{30s} and the Rec_{tot} (Table 22) decrease from one week to six months.

Furthermore, the distance between the moduli, over time, in A3_F1 (42%) increases more than in sample A1_F1 (15%), as reported in Table 22. The end of LVER is comparable to sample A1_F1, and so higher than that of standard.

The storage stability over time is less good than in sample A1_F1.

Nevertheless, sample A3_F1 still appears a good A component, since exhibits medium-high recoveries and a greater LVER than that in Filler_2A, having also a moderate storage stability.

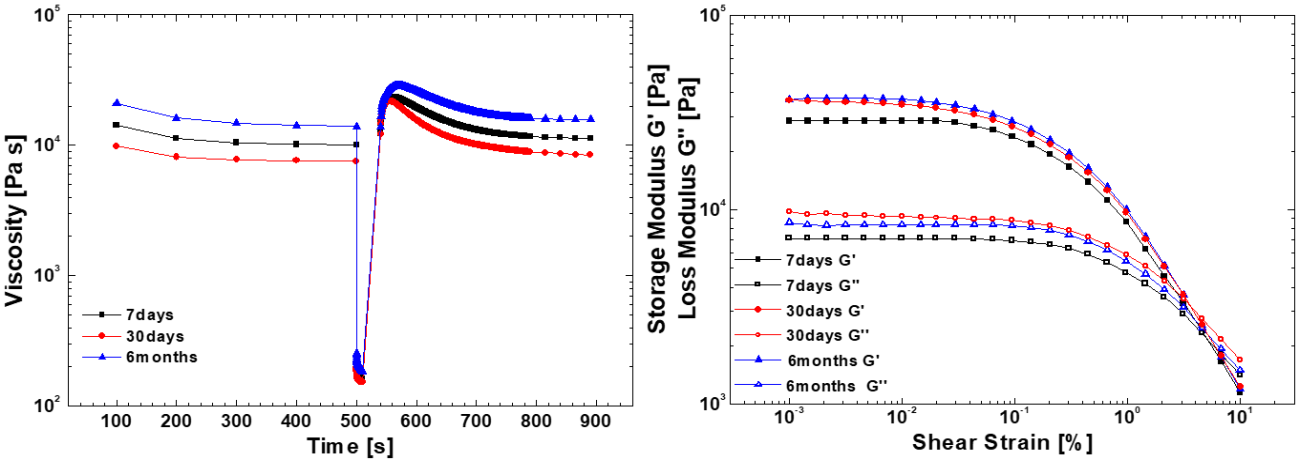

Figure 90: recovery test (left) and amplitude sweep test (right) of sample A3_F1

B components

For the B component, the recovery percentage after 30s, the total recovery percentage and the distance between the moduli, its increment in percentage after one month and after six months respect to the measure performed at one week and the end of LVER are reported in Table 23.

Sample	Times	Rec_{30s} [%]	Rec_{tot} [%]	G'-G'' [kPa]	Δ(G'-G'') [%]	LVER End [%]
Filler_2B	7 days	56	50	12	-	0.005
	6 months	49	50	14	16.7	0.005
B2_F1	7 days	67	64	18	-	0.005
	30 days	62	55	25	38.9	0.005
	6 months	43	23	132	633	0.005
B4_F1	7 days	61	92	1.5	-	0.010
	30 days	74	90	6.9	360	0.010
	6 months	60	55	12	700	0.010

Table 23: rheological data of recovery and amplitude sweep tests of B components

Sample B2_F1 recovery test and amplitude sweep test are reported in Figure 91.

It shows a particular thixotropic behaviour: in all measurements, the recovery (Table 23) is not total and over time, after 30 days and after 6 months, it tends to decrease after a slight elastic behaviour

between 500 and 600s. Respect to the standard, the recoveries of samples are lower.

From the amplitude sweep test, the measure after 6 months exhibits a higher separation between moduli (132kPa) than the measures after 7 (18kPa) and 30 days (25kPa), with an increment percentage, after six months, of 633%. This increment is much higher than that of the standard.

The end of LVER is detectable at shear strain 0.005%, as that of standard. In addition, the viscosity tends to increase significantly over time. Summing up the storage stability is scarce.

These results permitted to consider this sample inadequate for use as filler for hull.

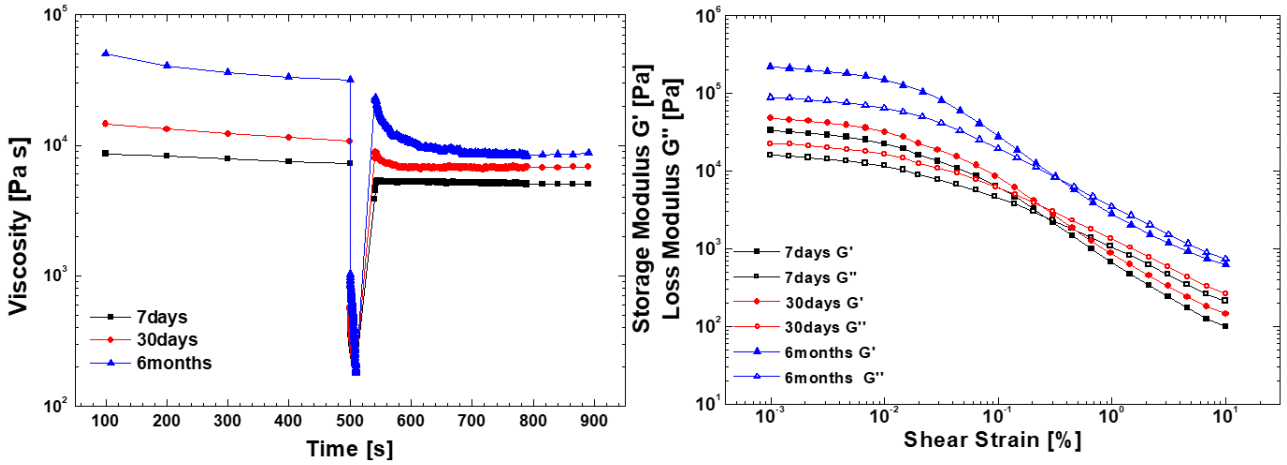

Figure 91: recovery test (left) and amplitude sweep test (right) of sample B2_F1

Sample B4_F1 recovery test and amplitude sweep test are reported in Figure 92.

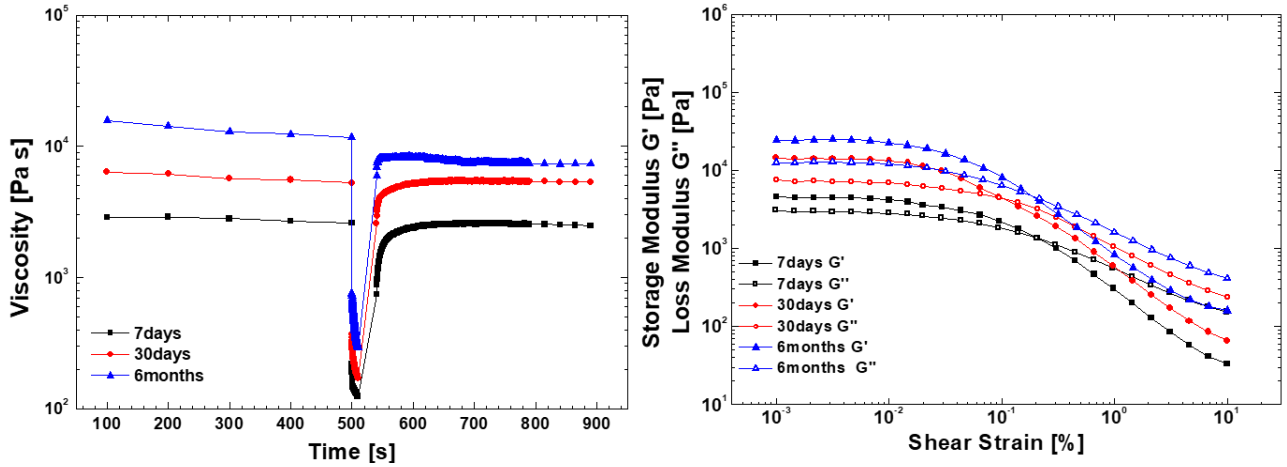

Figure 92: recovery test (left) and amplitude sweep test (left) of sample B4_F1

B4_ F1 shows a recovery that tends to decrease over time, but its recoveries are, generally, higher respect those of standard and of B2_F1 sample, as visible in Table 23.

The measure after 7 days exhibits a slightly separation between moduli (1.5 kPa), but this separation

increases a lot over time until an increment percentage, after six months, of 700%. Similar to sample B2_F1, the increment is much higher than that of the standard.

The LVER is greater than in sample B2_F1 and its end is detectable at shear strain 0.01%, value higher than in standard. The viscosity tends to increase significantly over time, and so the storage stability is scarce.

From rheological analyses, this sample could be used as filler for hull, once improved the storage stability.

MECHANICAL ANALYSIS

The three-point bending test results are reported in Table 24, where E_b is the Young's modulus, the σ_b is the stress and the ε_b is the deformation. For F1 samples, increasing the fibre percentage the E_b increases: sample A3+B4_F1 has a 68% more of the F1 than A1+B2_F1 and the Young's modulus is 22% higher. E_b, is also higher than in standard, nevertheless the mechanical properties appear acceptable for the applications of fillers for hull.

Sample	E_b [MPa]	σ_b [MPa]	ε_b [%]
Filler_2A+2B	1200	17.01	1.90
A1+B2_F1	1461	16.07	1.19
A3+B4_F1	1779	22.10	1.30

Table 24: three-point bending results of F1 cross-linked samples

6.1.2 NATURAL FIBRES: F2

This fibre, in Filler_2A, has substituted two extenders: fumed silica (OA=320 g/100$g_{\text{fumed silica}}$) and alumina-silicate spheres (OA=60 g/100$g_{\text{alumina-silicate spheres}}$).

In the B components, since fumed silica is not present, F2 has replaced carbonates and alumina-silicate spheres.

For both two components also other extenders percentage were slight modified in order to have a total adsorption value similar to standards.

Different formulations were tested and in Table 25 the percentage of F2, the extenders replaced and total adsorption of filler are reported.

Sample	F_2	Alumina-silicate spheres	Talc	Microspheres	Silica	Carbonates	Total adsorption
	[%]						
Filler_2A	-	5.7	3.5	9.0	3.0	-	39.2
A1_F2	7.0	2.8	3.5	10.8	-	-	41.6
A3_F2	6.7	-	8.2	10.8	-	-	41.6
Filler_2B	-	9.0	-	9.5	-	31.8	38.5
B2_F2	7.0	-	-	9.5	-	34.0	38.0
B4_F2	11.0	-	-	5.0	-	34.5	39.9

Table 25: extenders and total adsorption percentage of flillers with F2

COATINGS TESTS

The specific weight (*S.W.*) was measured at two different times: after one week from the production and after three months to evaluate the stability of products. The measures after six months are not reported since they are still in progress. These values and the increase percentage (Δ) are reported in Table 26.

Sample	$S.W._{7days}$ [g/cm^3]	$S.W._{3months}$ [g/cm^3]	Δ [%]
Filler_2A	0.700	0.741	5.86
A1_F2	0.742	0.796	7.28
A3_F2	0.741	0.798	7.69
Filler_2B	0.720	0.789	9.58
B2_F2	0.714	0.797	11.6
B4_F2	0.803	0.905	12.7

Table 26: specific weight at two different times and their increment in percentage of F2 samples

The specific weight after three months increases for all samples and this increase is higher than in the standards. However, the specific weight of samples appear still acceptable to use as filler for hull.

The values of hardness test, after 7 days from application, are reported in Table 27. Compared to the standard, the Shore D values for F2 samples are slightly higher. In addition, the samples appear quite homogeneously cross-linked, in fact the instantaneous measures and the one after 15s are very similar.

Sample	Shore D_{7days}
Filler_2A+2B	61/60
A1+B2_F2	64/63
A3+B4_F2	66/65

Table 27: Shore D values of F2 cross-linked samples

RHEOLOGICAL ANALYSIS

The same rheological analyses of samples with F1 were carried out on samples with F2. In this case the measurements are still in progress, as the specific weight, and so the data related to six months are replaced to that of three months.

A components

In Table 28 are reported the recovery percentage after 30s (Rec_{30s}), the total recovery percentage (Rec_{tot}), the distance between the moduli (G'-G'') its increment in percentage after one month and after three months respect to the measure performed at one week, $\Delta(G'-G'')$, and the end of Linear Viscoelastic Range (*LVER*), obtained from RheoCompass s1.19.

Data of A component standard are reported in Table 28 to compare them with the new samples.

Sample	Times	Rec_{30s} [%]	Rec_{tot} [%]	G'-G'' [kPa]	Δ(G'-G'') [%]	LVER end [%]
Filler_2A	7 days	53	92	25	-	0.005
	3 months	56	89	26	4.00	0.005
A1_F2	7 days	100	97	6.5	-	0.005
	30 days	101	103	12	84.6	0.003
	3 months	95	117	16	146	0.003
A3_F2	7 days	113	116	4.9	-	0.005
	30 days	140	118	9.9	102	0.005
	3 months	128	140	12	145	0.005

Table 28: rheological data of recovery and amplitude sweep tests of A components

Sample A1_F2 recovery test and amplitude sweep test are reported in Figure 93.

As visible from the figure and from Table 28, A1_F2 shows a good thixotropic behaviour, quite different from samples with F1: the recovery after 30s is lower than in samples with F1 (see Table

22), but the total recovery is similar. This thixotropic behaviour is better than in standard: A1_F2 exhibits a higher Rec_{30s} (over 100%) respect to standard (below 60%).

This is valid for all measurements over time. It is also highlighted the Rec_{tot} increases over time unlike the standard.

From the amplitude sweep test and from Table 28, the sample exhibits a lower separation between the moduli than in samples with F1; the separation between moduli increases more, over time, compared to the standard and to the samples with F1.

Furthermore, the end of LVER is detectable at lower shear strain (0.005-0.003%) than that of samples with F1, but comparable with the standard (0.005%).

Both measurements show that A1_F2 is quite stable over time: after one month the viscosity tends to stabilize.

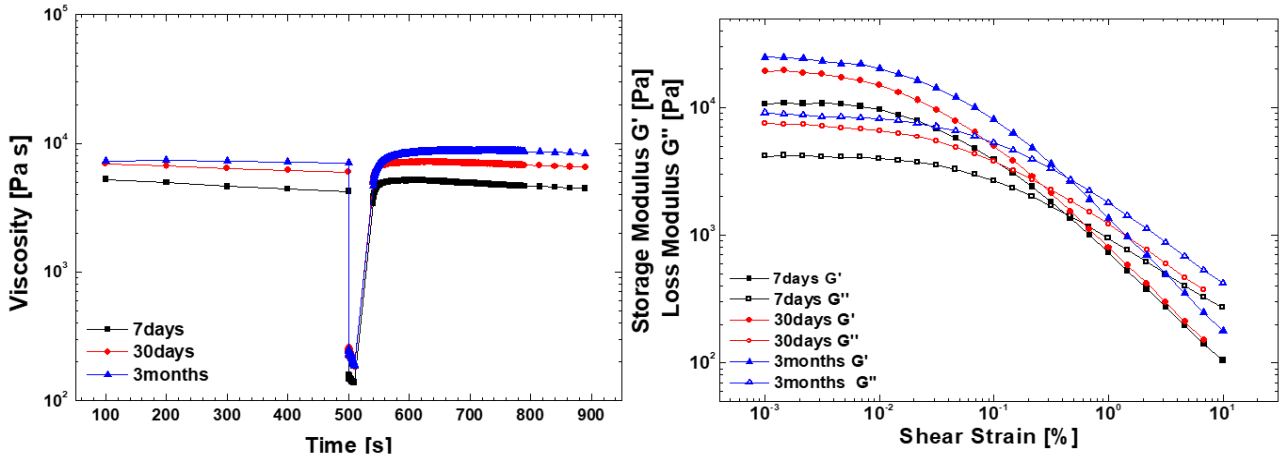

Figure 93: recovery test (left) and amplitude sweep test (right) of sample A1_F2

Consequently, from the rheological point of view, A1_F2 appears a quite good A component: it is applicable greater thickness (high Rec_{30s} and Rec_{tot}). Furthermore, the LVER is comparable with the standard and the storage stability is quite good.

Sample A3_F2 recovery test and amplitude sweep test are reported in Figure 94.

A3_F2 shows a thixotropic behaviour similar to sample A1_F2, but more intense. Indeed, the Rec_{30s} and the Rec_{tot} are higher than in sample A1_F2, as reported in Table 28.

From the amplitude sweep test and from Table 28, the sample exhibits a separation between the moduli similar to sample A1_F2 for the measure after one week, and after six months. The end of LVER is detectable at around shear strain 0.005% for all measurements, comparable with the standard.

Both measurements show that A3_F2 is quite stable over time, similarly to sample A1_F2.

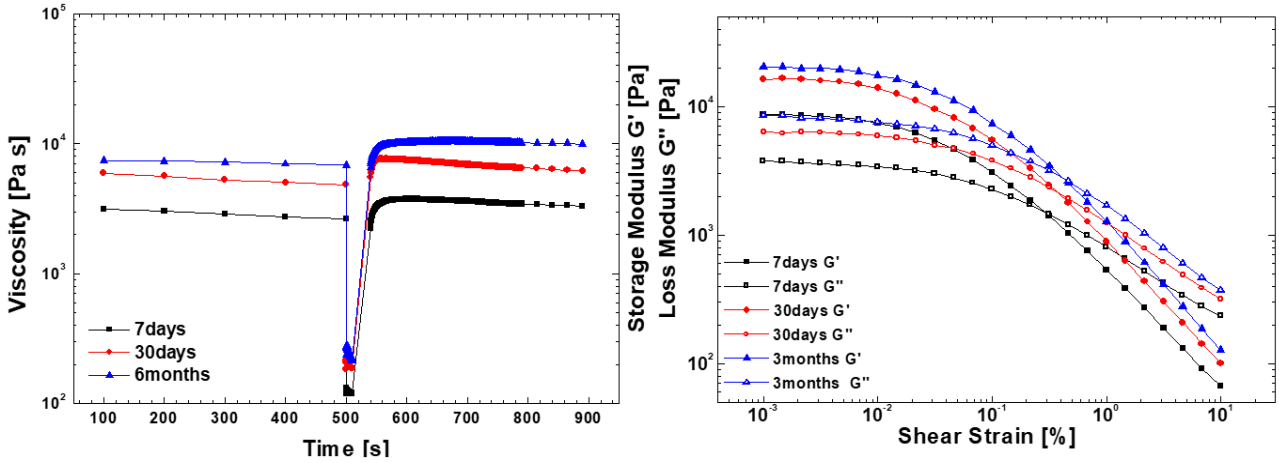

Figure 94: recovery test (left) and amplitude sweep test (right) of sample A3_F2

This sample appears a not bad A component filler for its thixotropic behaviour, showing high recoveries, that increase over time, even if its storage stability is not very good.

B components

For the B component, the recovery percentage after 30s, the total recovery percentage, the distance between the moduli, its increment in percentage after one month respect to the measure performed at one week, and the end of LVER are reported in Table 29.

From the visual aspect to spatula (see 3.2 "Coating tests"), the B component samples, after two months, appeared hard and dry, as visible in Figure 95 (right), so the rheological measurements were performed until one month.

Figure 95: sample B2_F2 after one week (left) and after two months from the production (right)

Sample	Times	Rec_{30s} [%]	Rec_{tot} [%]	G'-G'' [kPa]	Δ(G'-G'') [%]	LVER end [%]
Filler_2B	7 days	56	50	11	-	0.005
	30days	53	50	12	9.09	0.005
B2_F2	7 days	125	85	74	-	0.005
	30 days	92	63	300	305	0.001
B4_F2	7 days	180	104	63	-	0.003
	30 days	101	65	93	47.6	0.003

Table 29: rheological data of recovery and amplitude sweep tests of B components

Sample B2_F2 recovery test and amplitude sweep test are reported Figure 96.

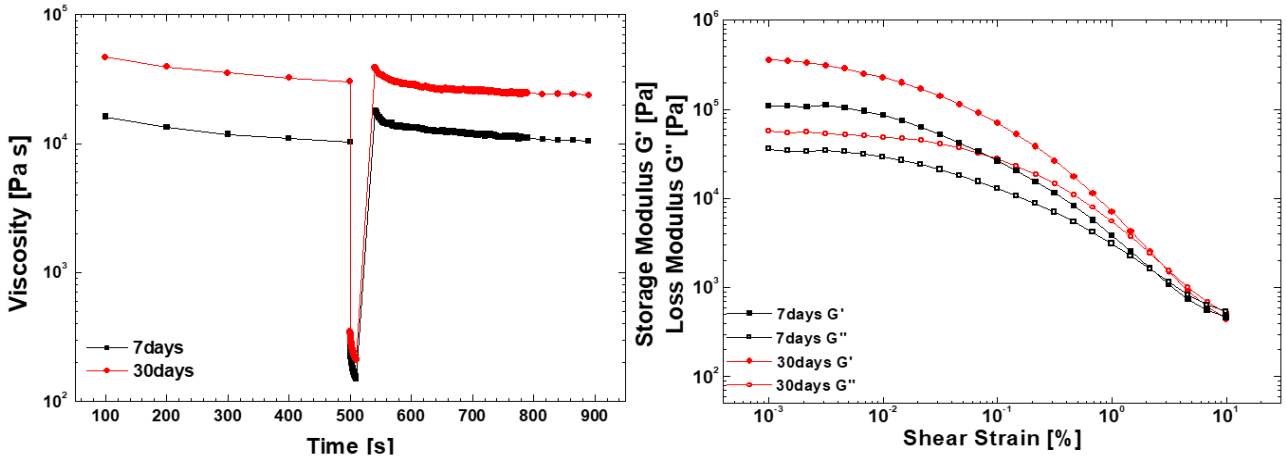

Figure 96: recovery test (left) and amplitude sweep test (right) of sample B2_F2

It shows a really good thixotropic behaviour; indeed the recoveries (Table 29) are much higher than in sample B2_F1 and in standard. However, both the Rec_{30s} and the Rec_{tot}, over time, decrease respectively from 125 to 92% and from 85 to 63%.

From the amplitude sweep test, the sample exhibits a good separation between the moduli, higher than in B2_F1 and in standard; the separation between the moduli increases a lot over time, until an increment percentage of 305%.

The end of LVER is detectable at around shear strain 0.005% for the sample measured after one week, while at 0.001% for the sample measured after 30days. Both measurements show that B2_F2 is not stable over time: after one month the viscosity increases considerably.

Even if the sample exhibits really good recoveries, they decrease over time. Anyway, the storage stability is too low as seen from the aspect to spatula test after two months and so this sample appear inadequate with this formulation for use as filler for hull.

Sample B4_F2 recovery test and amplitude sweep test are reported in Figure 97.

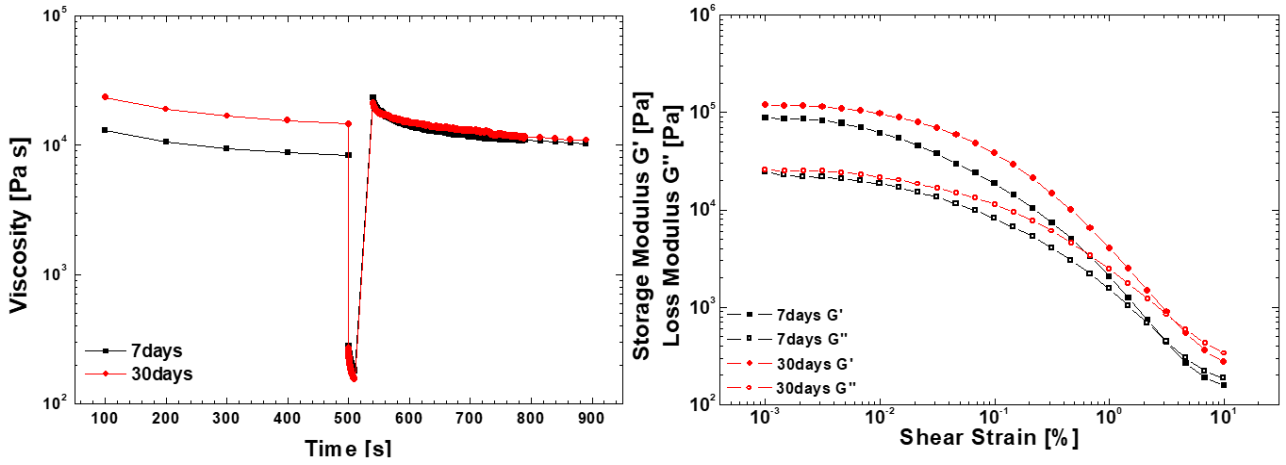

Figure 97: recovery test (left) and amplitude sweep test (right) of sample B4_F2

It shows an excellent thixotropic behaviour with similar trend to sample B2_F2, but more intense; indeed, the recoveries of B4_F2 are higher than in B2_F2. The same behaviour is evident for the measure after one month.

From the amplitude sweep test, the sample exhibits a good separation between the moduli that increases, over time, less than in sample B2_F2. The end of LVER is detectable at around shear strain 0.003%, value lower than in standard.

Both measurements show that B4_F2 is not too much stable over time: after one month, the viscosity increases, but less than in B2_F2.

From the results, even if the sample exhibits an excellent thixotropic behaviour and a higher stability than B2_F2, it appears inadequate for use as filler for hull. However as for B4_F1, by acting on the formulation, for instances, testing different rheological additives, it may be possible to implement the stability of this sample.

MECHANICAL ANALYSIS

The three-point bending test results are reported in Table 30.

For samples with F2, increasing the fibre percentage E_b decreases: sample A3+B4_F2 has a 27% more of the F2 than sample A1+B2_F2 and the Young's modulus is lower of 9%.

E_b, in F2 samples, is higher than in standard, nevertheless the mechanical properties appear acceptable for applications of the fillers for hull. The reinforced effect of F2 is lower than that F1.

Sample	E_b [MPa]	σ_b [MPa]	ε_b [%]
Filler_2A+2B	1200	17.0	1.9
A1+B2_F2	1431	15.0	1.2
A3+B4_F2	1298	17.2	1.4

Table 30: three-point bending results of F2 cross-linked samples

MORPHOLOGICAL CHARACTERISATION

SEM images of samples A1_F2 and B2_F2 are reported in Figure 98 (up and down respectively). The extenders appear quite dispersed. The wood fibres are clearly visible in Figure 98b and d. There is a good adhesion between extenders and matrix.

For sample A3_F2 and B4_F2 are valid the same consideration of sample A1_F2 and B2_F2.

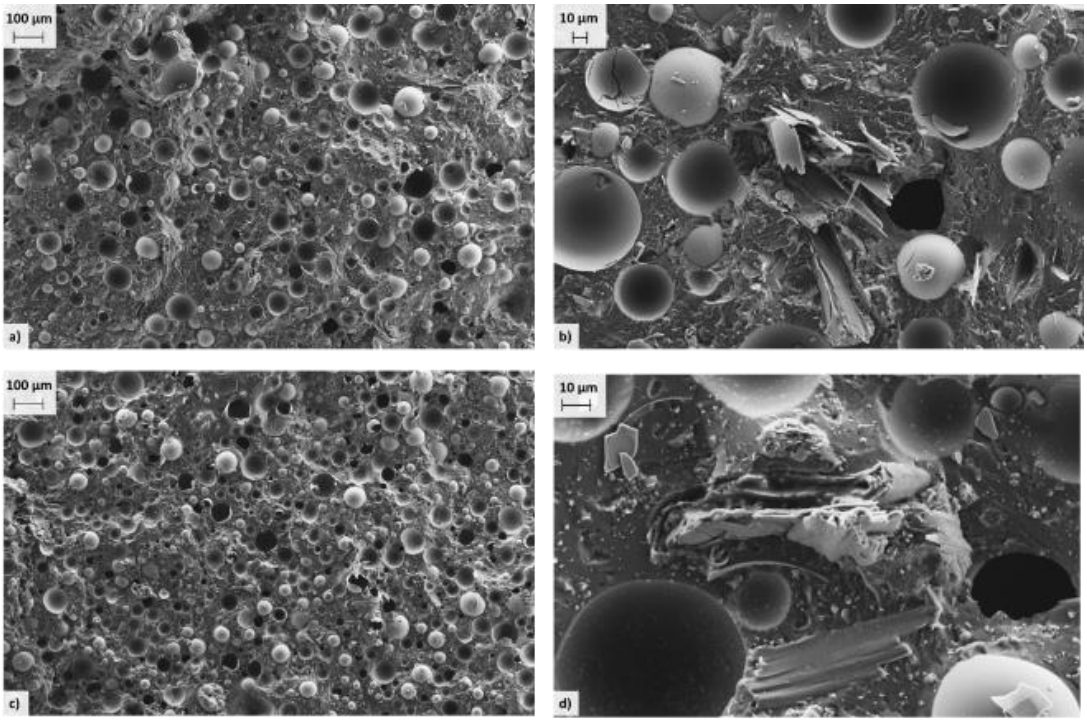

Figure 98: SEM images of samples A1_F2 (up) and B2_F2 (down)

6.2 HOLLOW POLYMERIC MICROSPHERES

In the past decades, polymeric micro- and nanoparticles have attracted great attention because of their broad applications in both traditional industry and modern technology, such as in drug delivery systems, catalysts, photonic crystals, biotechnology, and coatings.

The microspheres advantages, thanks to their spherical shape are: 1) low surface area, which means a low resin demand and 2) the ability to roll past one another, hence there is minimal impact on viscosity when they are added to a resin.

Furthermore, the hollow polymeric microspheres have thin shell and show high resilience and high compressibility. Therefore, they can be deformed under stress (during high shear mixing or pumping), and their breakage is very low or absent [83 - 88].

In the traditional formulation of fillers, hollow glass microspheres ($175g/100g_{glass\ microspheres}$) were used. An attempt to replace these extenders, in both standard components, with polymeric hollow microspheres was carried out in order to improve the rheological properties of the single components. For both two components also other extenders percentage were slight modified in order to have a total adsorption value similar to standards.

The apparent density and the oil adsorption values of polymeric microspheres, called PM, are respectively 0.07 g/cm^3 and $300g/100g_{PM.}$

In Table 31 the percentage of PM, the extenders replaced and total adsorption of filler are reported.

Sample	PM	Alumina-silicate spheres	Talc	Microspheres	Carbonates	Total adsorption
	[%]					
Filler_2A	-	5.7	3.5	9.0	-	39.2
A1_PM	8.0	5.7	4.5	-	-	39.3
Filler_2B	-	9.0	-	9.5	31.8	38.5
B2_PM	8.5	8.5	-	-	33.3	38.3

Table 31: extenders and total adsorption percentage of filler with PM

6.2.1 COATINGS TESTS

The specific weight was measured at two different times: after one week from the production and after six months. These values and the increment in percentage are reported in Table 32.

Sample	S.W.$_{7days}$ [g/cm^3]	S.W.$_{6months}$ [g/cm^3]	Δ [%]
Filler_2A	0.700	0.750	7.14
A1_PM	0.605	0.635	4.96
Filler_2B	0.720	0.795	10.4
B2_PM	0.618	0.658	6.47

Table 32: specific weight at two different times and their increment in percentage of PM samples

Both components show a slight increment over time, lower than that of standards, and therefore, these formulations have better performance than standard for the application of the filler on hull.

The values of hardness test are reported in Table 36. These values are too low to be used in field application. Despite this, the samples appear quite homogeneously cross-linked, in fact the instantaneous measures and the one after 15s are quite similar.

Sample	Shore D$_{7days}$
Filler_2A+2B	61/60
A1+B2_PM	45/43

Table 33: Shore D values of PM cross-linked samples

6.2.2 RHEOLOGICAL ANALYSIS

The same rheological analyses of samples with F1 were carried out on samples with polymeric microspheres.

A components

The recovery percentage after 30s (Rec_{30s}), the total recovery percentage (Rec_{tot}), the distance between the moduli (G'-G'') its increment in percentage after one month and after six months respect to the measure performed at one week, $\Delta(G'-G'')$, and the end LVER are reported in Table 34.

The rheological data of the A component standard are reported in Table 34 to compare them with the samples.

Sample	Times	Rec_{30s} [%]	Rec_{tot} [%]	G'-G'' [kPa]	Δ(G'-G'') [%]	LVER end [%]
Filler_2A	7 days	53	92	25	-	0.005
	6 months	57	85	27	8.00	0.005
A1_PM	7 days	68	82	7.1	-	0.010
	30 days	66	90	8.3	16.9	0.010
	6 months	70	96	14	97.2	0.010

Table 34: rheological data of recovery and amplitude sweep tests of A components

Sample A1_PM recovery test and amplitude sweep test are reported in Figure 99.

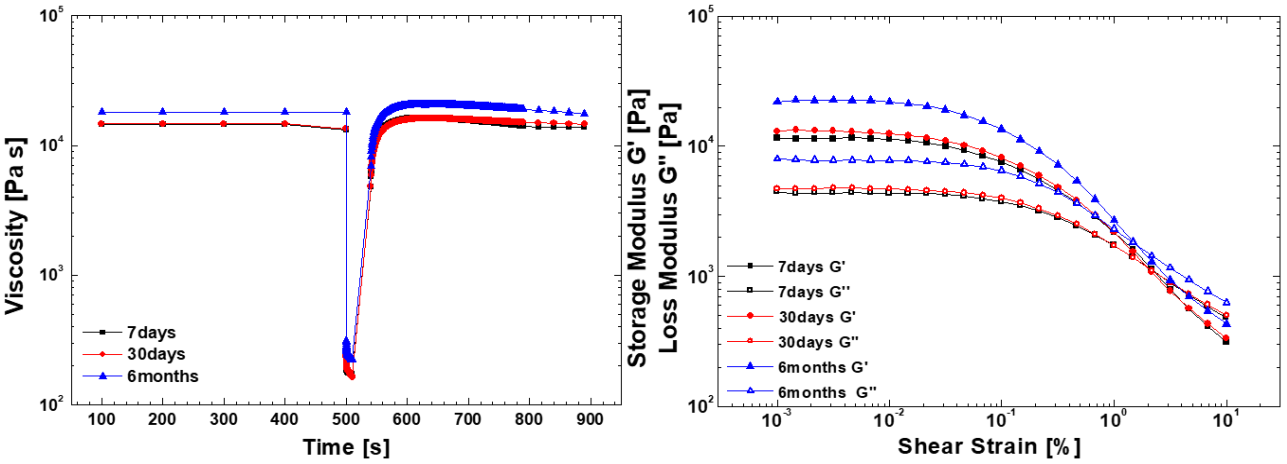

Figure 99: recovery test (left) and amplitude sweep test (right) of sample A1_PM

A1_PM shows a discrete thixotropic behaviour: both the recoveries are lower than in samples with wood fibres; however, they are, generally, a bit higher than in standard and they increase over time, as visible in Table 34.

Considering amplitude sweep tests, sample exhibits a good separation between moduli, comparable with F2 samples, lower than in standard and in F1 samples. Over time, the separation increases until 14kPa. The end of LVER is higher (0.01%) than in standard (0.005%) for all measurements. After one month, the viscosity tends to increase a bit.

From the rheological analyses, A1_PM appears a good A component, indeed, the recoveries are higher than standard and they increase over time instead to decrease as for standard. Furthermore, the LVER is higher than standard and so the sample can suffer shear strain higher without disrupting its internal structure. In addition, the storage stability is quite good.

B components

As to the A component, the recovery percentage after 30s, the total recovery percentage, the distance between the moduli, its increment in percentage after one month and after six months respect to the measure performed at one week, indicated as *Δ(G'-G'')* and the end of LVER. Table 35

Sample	Times	Rec_{30s} [%]	Rec_{tot} [%]	G'-G'' [kPa]	Δ(G'-G'') [%]	LVER End [%]
Filler_2B	7 days	56	50	12	-	0.005
	6 months	49	50	14	16.7	0.005
B2_PM	7 days	130	91	0.6	-	0.006
	30 days	481	166	5.8	866	0.005
	6 months	460	264	15	2400	0.005

Table 35: rheological data of recovery and amplitude sweep tests of B components

Sample B2_PM recovery test and amplitude sweep test are reported in Figure 100.

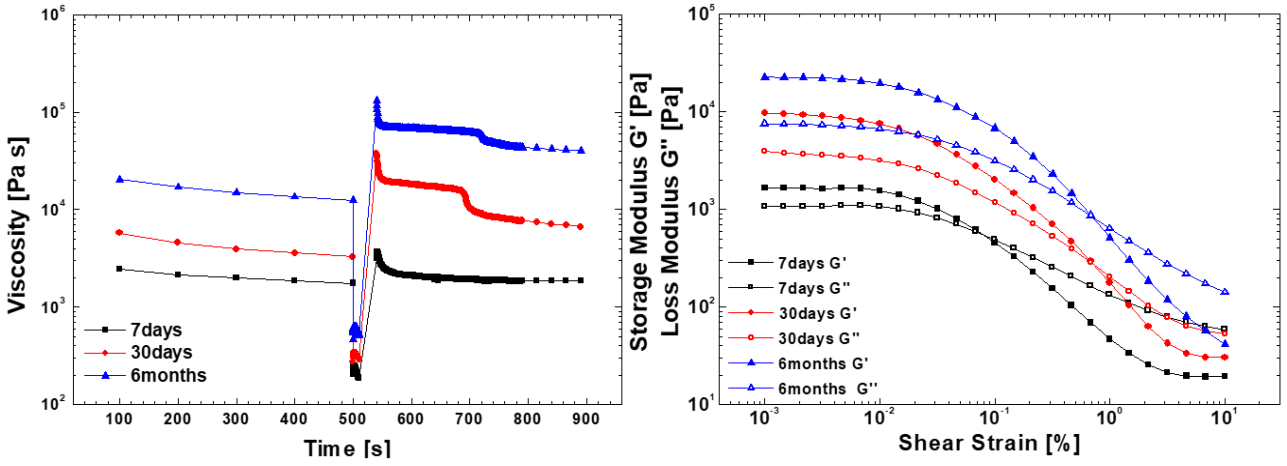

Figure 100: recovery test (left) and amplitude sweep test (right) of sample B2_PM

B2_PM shows an excellent thixotropic behaviour: the polymeric microspheres give a remarkable elastic contribution. Indeed, the recoveries are the highest among the samples discussed until now, as reported in Table 35.

Considering amplitude sweep tests, sample exhibits the smallest separation between the moduli (0.6kPa) among all the samples seen so far, when measured after one week. However, for measurements after 30 days and after 6 months, this separation grows to become the highest of among all samples, until an increment percentage of 2400%.

The end of LVER is detectable at around shear strain 0.005%, as for the standard. Both measurements show that B2_PM is not very stable over time.

The sample exhibits an excellent thixotropic behaviour and a separation between moduli that increases really much over time. Even if the storage stability must be improved, the sample appears a really good B component filler.

6.2.3 *MECHANICAL ANALYSIS*

The three-point bending test results are reported in Table 36.

The data are really lower than in standard and in samples with wood fibres. The reinforcement effect is scarce and so the mechanical properties are inadequate for filler for hull.

Sample	E_b [MPa]	σ_b [MPa]	ε_b [%]
Filler_2A+2B	1200	17.01	1.90
A1+B2_PM	189	4.5	4.7

Table 36: three-point bending results of PM samples

6.2.4 *MORPHOLOGICAL CHARACTERISATION*

SEM images of sample A1_PM and sample B2_PM are reported in Figure 101 (up and down respectively).

The extenders appear quite dispersed (Figure 101b) and polymeric microspheres are clearly visible.

Figure 102 reports in more detail the polymeric microspheres in sample A1_PM. The adhesion matrix-extenders is really good.

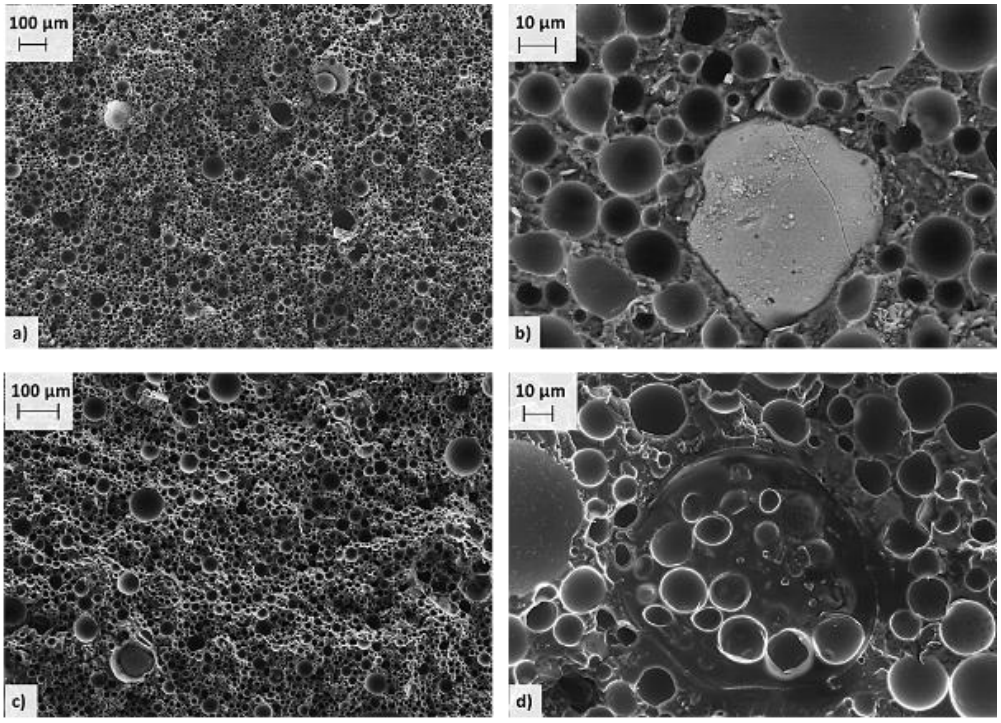

Figure 101: SEM images of samples 1_PM (up) and 2_PM (down)

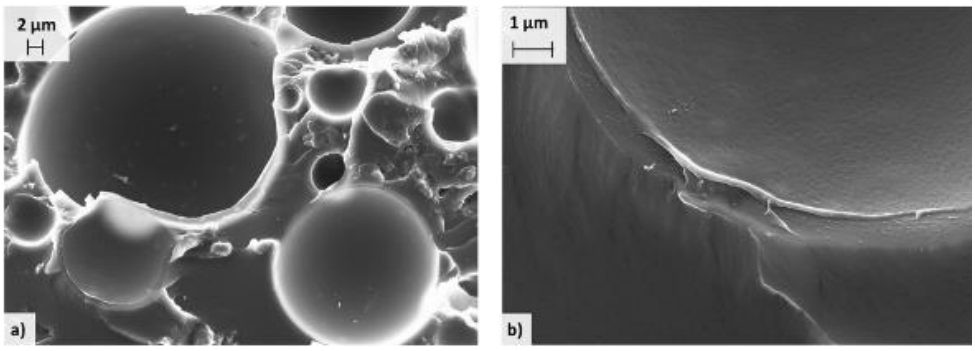

Figure 102: SEM images of sample 1_PM at high magnifications

6.3 CONCLUSIONS

Wood fibres and polymeric hollow microspheres are used to formulate new fillers, replacing different standard extenders.

Considering the results obtained from the analyses on wood fibres, F1, it is highlighted that the two samples of A component are really good fillers both from coatings tests (even if the specific weight is higher than standard) and from the rheological point of view. On the other hand, the samples of B component must be improved, for instances testing different rheological additives, as in B2_F1, or

playing on the percentage of extenders, as in B4_F1. Indeed, B2_F1 is acceptable as filler for hull, considering coatings test, but not usable considering its thixotropic behaviour that is too low, moreover it is scarcely stable.

Sample B4_F1 is not usable as filler for hull due to the high specific weight, but its rheological properties appear quite good and so acting on formulation, for instance reducing the extenders with high oil adsorption value, the specific weight can be stabilised.

From the point of view of mechanical analysis, both the samples appear acceptable to use as filler for hull.

Considering the results obtained from the analyses, until three months, on wood fibres, F2, it is highlighted that the two samples of A component are similar to F1 samples, but they are less performant and less stable than F1 samples. In spite of that, these samples can be used as filler for hull. Whereas samples of B component exhibit a really good thixotropic behaviour, but unfortunately after two months from the production they appeared hard and dry. Therefore, they cannot be used as filler for hull. Tests are necessary to improve the stability and the aspect to spatula, for instances, working on the percentage of extenders with high oil adsorption value.

The cross-linked product is acceptable as filler for hull, since the mechanical properties are good and the adhesion matrix-extenders is strong.

Considering the results obtained from the analyses on polymeric microspheres, it is highlighted that: both A and B components with PM exhibit a very low specific weight, really good rheological properties and a strong adhesion matrix-polymeric microspheres. Unfortunately, the reinforced effect is too low for the filler for hull applications.

Future developments will concern the B components:

- ✓ for wood fibres samples, further tests will be needed to implement the rheological properties and the specific weight. Moreover, these fibres can be used in fillers for deck, that have specific weight, rheological properties and finishing less restrictive than fillers for hull.
- ✓ for polymeric microspheres samples, it will be necessary to work on the other extenders to improve the mechanical properties, for instance trying samples with natural fibres and hollow polymeric microspheres to take advantage of their best properties.

The formulations tested have allowed the company to investigate new raw materials permitting it to explore new areas of research. Indeed, also if some formulations are not usable as fillers for hull applications, they can be considered the trailhead to use the new extenders in the future.

CHAPTER 7: DISPERSANTS STUDY

As previously discussed (see "Chapter 5: Extenders study") there were two types of hollow glass microspheres used in different field of applications: the GM_1 were employed in commercial fillers while GM_2 were used in the new filler development (see "Chapter 9: Development of a new filler"). Although the adhesion of GM_1 with the matrix was scarce respect the GM_2, they were used in commercial filler due to the lower density and cost, respect GM_2.

Therefore, to improve the wettability and the adhesion of GM_1 with the matrix, different dispersing agents (see 2.3.1 "Dispersant") were investigated.

In order to simplify the study and reduce the number of variables, ad hoc formulations were prepared: each sample included the epoxy resin, from bisphenol A and bisphenol F, matrix of Filler_2A, an anti-foam agent, necessary to avoid the foam formation during dispersion, hollow glass microspheres and different dispersing agents. These agents used were selected from the many products available on the market, taking into account the coating system within which they must be inserted. They are shown in Table 37, their nature is reported according to the technical data sheet from the producer.

Dispersing Agent	Nature
Additive 1	Self-emulsifying soy lecithin
Additive 2	N- tallow alkyl trimethylene diamine dioleate
Additive 3	Hyperbranched polyester
Additive 4	tetra(2,2 diallylxymethyl) butyl, di(ditridecyl) phosphite titanate

Table 37: dispersing agents

In Table 38, the considered samples are reported:

- sample 0: without dispersing agent was used as reference,
- samples 1-4: with four different dispersing agents.

A Component	Epoxy Resin	Dispersing Agent	Microspheres	Anti-Foam Agent
Sample	(% w/w)			
Sample 0 (without dispersing agent)	81.2	0.0	18.3	0.5
Sample 1 (with additive 1)	80.0	1.5	18.0	0.5
Sample 2 (with additive 2)	80.0	1.5	18.0	0.5
Sample 3 (with additive 3)	80.0	1.5	18.0	0.5
Sample 4 (with additive 4)	81.0	0.1	18.4	0.5

Table 38: samples composition

After the samples preparation, the polyamide resin (B matrix) was added to obtain a cross-linked product. The polyamide resin amount was calculated based on the content of epoxy resin in each sample: 40.6% for sample 0, 40.0% for samples 1-2-3, 40.5% for sample 4. Therefore, rheological and mechanical analyses and a morphological characterisation were carried out.

7.1 RHEOLOGICAL ANALYSIS

The rheological measurements in oscillatory mode, amplitude sweep test (AS), were performed on uncross-linked components at two different times: t_1, after one week and t_2, after six months by the production. Time t_1 is representative for the first step of the supply chain (from manufacturer to shipyard), and t_2 is representative of the life-cycle of the product.

The measurements were carried out to evaluate the viscoelastic properties over time, considering storage modulus, G', loss modulus, G'', and complex modulus, G* (see 3.5 "Rheological analysis"). Triplicate measurements were carried out and the curves reported in each plot represent the mean of the three curves.

7.1.1 MEASURES AFTER ONE WEEK FROM THE PRODUCTION

In Figure 103 and Figure 104 are reported respectively G' and G'' and G* versus the shear strain. Considering the first figure, it is worth noticing that the samples can be divided in two groups: samples 0, 1 and 2 show a similar behaviour, samples 3 and 4 exhibit a different behaviour, but they are similar to each other. In the same figure, it is also reported the curve of the matrix (pure epoxy resin without additives and microspheres), as further comparison.

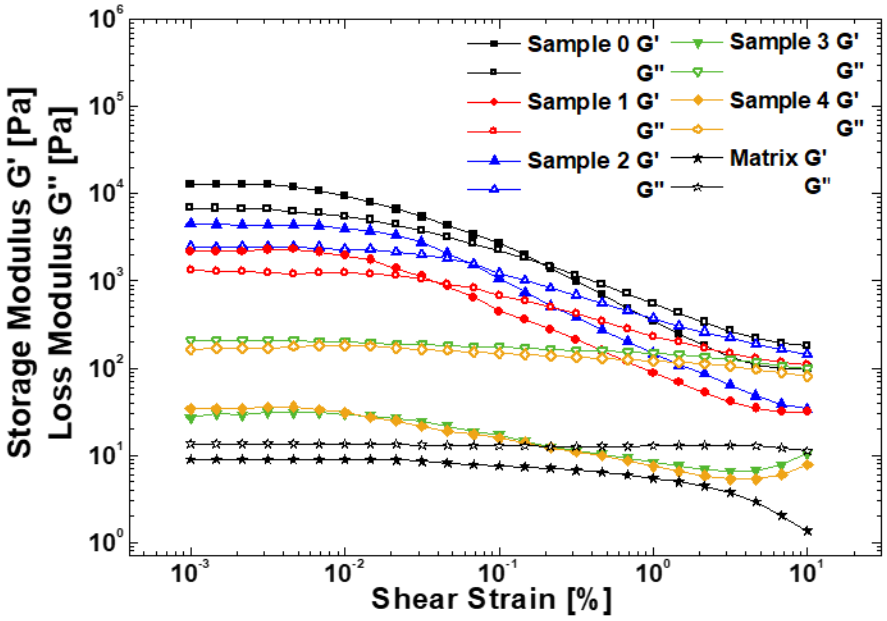

Figure 103: amplitude sweep test of samples and matrix performed after one week from the production

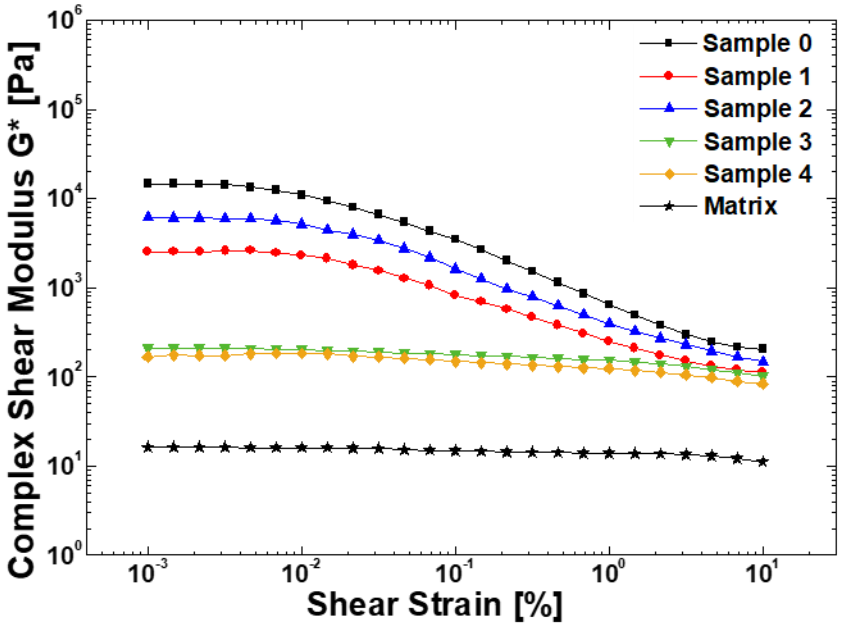

Figure 104: complex shear modulus of samples and matrix performed after one week from the production

Considering Figure 104, the first group of samples (0, 1 and 2) shows initially high values of complex modulus (G*) that decrease rapidly increasing the shear strain. On the contrary, the second group (samples 3 and 4) exhibits initially low values of G* that decrease very slowly increasing the shear strain, as in the matrix curve.

These results were examined taking to account the Payne effect; this effect has been deeply studied for elastomer composites loaded with carbon black and silica [89 - 97], but few works have been reported on the non-elastomeric composites, and in particular, nothing is reported in literature about filled epoxy resins for nautical field.

The mechanism responsible for the Payne effect is still controversial, but the most commonly accepted hypothesis is the progressive destruction of extenders network upon application of oscillatory shear. Indeed, the extenders form a secondary network (extender-extender) within the polymer matrix, offering high resistance to the small amplitudes (high G*) that tend to virtually disappear ad high amplitude (low G*), where deformation destroy the secondary structure [96 - 98].

Table 39 collects the means and the standard deviations of values of complex modulus, G_0*, in the LVER, at very low strain (0.001%), complex modulus G_∞*, at high strain (10%), and Payne amplitude, defined as $\Delta G^* = G_0^* - G_\infty^*$. Samples 0, 1 and 2 show a higher ΔG^* (over 1500 Pa) than samples 3 and 4 (below 150 Pa). As a result, it is possible to observe a strong extender-extender network, in the first samples group, while a secondary network is clearly less strong in samples 3 and 4 that exhibit the same behaviour of matrix, but with a higher viscosity due to presence of hollow glass microspheres. In this case, the extender-matrix interactions are much stronger than extender-extender ones: the particles are well dispersed and separated from each other, so they have a reinforcing effect. Additives 3 and 4 are more performant than the other additives

Sample	G_0*	G_∞*	ΔG*
	[Pa]		
Matrix	16 ± 1	11 ± 1	5 ± 1
Sample 0	14548 ± 130	204 ± 15	14344 ± 145
Sample 1	2546 ± 70	104 ± 9	12442 ± 61
Sample 2	5122 ± 143	148 ± 13	4974 ± 127
Sample 3	211 ± 15	101 ± 3	110 ± 16
Sample 4	167 ± 22	83 ± 4	84 ± 3

Table 39: G_0, G_∞* and ΔG*, values of matrix and samples measured after one week from the production*

7.1.2 *MEASURES AFTER SIX MONTHS FROM THE PRODUCTION*

In Figure 105 and Figure 106 are reported respectively G' and G'' and G* versus the shear strain.

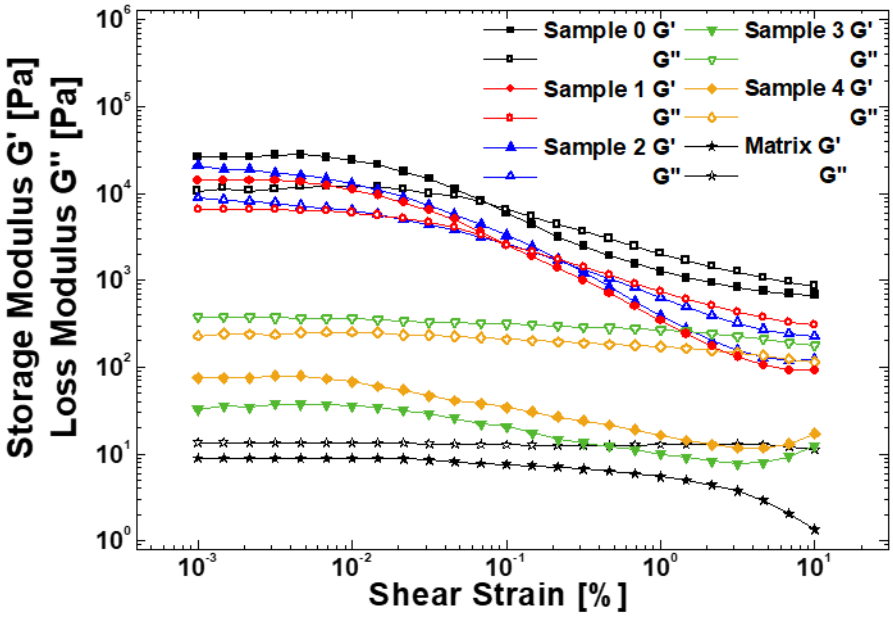

Figure 105: amplitude sweep test of samples and matrix performed after six months from the production

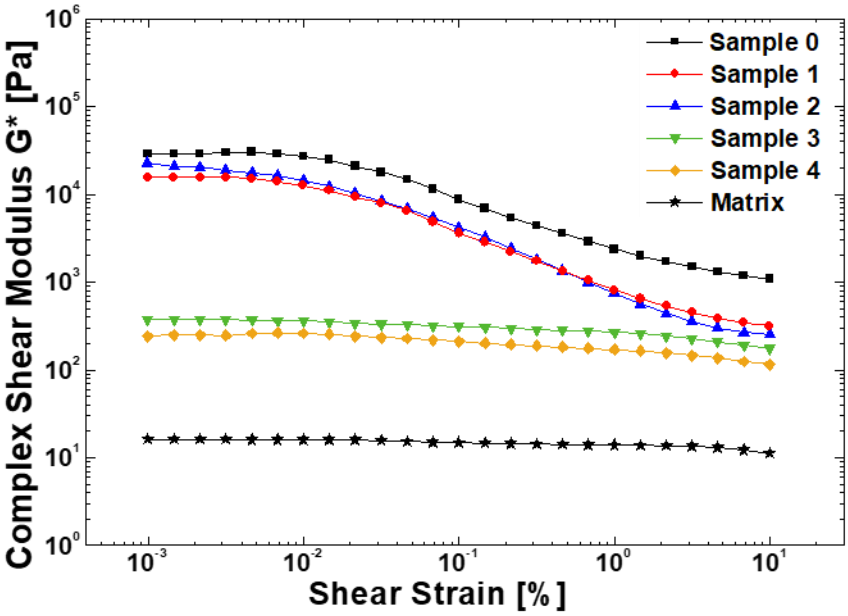

Figure 106: complex shear modulus of samples and matrix performed after six months from the production

The trend of samples measured at t_2 is analogous to that of samples measured at t_1, and so the samples can be again classified in two groups: 0, 1, 2 and 3, 4.

The Payne effect increases definitely for samples 0, 1 and 2, while for samples 3 and 4 the increment is very slight, as reported in Table 40. Moreover, samples 0, 1 and 2 show a higher ΔG^* (over 15000

Pa) than the ones at t_1 (over 1500Pa), while samples 3 and 4, measured at t_2 exhibit a ΔG^* a bit higher (below 200) than that measured at t_1 (below 150).

Therefore, the already strong interaction extenders-extenders, present at t_1 in 0, 1 and 2, is increased further at t_2. Instead, for samples 3 and 4 the secondary network is stronger than in measures at t_1, but they are still able to follow the trend of the matrix, and so they have particles well-dispersed also after six months of storage.

Sample	G_0^*	G_∞^*	ΔG^*
	[Pa]		
Matrix	17± 1	9 ±2	8 ± 1
Sample 0	28686 ± 693	1087 ± 74	27599± 343
Sample 1	15693 ± 102	317 ± 29	15376 ± 81
Sample 2	22700 ± 525	256 ± 49	22444 ± 301
Sample 3	360 ± 84	168 ± 26	192 ± 69
Sample 4	240± 65	115± 10	125 ± 32

Table 40: G_0^*, G_∞^* and ΔG^*, values of matrix and samples measured after six months from the production

Therefore, the measurements performed at t_2, confirm the results obtained at t_1 and show the good performances of additives 3 and 4.

7.2 MECHANICAL ANALYSIS

The efficacy of dispersing agent in the uncross-linked formulation is reflected on the reinforcing effect of extenders in the cross-linked product. To evaluate the importance of this effect, three-point bending mechanical tests were performed (see 3.6.2 “Uniaxial tests”).

Samples with parallelepiped shape and definite size were realised, curing samples 0 to 4 with polyamide resin.

The tests results are reported in Table 41 where E_b is the Young’s modulus (MPa), σ_b is the stress (MPa) and ε_b is the deformation (%).

Sample	E_b [MPa]	σ_b [MPa]	ε_b [%]	Matrix-Extender Distance (μm)
Sample 0	1454 ± 178	18.9 ± 2.7	1.17 ± 0.27	0.254 ± 0.047
Sample 1	1444 ± 31	17.7 ± 0.9	1.24 ± 0.11	0.235 ± 0.023
Sample 2	1460 ± 53	18.0 ± 0.7	1.21 ± 0.07	0.249 ± 0.051
Sample 3	1886 ± 32	24.9 ± 1.3	1.39 ± 0.13	0.091 ± 0.007
Sample 4	1897 ± 59	24.4 ± 1.5	1.46 ± 0.14	0.085 ± 0.004

Table 41: three-point bending test and the morphological results

Samples 0, 1 and 2 show lower Young's modulus, stress and deformation than samples 3 and 4. In particular, Young's modulus confirms that in samples 3 and 4 extenders have a significant reinforcement effect, so these dispersing agents result more efficient than those in sample 1 and 2.

7.3 MORPHOLOGICAL ANALYSIS

Morphological characterisation was carried out to observe the adhesion between matrix and hollow glass microspheres. SEM images of samples 0, 1, 2, 3 and 4 were reported, respectively, in Figure 107, Figure 108, Figure 109, Figure 110 and Figure 111.

In the images, the microspheres and the matrix are visible. In particular, in Figure 107b), c) and d) it is possible to identify gaps between the extenders and the matrix. The same observations are valid for samples 1 and 2.

Also in sample 3 (Figure 110), the extenders and the matrix are visible, but in this case gaps are not present and the matrix has a strong adhesion with the extenders. The same observation is valid for sample 4.

To summarise SEM images show a better adhesion of the microspheres on the resin for the samples 3 and 4, than for samples 0, 1, 2.

In Table 41 the distance between matrix and hollow glass microspheres surfaces, measured with the help of ImageJ, is reported. Samples 0, 1 and 2 show greater gaps (~0.200-0.250 μm) than samples 3 and 4 (~0.090 μm). These observations are in good agreement with the rheological and mechanical measurements.

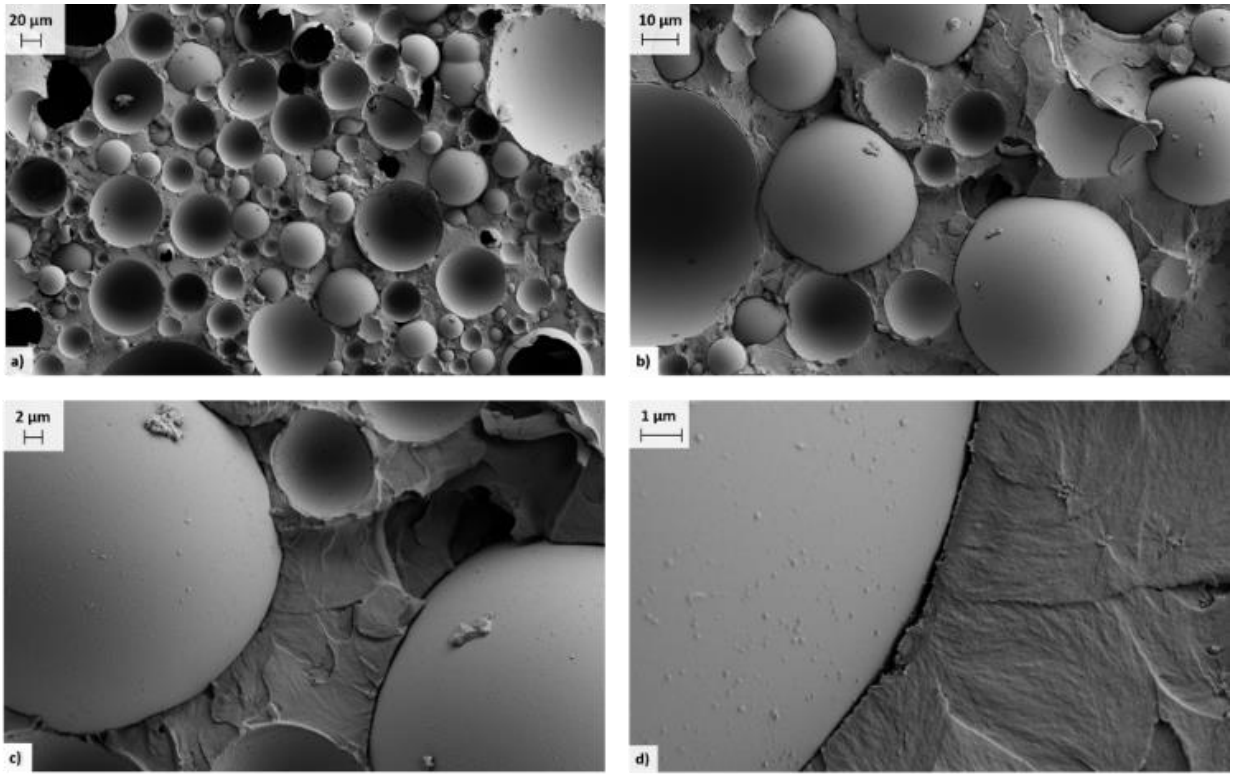

Figure 107: SEM images of sample 0

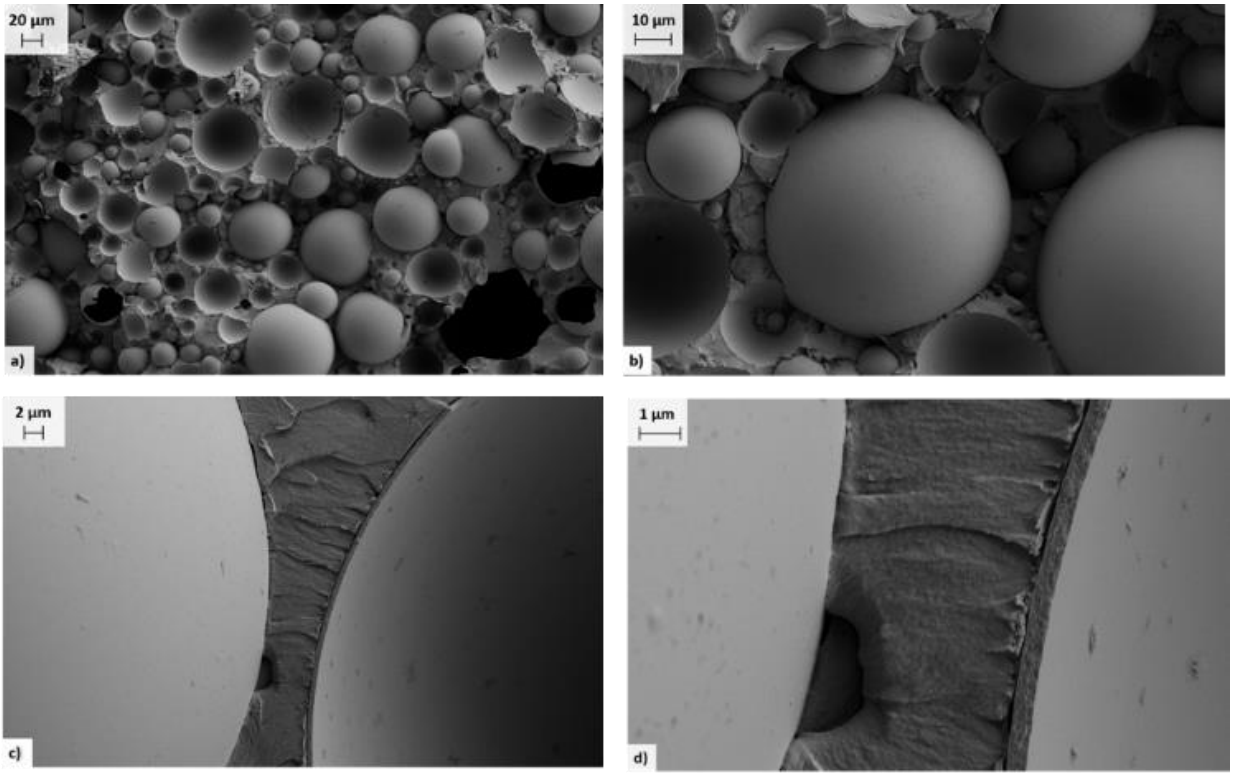

Figure 108: SEM images of sample 1

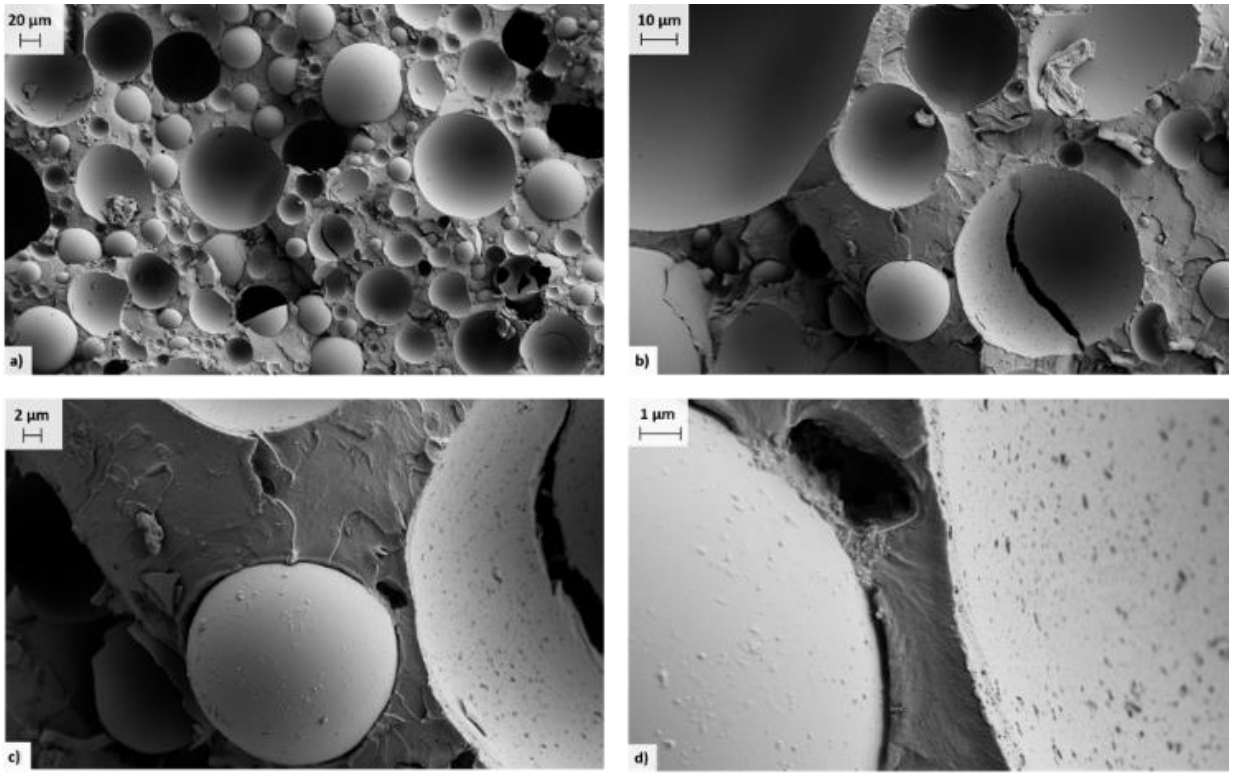

Figure 109: SEM images of sample 2

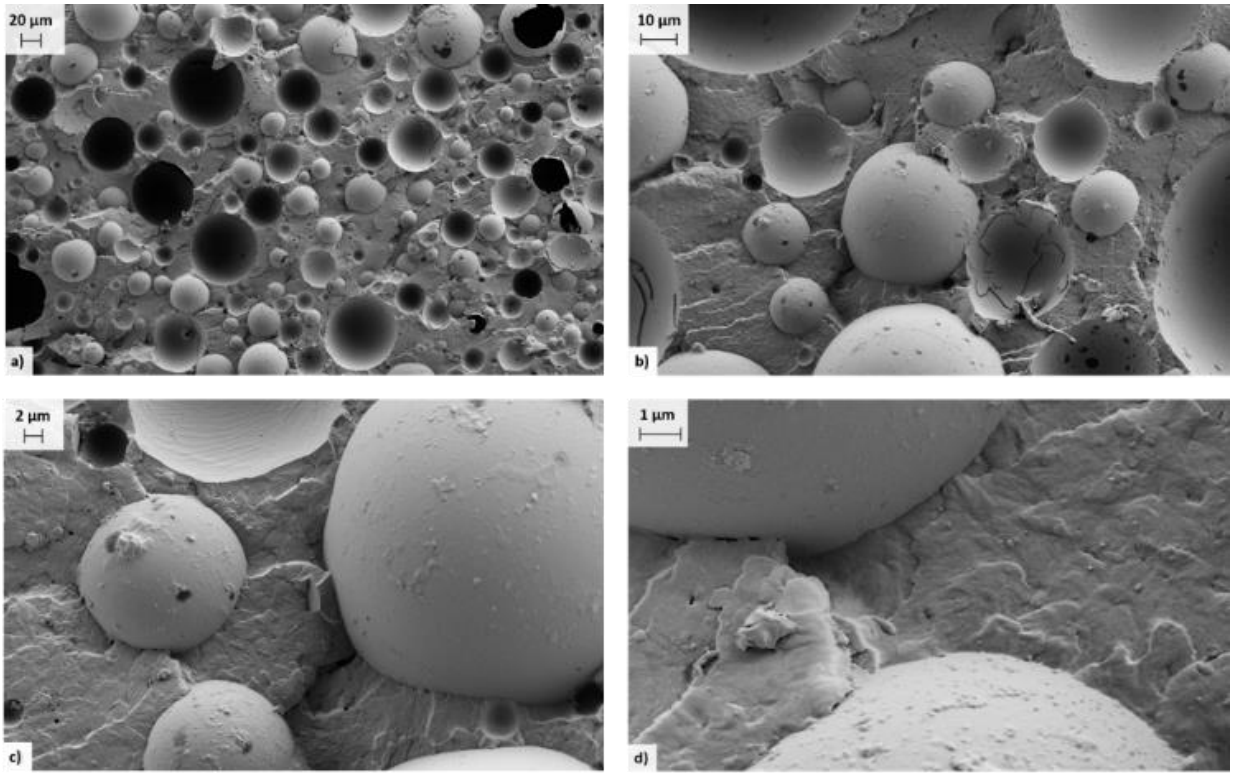

Figure 110: SEM images of sample 3

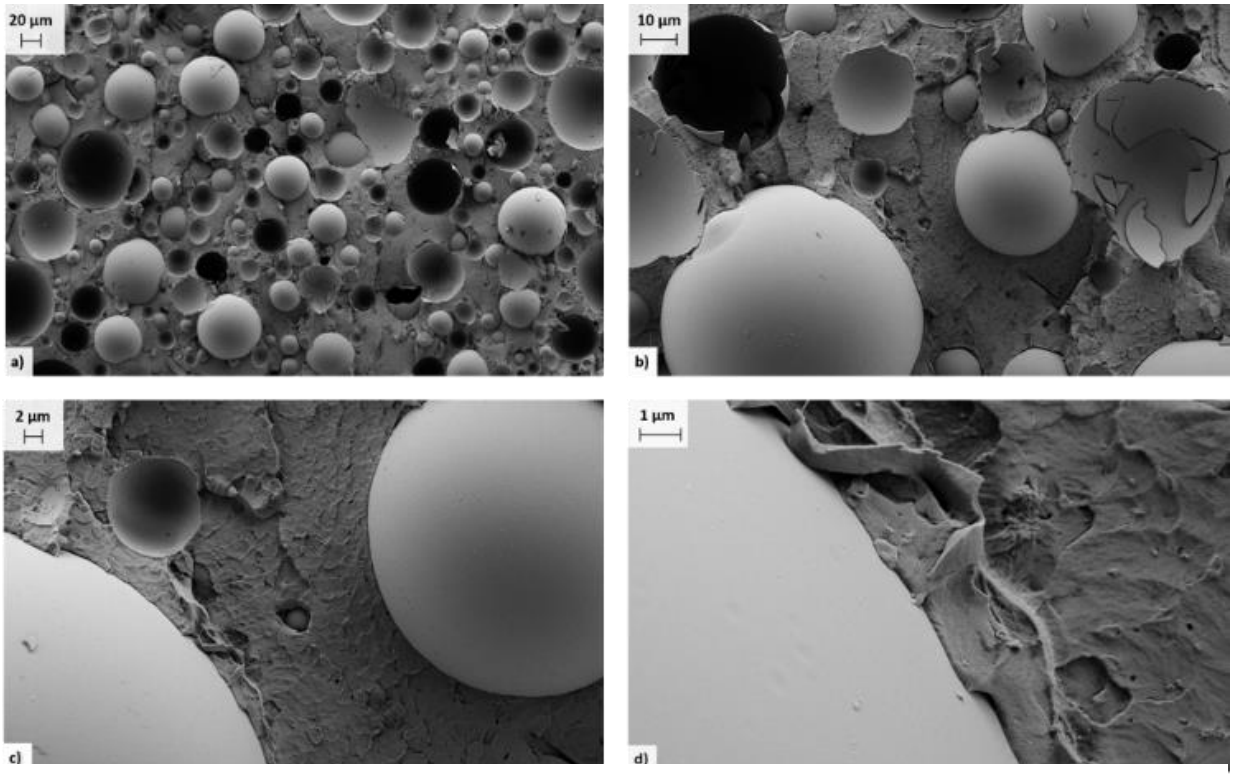

Figure 111: SEM images of sample 4

7.4 CONCLUSIONS

Considering the results obtained, additives can be divided into two groups: additives 1 and 2 on the one hand and additives 3 and 4 on the other hand.

Self-emulsifying soy lecithin (additive 1) and N- tallow alkyl trimethylene diamine dioleate (additive 2) wet poorly the extenders, showing high interaction extenders-extenders, that increase over time, a low Young's modulus of the cross-linked product and a scarce adhesion between matrix and extenders (GM_1).

On the contrary, hyperbranched polyester (additive 3) and phosphite titanate (additive 4), present in samples 3 and 4 respectively, wet very well the glass hollow microspheres. In fact, these two samples showed:

- a good stability during the storage in the can until six months,
- a more fluid behaviour, visible from the rheological measurements, compared to samples 0, 1 and 2,
- a high Young's modulus, observed in the mechanical measurements of the cross-linked product,

- a good adhesion of the matrix to the microspheres, visible in the morphological characterisation.

The different performance of the two groups of dispersants is related to the diverse chemical nature of their hydrophilic groups, therefore to the different type of stabilization. Additives 1 and 2 are ionic dispersants, in particular, lecithin is a Zwitterionic surfactant and the diamine dioleate is cationic, while samples 3 and 4 are non-ionic dispersants. Even if the lecithin is traditionally used as dispersing agent in coating formulations, in the fillers, the steric stabilization, typical of non-ionic dispersants, is the better method for the inhibition of particle aggregation.

CHAPTER 8: RHEOLOGICAL MODIFIERS STUDY

In chapter 8, the rheological modifiers (see 2.3.2 “Rheological modifiers”) were studied to improve the rheological properties of fillers. A systematic screening of ten different rheological modifiers were performed, using recovery test, on both the single components. After that, four additives were selected and monitored, over time, until one year for both A and B components obtaining a complete rheological characterisation. Rheological analysis produces a very large amount of information and so statistical methods are useful to elaborate the data. In this chapter, these data were treated both with univariate analysis (ANOVA) and, for the first time, with multivariate data processing, using PCA after low-level data fusion (see 3.8 “Univariate and Multivariate analyses”). The employment of the statistic methods is used in this chapter for the really high number of data correlated between them.

Furthermore, cross-linked products of these four samples were analysed with dynamic mechanical thermoanalysis in order to evaluate the influence of temperature on the mechanical properties. The data obtained are treated with multivariate analysis.

The additives tested belonged to both inorganic rheological modifiers, such as bentonites, and organic rheological modifiers, as polyamides and castor oils [33, 34, 99 - 106]. Generally, the particles surface of inorganic additives is opportunely treated as a function of the coating system where they will be used, in order to have the best performance in that system. Indeed, in the technical data sheets (*TDS*) is indicated the coating system.

In Table 42 are reported the nature of the rheological modifiers tested, the coating system recommended, their density and melting point. All data reported are obtained from their TDS. As for the dispersing agents, the rheological modifiers were commercial product and so the specific composition was not available.

Additive	Family	Coating system recommended	Density [g/cm^3]	Melting point [°C]
Additive STD	Castor oil derivative	-	1.02	136-140
Additive1	Bentonite modified	Polar	1.70	-
Additive2	Bentonite modified	Non polar	1.71	-
Additive3	Polyamide modified	-	1.02	120-130
Additive4	Castor oil derivative	-	1.01	84-88
Additive5	Bentonite modified	Polar	1.47	-
Additive6	Bentonite modified	Polar	1.62	-
Additive7	Polyamide modified	-	1.05	120-130
Additive8	Bentonite modified	Non polar	1.70	-
Additive9	Polyamide modified	-	1.04	120-130
Additive10	Castor oil derivative	-	1. 02	80-86

Table 42: rheological modifiers tested and data reported in TDS

These ten additives were experimented on the formulations of the A and B standards, replacing, with the same amount, their rheological modifiers. The approximate composition of the two components is listed in Table 43.

Component	A	B
	[% w/w]	
Resin	70-80	40-50
Extender	10-20	40-50
Glass microspheres	0-5	0-5
Additives	1-2	0-5
Rheological modifiers	3	3

Table 43: A and B components composition

8.1 SCREENING TEST

The screening test was carried out using recovery test (see 3.5.2 "Recovery test"), since it is quite fast and with the use of the recovery percentage after 30s and the total recovery percentage (see 3.5.2 "Recovery test") it is possible to compare the thixotropic behaviour of different samples numerically.

In Table 44 the recovery after 30s (Rec_{30s}) and the total recovery (Rec_{tot}) of samples and of standards are reported. Each sample is called with the number of the additive and the letter of component, e.g. sample 1A is the A component with the additive 1.

A component	Rec_{30s} [%]	Rec_{tot} [%]	B component	Rec_{30s} [%]	Rec_{tot} [%]
Filler_2A	53	92	**Filler_2B**	56	50
1A	60	86	**1B**	49	83
2A	59	88	**2B**	24	76
3A	62	89	**3B**	116	64
4A	64	88	**4B**	86	79
5A	88	95	**5B**	29	85
6A	63	81	**6B**	23	75
7A	52	80	**7B**	52	95
8A	68	92	**8B**	35	100
9A	75	98	**9B**	80	89
10A	85	96	**10B**	61	93

Table 44: recoveries after 30s and total recoveries of ten samples and of standards

The recovery tests of the A component samples and of the B component samples are reported respectively in Figure 112 and in Figure 113.

From the curves and from the table, it is visible for both the components that Rec_{30s} varies more than Rec_{tot}. Furthermore, the B component recoveries are more variable than in A component. In fact, both the initial viscosity (first step of recovery test) and the shape of recovery result quite different among the B component samples. For instance, the sample 6B exhibits the lowest initial viscosity and a different shape of recovery compared to sample 3B that has the highest initial viscosity among the B component samples.

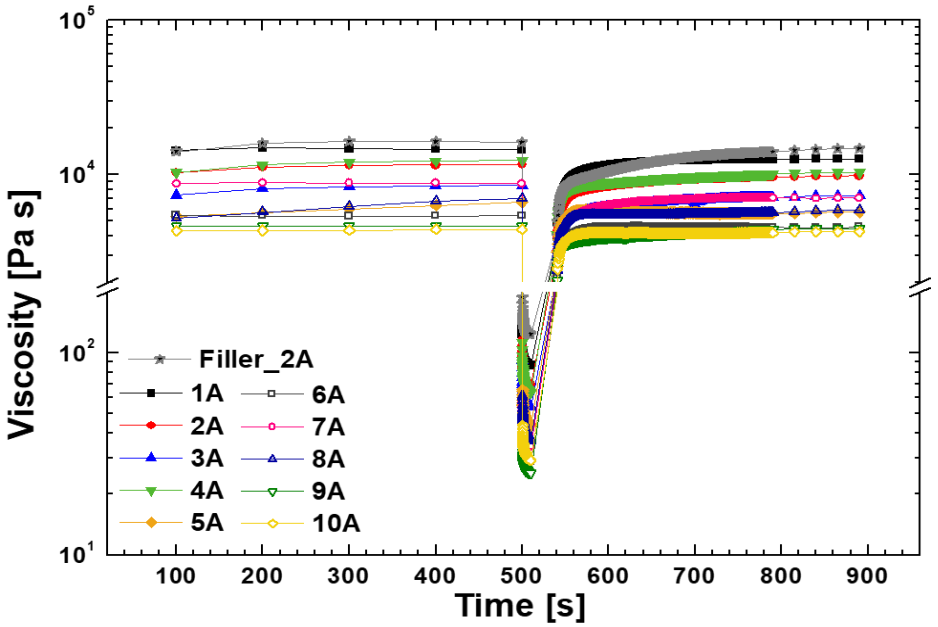

Figure 112: recovery test of A component samples

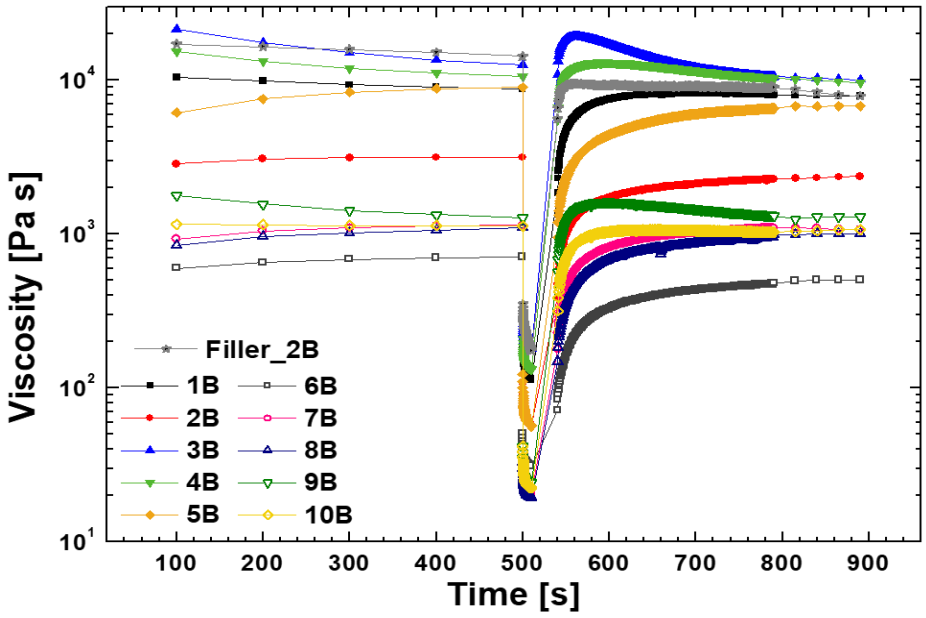

Figure 113: recovery test of B component samples

Considering the A components, almost all samples exhibit a better Rec_{30s} compared to the standard (53%), an exception is sample 7A (52%) that is equal to the standard. Instead, few samples (5A, 9A and 10A) show a better total recovery than the standard (92%). Apparently, there is no correlation with the performance and the family of the additives.

Considering the B component samples, just four samples (3B, 4B, 9B and 10B) present a better Rec_{30s} compared to the standard, the others have really low values. These samples have additives belonging

to the polyamide or castor oil families. Also, sample 7B and the standard have rheological modifiers belonging, respectively, to polyamide and castor oil, and so their composition must be different respect to those in samples 3B, 4B, 9B and 10B. On the contrary, respect to A component samples, the total recoveries are all better (over 60%) than in the standard (50%).

From these results, the first four samples were considered for the complete rheological characterisation and for the data treatment with the statistical analysis. The samples were chosen since "representative" of three families and for different coating systems (polar, non polar). Furthermore, they exhibit really different thixotropic behaviour in the B components.

8.2 RHEOLOGICAL ANALYSIS

The rheological analyses were performed both in rotatory mode, viscosity (see 3.5.1 "Viscosity test") and recovery tests (see 3.5.2 "Recovery test"), and in oscillatory mode, amplitude sweep tests (see 3.5.3 "Amplitude sweep test").

All rheological measurements were performed at two different times: 1) after one week from the production (t_1) and 2) after one year from the production (t_2), Time t_1 is representative for the first step of the supply chain (from manufacturer to shipyard), and t_2 is representative for the shelf-life of the product.

Three measurements for each sample were carried out and the results represent the mean values.

8.2.1 A COMPONENTS

VISCOSITY TEST

Figure 114 reports the viscosity flow curves of different A components and, in Table 45, the zero shear rate viscosity, η_0, modelled with the Carreau equation (see 3.5.1 "Viscosity test"), and the initial viscosity measured at $\dot{\gamma} = 0.01s^{-1}$, indicated as $\eta_{0.01\_F}$, are reported.

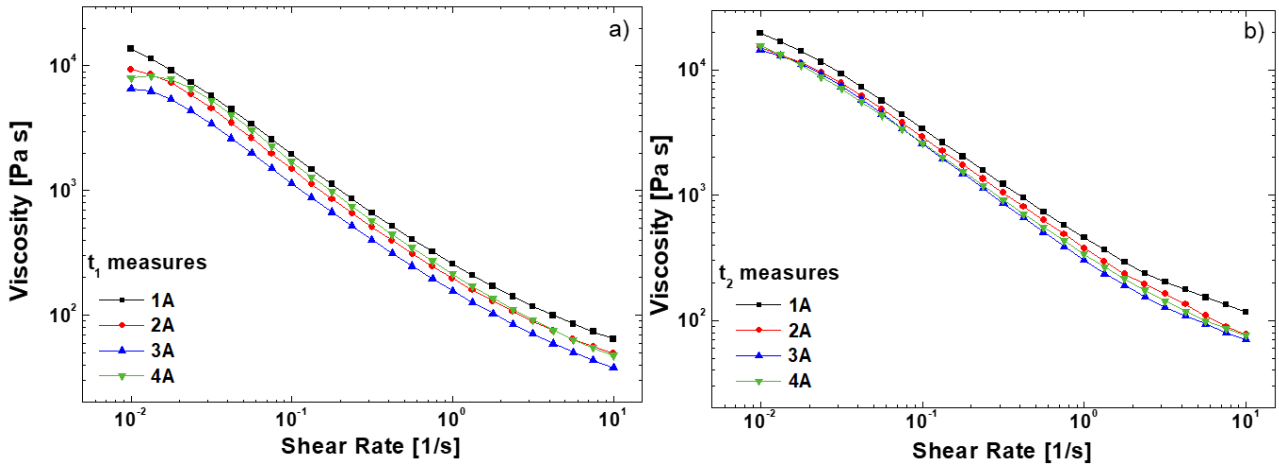

Figure 114: viscosity test of A components after one week (a) and after one year (b) from the production

All curves show a shear thinning behaviour (typical for paints) and the Newtonian plateau is not visible in the investigated shear rate range.

All curves at t_1 (Figure 114a) are quite similar: sample 1A shows a higher viscosity in the whole interval of shear rate ($\eta_{0.01\_F}$ = 13.4kPa s). On the other hand, sample 3A exhibits the lowest viscosity ($\eta_{0.01\_F}$ = 7.31kPa s). 2A and 4A curves show intermediate values ($\eta_{0.01\_F}$ around 10kPa s) and are overlapped. Over time (measures at t_2) 2A, 3A and 4A curves tend to overlap, while 1A sample maintain the highest viscosity, such as in t_1 measures (Figure 114b).

	t_1 (after one week from the production)			t_2 (after one year from the production)		
Sample	η_0	$\eta_{0.01\_F}$	$\eta_{0.01\_R}$	η_0	$\eta_{0.01\_F}$	$\eta_{0.01\_R}$
	[kPa s]					
1A	16.8±0.5	13.4±2.2	14.6±2.6	20.8±2.5	18.4±1.2	18.2±1.8
2A	10.7±1.4	10.2±1.2	11.2±1.3	17.6±1.1	14.8±0.7	14.5±0.6
3A	8.5±1.6	7.3±1.5	8.2±1.1	17.9±3.7	14.2±1.8	14.1±2.3
4A	9.6±0.4	10.4±3.8	11.7±0.3	16.5±0.6	15.2±0.9	13.5±0.7

Table 45: rheological data from viscosity and recovery tests of A components

RECOVERY TEST

In Figure 115, the recovery tests for the A components is shown and, in Table 45, viscosities in the first interval at $\dot{\gamma}$ = 0.01 s^{-1} ($\eta_{0.01\_R}$) are collected.

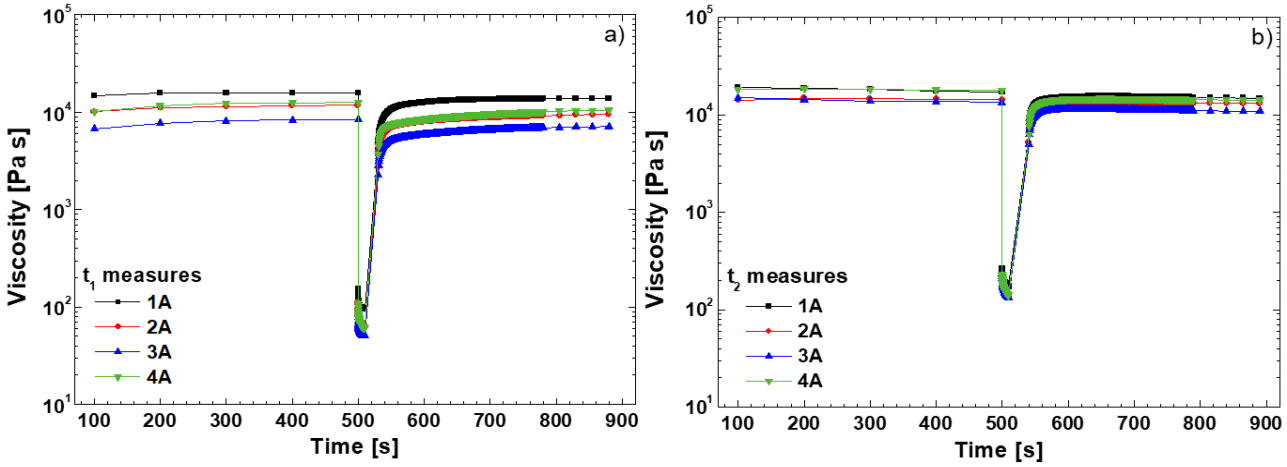

Figure 115: recovery test of A components after one week (a) and after one year (b) from the production

Analysing the first interval of the curves at t_1 (Figure 115a), a higher initial viscosity is observed for sample 1A and a lower one for sample 3A, according to the flow curves. Again, curves related to samples 2A and 4A are overlapped. After one year (t_2 measures in Figure 115b), the samples appear poorly discriminable, with a noticeable overlap of samples 1A and 4A and samples 2A and 3A respectively.

Moreover, in Table 46, the Rec_{30s} and the Rec_{tot} are listed. At t_1, Rec_{30s} are about the same for all samples and over time they tend, generally, to increase a bit. For Rec_{tot} the same observation is valid at t_1 and at t_2.

	t_1 (after one week from the production)				t_2 (after one year from the production)			
Sample	**Rec_{30s}**	**Rec_{tot}**	**G'-G''**	**tanδ**	**Rec_{30s}**	**Rec_{tot}**	**G'-G''**	**tanδ**
	[%]		[kPa]	[1]	[%]		[kPa]	[1]
1A	60±9	86±2	6.5±0.87	0.27±0.01	71±3	82±1	16±1.8	0.39±0.03
2A	59±8	88±8	5.5±0.63	0.30±0.03	71±3	81±2	7.1±0.43	0.29±0.01
3A	62±10	89±8	4.5±0.11	0.30±0.02	70±4	79±7	25±4.2	0.26±0.01
4A	64±6	88±2	9.7±0.56	0.26±0.01	66±2	72±10	6.9±0.86	0.30±0.02

Table 46: rheological data from recovery and amplitude sweep tests of A components

AMPLITUDE SWEEP TEST

Regarding oscillatory measurements, amplitude sweep test is reported in Figure 116 and in Table 46 the distance, at very low strain (0.001%), between the moduli of A component samples, indicated as

G'-G'', and the loss factor (*tanδ*) corresponding to the end of Linear Viscoelastic Region (*LVER*), obtained from the RheoCompass s1.19, are registered.

For all samples, a viscoelastic solid-like behaviour is visible until to the cross-point, where the modules cross each other. From this point, the sample is characterised by a fluid-like behaviour.

Considering the distance between the moduli, at t_1 the samples exhibit comparable values, while for the measures at t_2, sample 3A (25kPa) has the highest distance between the moduli followed by sample 1A (16kPa) and by samples 2A and 4A that have values comparable (below 8.0kPa).

Over time, for all samples the distances increase, in particular for samples 1A (from 6.5 to 16kPa) and 3A (from 4.5 to 25 kPa), with the exception of sample 4A, in which the distances decreases.

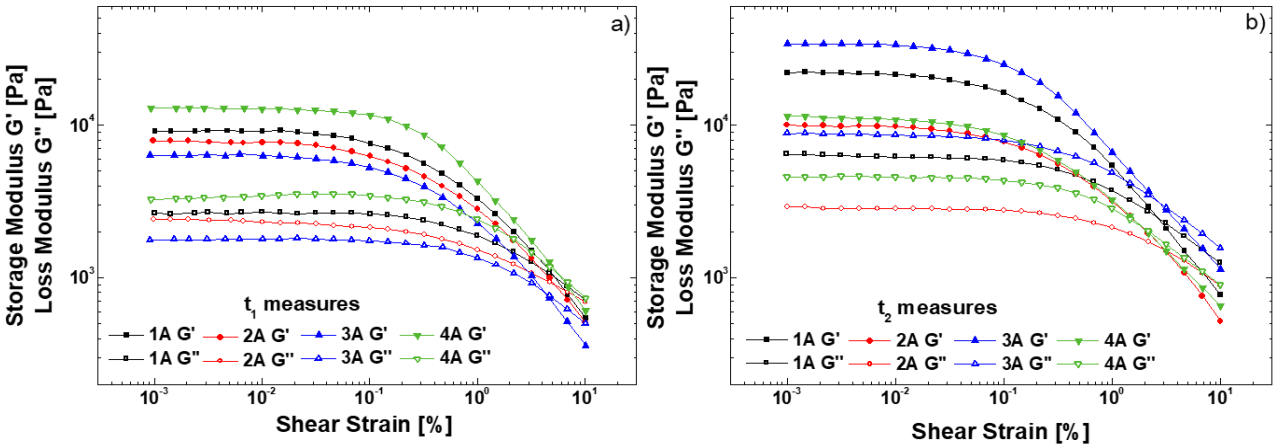

Figure 116: amplitude sweep test of A component after one week (a) and after one year (b) from the production

The loss factor is reported in Figure 117. In the first part of the curve (until γ=0.01%), the loss factor is almost constant; this is ascribable to the LVER: structural variations that occur in this region are reversible. Increasing the shear strain, the loss factor increases, so the viscous behaviour becomes more relevant with respect to elastic behaviour. As long as tanδ remains lower than 1, the structure shows a rigid-like behaviour, when tanδ is higher than 1 the material assumes a liquid-like behaviour.

It is worth noting that the curves are little differentiated for both the measurements after one week and after one year from the production.

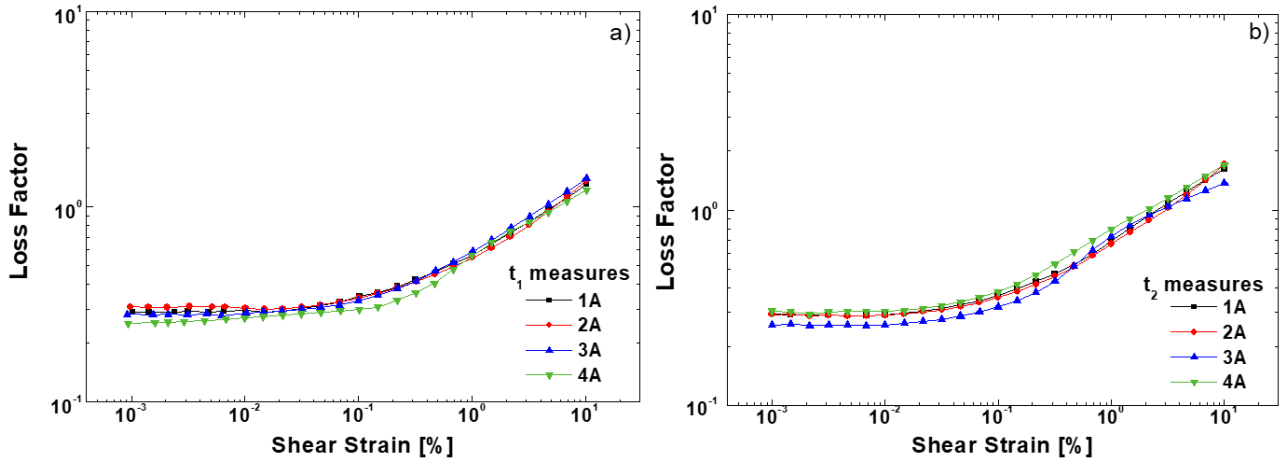

Figure 117: loss factor of A component after one week (a) and after one year (b) from the production

8.2.2 B COMPONENTS

VISCOSITY TEST

Figure 118 reports the viscosity flow curves of different B components and, in Table 47, the zero shear rate viscosity, η_0, modelled with the Carreau equation, and the initial viscosity measured at $\dot{\gamma}$ = 0.01s^{-1}, indicated as $\eta_{0.01\_F}$, are reported.

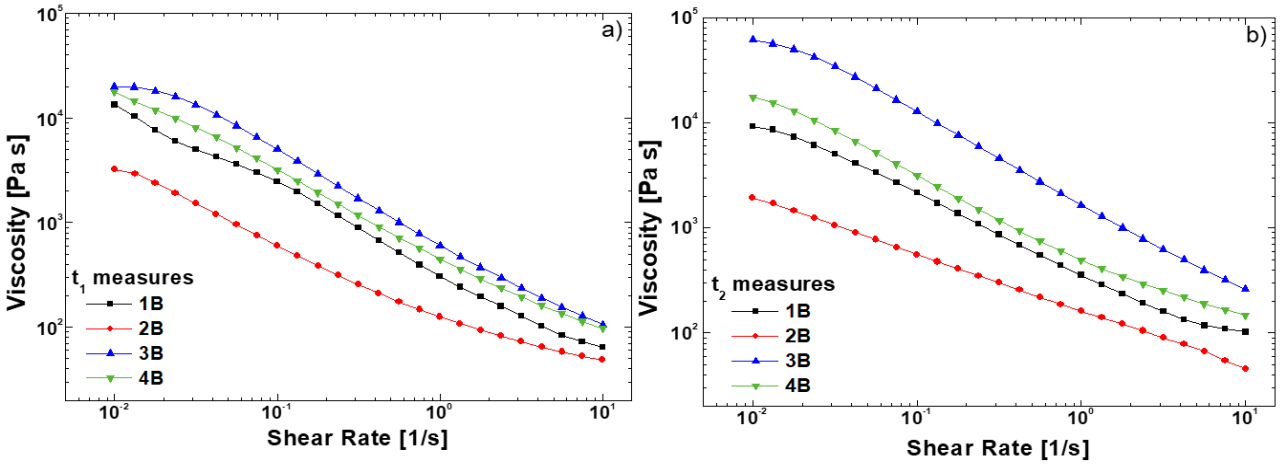

Figure 118: viscosity test of B components after one week (a) and after one year (b) from the production

Also in this component, the Newtonian plateau is not visible in the investigated shear rate range; the 1B, 3B and 4B curves at t_1 (Figure 118a) are quite similar, while 2B sample is different, showing a lower slope with respect to the others, and the shear thinning behaviour is less noticeable. Sample 3B shows a higher viscosity in the whole interval of shear rate, $\eta_{0.01\_F}$ = 20.5kPa s. Sample 2B, exhibits the lowest viscosity, $\eta_{0.01\_F}$ = 3.41kPa s. Over time (t_2 measures in Figure 118b), the curves tend to

differ more, maintaining the trend of t_1: sample 3B, with higher viscosity, followed by samples 4B, 1B and 2B.

Sample	t_1 (after one week from the production)			t_2 (after one year from the production)		
	η_0	$\eta_{0.01\_F}$	$\eta_{0.01\_R}$	η_0	$\eta_{0.01\_F}$	$\eta_{0.01\_R}$
	[kPa s]					
1B	13±1.7	11±2.7	9.5±0.4	13±2.5	10±1.3	8.1±1.0
2B	3.7±0.5	3.4±0.8	3.1±0.2	3.5±2.0	3.4±0.6	4.0±0.5
3B	22±2.4	21±3.8	18±0.7	61±2.6	58±4.5	61 ±9.7
4B	21±2.6	17±3.0	13±1.7	19±3.2	17±3.1	16±2.7

Table 47: rheological data from viscosity and recovery tests of B components

RECOVERY TEST

In Figure 119, the recovery tests for the B components is shown in Table 48, viscosities in the first interval at $\dot{\gamma} = 0.01\ s^{-1}$ ($\eta_{0.01\_R}$) are collected.

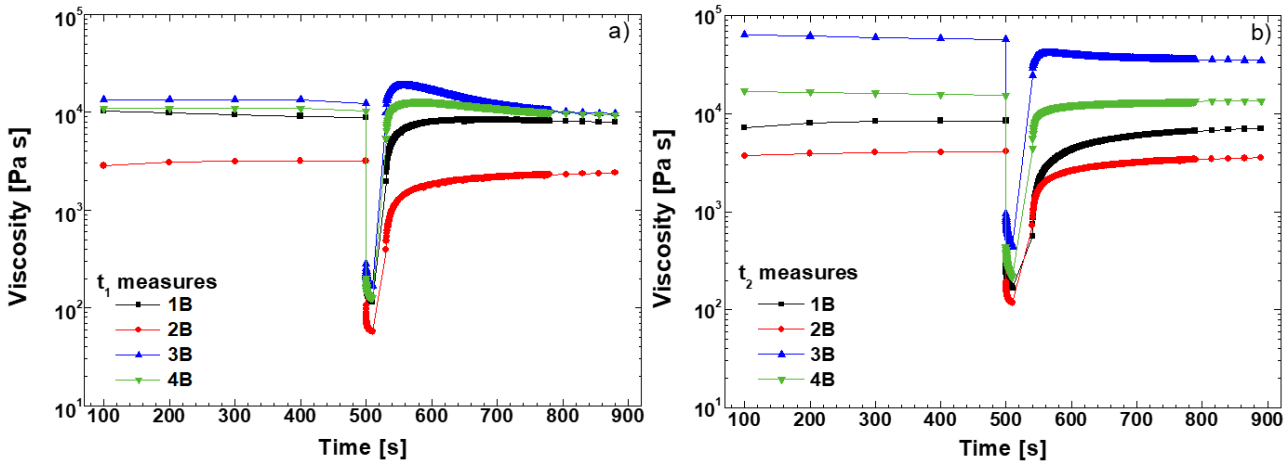

Figure 119: recovery test of B component after one week (a) and after one year (b) from the production

Analysing the first interval of the curves at t_1 (Figure 119a), it is observed a higher viscosity for the 3B sample and a lower viscosity for the 2B, according to the flow curves. After one year (t_2 measures in Figure 119b), the samples tend to differ more, while maintaining the trend of t_1, such as in flow curves measures.

In Table 48, the Rec_{30s} and the Rec_{tot} are listed. At t_1, the Rec_{30s} varies a lot: samples 3B and 4B exhibit the highest values, respectively 116% and 86% that decrease quite over time, while samples 1B and 2B exhibit the lowest values, respectively 49% and 24%. At t_1, the Rec_{tot} values are more

similar between them than Rec_{30s} and, over time, all values tend to increase, with the exception of sample 2B.

Sample	t_1 (after one week from the production)				t_2 (after one year from the production)			
	Rec_{30s}	Rec_{tot}	G'-G''	tanδ	Rec_{30s}	Rec_{tot}	(G'-G'')	tanδ
	[%]		[kPa]	[1]	[%]		[kPa]	[1]
1B	49±4	83±3	4.8±0.33	0.46±0.01	45±5	85±1	0.74±1.9	0.90±0.05
2B	24±10	76±4	1.0±0.22	0.57±0.04	25±1	59±7	1.3±0.94	0.74±0.03
3B	116±6	64±1	25±1.4	0.32±0.01	71±4	88±1	110±3.7	0.28±0.01
4B	86±5	79±3	17±0.91	0.34±0.01	58±3	83±4	7.8±1.6	0.45±0.02

Table 48: rheological data from recovery and amplitude sweep tests of B components

AMPLITUDE SWEEP TEST

Regarding oscillatory measurements, amplitude sweep test is reported in Figure 120 and in Table 48 the distance, at very low strain, between the moduli of B component samples (G'-G''), and the tanδ corresponding to the end of LVER, obtained from the RheoCompass s1.19, are registered.

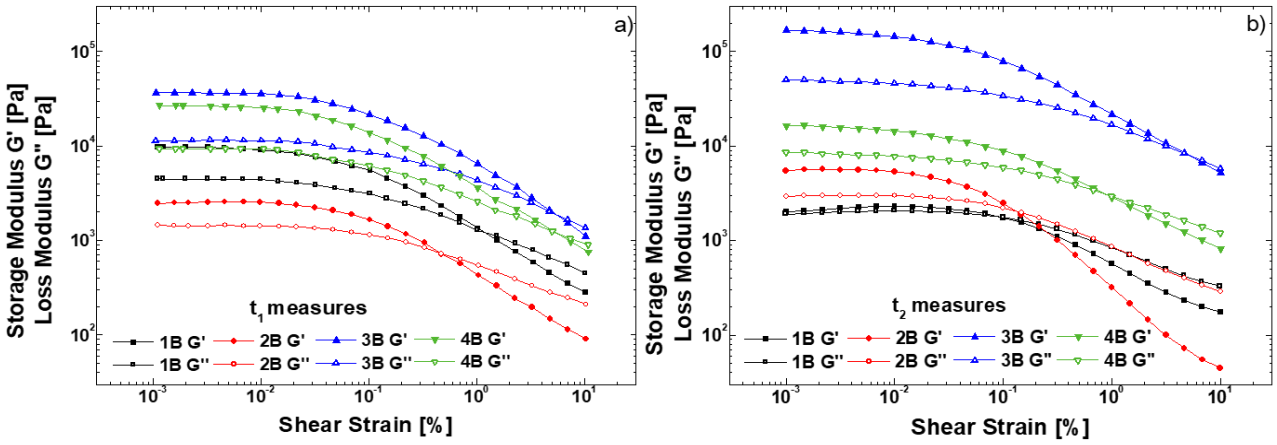

Figure 120: amplitude sweep test of B component after one week (a) and after one year (b) from the production

For all samples, a viscoelastic solid-like behaviour is visible until a cross-point, where the modules cross each other. From this point the sample is characterised by a fluid-like behaviour.

Considering the distance between the moduli, for the measures at t_1, almost all the samples exhibit a remarkable difference that is accentuated at t_2, increasing for sample 3B, while for 1B and 4B decreases. For sample 2B, the distance between the moduli appears quite stable.

The loss factor is reported in Figure 121. At time t_1 the curves show an increase in loss factor increasing shear strain with similar trend for all samples. On the other hand, at time t_2, sample 2B shows a more rapid increase if compared to other ones.

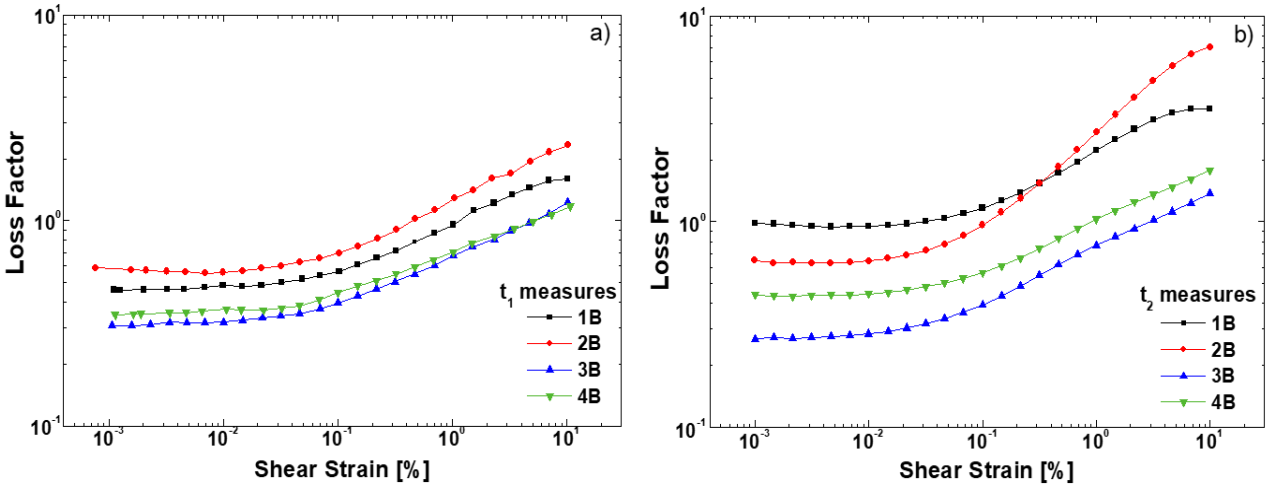

Figure 121: loss factor of B component after one week (a) and after one year (b) from the production

8.3 UNIVARIATE AND MULTIVARIATE ANALYSES

Statistical analysis was carried out to evaluate the difference in the rheological behaviour between samples and over time, both with univariate and multivariate statistical approach.

For both measurements at t_1 and t_2, the initial viscosity, $\eta_{0.01\_F}$, measured at shear rate $0.01s^{-1}$ with viscosity test and the initial viscosity, $\eta_{0.01\_R}$, measured at shear rate $0.01s^{-1}$ with recovery tests were analysed with univariate statistical analysis at $p<0.05$ significance level. In more detail, Student's t test, one-way analysis of variance (ANOVA) and the Bonferroni post-hoc test were used to compare the rheological results. Also, the percentage of recovery and loss factor values, corresponding to the end of LVER, were analysed using univariate statistical analysis. The loss factor obtained from the amplitude sweep allowed to consider just one curves instead two different curves, i.e. storage and loss moduli, and therefore simplify the analysis.

The multivariate approach was used on all rheological data in one-step, thanks to a low-level data fusion methodology. Each measurement (viscosity test, amplitude sweep test) produced 25 data-points (viscosity curve, storage modulus, loss modulus, loss factor) with the exception of recovery test (609 data-points) and, so, to give the same importance a-priori to each curve, the block-scaling pre-treatment was performed prior to concatenation of signals. After that, principal component

analysis was performed on this concatenated data matrix, with the aim of extracting the information related to differences between additives in the two components.

8.3.1 UNIVARIATE ANALYSIS

A COMPONENT

Considering the viscosity and the recovery tests, it is possible to find a good agreement between $\eta_{0.01\_F}$ and $\eta_{0.01\_R}$ for both measures at t_1 and t_2 as reported in Table 45, indeed the slight differences are not statistically significant according to Student's t test ($p<0.05$).

Considering the recoveries reported in Table 46, ANOVA confirms that no differences are statistically detectable between the recoveries after 30s of four samples, the same is valid for the total recovery, at t_1. The same consideration can be done for measurements performed at t_2.

For the statistical analysis of the samples loss factor at the end of LVER, ANOVA proves that they are not significantly different ($p<0.05$) both at t_1 and t_2.

As a conclusion, from these statistical results none of the additives shows a different performance in the epoxy system (A component) studied.

B COMPONENT

Considering the viscosity and the recovery tests, it is possible to find a good agreement between $\eta_{0.01\_F}$ and $\eta_{0.01\_R}$ for both measures at t_1 and t_2 as reported in Table 47, indeed the slight differences are not statistically significant according to Student's t test ($p<0.05$).

Considering the recoveries reported in Table 48, ANOVA confirms that the values of the samples recovery after 30s and total recovery are different from each other ($p<0.05$), both in t_1 and t_2 measures. In t_1, a post-hoc comparison (Bonferroni's test) shows that for Rec_{30s} only samples 1B and 2B are not different in a significant way; while for the Rec_{tot} only samples 1B and 3B are different. Instead, in t_2 a post-hoc comparison (Bonferroni's test) proves that for Rec_{30s} and Rec_{tot} only 2B sample is different from other samples. Furthermore, in the Rec_{30s}, samples 1B and 3B are significant different.

For the statistical analysis of the samples loss factor at the end of LVER, ANOVA proves that they are significantly different ($p<0.05$) for both t_1 and t_2. A post-hoc comparison (Bonferroni's test) shows that, at time t_1, only 3B and 4B samples are not different in a significant way while, at time t_2, only 1B and 2B samples are not significantly different.

From these statistical results, with polyamide matrix (B component), it is possible to conclude that the additives show a different performance. In particular, the best is the third one, which is of

polyamide nature as the matrix, and the worst is the second one, the bentonite for non-polar coating systems.

8.3.2 *MULTIVARIATE ANALYSIS*

A COMPONENTS

In Figure 122, PCA of A component is reported. In detail, Figure 122a represents the score plot of t_1 (red diamonds) and t_2 (green squares) together.

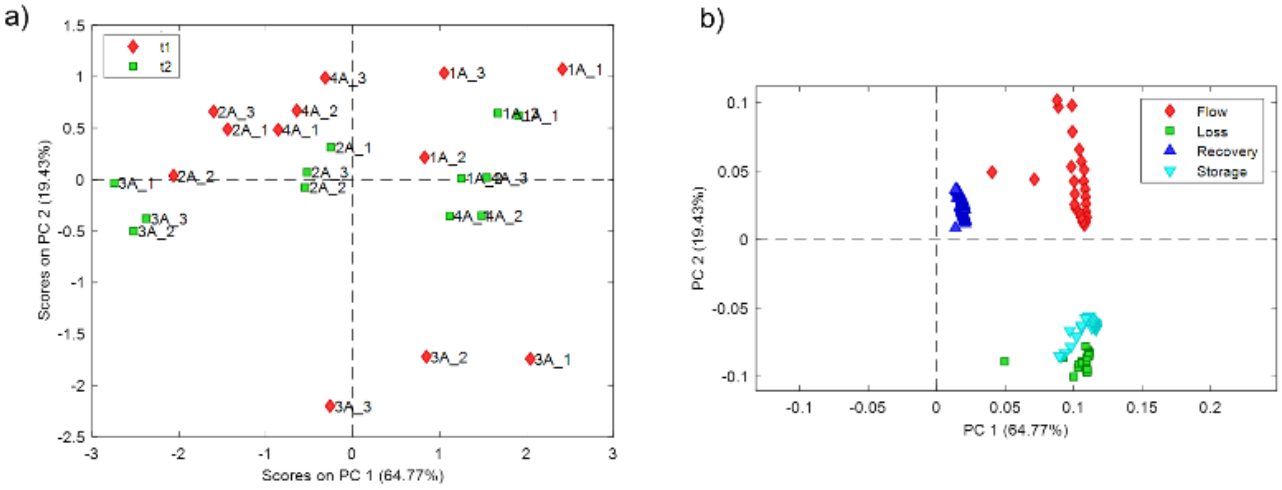

t1	1A	2A	3A	4A
1A	0.00	17.50	0.22	7.68
2A	17.50	0.00	6.96	10.08
3A	0.22	6.96	0.00	2.35
4A	7.68	10.08	2.35	0.00

t2	1A	2A	3A	4A
1A	0.00	45.73	179.30	0.48
2A	45.73	0.00	108.92	61.04
3A	179.30	108.92	0.00	262.57
4A	0.48	61.04	262.57	0.00

Figure 122: PCA for component A; score scatter plot and related FW table (a) and loading scatter plot (b)

From an exploratory point of view, it results evident how the highest amount of information is associated to PC1, explaining 64.77% of data variance. Groups of points corresponding to different additives appear quite overlapped, especially concerning additives 1 and 3. A more resolved separation is detectable after one year of storage (t_2). These considerations are confirmed by Fisher weights (FW), reported in Figure 122a, permitting to evaluate the separation degree between pairs of data groups, considering also the dispersion within each group. In particular, due to the important modifications occurred in the sample containing additive 3, the differences between sample A3 and sample A1 evolve from a FW lower than 1 (0.22) to a FW higher than 100 (179.30).

This particular behaviour of sample A3 at t_2 is confirmed also by the high FW values related to the comparison of this sample with both A4 and A2.

The results of multivariate analysis confirm the conclusions of univariate analysis.

Considering the loading plots (Figure 122b), it clearly appears how differences between groups of samples according to the type of additive are mainly influenced by continuous rotational measurements, in particular by flow curves.

B COMPONENTS

Regarding B component, PCA is reported in Figure 123.

Looking at the score plot (Figure 123a), it is possible to notice that all the sample groups are well separated depending on the additive; moreover, the dispersion within each group is lower, with the exception of sample 3B. This conclusion is confirmed by the FW values reported in Figure 123a, with values higher than 1 for all the pairs of samples. The increase of the differences at t_2 becomes strongly evident, with huge FW values (even higher than 1500, in the case of B2 vs. B3). It means that differences in the B component were important at t_1 and become remarkably more important with time.

Considering the loading plots (Figure 123b), it clearly appears how differences between groups of samples according to the type of additive are mainly influenced by continuous rotational measurements, in particular by flow curves.

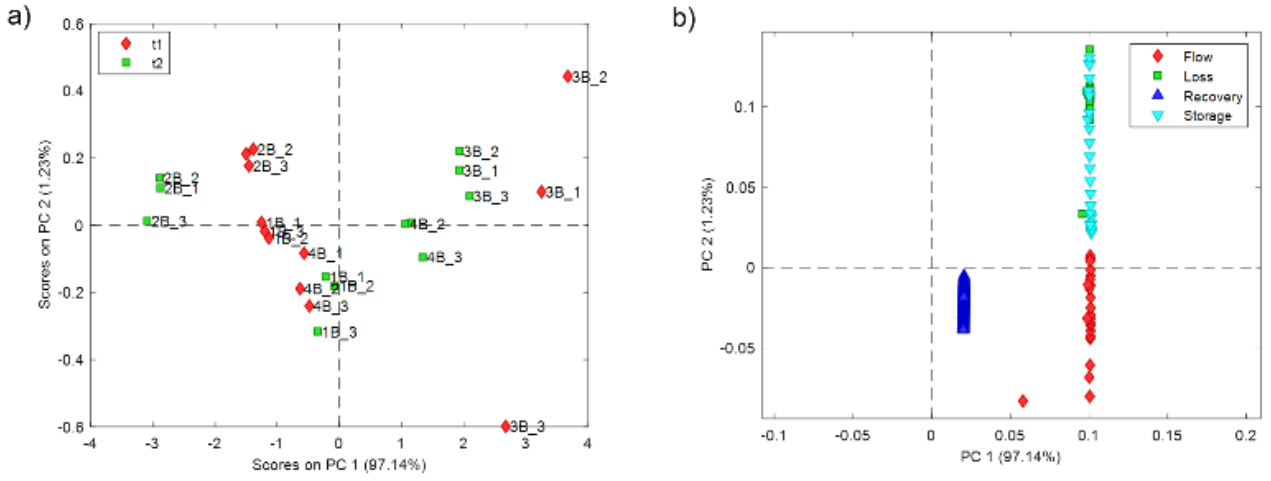

t1	1B	2B	3B	4B
1B	0.00	13.72	113.68	65.09
2B	13.72	0.00	127.13	128.02
3B	113.68	127.13	0.00	82.55
4B	65.09	128.02	82.55	0.00

t2	1B	2B	3B	4B
1B	0.00	336.81	258.38	74.98
2B	336.81	0.00	1568.54	746.94
3B	258.38	1568.54	0.00	33.15
4B	74.98	746.94	33.15	0.00

Figure 123: PCA for component B; score scatter plot and related FW table (a) and loading scatter plot (b)

8.4 MECHANICAL ANALYSIS

The same four samples characterised rheologically were analysed with the dynamic mechanical thermoanalysis (see 3.6.1 “Dynamic mechanical thermoanalysis (DMTA)”) after the cross-linking. Each A component sample was mixed with a suitable amount of polyamide resin and the same was performed for each B component sample, but with the epoxy resin. To have a complete cross-linking, the samples were measured after one week.

8.4.1 DYNAMIC MECHANICAL THERMOANALYSIS (DMTA)

As for the rheological characterisation, three measurements for each sample were carried out and the results represent the mean values. The measurements were performed in torsional mode (see 3.6.1 “Dynamic mechanical thermoanalysis (DMTA)”, after the identification of LVER using an amplitude sweep tests, as reported in Figure 124.

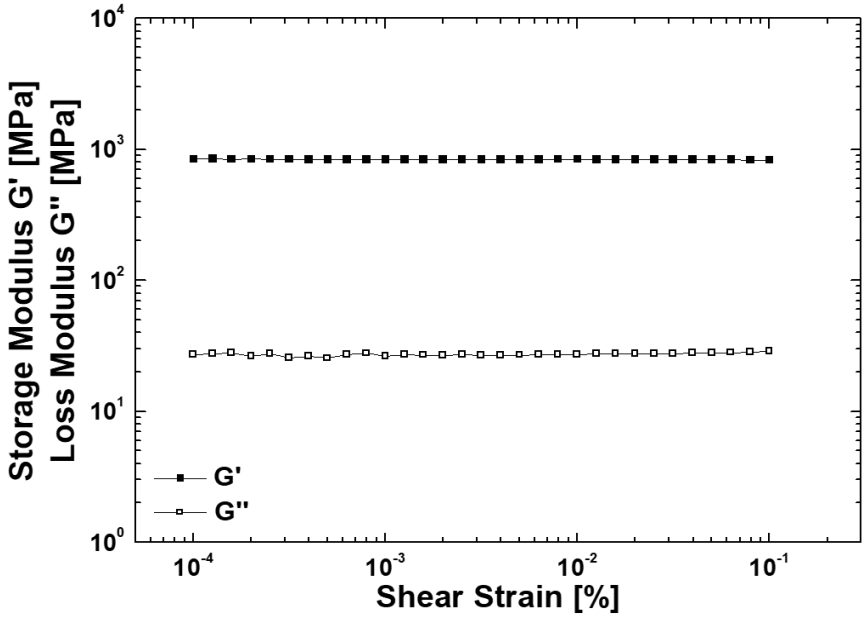

Figure 124: DMTA amplitude sweep test of sample 1A

The DMTA of both cross-linked A and B samples are reported, respectively, in Figure 125 and in Figure 126. On the left of plot, the storage and loss moduli are reported, while on the right the loss factor is represented.

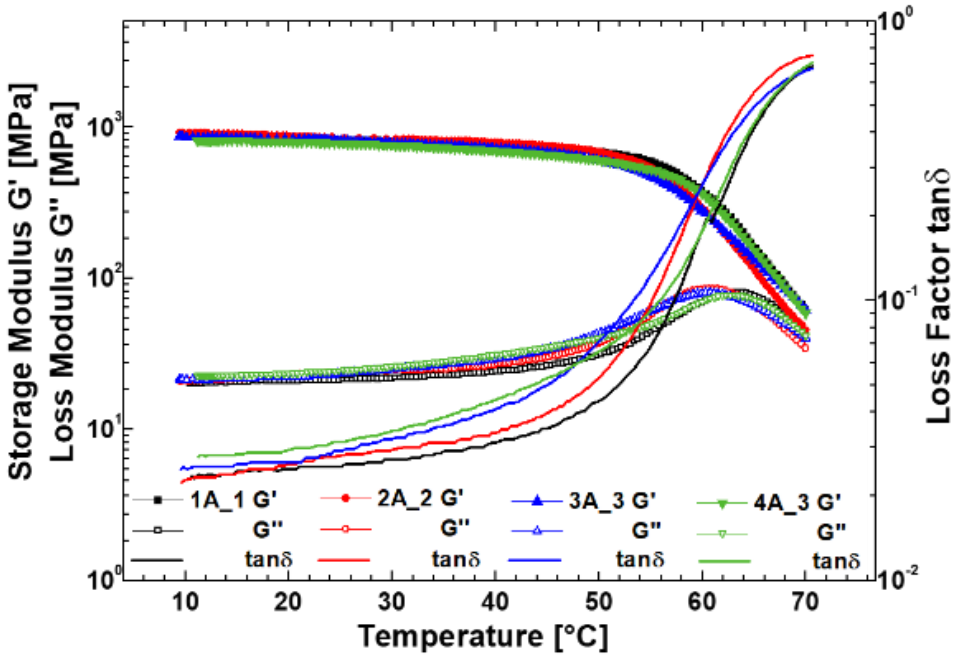

Figure 125: A component samples DMTA in torsion

In Figure 125, the A components curves appear quite similar and overlapped, indeed, the distances between the moduli is around the same for all samples. Also the Tg are around the same for all samples (~70°C).

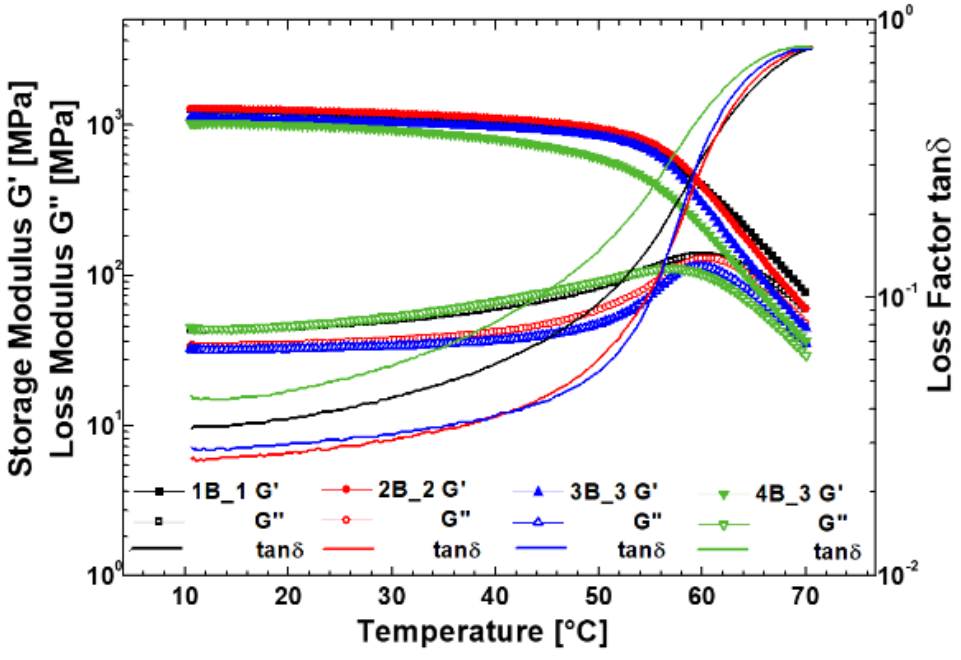

Figure 126: B component samples DMTA in torsion

In Figure 126 the B component curves appear a little bit less overlapped than for the A component samples. In this case, the samples 4B and 1B exhibit a lower distances between the moduli compared with the others. The Tg are around the same for all samples (~70°C).

8.4.2 *MULTIVARIATE ANALYSIS*

The DMTA data were treated with multivariate analysis since, as previously discussed, the results coincide with the univariate, but the treatment is faster.

Therefore, a low-level data fusion on the storage and loss moduli were performed. In this case, the number of variables is the same for both the block of data (150 data-points) and so the block-scaling pre-treatment was not performed.

In Figure 127, PCA of A cross-linked samples DMTA is reported. In more detail, Figure 127a represents the scores plot of A component samples, while Figure 127b represents the loadings plot. From an exploratory point of view, the highest amount of information is associated to PC1, explaining 58.6% of data variance. Groups of points corresponding to different rheological modifiers are scarcely separated. Considering the loading plots (Figure 127b) it is visible how all variables have the same importance for all samples, in fact they are distributed more or less circularly around the origin.

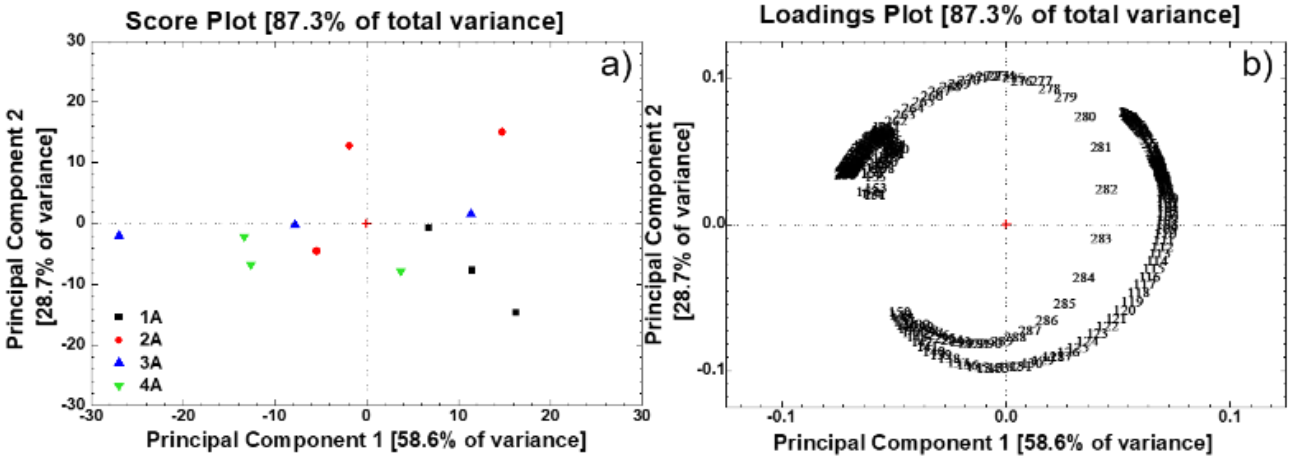

Figure 127: PCA of cross-linked A samples DMTA; score scatter plot (a) and loading scatter plot (b)

In Figure 128, PCA of B cross-linked samples DMTA is reported. In more detail, Figure 128a represents the scores plot of B component samples, while Figure 128b represents the loadings plot. The highest amount of information is associated to PC1, explaining 58.6% of data variance. Groups of points corresponding to different rheological modifiers appear quite well separated.

Considering the loading plots (Figure 128b), it is visible a different distribution of variables compared to the loading plot of A component: in this case, it is identifiable a semicircle where the variables at right represent the storage modulus, while the variables at left represent the loss modulus. The 2B samples are, so, mainly influenced by the storage modulus, while the 4B samples are mainly influenced by loss modulus. These observations are in agreement with the B component curves of

DMTA (Figure 123) in which the 2B samples exhibit a higher storage modulus than other samples whereas 4B samples show higher loss modulus compared with other samples.

Therefore, also in the cross-linked products the rheological modifiers have some effects on the B component samples.

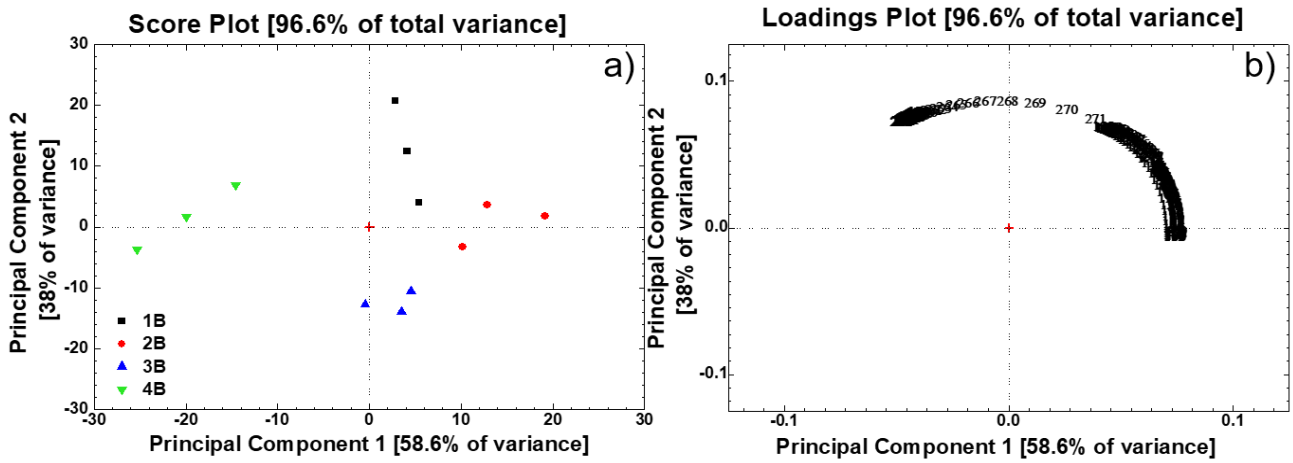

Figure 128: PCA of B cross-linked samples DMTA; score scatter plot (a) and loading scatter plot (b)

This result is particularly interesting because it shows that rheological modifiers, inserted in the formulation to obtain the right behaviour during the storage and the application of the product, have an effect on the mechanical properties of the cured filler. As consequence, their choice must be done keeping in consideration these aspects.

8.5 CONCLUSIONS

A systematic study of ten different rheological modifiers were carried out using recovery test. From the results, A components don't show relevant differences between them, while for the B components the rheological curves have rather different trends.

Four additives of those were studied in more details, performing a complete rheological characterisation over time, until one year. On the rheological data, both univariate and multivariate statistical analyses were carried out.

It was clear that the additives have no significant influence on the A component, while they have a remarkable influence on the B component. It was also noticeable that, along time (from the production t_1 along a year t_2), the very slight differences between additives on the A component tend to further decrease while, on the B component, the differences tend to increase. Furthermore, on the B

component, in both t_1 and t_2, the more performant additive is the polyamide and the worse one is the bentonite for non-polar coating systems. The reason must be searched in the matrix-additive interactions.

These interactions are caused by the hydrogen bonds formation. They create a structure, which can be destroyed by a stress and regenerated after the stress removal: this phenomenon is clearly evident in the recovery test. The different nature of A and B component consists in having acceptor and/or donor groups of the hydrogen bond: the epoxy matrix has only acceptor groups, while the polyamide matrix has both the acceptor groups and the donors. Therefore, B component allows to create stronger bond with polar systems, in particular with additive 3, which is of polyamide nature as itself.

Considering the data analysis and using a univariate statistical approach, a single data treatment for each type of rheological method is necessary. In this way, a lot of time is spent and correlations between different techniques may be not understood. On the contrary, multivariate analysis provides a "picture" of samples variance allowing to highlight correlations between the constituents of formulation and simplifying the analysis of large amounts of data.

From this study it is observed how, for the two components, it is necessary have two different additives, instead in the commercial fillers the rheological modifiers in both the components were the same.

On eight samples also a mechanical analysis (DMTA) was performed. On these data multivariate treatment was carried out. From the statistical results, A cross-linked samples appear quite overlapped while the B cross-linked samples are rather separated. Therefore, it is evident also for the cross-linked product of B component samples, an influence of rheological modifiers.

CHAPTER 9: DEVELOPMENT OF A NEW FILLER

Chapter 9 is focalised on the new specific filler formulation for the North European market. In this region, the fillers are extruded with the use of gear pumps at high operating pressures (typically 45 bar). This system involves the breakage of the standard microspheres, used in commercial fillers, with the consequence of chemical-physical modifications of the fillers, which cause problems during the application.

Therefore, different formulations were investigated both to optimise the compression resistance of filler, testing both GM_1 and GM_2, and to optimise their rheological behaviour.

Once identified the best formulations for A and B component among those tested, the new filler was compared to those commercials used as benchmark. In addition, a comparison between the new filler before and after in-field application was carried out.

9.1 OPTIMISATION OF COMPRESSION RESISTANCE

The first step to the development of the new filler was to test the compression resistance of A and B components containing both GM_1 and GM_2. GM_1, as already mentioned (see "Chapter 5: Extenders study") are less expensive and with lower density than GM_2 and so they are used in commercial fillers.

From the TDS of microspheres, GM_2 have more crush resistance than GM_1 and so they should have resisted to the compression of mechanical pumps.

Therefore, the fillers with GM_1 and GM_2 were undergone to compression tests to evaluation their crush resistance. A cylindrical stainless container (diameter 75 mm), where a single component of filler was placed, was compressed in two steps: the first one at 19bar and the second one at 38bar. This limit, 38bar, was imposed from the instrument (maximum load 38bar) and from the amount of filler, which had to be enough to measure the specific weight. After each compression step, the specific weight was registered and compared with the measure performed before the test. The GM_2 were tested in both A and B components of Filler_2 replacing the GM_1 and respectively called Filler_2AGM_2 and Filler_2BGM_2.

Figure 129: cylindrical stainless container used to test the compression resistance of the fillers

In Table 49 are reported the different values of specific weight before compression ($S.W._i$), after first compression ($S.W._{19bar}$), after the second compression ($S.W._{38bar}$) and the related increments in percentage, codified respectively as Δ_{19bar} and Δ_{38bar}.

Filler	$S.W._i$	$S.W._{19bar}$	$S.W._{38bar}$	Δ_{19bar}	Δ_{38bar}
	[g/cm^3]			[%]	
Filler_1A	0.62	0.72	0.99	16.1	59.7
Filler_1B	0.53	0.61	0.85	15.1	67.9
Filler_2A	0.70	0.75	0.87	7.14	24.2
Filler_2B	0.72	0.73	0.89	1.39	23.2
Filler_2AGM_2	0.80	0.80	0.81	0	1.25
Filler_2BGM_2	1.01	1.01	1.01	0	0

Table 49: specific weights and their increment in percentage, after compression, of commercial filler and new filler

The increment of specific weight is related to the breakage of microspheres that involves an increase of weight and a decrease of volume respect to the same sample with whole microspheres. Considering the commercial fillers, containing GM_1, it is visible a remarkable increment of specific weight. In particular, Filler_1 exhibits an upper increment in percentage than Filler_2, indeed, it has a higher percentage of GM_1 in formulation. Instead, the specific weight of Filler_2AGM_2 and Filler_2BGM_2 is stable and so, it is possible to conclude that GM_2 were not broken, during the compression.

In particular, considering the curves obtained from the dynamometer of Filler_2A (with GM_1) and of Filler_2AGM_2, reported in Figure 130, it is possible to observe, for the first one, two steps of compression in the range 0-6min and 6-12min.

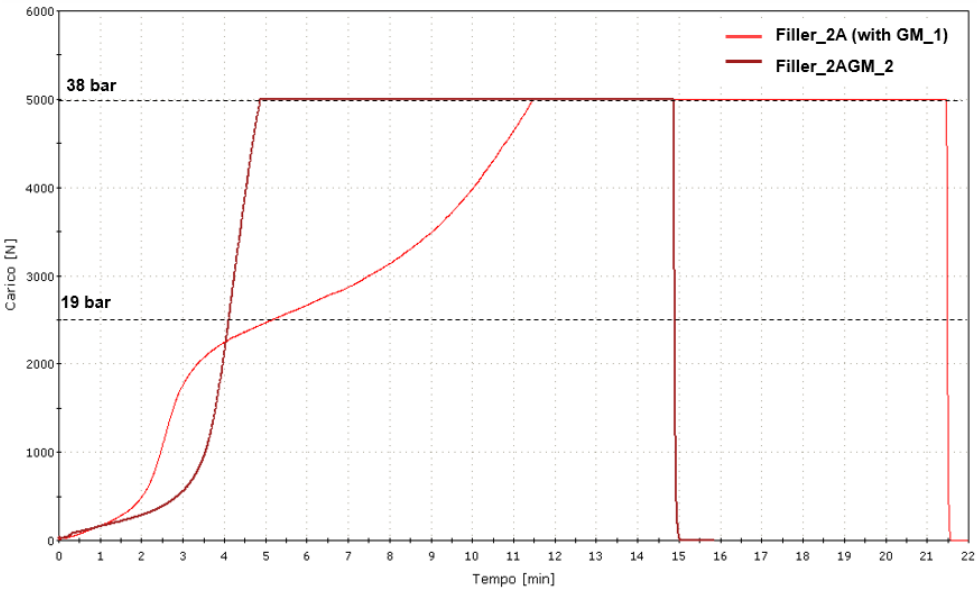

Figure 130: load vs. time for Filler_2A both with GM_1 and with GM_2

These two steps were always present in all samples, with the exceptions of Filler_2AGM_2 and of Filler_2BGM_2. The first step could be related to the release of air that involved in a small increment of specific weight and then, in the second step, the increment in specific weight was related to the breakage of the hollow glass microspheres.

9.2 OPTIMISATION OF RHEOLOGICAL BEHAVIOUR

Verified that the GM_2 can be used in filler extruded with gear pumps, different formulations for A and B component were tested to optimise their rheological properties. The formulations of Filler_2A and Filler_2B were used as a starting point for the new formulation.

In Table 50, all formulations of A component are listed reporting the percentage of extenders and total adsorption. From the results obtained in “Chapter 8: Rheological modifiers study”, the rheological modifiers, belonging to the bentonites, polyamide and castor oil families, had no particular influence on rheological behaviour and so they were tested in A component formulations of new filler.

Sample	Rheological additive family	Alumina-silicate spheres	Talc	Microspheres	Silica	Total adsorption
	-	[%]				
Filler_2A	Castor oil derivative	5.7	3.5	9.0	3.0	39.2
1A	Castor oil derivative	5.7	3.5	9.0	3.0	36.0
3A	Castor oil derivative	8.3	-	9.0	4.5	34.2
5A	Castor oil derivative	6.3	2.0	10.5	4.5	36.5
7A	Polyamide modified	7.5	-	10.5	4.5	37.2
9A	Polyamide modified	8.3	2.0	9.5	3.0	32.6
11A	Bentonite modified for non polar system	8.3	2.0	9.5	3.0	32.6
13A	Bentonite modified for polar system	8.3	2.0	9.5	3.0	32.6

Table 50: A component formulations for new filler

As in “Chapter 8: Rheological modifiers study”, recovery tests were performed on samples in order to have comparable data from the rheological point of view. 1A and 5A samples were exclude from the recovery test, since too viscous based on aspect to spatula test.

In Figure 131, the recovery tests are reported. As already discussed, the recovery curves of A component samples appear really similar.

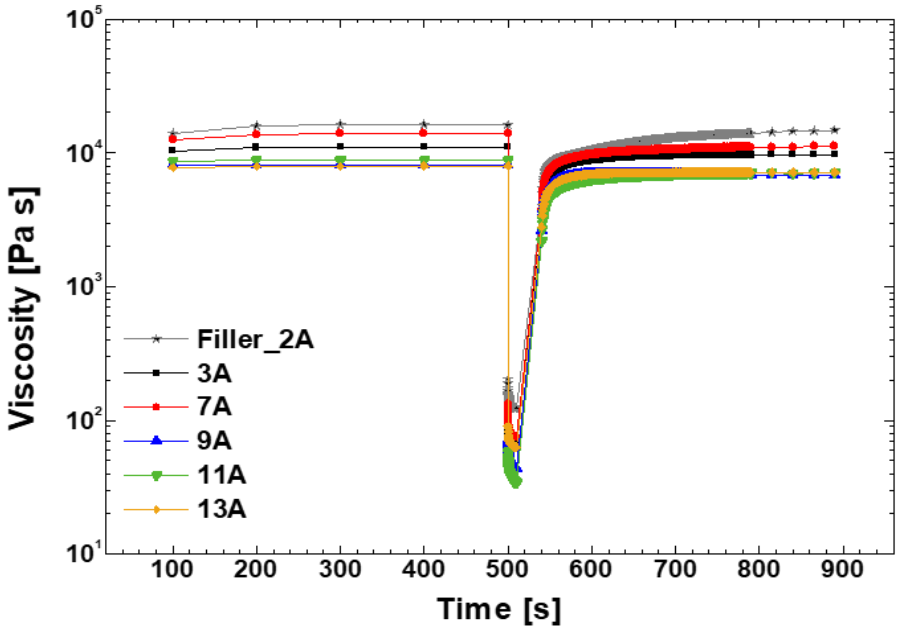

Figure 131: recovery test of A components

The recoveries of samples reported in Figure 131 are listed in Table 51. From the results, the formulation with the best rheological performance was 13A, since its Rec_{30s} and Rec_{tot} were higher than in other samples and in the standard. Therefore, this formulation was selected for the new filler A component.

A component	Rec_{30s}	Rec_{tot}
	[%]	
Filler_2A	53	92
3A	59	89
7A	54	81
9A	67	84
11A	52	80
13A	80	91

Table 51: recovery after 30s and total recovery of A components

In Table 52, all formulations of B component are listed reporting the percentage of extenders and total adsorption. The microspheres of Filler_2B were GM_1 while in other samples GM_2. From the results obtained in "Chapter 8: Rheological modifiers study", the rheological modifiers used were polyamide.

Sample	Alumina-silicate spheres	Microspheres	Carbonates	Silica	Total adsorption
	[%]				
Filler_2B	9.0	9.5	31.8	3.0	38.5
2B	7.0	13.5	28.6	1.5	39.2
4B	9.3	16.3	18.3	1.0	41.5
6B	9.4	16.3	18.5	1.0	41.6
8B	10.5	13.4	27.0	1.5	40.8
10B	9.4	15.3	28.6	1.0	49.6
12B	11.0	13.4	15.0	1.0	38.3
14B	11.0	13.4	15.0	1.5	38.3
15B	11.0	13.4	15.0	1.5	38.3
16B	11.0	13.4	15.0	1.5	38.3
17B	11.0	13.4	15.0	1.5	38.3
18B	11.0	13.4	20.0	1.5	39.5
19B	11.0	13.4	20.0	1.5	39.5
20B	12.0	13.4	23.6	1.7	36.1

Table 52: B component formulations for new filler

As in A component, some samples were excluded from the recovery test (Figure 132). The recovery curves of B component samples exhibit trends really different.

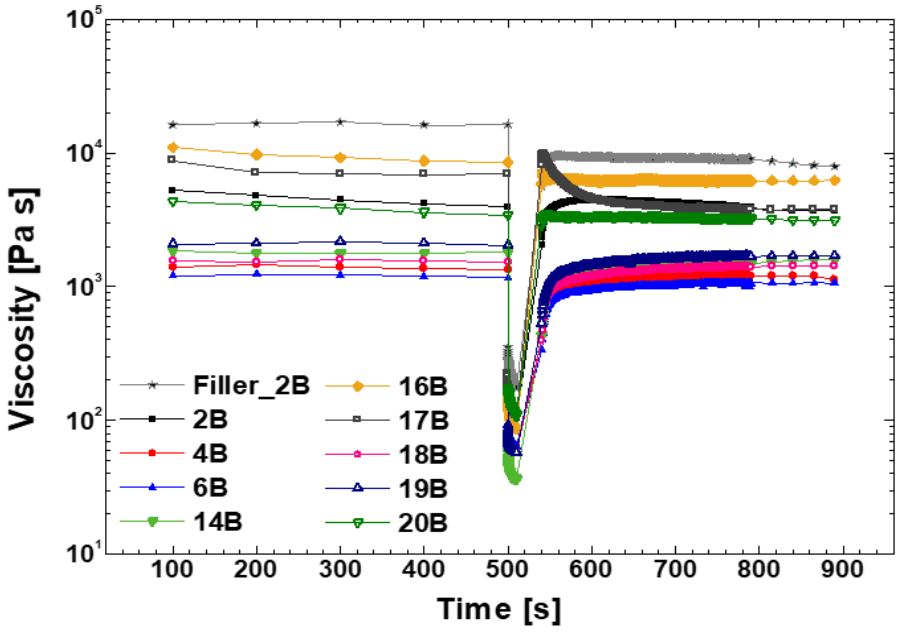

Figure 132: recovery test of B components

The recoveries of samples reported in Figure 132 are listed in Table 53. 16B and 20B samples showed higher Rec_{30s} than in the other samples and in the standard, nevertheless, the 20B sample was selected as B component of the new filler, since 16B had lower Rec_{tot} than other samples.

B component	Rec_{30s}	Rec_{tot}
	[%]	
Filler_2B	56	50
2B	82	82
4B	63	86
6B	61	88
12B	53	85
14B	69	66
16B	109	51
18B	58	91
19B	52	80
20B	94	80

Table 53: recoveries after 30s and total recoveries of B components

The samples 13A and 20B will be called respectively Filler_NA and Filler_NB, and the cross-linked product will be called Filler_N.

9.3 LABORATORY TEST

The following characterisations and studies were carried out on the Filler_N in the laboratory.

9.3.1 COATINGS TESTS

The specific weight of both components of Filler_N, is reported in Table 54. The compression of Filler_NA and of Filler_NB was also preformed and the corresponding data are listed in Table 54.

	S.W. [g/cm^3]	S.W.$_{38bar}$ [g/cm^3]	Δ_{38bar} [%]
Filler_1A	0.62	0.99	59.7
Filler_1B	0.53	0.85	67.9
Filler_2A	0.70	0.87	24.2
Filler_2B	0.72	0.89	23.2
Filler_NA	0.83	0.85	2.4
Filler_NB	0.76	0.78	2.7

Table 54: specific weight of commercial fillers and Filler_N before and after compression and its increment in percentage

As visible, Filler_N shows upper specific weight than commercial fillers; this is related to their formulations and to different density of two hollow glass microspheres types (GM_2 has higher density than GM_1). The really slight increment of specific weight could be related to the loss of incorporated air during the production.

In Table 55, the pot life, measured at 20°C and the hardness test values of Filler_N are reported. The Shore D values of Filler_N are a little bit greater than in other fillers, but for the use as a filler for hull it is acceptable. In addition, Filler_N appears homogeneously cross-linked, in fact the instantaneous measure and the one after 15s are very similar.

	Pot Life [min]	Shore D_{7days}
Filler_1	60	55/50
Filler_2	60	61/60
Filler_N	40	68/66

Table 55: pot life and shore D values of commercial fillers and of Filler_N

In Figure 133, the measure of Shore D is reported.

Figure 133: Shore D measure

9.3.2 *INFRARED SPECTROSCOPY ANALYSIS*

The infrared analysis was used to study the mixing ratio of the Filler_N.

STUDY OF MIXING RATIO

As already explained the mixing ratio knowledge is essential for the fillers application control. One possibility to do that is the use of a calibration line obtained from IR spectra of different known mixing ratios. To create the calibration line, the ratio between the intensity of epoxy and polyamide typical signals, called R, is plotted versus the mixing ratio (A/B). There are different typical signals for epoxy and polyamide, as already discussed, but in this chapter are considered the follow peaks: 827cm^{-1} for epoxy and 711cm^{-1} or 872cm^{-1} for polyamide matrix. These peaks were chosen because they are constant during the cross-linking and they were not overlapped.

Therefore, five samples were prepared with the following mixing ratios A/B: 0.92, 1.04, 1.14 (stoichiometric, because the ratio fifty/fifty of A/B is related to the extenders percentage present in the formulations), 1.27, 1.43 and after cross-linking they were analysed with IR.

Five IR spectra were collected for each sample in order to obtain a more precise measurement.

For both the I827/I711 and I827/I872 ratio, called respectively $R_{827/711}$ and $R_{827/872}$, calibration lines ($y=ax+b$) were constructed and they are reported in Figure 134.

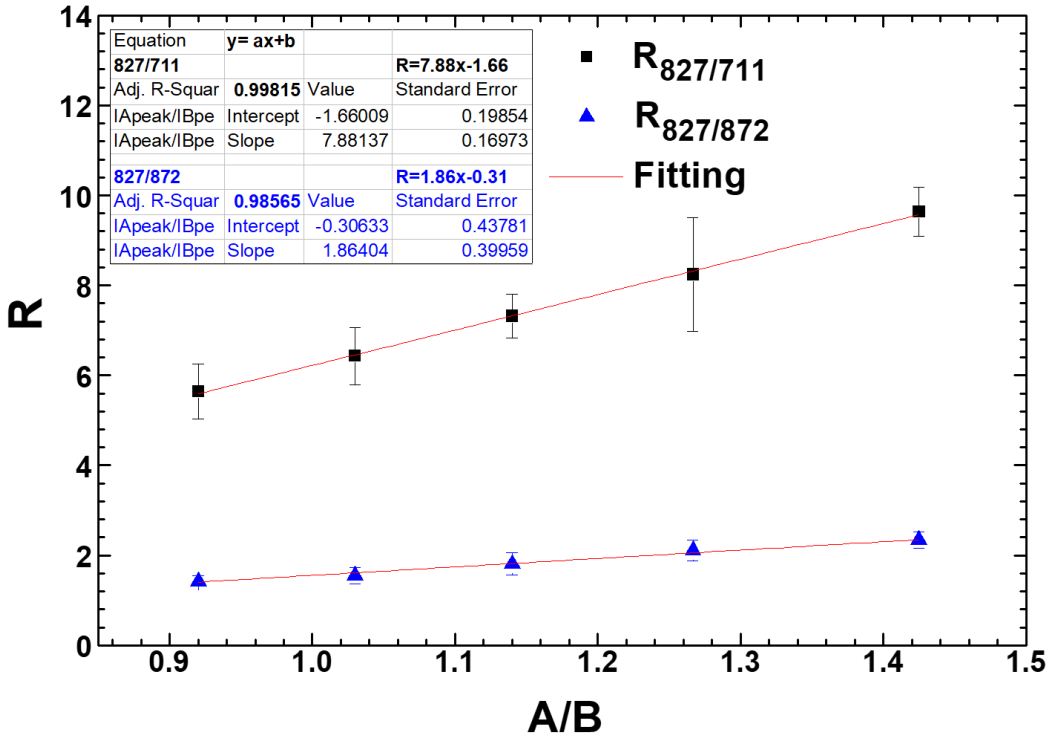

Figure 134: calibration lines for Filler_N

As visible, the linearity is really good for both. $R_{827/872}$ has R^2 higher than in $R_{827/711}$, in addition, $R_{827/872}$ allows a better identification of the samples, being more sloping and therefore, it is considered to calculate the mixing ratio; however, $R_{827/872}$ has higher standard deviations compared to $R_{827/711}$. Therefore, the equation of the calibration line is:

$$R = 7.88x - 1.66 \tag{25}$$

The mixing ratio A/B can be calculated with the following expression:

$$\frac{A}{B} = \frac{R + 1.66}{7.88} \tag{26}$$

In Figure 135 and in Figure 136, the IR spectra of the mixing ratios tested and the magnification of these spectra in range 890-650cm^{-1} are respectively reported.

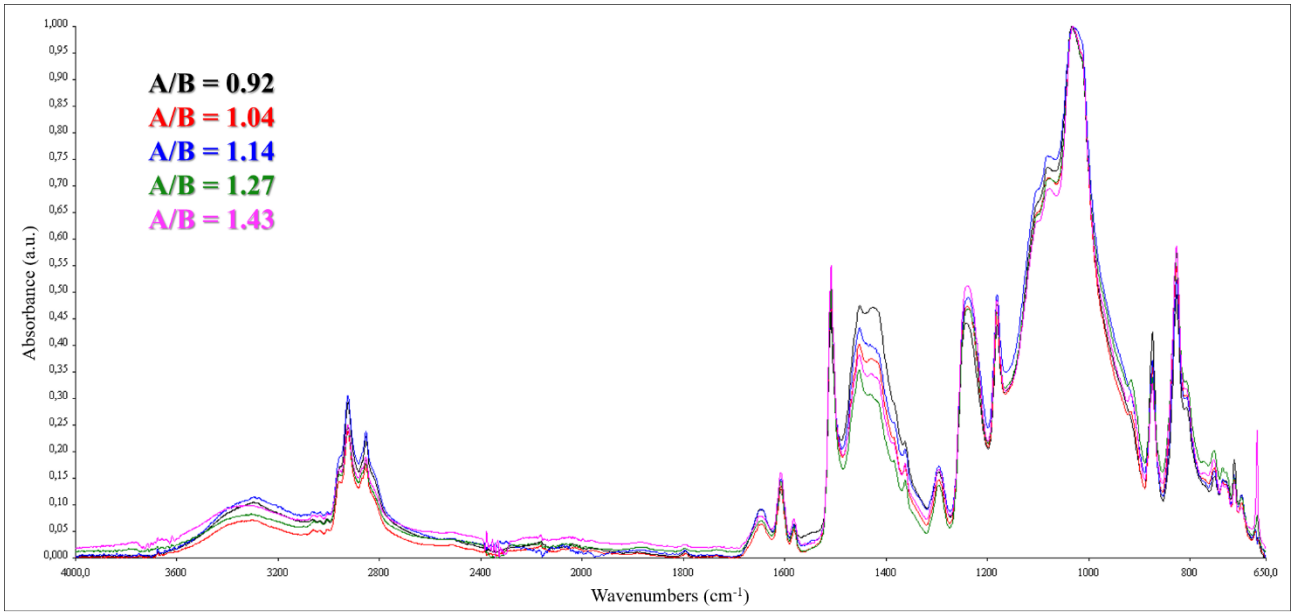

Figure 135: IR spectra of mixing ratios

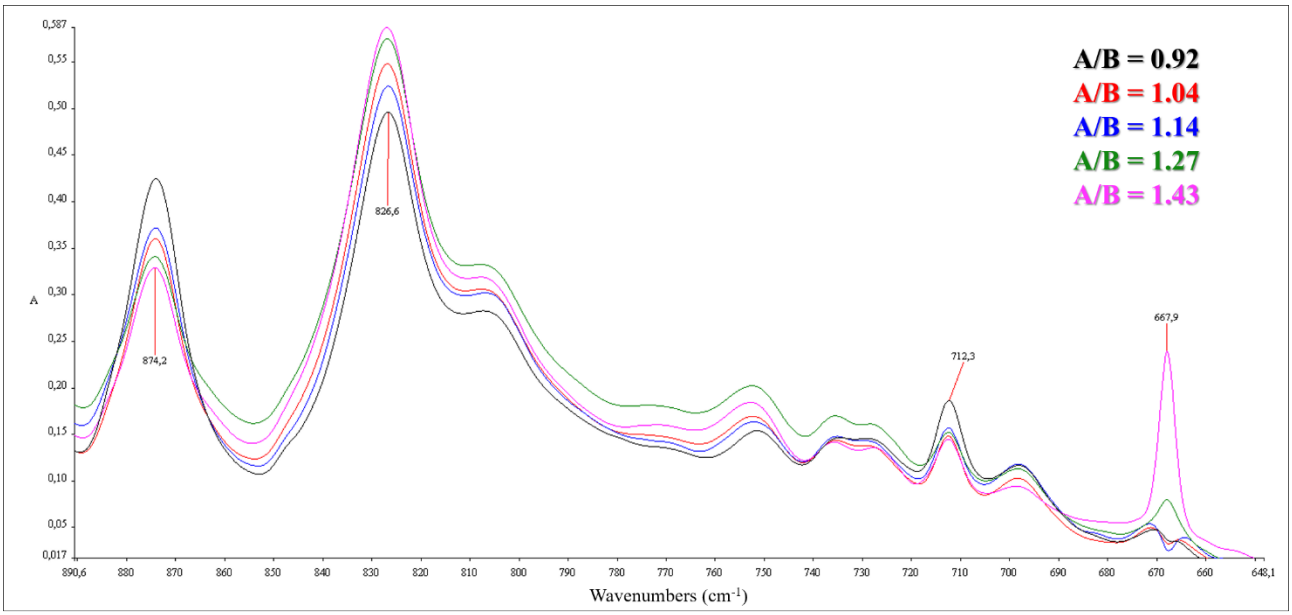

Figure 136: IR spectra of mixing ratios; magnification in range 890-650cm^{-1}

Therefore, withdrawing the samples from the hull and analysing them with IR, the R ratios between the intensity of typical signals of A and B component, are obtained. Subsequently, inserting them in the calibration line the mixing ratio was identified.

9.3.3 THERMAL ANALYSIS

THERMOGRAVIMETRIC ANALYSIS (TGA)

TGA was performed to determine the degradation temperature of the resins and the residual of filler. The TGA curve of Filler_N is reported in Figure 137.

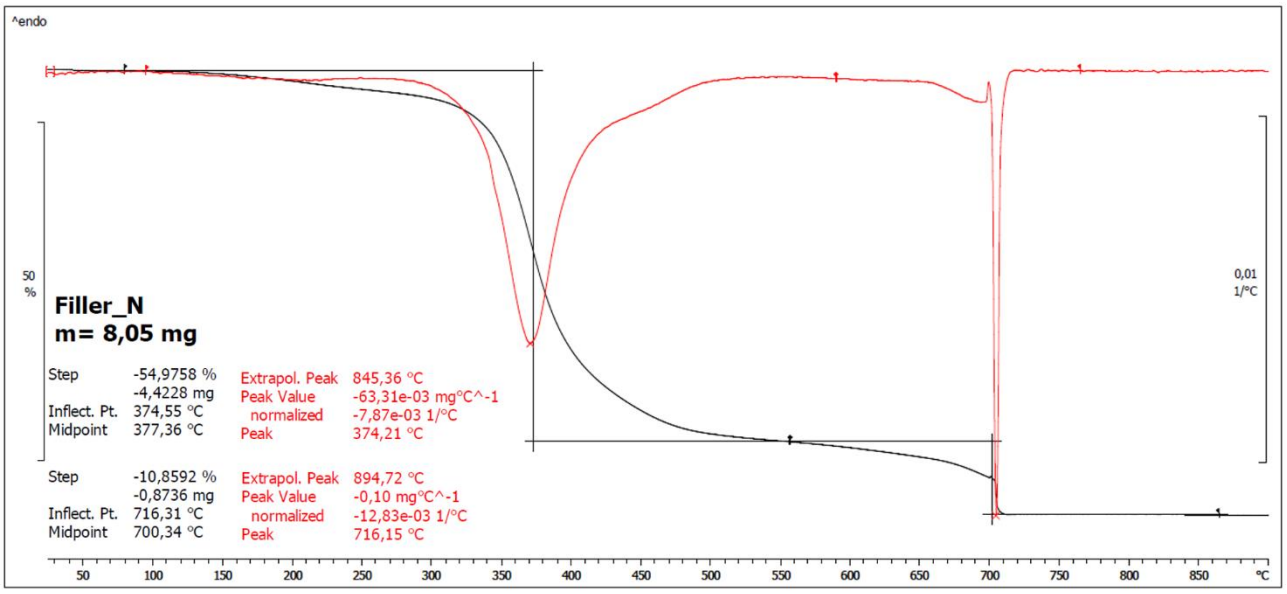

Figure 137: TGA curves of Filler_N

It shows a first loss at around 150 °C, due to the loss of low molecular weight molecules into the filler. Then the loss of material (54.98%wt) in the range 300–700 °C is due to real decomposition of the organic part of the resins, confirming their thermal resistance up to 350 °C. Moreover, at 700 °C, it is observed the switch from N_2 to O_2 atmosphere and the residue of 34.16% wt is ascribed to the inorganic extenders.

The trend of TGA curve is totally analogous to commercial fillers.

DIFFERENTIAL SCANNING CALORIMETRY (DSC)

The DSC curves, used to determine the temperature of glass transition (*Tg*), are reported in Figure 138, the trend of the three fillers is around the same.

The Tg of Filler_N, considering the midpoint, is 46°C, value slightly higher than those of Filler_1 and of Filler_2 respectively 43 and 41°C. This Tg value is in agreement with the mechanical properties (Shore D values, Young's modulus and so on), that are higher than in commercial fillers.

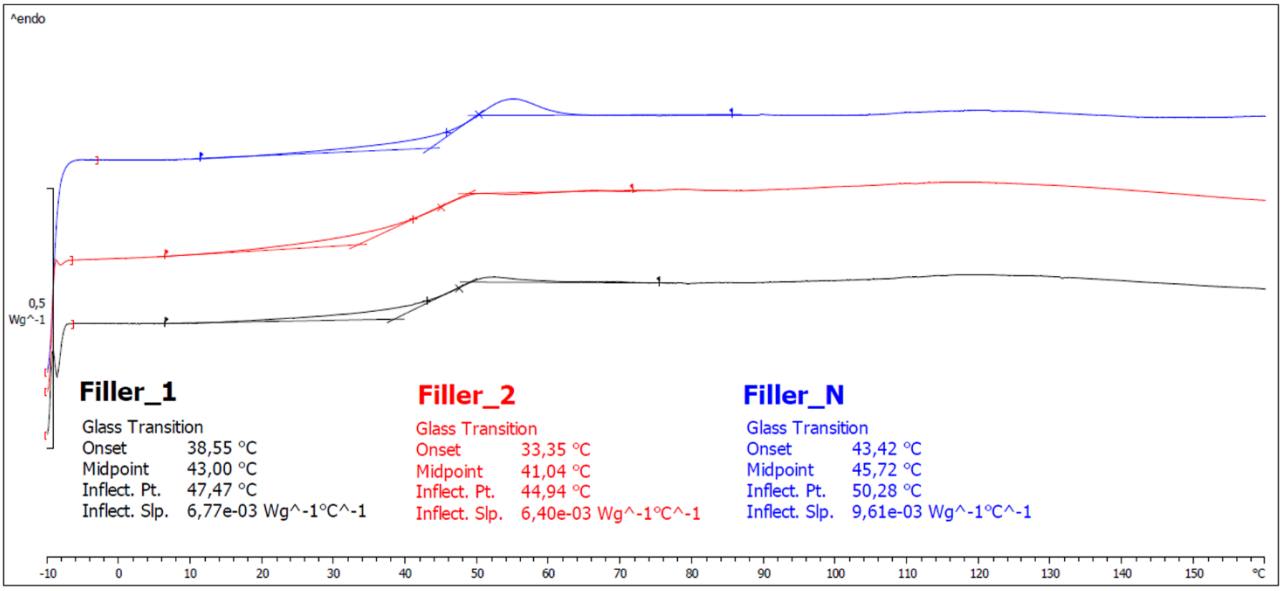

Figure 138: DSC curves of commercial fillers and of Filler_N

THERMAL PROPERTIES OF DIFFERENT A/B RATIO

On the five samples with different mixing ratio A/B, DSC analyses were performed and the curves are reported in Figure 139, while in Table 56 the Tg values are listed.

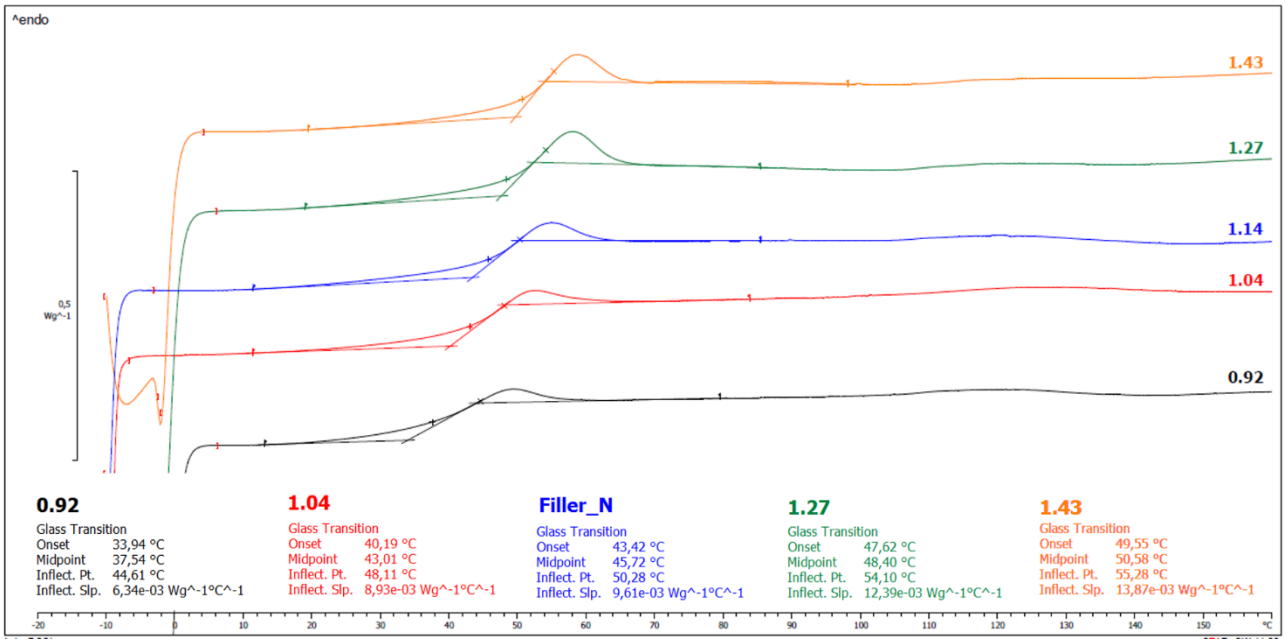

Figure 139: DSC curves of samples with different mixing ratios

From the Tg values reported below and from the Figure 140, in which the Tg is plotted against the mixing ratio, it is possible to observe a specific trend: firstly the Tg values increase rapidly and then they tend to stabilise. Indeed, from mixing ratio 0.92 (excess of 19% of B component) to

stoichiometric ratio there is a sharp increment of Tg and subsequently, increasing further the A component (25% in excess), the raise of Tg slows down up to a quite stable value of about 48°C.

A/B	Tg [°C]
0.92	37
1.04	43
1.14	46
1.27	48
1.43	50

Table 56: Tg of samples with different mixing ratio A/B

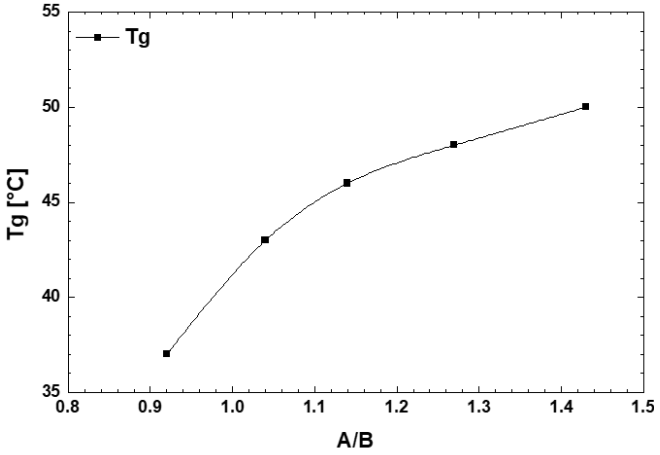

Figure 140: Tg vs. A/B mixing ratio

9.3.4 RHEOLOGICAL ANALYSIS

Different rheological tests were performed on both two components of Filler_N. The measurements were carried out at two different times: 1) after one week (t_1) and 2) after one year (t_2) from the production. Triplicate measurements have been carried out on each samples.

In Table 57 are reported, for Filler_2 and Filler_N the means and the standard deviations of initial viscosity ($\eta_{0.01\_F}$), the recovery percentage after 30s (Rec_{30s}), the total recovery percentage (Rec_{tot}), the distance between the moduli, indicated as G'-G'', its increment in percentage after one year respect to the measure performed at one week, $\Delta(G'-G'')$, and the end of LVER, obtained from the software RheoCompass s1.19.

Filler	Times	$\eta_{0.001\_F}$ [kPa s]	Rec_{30s} [%]	Rec_{tot} [%]	G'-G'' [kPa]	Δ(G'-G'') [%]	LVER end [%]
Filler_2A	7days	16±1	53±5	92±6	25±2	-	0.005
	1years	25±1	55±3	85±4	31±2	24.0	0.005
Filler_NA	7days	11±5	80±4	89±3	14±3	-	0.030
	1years	13±5	63±4	82±1	31±5	121	0.030
Filler_2B	7days	12±2	56±3	50±1	12±1	-	0.005
	1years	21±2	44±5	45±1	20±1	66.7	0.005
Filler_NB	7days	5±1	94±2	80±01	13±4	-	0.010
	1years	9±4	89±3	80±6	15±9	15.4	0.010

Table 57: the rheological data from viscosity, recovery and amplitude sweep tests of Filler_2 and Filler_N

VISCOSITY TEST

Figure 141 reports the flow curves of both A and B components of Filler_N and Filler_2.

Considering the A components, as visible in Figure 141a) and as reported in Table 57, Filler_NA appears more stable than Filler_2A that exhibits, over time, a remarkable increase of viscosity. The trend of Filler_2A and Filler_NA curves is comparable.

Regarding the B components (Figure 141b), the Filler_NB trend is quite different compared to the Filler_2B, indeed Filler_NB has a smaller slope compared to the commercial filler. This behaviour involves a milder dependence of viscosity on shear rate respect commercial filler.

The Filler_NA appears more stable over time than Filler_NB.

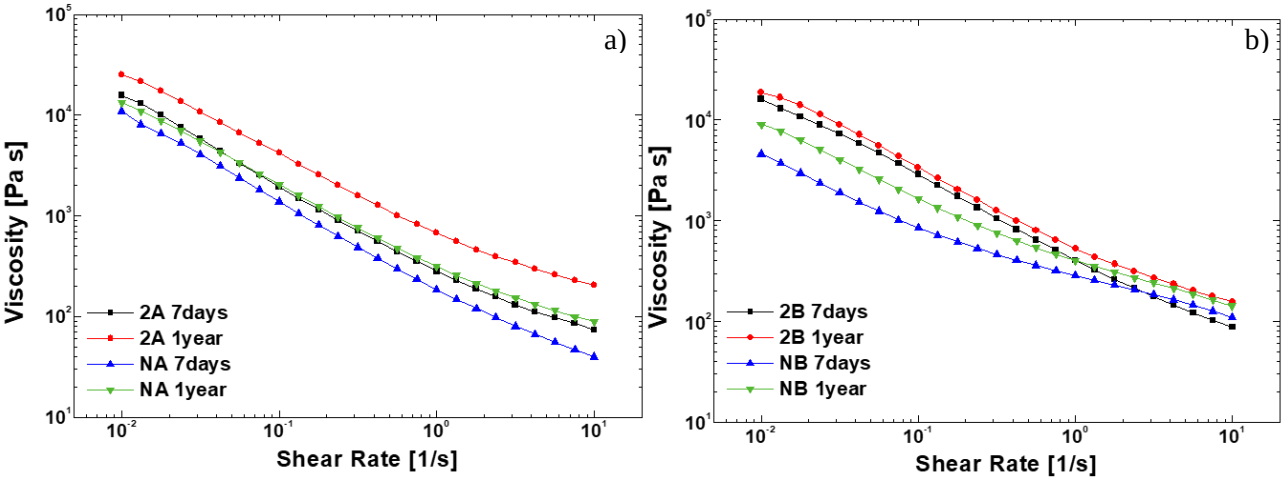

Figure 141: viscosity test of Filler_2 and Filler_N; A components (a) and B components (b)

RECOVERY TEST

Figure 142 reports the recovery test of A component Figure 142a) and of B component Figure 142b) of Filler_2 and Filler_N. Over time, all recoveries decrease, but there are some differences to highlight. Considering the A components, as for the flow curves, the trends of Filler_2A and Filler_NA are comparable. However, as reported in Table 57, the recoveries of Filler_NA appear higher than in Filler_2A. The same consideration can be done for the measurements over time.

Considering the B components, the recoveries are really good both at t_1 and at t_2 for the Filler_NB, indeed they are higher than in Filler_2B.

Filler_NA results a good A component and in particular the B component of this new filler results better than Filler_2 for the filler requirements, indeed, as already mentioned, the faster is the recovery the higher is the applicable thickness (see 3.5.2 “Recovery test”).

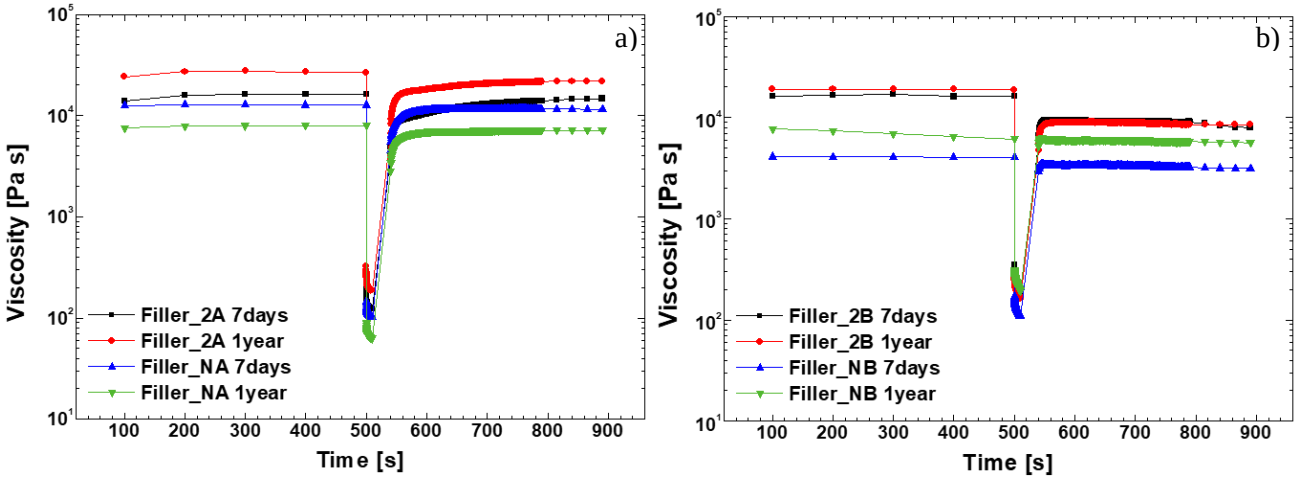

Figure 142: recovery test of Filler_2 and Filler_N; A components (a) and B components (b)

AMPLITUDE SWEEP TEST

Figure 143 reported the amplitude sweep test of A component Figure 143a) and of B component Figure 143b) of Filler_2 and of Filler_N.

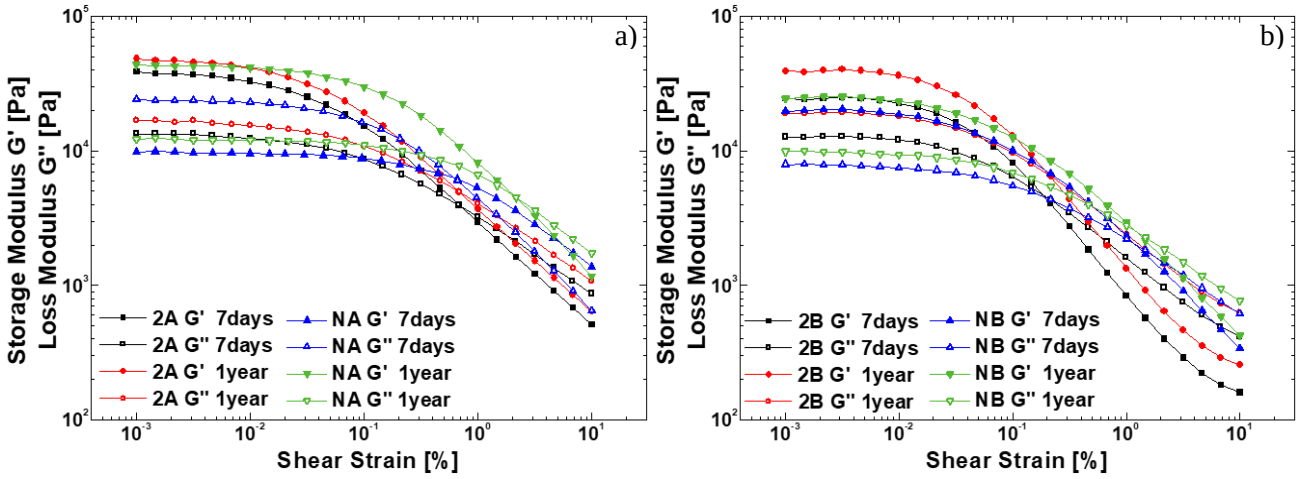

Figure 143: amplitude sweep test of Filler_N; A components (a) and B components (b)

As visible from the amplitude sweep test, all the samples exhibit a good separation between moduli (over 10kPa), that increases over time.

Considering the A components, Filler_NA shows an increment in percentage of the distance between the moduli of 121%, while Filler_2A of 24%. The end of LVER, instead, is higher in Filler_NA (0.030%) than in Filler_2A (0.005%) and so Filler_NA can suffer shear strain higher without disrupting its internal structure. Over time, Filler_N appear less stable than Filler_2.

Considering the B components, the Filler_NB exhibits lower separation between the moduli respect to the Filler_2B, and over time, its increase (15%) is lesser than the Filler_2B (67%).

Finally, as for the A components, in the Filler_NB the end of LVER is upper than in Filler_2B.

In this case, the Filler_NB appears more stable than Filler_2B.

Generally, the B component of Filler_N is the most stable among all samples, in amplitude, and this is an important goal for the new filler. Indeed, in all samples already discussed, the B components show a limited stability over time. Furthermore, the end of LVER both for A and B components of Filler_N is higher than in Filler_2. Therefore, for the application point of view, Filler_N appears really good.

9.3.5 MECHANICAL ANALYSIS

Among the several filler requirements, mechanical properties represent a fundamental aspect to taking into consideration (see "Chapter 2: Fillers").

Therefore, mechanical characterisation of filler was clearly necessary. Torsional oscillatory tests, belonging to the dynamic mechanical thermoanalysis (*DMTA*), tensile tests, three-point bending tests and compression were carried out, on the cross-linked product, obtained mixing A and B components.

To have a complete cross-linking, the samples were measured after one week from the application.

DYNAMIC MECHANICAL THERMOANALYSIS

The measurements were performed in torsional mode (see 3.6.1 "Dynamic mechanical thermoanalysis (DMTA)"), using the LVER determined for commercial fillers and the same heating profile (see Figure 55 in "Chapter 4: Characterisation of commercial fillers").

Three measurements for each sample were carried out and the results represent the mean values.

Filler_N and the commercial fillers DMTA in torsion are reported in Figure 144.

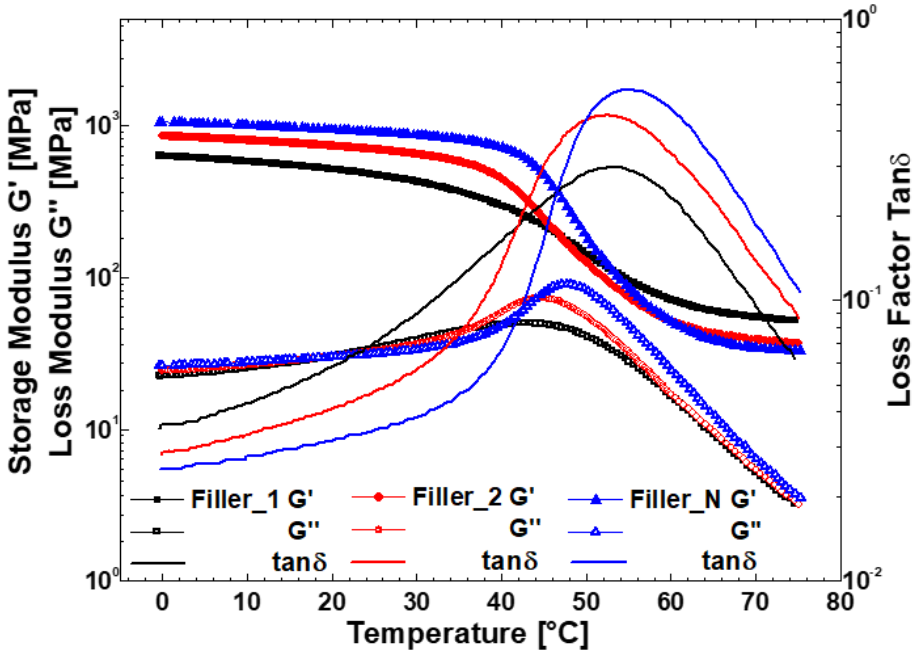

Figure 144: DMTA of commercial fillers and of Filler_N

From the DMTA, the glass transition temperatures were obtained considering the loss factor peaks. The mean is reported in Table 58 with the corresponding standard deviation.

The coefficients of thermal expansion, α, were also calculated from the DMTA data (see "Chapter 4: Characterisation of commercial fillers"). As for the commercial fillers the ΔT considered were related to the glass transition temperature. In Table 58 are reported α_1 (measured before the Tg), α_2 (measured after the Tg), and their increment in percentage ($\Delta\%$).

Filler	T_g [°C]	α_1 [$10^{-4} \cdot$ °C]	α_2 [$10^{-4} \cdot$ °C^{-1}]	$\Delta\alpha$ [%]
Filler_N	54.9±0.2	1.26	1.69	34.1

Table 58: glass transition temperatures and its coefficients of expansion of Filler_N

Considering the values of commercial fillers (see Table 8), the Tg of Filler_N is comparable, as α_1, while the α_2 is a little bit higher.

The values of coefficients of thermal expansion are just indicative, since this is not the correct method to determine α, however they can be used to have a preliminary comparison.

UNIAXIAL TEST

Three measurements for each sample were carried out and the results, reported in tables, are the means and the standard deviation. Analogously to the uniaxial test of commercial fillers, also Filler_N was mechanically analysed at three different temperatures 0, 20 and 30°C. Besides, the samples with different ratio were analysed to evaluate its influence on the mechanical properties with three-point bending test.

Tensile Test

In Table 59, are listed the Young's modulus (MPa), E_t, the stress (MPa), σ_t, and the deformation (%), ε_t of Filler_N. The values of commercial fillers are reported in Table 9.

Filler	Temperature [°C]	E_t [MPa]	σ_t [MPa]	ε_t [%]
Filler_N	0	1204 ± 53	13.66 ± 0.36	0.71± 0.21
	20	1020 ± 95	11.90 ± 3.40	1.05 ± 0.25
	30	985 ± 49	9.70 ± 1.87	1.90 ± 0.80

Table 59: tensile values of Filler_N

In Figure 145, the stress (σ_t) is plotted against the deformation (ε_t) for the commercial fillers and of Filler_N. The measures exhibit standard deviations quite high, above all for the Filler_N at 20 and 30°C. Nevertheless, the influence of temperature on Filler_N appears comparable with Filler_1.

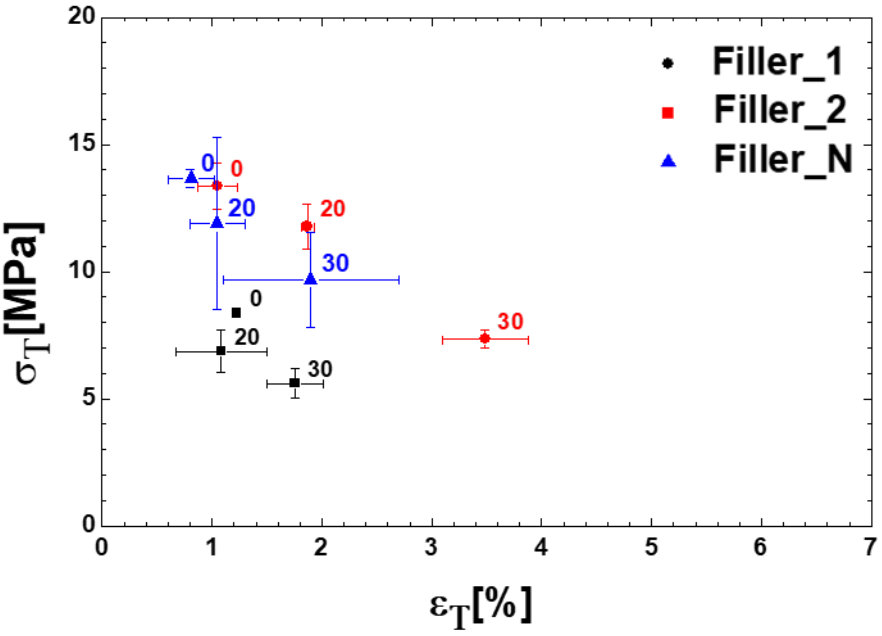

Figure 145: tensile results for Filler_N and commercial fillers

Three-point bending Test

In Table 60 are listed the Young's modulus (MPa), E_b, the stress (MPa), σ_b, and the deformation (%), ε_b, of Filler_N. The values of commercial fillers are reported in Table 10. In Figure 146, the stress (σ_t) is plotted against the deformation (ε_t).

Filler	Temperature [°C]	E_t [MPa]	σ_t [MPa]	ε_t [%]
Filler_N	0	2647 ± 21	25.2 ± 0.6	1.00 ± 0.03
	20	2287 ± 41	22.2 ± 1.1	1.06 ± 0.06
	30	1930 ± 28	20.7 ± 0.9	1.25 ± 0.09

Table 60: three-point bending values of Filler_N

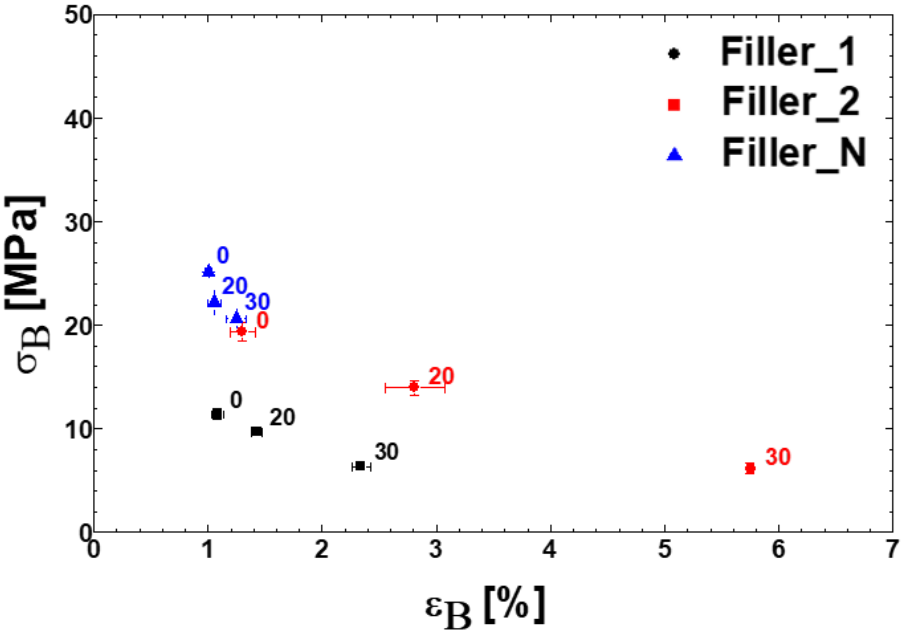

Figure 146: three-points bending test results of commercial fillers

Filler_N shows a less dependence from the temperature than other two fillers. In addition, standard deviations are always very low.

COMPRESSION TEST

The means and the standard deviations of E_b, σ_b, and the ε_b are shown in Table 61, while in Figure 147 the stress (σ_t) is plotted against the deformation (ε_t).

Filler	Temperature [°C]	E_t [MPa]	σ_t [MPa]	ε_t [%]
Filler_N	0	1493 ± 307	44.6 ± 0.7	3.56 ± 0.45
	20	1120 ± 83	37.9 ± 1.2	3.59 ± 0.31
	30	872 ± 111	32.7 ± 0.7	3.90 ± 0.11

Table 61: compression values of Filler_N

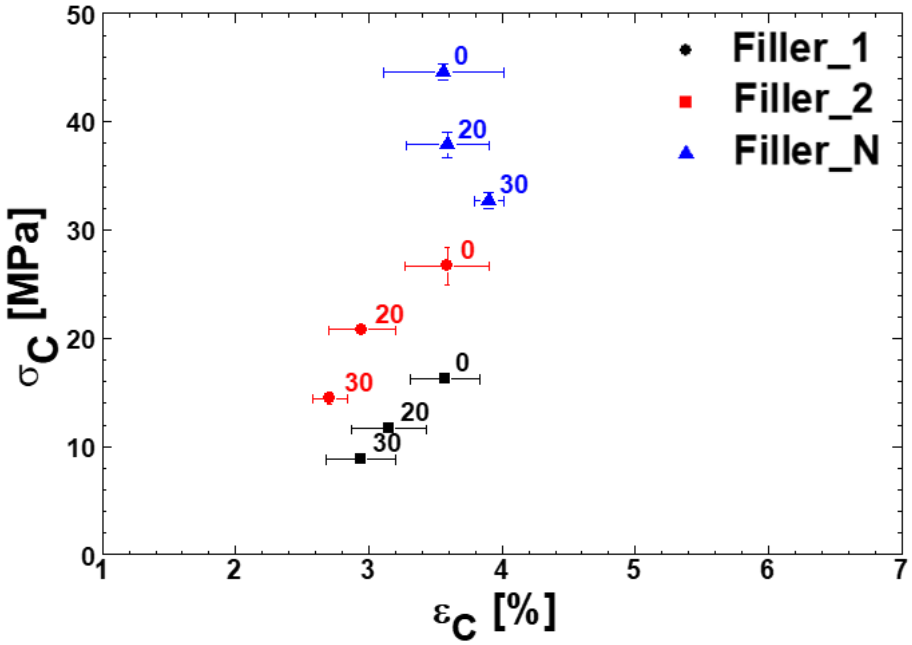

Figure 147: compression results of commercial fillers

According to the compression test, the fillers are not relevantly different considering the deformation. On the other hand, considering the stress Filler_N is more resistant than Filler_1 and Filler_2.

MECHANICAL PROPERTIES OF DIFFERENT A/B RATIO

The same mixing ratios already analysed with the IR for the creation of the calibration line were mechanically characterised through three-point bending test. In Table 62 the Young's modulus (MPa), E_b, the stress (MPa), σ_b, and the deformation (%), ε_b, of mixing ratios of Filler_N are listed.

A/B	E_b [MPa]	σ_b [MPa]	ε_b [%]
0.92	2000±81	19.8 ±0.2	1.12 ±0.06
1.04	2253±19	21.0 ±0.7	1.01 ±0.03
1.14	2307±78	20.5 ±0.8	0.94 ±0.04
1.27	2932±20	24.0 ±1.3	0.86 ±0.05
1.43	2474±77	20.9 ±1.0	0.89 ±0.04

Table 62: three-point bending results of different mixing ratios

In Figure 148, the stress (σ_t) is plotted against the deformation (ε_t) for all samples with different mixing ratios. From the results obtained, the product thus formulated bears well both an excess and a deficiency of one component respect the other, even by 20%. The reproducibility of the measurements is good, with low standard deviations.

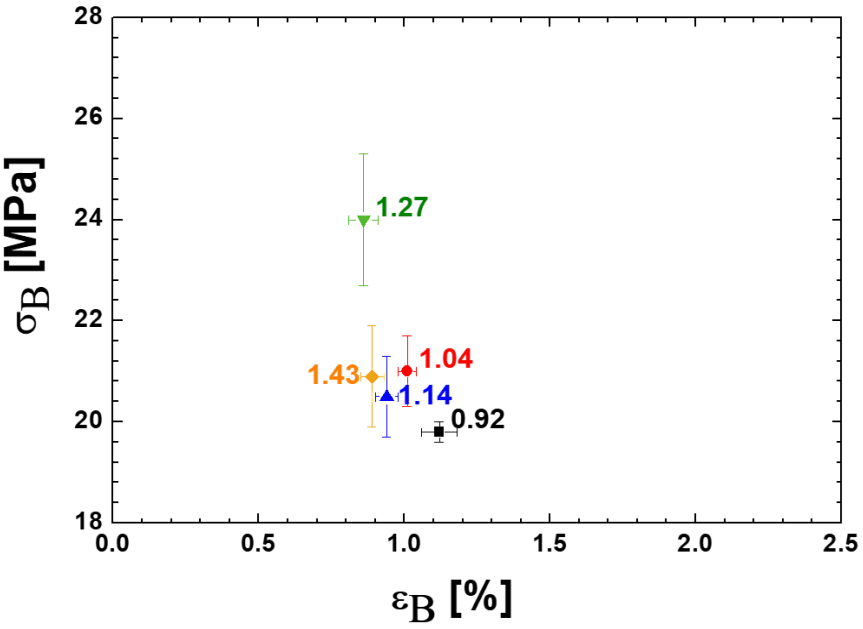

Figure 148: bending results of different mixing ratios A/B

9.3.6 MORPHOLOGICAL CHARACTERISATION

The morphological characterisation was performed to see the adhesion between matrix and extenders and to understand if extenders agglomerates.

SEM images of Filler_N are reported in Figure 149, it is clearly visible the good adhesion between matrix and hollow glass microspheres, easily identifiable. Interesting in Figure 149b) and c) a portion of matrix that is strongly adhered to the hollow glass microspheres surface. The other extenders appear quite well dispersed.

To obtain a quantitative analysis of samples, manual image analysis was carried out on digitalised SEM images, by using the image analysis open source software ImageJ 1.51 to measure: 1) the microspheres diameter, 2) the wall thickness and 3) the distance matrix-hollow glass microspheres. These values are reported in Table 63 and each value is a mean of fifty measures. The microspheres diameter and the wall thickness are in agreement with the measures already reported in Table 12, related to the commercial fillers and in Table 14 related to microspheres.

The distance matrix-hollow glass microspheres is not detected (~0μm) and also this is in agreement with the observations to GM_1 and GM_2 microspheres (see “Chapter 5: Extenders study”).

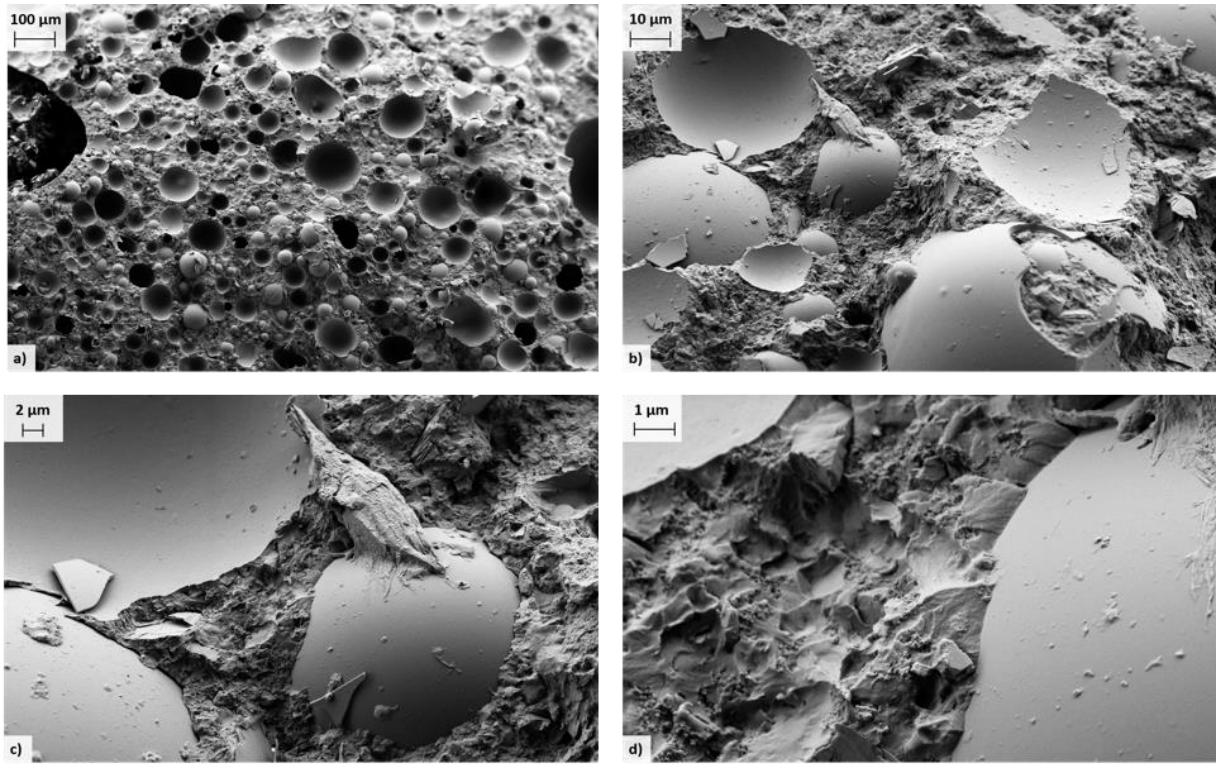

Figure 149: SEM images of Filler_N

Filler	Microspheres diameter	Wall thickness	Matrix-microspheres distance
	[µm]		
Filler_N	42.73 ± 8.15	0.816 ±0.110	~ 0

Table 63: morphological results of Filler_N

9.4 IN-FIELD TEST

The following characterisations were performed on the Filler_N, after extrusion with the gear pumps directly in the Holland shipyards, and therefore called in-field test. In Figure 150 are reported some pictures of a) gear pump, b) gear pump with the two components of Filler_N and c) extrusion of both components mixed.

In Figure 151, the application of Filler_N is shown.

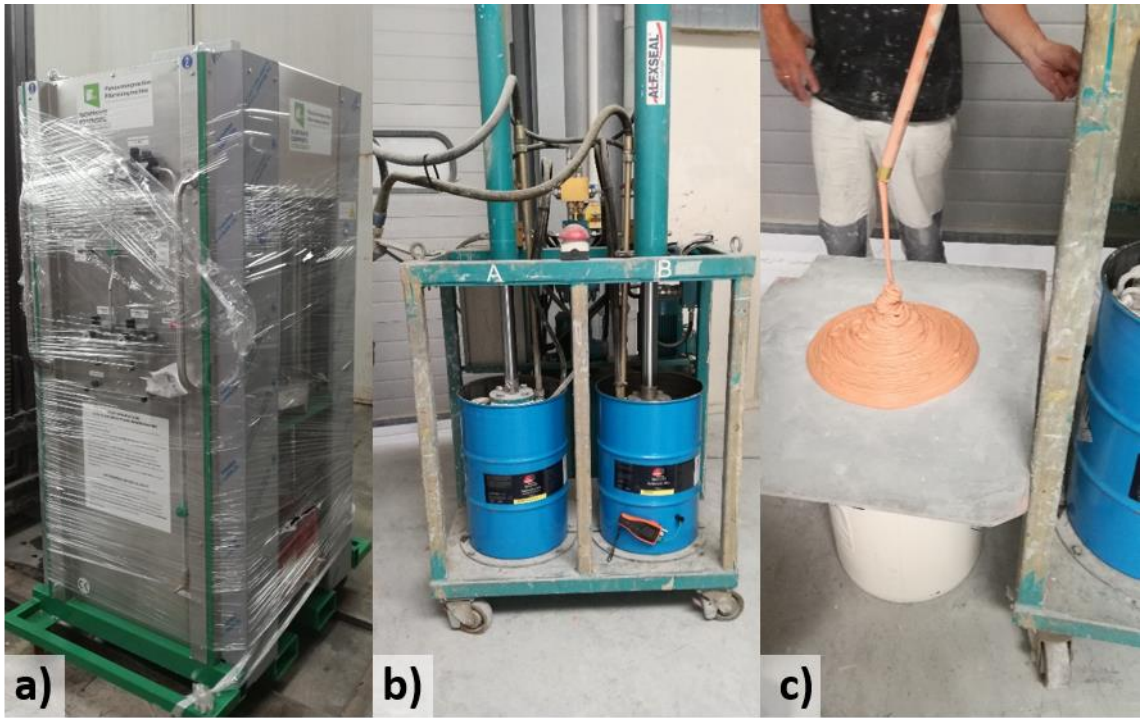

Figure 150: a) gear pump, b) gear pump with the drums of two components of Filler_N and c) A and B components mixed and extruded

Figure 151: application after extrusion of Filler_N

9.4.1 COATINGS TESTS

The specific weight of both components of Filler_N, measured before the extrusion ($S.W._i$), after the extrusion ($S.W._{extruded}$) and its increment in percentage are reported in Table 64.

	S.W.$_i$ [g/cm^3]	**S.W.$_{extruded}$** [g/cm^3]	**Δ** [%]
Filler_NA	0.83	0.86	3.6
Filler_NB	0.76	0.84	10.5

Table 64: specific weight before and after compression and its increment in percentage of Filler_N

As visible from the results, the specific weight of A component is little bit higher than that observed in the laboratory, but totally comparable; for the B component, instead the increment in percentage is of 11%. This value is unexpected respect to laboratory measurements.

This anomaly is probably associated with several factors such as:

- the air incorporated within the material: in the-field tests 50L drums were used, in this condition the material may have incorporated air in the production phase, as well as in the packaging phase;
- the mechanical stress imposed from the gears pumps is not exactly the same imposed in laboratory compression tests.

To complete the in-field tests, different samplings of applied and cross-linked Filler_N were carried out and analysed. The samplings were the follows:

(1) sample collected manually from the drums and manually mixed, called Filler_N$_{manually}$

(2) sample extruded with machine and mixed manually, called Filler_N$_{hands}$ and

(3) sample extruded and mixed with machine, called Filler_N$_{extruded}$.

In Table 65, the Shore D values of the three different samplings and the value obtained in laboratory test, called Filler_N$_{laboratory}$, are listed.

Samples	Shore D_{7days}
Filler_$N_{laboratory}$	68/66
Filler_$N_{manually}$	65/64
Filler_N_{hands}	75/67
Filler_$N_{extruded}$	75/70

Table 65: Shore D values of Filler_N

From the results, the fillers extruded and mixed manually or with machine have hardness higher than that collected and mixed manually. The last one value is in agreement with the measurement performed in laboratory. These results are in agreement with the idea that the extruded products, Filler_N_{hands} and Filler_$N_{extruded}$, without embedded air, are more compact than Filler_$N_{laboratory}$.

9.4.2 INFRARED SPECTROSCOPY ANALYSIS

To check the mixing ratio of the extruded product some cross-linked samples of Filler_$N_{extruded}$ were withdrawn in different parts of yacht. Therefore, collecting the IR spectra of these samples and using the equation of calibration line (26), the mixing ratio was identified. The results indicate a mixing ratio of 1.20, value higher than that of Filler_$N_{laboratory}$ (mixing ratio stoichiometric 1.14).

Moreover, the same analysis was carried out on the samples, already seen in the hardness test. The different mixing ratios are:

(1) 1.13 for Filler_$N_{manually}$

(2) 1.19 for Filler_N_{hands}

(3) 1.21 for Filler_$N_{extruded}$.

Consequently, the extruded products (Filler_N_{hands} and Filler_$N_{extruded}$) exhibit a little bit higher amount of A component than Filler_$N_{laboratory}$. Nevertheless, from the mechanical analysis performed on all the samples (see 9.4.4 “Mechanical analysis”) these mixing ratios result acceptable for the application as a filler for hull.

In Figure 152 and in Figure 153 are reported respectively the IR spectra of samples and the magnification of these spectra in range 890-650cm^{-1}.

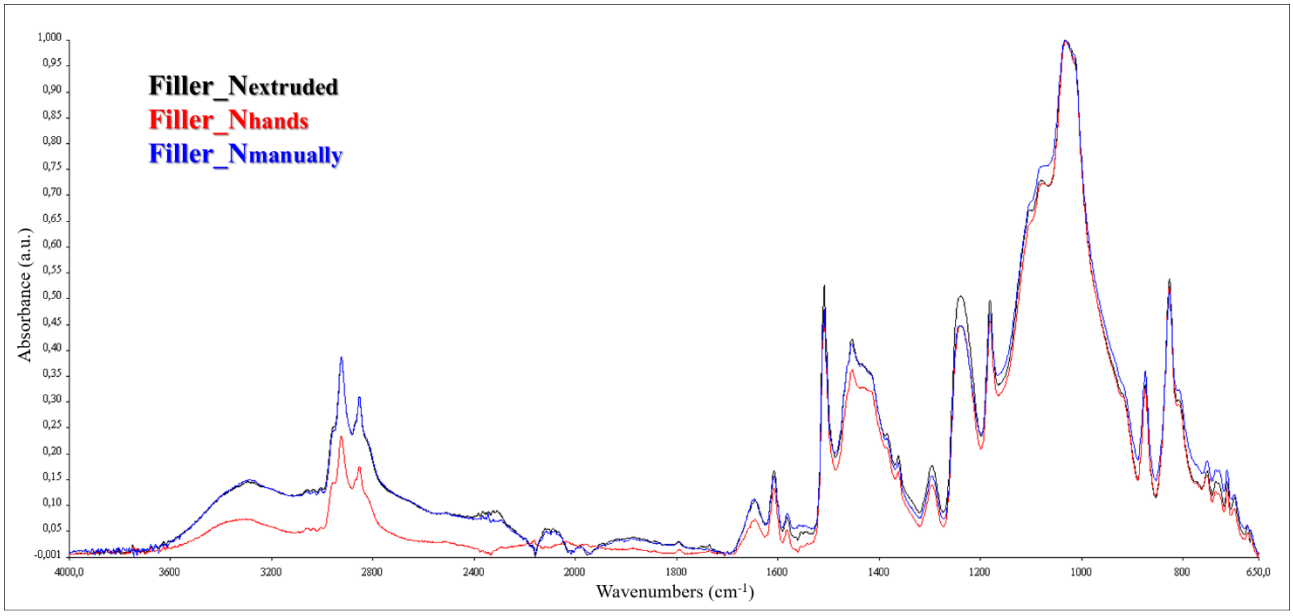

Figure 152: IR spectra of samplings of Filler_N

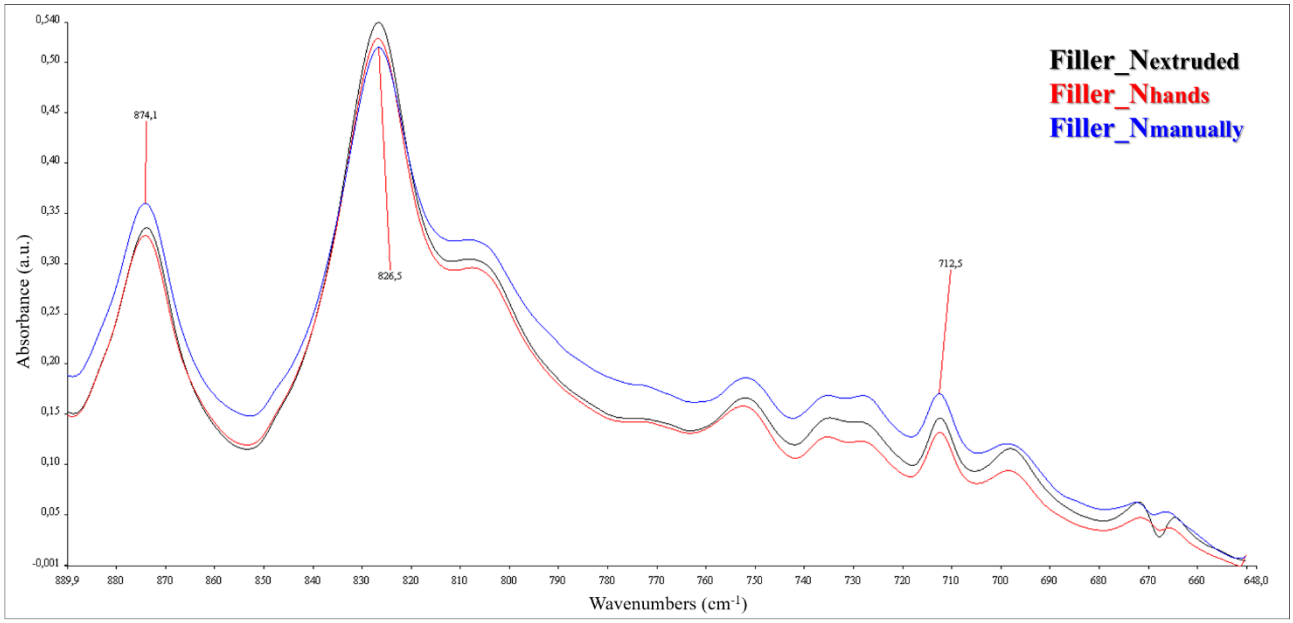

Figure 153: IR spectra of samplings of Filler_N; magnification in range 890-650cm^{-1}

9.4.3 THERMAL ANALYSIS

In Figure 154, the DSC curves of Filler_ $N_{laboratory}$, Filler_N_{hands} and Filler_$N_{extruded}$ are reported.

The Tg of both the Filler_N_{hands} and Filler_$N_{extruded}$, considering the midpoint, is 48°C, a little bit higher than in Filler_$N_{laboratory}$ (46°C) and this is in agreement with the mechanical properties (Shore D values, Young's modulus and so on).

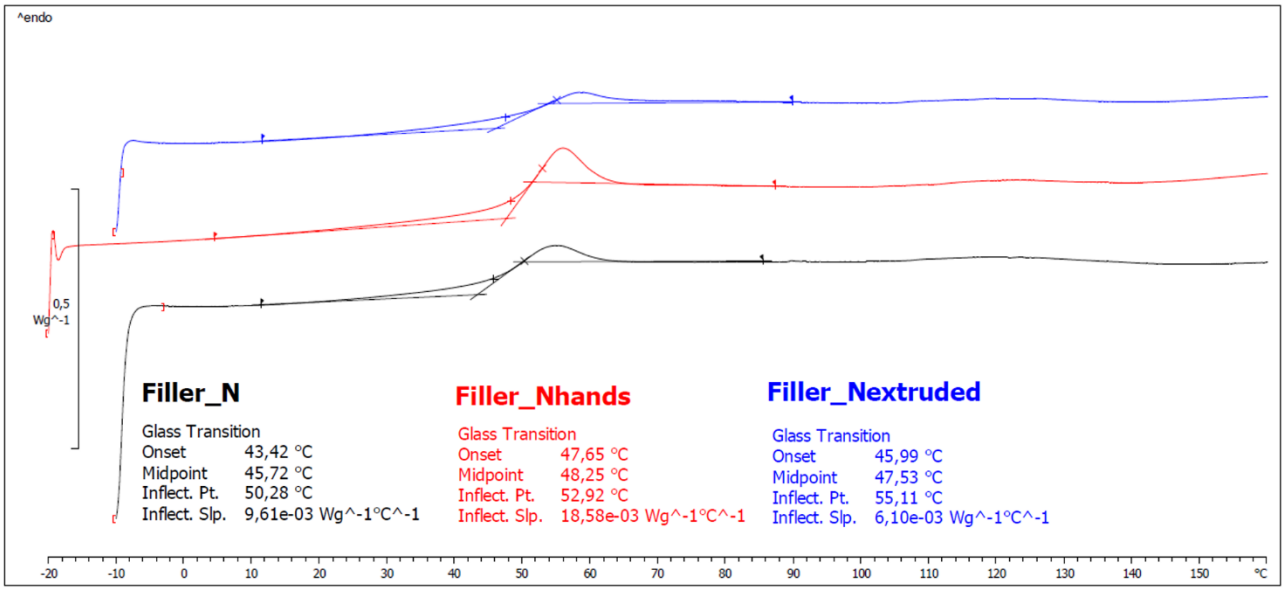

Figure 154: DSC curves of samplings of Filler_N

9.4.4 MECHANICAL ANALYSIS

On the Filler_$N_{manually}$, Filler_N_{hands} and of Filler_$N_{extruded}$ three-point bending test was also performed. In Table 66 the Young's modulus (E_b) the stress (σ_b) and the deformation (ε_b) are listed.

	E_b [MPa]	σ_b [MPa]	ε_b [%]
Filler_$N_{laboratory}$	2307±78	20.5 ±0.8	0.94 ±0.04
Filler_$N_{manually}$	2360±53	22.8±0.9	1.08±0.09
Filler_N_{hands}	2514±25	23.5 ±1.1	1.04 ±0.05
Filler_$N_{extruded}$	2499±30	22.23 ±0.5	0.97 ±0.02

Table 66: three-point bending results of mixed by hands and extruded samples of Filler_N

According to E_b, the values of Filler_$N_{laboratory}$ and of Filler_$N_{manually}$ are comparable and the extruded products appear a little more rigid respect to that of laboratory. These data are in agreement with the results of infrared and thermal analyses, indeed the mixing ratios of extruded products are higher as well as the Tg and the Shore D values respect the Filler_$N_{laboratory}$ and Filler_$N_{manually}$.

9.5 CONCLUSIONS

New filler for North European market was formulated and already commercialised. This type of filler had to be applicable with extruding machines, i.e. it had to resist to important mechanical stresses without loosing its properties.

Different mechanical and rheological tests were carried out and to optimise the new filler formulation. Some characterisations of new filler took place to study its properties such as thermal, mechanical, morphological and so on. In addition, its mixing ratio was studied, creating a calibration line, to control the cross-linked product properties also when the mixing ratio was not stoichiometric. Remembering that, in-field application, a certain degree of variation in mixing ratio were considered, due to the calibration of the extruding machine and/or the operator precision during his work.

The new filler exhibits some innovative characteristics, listed below:

- the presence of GM_2, instead GM_1, not only permits high pressures of extrusion (45bar), but also to have a really strong adhesion matrix and hollow glass microspheres, as already discussed in Chapter 5: Extenders study;
- the possibility to extrude the filler at lower pressures than other commercial fillers of competitors: from in-field test it was observed that “only” 30-35 bar is enough to extrude the products;
- the rheological behaviour of B component is particularly interesting, indeed respect to the other commercial fillers, it has higher recoveries and exhibits more storage stability;
- the product bears a variation in the mixing ratio, even by 20%: this property permits an easier in-field use;
- the low influence of temperature on the mechanical properties respect to the commercial fillers.

The characterisations performed on filler extruded in field show that the extrusion involves an amount of A component a bit higher than that required for stoichiometric mixing.

Concluding, the new filler appears a really good product that responds well to North European market demands.

CHAPTER 10: CONCLUSIONS

Fillers for yachting industries have been extensively studied to improve the existing formulations, using also sustainable materials, to develop a new filler for specific market and to allow the company to transform traditional and empirical know-how, into scientific knowledge.

Considering these targets the starting point of this work was a characterisation of commercial fillers, from which it is obtained that:

- the FTIR spectroscopy allows to monitor the curing process by following changes in intensity of some diagnostic bands detectable even in such a complex matrix;
- the curing process depends on the temperature and it is not influenced by humidity at room temperature, while at low temperatures humidity has a slight effect, causing the incomplete cross-linking;
- the commercial fillers have slight differences between them, such as in rheological behaviours and in mechanical properties.

Furthermore, the characterisation has made possible: 1) the use of commercial fillers as benchmark for the product subsequently developed, 2) the quality control and/or the investigation of anomalies, following in-field problems and 3) the setup of experimental methods useful in the development of new products.

Once characterised the commercial fillers, it is deepened the knowledge of extenders that have remarkable importance on the two components, particularly for the B component, in which their percentage is over 50%. The systematic characterisation of extenders allowed to perform quality control of these incoming raw materials avoiding eventual problems in the final product, due to their altered batches.

Among the extenders, the hollow glass microspheres have an essential role, since they permit to reduce the specific weight of the filler, having low density are used in high percentages in the formulations. Two types of hollow glass microspheres, GM_1 and GM_2, have been considered: the first are employed in the commercial fillers because they are less dense and less expensive than GM_2. From the results related to the morphological characterisation, it was observed that GM_2 exhibits a really good adhesion with the matrix also without the dispersing agent, unlike GM_1. Moreover, the formulations with microspheres were studied from the rheological point of view. Relative high percentages could be well inserted in the A and B formulations without loss the rheological performances.

Among the targets of this research project the use of sustainable materials was present and therefore, formulations with wood fibres, replacing standard extenders, were investigated, since they come from renewable source with low density and at low cost. In addition, polymeric hollow microspheres were considered, since more performant, from the rheological point of view, than hollow glass microspheres. The polymeric microspheres are also characterised by high resilience and high compressibility allowing deformations under stress (during high shear mixing or pumping) with breakage absent or really low.

From these tests both the two innovative extenders perform really good in the A component, besides, the substitution of hollow glass microspheres with wood fibres permits to save time, especially at the production site, since the dispersion of hollow glass microspheres in the matrix requires the substitution of cowles with butterfly.

On the other hand, in the B components, the wood fibres allowed to improve the sustainability, but they had an unsatisfactory rheology and so they have to be further tested, for instances, with different rheological modifiers. The hollow polymeric microspheres permitted to improve remarkably the rheology, but had scarce mechanical properties, and so they have to be combined with other extenders, which increase the mechanical performances. Nevertheless, these formulations allowed the company to investigate new raw materials permitting it to explore new areas of research and they can be considered the trailhead to use the new extenders in the future.

Afterwards, the additives were investigated, even if their amount in the formulation is usually less than 5%, their effect is really significant. The first type of additive studied were the dispersants to optimize the adhesion of GM_1 with the matrix that was lower than that of GM_2.

Among the commercial additives, it was observed that the hyperbranched polyester and phosphite titanate wet very well the glass hollow microspheres. In fact, the samples with these two additives showed, for the single component, a good stability during the storage in the can and a more fluid behaviour. In the cross-linked product, the samples with the two additives exhibited a high Young's modulus and a good adhesion of the matrix also to the GM_1.

The better performance of these additives (3 and 4) respect others (1 and 2) is related to the type of stabilization. Indeed, these, being non-ionic dispersants, exhibited steric stabilisation. These results are particularly interesting considering that traditionally, in coating formulations, are used dispersing agents as lecithin that is a Zwitterionic surfactant, and so an ionic dispersant.

Subsequently, the rheological modifiers were systematically investigated with rheological measurements. The rheological analysis produces a large amount of data that can be useful to treat with univariate and multivariate statistical analyses.

The rheological modifiers study was made up into two steps: a quick screening to identify which additives were interesting to test and a second step in which these additives were rheologically monitored for one year.

In the first step, several rheological modifiers, belonging to bentonites for polar and non-polar coating systems, polyamide and castor oil families, were experimented. The selected method was the recovery test, since it is quite fast and with the use of recovery percentage after 30s and the total recovery percentage it is possible to compare the thixotropic behaviour of different samples numerically.

From this screening the A components did not show relevant differences between them, while for the B components the rheological curves have rather different trends. Rheological modifiers belonging to different families were studied in more details, performing a complete rheological characterisation until one year, treating the data with statistical analyses.

From the results, the additives have no significant influence on the A component, while they have a remarkable influence on the B component, showing the following performance trend: polyamide (the best one), castor oil, bentonite for polar system and finally bentonite for non-polar system (the worst). These differences must be searched in the matrix-additive interactions due to the hydrogen bonds formation. The different nature of A and B consists in having acceptor and/or donor groups of the hydrogen bond: the epoxy matrix has only acceptor groups, while the polyamide matrix has both the acceptor groups and the donors. Therefore, B component allows to create strong bond with polar systems, in particular with polyamide. From this study, it was observed how, for the two components, it is necessary to have two different additives, instead in the commercial fillers the rheological modifiers in both the components were the same.

The statistical approaches were in agreement between them, but using a univariate statistical approach (analysis of variance), a single data treatment for each type of rheological method was necessary, while with multivariate analysis (Principal component analysis after low-level data fusion), one single treatment was necessary for all rheological data. Therefore, it provided a “picture” of samples variance allowing to highlight correlations between constituents and simplifying the analysis of large amounts of data.

On the samples characterised rheologically over time also a dynamic mechanical analysis (DMTA) were performed and the data are treated with the multivariate analysis, showing as, also in this case, the A components were not influenced by rheological modifiers, but B components were influenced. This was an interesting result, since the rheological modifiers have an effect also on the mechanical properties of the cross-linked filler. As consequence, their choice must be done keeping in consideration these aspects.

All the results obtained have permitted to develop a new filler for the North European market: the filler had to be applicable with extruding machines, i.e. it had to resist important mechanical stresses without losing its properties. Therefore, to formulate the new A and B components of this filler, different steps were carried out:

1. first of all, compression tests were performed on filler with both GM_1 and GM_2, showing for the filler with GM_2 a higher compression resistance respect than GM_1. The use of GM_2 not only permits high pressures of extrusion (45bar), but also permits to have a really strong adhesion matrix-hollow glass microspheres, unlike the GM_1, as previously seen in the extenders study;
2. identified the type of microspheres to use, it was necessary to optimise the rheological performance of the A and B formulations, using the best rheological additives for the two components already investigated in the study of rheological modifiers;
3. obtained the two formulations, some characterisations of new filler took place to study its properties such as thermal, mechanical, morphological and so forth, using the commercial fillers as benchmark;
4. the A/B mixing ratio was studied, creating a calibration line, to control the cross-linked product properties. This was an important check for in-field application, indeed it was useful for the calibration of the extruding machine and to control the operator precision during his work;

The new filler exhibited some innovative characteristics compared to the commercial ones, below listed:

- the presence of GM_2, that permitted high pressures of extrusion, and a really strong adhesion matrix-hollow glass microspheres;
- the possibility to extrude the filler at lower pressures than that of other competitors: from in-field test it was observed that “only” 30-35 bar was enough to extrude the products;
- the rheological behaviour of B component was particularly interesting, indeed it had higher recoveries and exhibited high storage stability;
- the product bore well some variations in the mixing ratio, even by 20%, permitting an easier in-field use;
- the low influence of the temperature on the mechanical properties, positive for the application in North Europe.

Considering all these aspects, the new filler appeared a really good product that responded well to North European market demands. Actually, the filler is commercialized in Holland.

Concluding, the work performed in these three years, from a scientific point of view, permitted:

1) to deepen the knowledge of these materials, with the direct observation in laboratory and not only in-field, therefore transforming traditional and empirical know-how, into scientific knowledge;
2) to carry out a systematic study of the raw materials, from the extenders to the additives, characterising them and observing their effects both on the single components and on the cross-linked products;
3) to better know the mechanism and time involved in the curing process, through the study of process by spectroscopic and calorimetric analysis in different environmental conditions (humidity and temperature);
4) to treat rheological data with advanced statistical analysis such as multivariate analysis that is not common in literature;

From an industrial point of view, the work permitted:

4) the better knowledge of the raw materials used, which is translated into the possibility of having increasingly performing trials;
5) the investigation of new raw materials such as wood fibers or polymeric microspheres, further introducing the company in the sustainable sector;
6) the development of A and B components for a filler that meets the requirements of a specific market, obtaining a product that shows also better characteristics than the commercial ones.

SUMMARY

The nautical field is a key market for the Italian economy, in fact Italy has a prominent place among world boat manufacturers and is ranked second (after Holland) in the European framework. In this field, the coatings for the external surfaces of ships play a fundamental role, because they have to provide all the aesthetic properties typical of a luxury product as brightness, light reflection and their durability over the time. In addition, they have to protect the substrate, resist to aggressive environment, thermal and mechanical stresses respecting the Safety of Life at Sea (*S.O.L.A.S.)* rules. It is therefore clear the need of the industry to invest in the search for appropriate materials to be used in the protection of ships surface to maintain high levels in the world production.

To respond to all demands of the market the multi-coat systems are essential. These types of coatings are protective systems based on the overlap of different layers (primer, filler, finishing filler, a second primer, undercoat and topcoat) with different thicknesses, nature and aim. They result the best systems to protect the yachts external surface over the waterline. Within the multi-coat systems, the fillers represent the main layer from the point of view of mechanical properties; they are composite materials with the first aim to fill the surface imperfections. In addition, from the point of view of consumption of material, fillers constitute the most part of the multi-coat system.

Among the various coating layers used, epoxy fillers have received of particular attention, in recent years, by designers, builders and applicators. The main reason is the fact that these materials show good resistance to abrasion, corrosion, thermal variations and the possibility of increasing mechanical properties, with appropriate additives and so on.

Unfortunately, the producers have poor knowledge of the characteristics of these products and their development is focused on empirical, more than scientific, considerations following the historical recipes.

Considering these premises, in the present thesis, the fillers have been extensively studied. In details, targets of this research project were:

- the transition, from an industrial point of view, from very empirical knowledge to a more scientific and systematic know-how;
- the optimization of existing fillers through the systematic study of additives and extenders in the commercial formulations;
- the development of new product with specific properties for the North European market;
- the particular attention to eco-friendly materials as required from the market.

Since the thesis is carried out in collaboration with Boero Bartolomeo SpA, one of the oldest paint factories in Europe, leader in Italy in paint building sector and leader in world for the yachting field, it was not possible to publish some details of the research work, due to confidentiality agreements.

The thesis is divided into two sections: Section I (fundamentals) and Section II (experimental).

The first section reports the state of art of yacht coatings and it includes three chapters.

In Chapter 1, it is considered:

- the structure of the coatings, that is different in function of the substrate, of the yacht part and if it is above or below the waterline;
- the composition of coatings, that are complex mixtures of chemical substances that can be grouped in several basic categories: binders, pigments and/or extenders, additives and all;
- the surface preparation of hull, that is essential to realize a performant and long-lasting painting system, indeed the surface must be clean, to avoid poor coatings adhesion or corrosion phenomena, and it must have a definite roughness degree, to improve the mechanical adhesion between substrate and coatings;
- the coating applications that can be performed with several methods depending on many factors: whether the material to be applied is solid, liquid or powder; whether coated films should be thick or thin, or in function of the shape of the surface.

Chapter 2 is focalised on the two-component fillers that are studied in detail in this work. They consist of an A component (based on epoxy resin) and a B component (based on polyamide), also named curing agent; once mixed in opportune ratios they form the filler to be applied. Being composite materials, fillers have a dispersed phase based on different extenders (such as carbonates, talc, hollow glass microspheres, alumina-silicate spheres, fumed silica) and several additives (as dispersants, rheological modifiers and anti-foam agents). The extenders and additives are dispersed in the matrix with a dissolver equipped of cowles and butterfly.

The filler needs some specific properties: rheological, mechanical and thermal. The rheological properties are essential in order to have:

1. an ease of mixing, indeed the high filler thickness (~ 2 cm) and the wide yacht surface lead to mixing considerable materials volume,
2. thixotropy, that is essential in order to avoid sagging effect during or just after the application.

The mechanical properties of fillers are fundamental to ensure the painting system integrity, because they must be able to withstand the deformations suffered by the structure.

Considering all this, the several critical aspects of the nautical filler can be summarised in two broad categories:

- related to the rheology of single component:
  - ✓ viscous behaviour when subjected to stress and thixotropic behaviour;
  - ✓ material stability in the can;
- related to the cross-linked product:
  - ✓ filler application conditions: the environmental conditions, such as temperature, humidity and the variable thicknesses of the material play a fundamental role for the good application of the coating;
  - ✓ glass transition temperature (T_g) acceptable in the usage temperature and compatible with the possible thermal stresses;
  - ✓ thermal stresses: since the boats can undergo considerable temperature changes, for example on summer days the temperatures can reach peaks of 80 °C on dark-coloured hulls and on winter days the temperatures are well below zero, the filler must withstand both conditions;
  - ✓ mechanical properties once applied, including the elasticity to adapt to the substrate deformations;
  - ✓ the possible recycling of these materials (currently there are strong difficulties in their recycling).

All these aspects should be addressed in an economically acceptable and sustainable context.

In Chapter 3, a brief description of the techniques used in the thesis is reported: coatings test, infrared, thermal, rheological and mechanical analyses, morphological characterisation and univariate and multivariate statistical analysis.

The coatings tests are traditionally used by the formulators, such as oil adsorption values, specific weight, pot life, hardness. The infrared analysis was used to characterise the materials, but also to study the curing process and the mixing ratio, while thermal analysis was performed to characterise thermally the fillers and to study the curing process. Rheological analyses were used to investigate the rheological performance and the mechanical analysis to study the mechanical properties also at different temperatures. In addition, the morphological characterisation was employed to see the dispersion of extenders and their adhesion with the matrix. The statistical analyses were used to treat the rheological data with advanced approaches.

Section II is the experimental part that consists in seven chapters, in which the results obtained and the conclusions of this work are reported.

Considering the targets of the research project, the work was so structured:

- first of all, a characterisation and a study of commercial fillers and raw materials such as extenders were performed,
- subsequently, alternative and innovative extenders and the main additives (dispersants and rheological modifiers) were investigated,
- finally, a new filler for the North European market was developed.

Chapter 4 reports the characterisation of two commercial fillers, Filler_1 and Filler_2, different for three principal reasons: 1) resin content 2) the different extenders and 3) density.

The characterisation was carried out with different techniques: coatings tests, infrared spectroscopy, thermal, mechanical analyses and morphological characterisation. The rheological analysis was performed on single components and, since the rheological behaviour changes over time, the tests were performed at two different times: 1) after one week from the production, representative for the first step of the supply chain (from manufacturer to shipyard) and 2) after one year from the production, representative for the shelf-life of the product.

Furthermore, the study of curing process, through IR and DSC analysis, was described. From the results, it is obtained that:

- the FTIR spectroscopy allows to monitor the curing process by following changes in intensity of some diagnostic bands detectable even in such a complex matrix;
- the curing process depends on the temperature and it is not influenced by humidity at room temperature, while at low temperatures has a slight effect, causing the incomplete cross-linking;
- the commercial fillers have slight difference between them, such as in rheological behaviours and in mechanical properties.

The characterisation of commercial fillers is essential to deepen the knowledge of these materials used as benchmark for the filler subsequently developed, for quality control and/or the investigation of anomalies, following in-field problems, and for the setup of experimental methods useful in the development of new products.

Chapter 5 is focalised on the extenders that have a remarkable importance on the two components, particularly for the B component, in which their percentage is over 50%.

Among the extenders, the hollow glass microspheres have an essential role, since they permit to reduce the specific weight of the filler, having low density are used in high percentages in the formulations. There were two types of hollow glass microspheres, GM_1 and GM_2, and the first ones were employed in the commercial fillers because they are less dense and less expensive than GM_2. The chapter is characterised by two parts: the first is centred on the systematic characterisation through infrared and morphological analyses, while the second on the rheological analysis of samples with increasing amounts of GM_1.

The systematic characterisation of extenders allowed to perform quality control of these incoming raw materials avoiding eventual problems in the final product, due to their altered batches. From the morphological results, it was observed that GM_2 exhibited a really good adhesion with the matrix also without the dispersing agent, unlike GM_1.

The formulations with microspheres were studied from the rheological point of view. Relative high percentages could be inserted in the A and B formulations without loss the final properties.

Among the targets of this research project, the use of sustainable materials was present and, therefore, formulations with wood fibres were investigated, since they come from renewable source, with low density and at low cost. In addition, the polymeric hollow microspheres were considered, since they are rheologically more performant than hollow glass microspheres. The polymeric microspheres are also characterised by high resilience and high compressibility allowing deformations under stress (during high shear mixing or pumping) with breakage absent or really low.

Different percentage of the new extenders were introduced in the A and B formulations replacing other standard extenders as alumina silicate spheres or hollow glass microspheres. Several techniques were used: coatings tests, rheological and mechanical analyses and morphological characterisation.

Generally, from these tests both the two innovative extenders perform really good in the A component, besides, the substitution of hollow glass microspheres with wood fibres permit to save time, especially at the production site, since the dispersion of hollow glass microspheres in the matrix require the substitution of cowles with butterfly.

On the other hand, in the B components, the wood fibres allowed to improve the sustainability, but they have an unsatisfactory rheology and so they have to be further tested, for instances, with different rheological modifiers. The hollow polymeric microspheres, even if they permit to improve remarkably the rheology, they have scarce mechanical properties, and so they have to be combined, for instances, with other extenders which can increase the mechanical performances. Nevertheless, these formulations allowed the company to investigate new raw materials permitting it to explore new areas of research and they can be considered the trailhead to use the new extenders in the future.

As obtained from the Chapter 5, GM_1 microspheres exhibited scarce adhesion with the matrix, respect to GM_2, therefore, to improve their wettability and their adhesion with the matrix, four commercial dispersing agents were investigated. The techniques used were rheological and mechanical analyses and morphological characterisation. The additives were selected from the many products available on the market, taking into account the coating system within which they must be inserted.

From the results, the hyperbranched polyester and phosphite titanate wet very well the glass hollow microspheres. In fact, the samples with these two additives showed, for the single component, a good stability during the storage in the can and a more fluid behaviour. In the cross-linked product, the samples with the two additives exhibited a high Young's modulus and a good adhesion of the matrix also to the GM_1.

The better performance of these additives respect the others was related to the type of stabilization. Indeed, these, being non-ionic dispersants, showed steric stabilisation. These results are particularly interesting, considering that traditionally, in coating formulations, are used dispersing agents as lecithin that is a Zwitterionic surfactant, and so an ionic dispersant.

Chapter 8 is focused on the rheological modifiers that were systematically investigated through the rheological analysis to improve the rheological properties of fillers.

The Chapter was made up of two steps: a quickly rheological screening, through recovery test and a second step in which the promising additives were rheologically experimented for one year.

In the first step several rheological modifiers belonging to bentonites for polar and non-polar coating systems, polyamide and castor oil families were experimented. The selected method was the recovery test, since it is quite fast and with the use of the recovery percentage after 30s and the total recovery percentage it is possible to compare the thixotropic behaviour of different samples numerically.

From this screening, the A components did not show relevant differences between them, while for the B components the rheological curves have rather different trends. Chosen the rheological modifiers as a function of their families, they were studied in more details, performing a complete rheological characterisation until one year, treating the data with statistical analyses.

Indeed, the rheological analysis produces a large amount of data that can be treated with statistical analyses such univariate (analysis of variance, ANOVA) and multivariate (principal component analysis, PCA after low-level data fusion).

From the results, the additives have no significant influence on the A component, while they have a remarkable influence on the B component, showing a performance trend: polyamide (the best one), castor oil, bentonite for polar system and finally bentonite for non-polar system (the worst). Over

time, on the B component, the differences tend to increase. These differences must be searched in the matrix-additive interactions due to the hydrogen bonds formation. The different nature of A and B consists in having acceptor and/or donor groups of the hydrogen bond: the epoxy matrix has only acceptor groups, while the polyamide matrix has both the acceptor groups and the donors. Therefore, B component allows to create stronger bond with polar systems, in particular with polyamide. From this study it was observed how, for the two components, it is necessary have two different additives, instead in the commercial fillers the rheological modifiers in both the components were the same.

The statistical approaches were in agreement between them, but using a univariate statistical approach, a single data treatment for each type of rheological method was necessary, while with multivariate analysis, one single treatment was necessary for all rheological data. Therefore, it provided a "picture" of samples variance allowing to highlight correlations between constituents and simplifying the analysis of large amounts of data.

On the samples characterised rheologically over time, also a dynamic mechanical thermoanalysis (DMTA) were performed and the data were treated with the multivariate analysis, showing as also in this case the A components were not influenced by rheological modifiers, and B components were influenced. This is an interesting result, since the rheological modifiers have an effect also on the mechanical properties of the cross-linked filler. As consequence, their chose must be done keeping in consideration these aspects.

All the results obtained until now permitted to develop a new filler for the North European market: the filler had to be applicable with extruding machines, i.e. it had to be able to withstand important mechanical stresses without losing its properties.

Therefore, different formulations were investigated to optimise the compression resistance of filler, testing both GM_1 and GM_2 in A and B formulations. After that, several formulations were tested with the rheological analysis, to obtain the best rheological performances. Remembering the results of rheological modifiers study, in the A component the bentonites, both for polar and non-polar coating systems, polyamide and castor oil were tested, while for the B components only polyamide was experimented.

Once identified the best formulations among those tested, the new filler was compared to those commercials used as benchmark. In addition, a comparison between filler before and after in-field applications was carried out. Different analyses were performed: coatings test, infrared, rheological mechanical analyses and morphological characterisation.

Moreover, mixing ratio of A and B components was studied, creating a calibration line, to control the cross-linked product properties. Remembering that, in-field application, a certain degree of variation

in mixing ratio was used, due to the calibration of the machine or to the operator precision during his work.

The new filler exhibited some innovative characteristics respect to those commercial, below listed:

- the presence of GM_2, that permitted high pressures of extrusion (45bar), and a really strong adhesion matrix-hollow glass microspheres;
- the possibility to extrude the filler at lower pressures than that of other competitors: from in-field test it was observed that "only" 30-35 bar was enough to extrude the product;
- the rheological behaviour of B component was particularly interesting, indeed it had higher recoveries and exhibited high storage stability;
- the product bore well some variations in the mixing ratio, even by 20%, permitting an easier in-field use;
- the low influence of the temperature on the mechanical properties, positive for the application in North Europe.

Considering all these aspects the new filler appeared a really good product that responded well to North European market demands. Actually, the filler is already commercialised.

Concluding, the work performed in these three years, from a scientific point of view, permitted:

1) to deepen the knowledge of these materials, with the direct observation in laboratory and not only in-field, therefore transforming traditional and empirical know-how, into scientific knowledge.
2) to carry out a systematic study of the raw materials, from the extenders to the additives, characterising them and observing their effects both on the single components and on the cross-linked products.
3) to better know the mechanism and time involved in the curing process, through the study of the process by spectroscopic and calorimetric analysis, in different environmental conditions (humidity and temperature);
4) to treat rheological data with advanced statistical analysis such as multivariate analysis that is not common in literature.

From an industrial point of view, the work permitted:

1) the better knowledge of the raw materials used, which is translated into the possibility of having increasingly performing trials;

2) the investigation of new raw materials such as wood fibers or polymeric microspheres, further introducing the company in the sustainable sector;
3) the development of A and B components for the new filler that meets the requirements of a specific market, obtaining a product that shows also better characteristics than the commercial ones.

REFERENCES

[1] Confindustria nautica, "Analisi di mercato per l'anno 2018," *La Nuatica in Cifre*, no. 40, 2018.

[2] Il Sole 24 ore, "Nautica, riparte il mercato interno," 2016. [Online]. Available: https://st.ilsole24ore.com/art/impresa-e-territori/2016-09-22/nautica-riparte-mercato-interno-153054.shtml?uuid=ADKPoMPB.

[3] Boat International, "2019 Global Order Book," 2019. [Online]. Available: https://www.boatinternational.com/yacht-market-intelligence/luxury-yachts-on-order/annual-reports/2019-global-order-book--39251.

[4] Ansa, "Polo mega yacht Genova: Amico&Co, a ottobre pronti lavori," Ansa.it, Marzo 2019. [Online]. Available: https://www.ansa.it/mare/notizie/rubriche/shippingecantieri/2019/03/19/polo-mega-yacht-genova-amicoco-a-ottobre-pronti-lavori_ac771788-1e44-409d-940d-8b38a62775e2.html.

[5] Il sole 24 ore, "Amico & Co avvia il lavori per il polo megayacht di Genova," Marzo 2019. [Online]. Available: https://www.ilsole24ore.com/art/amico-co-avvia-lavori-il-polo-megayacht-genova-AB5pDwfB.

[6] A. B. Strong, Fundamentals of Composites Manufacturing - Materials, Methods and Applications, Dearborn, Michigan, USA: Society of Manufacturing Engineer, **2008**.

[7] A. M. Berendsen, Ship Painting Manual, Amsterdam, Nederland: De Boer Maritiem, **1975**.

[8] S. Paul, Surface Coatings: Science and Technology, Hoboken, New Jersey, USA: Wiley, **1996**.

[9] F. N. Jones, M. E. Nichols, S. P. Pappas, Organic Coatings: Science and Technology, Hoboken, New Jersey, USA: Wiley, **2017**.

[10] P. A. Schweitzer, Paint and Coatings: Applications and Corrosion Resistance, Boca Raton, Florida, USA: CRC Press, **2006**.

[11] F. Zhou, Antifouling Surfaces and Materials: from Land to Marine Environment, Berlin, Germany: Springer, **2015**.

[12] C. Hellio, D. Yebra, Advances in Marine Antifouling Coatings and Technologies, Boca Raton, Florida, USA: CRC Press, **2009.**

[13] R. Lambourne, T. A. Strivens, Paint and Surface Coatings, Sawston, UK: Woodhead Publishing, **1999.**

[14] G. D. Anderson, "Coatings Analysis: Introduction," in *Encyclopedia of Analytical Chemistry*, Hoboken, New Jersey, USA: Wiley, **2001**, 1782-1785.

[15] J. V. Koleske, Paint and Coating Testing Manual, West Conshohocken, Pennsylvania, USA: ASTM International, **2012**.

[16] S. D. Cramer, S. Bernard, J. Covino, Corrosion: Fundamentals, Testing, and Protection, Vol. 13A, West Conshohocken, Pennsylvania, USA: ASTM International, **2003**.

[17] T. J. Miranda, Surface Coatings: Raw Materials and Their Usage, Vol. 1, Amsterdam, Netherlands: Springer, **1993**.

[18] B. Müller, U. Poth, Coatings Formulation, Hanover, Germany: Vincentz Network, **2011**.

[19] A. Hammer, *Thermal analysis of polymer*, Mettler Toledo **2013**.

[20] M. Dornbush, U. Christ, R. Rasing, Epoxy Resins: Fundamentals and Applications, Hannover, Germany: Vincentz Network, **2016**.

[21] B. Ellis, Chemistry and Technology of Epoxy Resins, Berlin, Germany: Springer, **1993**.

[22] B. Bilyeu, W. Brostow, K. P. Menard, "Epoxy thermosets and their applications," *J. Mat. Edu.,* 22, 107–129, **2000**.

[23] J. I. Kroschwitz, Encyclopedia of Polymer Science and Engineering, Vol. 6, New York: Wiley & Sons, **1988**.

[24] F. Mark, N. M. Bikales, C. G. Overberger, G. Menges, Encyclopedia of Polymer Science and Engineering, Vol. 11, New York, USA: Wiley & Sons, **1988**.

[25] R. Allen, Epoxy Resins in Coatings, Philadelphia, Pennsylvania, USA: Federation Series of Coating Technology, **1972**.

[26] T. Theophanides, Infrared Spectroscopy – Materials Science, Engineering and Technology, London UK: InTech, **2012**.

[27] J. Macan, I. Brnardi, M. Ivankovi, H.J. Mencer, "DSC study of cure kinetics of DGEBA based epoxy resin with poly(oxypropylene) diamine," *J. Therm. Anal. Calorim*., 81, 369-373, **2005**.

[28] U. Braun, K. Brademann-Jock, W. Stark, "Cure monitoring of epoxy films by heatable in situ FTIR analysis: correlation to composite parts," *J. Appl. Polym. Sci.*,131, 39832–39841, **2014**.

[29] M. Delucchi, M. Castellano, S. Vicini, S.Vita, E. Finocchio, R. Ricotti, G. Cerisola, "A methodological approach for monitoring the curing process of fairing compounds based on epoxy resins," *Progr. Org. Coat.*, 123, 20–26, **2018**.

[30] M. Delucchi, E. Finocchio, M. Castellano, S. Vicini, S. Vita, G. Cerisola, R. Ricotti, "Application of DSC and FTIR techniques for monitoring the curing process of epoxy fillers used for yacht application," *Metall. Ital.*,109, 107-110, **2017**.

[31] Y. Calventusm S. Montserrat, J.M. Hutchinson, "Enthalpy Relaxation of Non-stoichiometric Epoxy-Amine Resins," *Polymer*, 42, 7081-7093, **2001**.

[32] A. Goldschmidt, H.-J. Streitberger, Handbook on Basic of Coating Technology, Hannover, Germany: Vincentz Network, **2007**.

[33] J. Bieleman, Additives for Coatings, Weinheim, Germany: Wiley-VCH, **2000**.

[34] L. J. Calbo, Handbook of Coatings Additives, New York, USA: Marcel Dekker, **1992**.

[35] I. Piirma, Polymeric Surfactants, New York, USA: Marcel Dekker Inc., **1992**.

[36] V. B. Fainerman, D. Mobius, R. Miller, Surfactants: Chemistry, Interfacial Properties, Applications, NewYork, USA: Elsevier, **2001**.

[37] K. Holmberg, Surfactants in Polymers, Coatings, Inks and Adhesives, Boca Raton, Florida, USA: CRC Press, **2003**.

[38] D. A. Skoog, F. J. Holler, S. R. Crouch, Principles of Instrumental Analysis, Boston, Massachusetts, USA: Thomson Brooks/Cole, **2007**.

[39] B. Stuart, Infrared Spectroscopy: Fundamentals and Applications, West Sussex, UK: John Wiley & Sons, **2004**.

[40] J. Kauppinen, J. Partanen, Fourier Transforms in Spectroscopy, Berlin, Germany: Wiley-VCH, **2001**.

[41] P. Gtiffithr, J. A. De Hasseth, Fourier Transform Infrared Spectrometry, Hoboken, New Jersey, USA: John Wiley & Sons, **2007**.

[42] H. Dannenberg, W. R. Harp, "Determination of Cure and Analysis of Cured Epoxy Resins," *Anal. Chem.*, 28, 1, 86-90, **1956** .

[43] B. Prime, "Differential scanning calorimetry of the epoxy cure reaction," *Polym. Eng. Sci.*, 13, 365–371, **1973**.

[44] K. Horie, H. Hiura, M. Sawada, I. Mita, H. Kambe, "Calorimetric investigation of polymerization reactions. III. Curing reaction of epoxides with amines," *J. Polym. Sci. A: Polym. Chem.*, 8, 1357–1372, **1970**.

[45] S. Mutlur, "Thermal Analysis of Composites Using DSC in Advanced Topics," in *Characterization of Composites*, Canada, M. R. Keller, **2004**.

[46] J. D. Menczel, R. B. Bruce Prime, Thermal Analysis of Polymers: Fundamentals and Applications, Hoboken, New Jersey, USA: John Wiley & Sons Inc., **2009**.

[47] G. W. H. Höhne, W. Hemminger, H.-J. Flammersheim, Diffrential Scanning Calorimetry, New York, USA: Springer, **1996**.

[48] J. Knoetze, L. Moolman, "The Prediction of Paint Properties from Rheological Data," in *European Congress of Chemical Engineering*, Copenhagen, Denmark: **2007**.

[49] H. A. Barnes, J. F. Hutton, K. Walters, An Introduction to Rheology, Amsterdam, Netherland: Elsevier Science Publisher B. V., **1989**.

[50] T. Mezger, Quality Assurance - Rheological Testing of the Sagging Behaviour of Coatings, Stuttgart, Germany: Paar Physica, **2002**.

[51] T. G. Mezger, Applied Rehology, Graz, Austria: Anton Paar GmbH, **2014**.

[52] T. G. Mezger, The Rheology Handook, Hanover, Germany: Vincentz Network, **2014**.

[53] H. A. Barnes, Handbook of Elementary Rheology, Aberystwyth, UK: Cambrian Printers, **2000**.

[54] P. J.Carreau, "Rheological equations from molecular network theories," *Tran. Soc. Rheol.*, 16, 99-127, **1972**.

[55] J. Mewis, N. J. Wagner, " Thixotropy," *Adv. Colloid. Interface Sci.*, 147, 214-217, **2009**.

[56] Vv.Aa., *Rheology Handbook*, East Windsor: Elementis Specialties Inc., **2008**.

[57] M. Osterhold, " Rheological methods for characterising modern paint systems," *Prog. Org. Coat.*, 40, 131-137, **2000**.

[58] K. P. Menard, Dynamic Mechanical Analysis a Practical Introduction, Boca Raton. Florida, USA: CRC press, **1999**.

[59] J. Goldstein, Practical Scanning Electron Microscopy: Electron and Ion Microprobe Analysis, Berlin, Germany: Springer Science & Business Media, **2012**.

[60] J. I. Goldstein, D. E. Newbury, P. Echlin, D. C. Joy, C. Fiori, E. Lifshin, Scanning Electron Microscopy and X-Ray Microanalysis, Berlin, Germany: Springer, **1981**.

[61] R. G. Miller, Beyond ANOVA: Basics of Applied Statistics, Boca Raton, Florida, USA: Chapman and Hall/CRC, **1997**.

[62] T. H. Wonnacott, R. J. Wonnacott, Introductory to Statistics, Hoboken, New Jersey, USA: Jhon Wiley and Sons, **1990**.

[63] M. Otto, Chemometrics: Statistics and Computer Application in Analytical Chemistry, Weinheim, Germany: Wiley - VCH, **2016**.

[64] I. T. Jolliffe, Principal Component Analysis, New York, USA: Springer-Verlag, **2002**.

[65] A. M. Harper, D. L. Duewer, B. L. Kowalski, J. L. Fasching, B. R. Kowalski (Ed.), "ARTHUR and Experimental Data Analysis: The Heuristic Use of a Polyalgorithm," in *Chemometrics: Theory and Application*, Washington, American chemical society, **1977**, 14-52.

[66] D. Lin-Vien, N. B. Colthup, W. G. Fateley, J. G. Grasselli, The Handbook of Infrared and Raman Characteristic Frequencies of Organic Molecules, San Diego, California, USA: Academic press Inc., **1991**.

[67] G. Nikolic, S. Zlatkovic, M. Cakic, S. Cakic, C.Lacnjevac, Z. Rajic, "Fast Fourier Transform IR Characterization of Epoxy GY Systems Crosslinked with Aliphatic and Cycloaliphatic EH Polyamine Adducts," *Sensors*, 10, 684-696, **2010**.

[68] K. E. Chike, M. L. Myrick, R. E. Lyon, S. M. Angel, "Raman and Near-Infrared studies of an epoxy resin," *Appl. Spectrosc.*, 47, 1631-1635, **1993**.

[69] L. S. Xu, J. R. Schlup, "Etherification versus amine addition during epoxy resin amine cure: an in situ study using near infrared spectroscopy," *J. Appl. Polym. Sci.*, 67, 895–900, **1998**.

[70] M. A. Escola, C. A. Moina, A. C.Nino Gomez, G. O. Ybarra, "The determination of the degree of cure in epoxy paints by infrared spectroscopy," *Polym. test.*, *2*4, 572-575, **2005**.

[71] M. Erdmann, V. Trappe, H. Sturm, U. Braun, E. Duemichen, "Cure conversion of structural epoxies by cure state analysis and in situ cure kinetics using nondestructive NIR spectroscopy," *Thermochim. Acta*, 650, 8-17, **2017**.

[72] H. Yamasaki, S. Morita, "Identification of the epoxy curing mechanism under isothermal conditions by thermal analysis and infrared spectroscopy," *J. Mol. Struct.*, 1069, 164-170, **2014**.

[73] E. Duemichen, M. Javdanitehran, M. Erdmann, V. Trappe, H. Sturm, U. Braun, G. Ziegmann, "Analyzing the network formation and curing kinetics of epoxy resins by in situ near-infrared measurements with variable heating rates," *Thermochim. Acta*, 49, 616, **2015**.

[74] P. Wu, H. W. Siesler, "Two-dimensional correlation analysis of variable-temperature Fourier transform mid- and near-infrared spectra of polyamide 11," *J. Mol. Struct.*, 521, 37-47, **2000**.

[75] C. Dell'Olio, Q. Yuan, R. J. Varley, "Epoxy/Poly(ethylene-co-methacrylic acid) blends as thermally activated healing agents in an epoxy/amine network," *Macromol. Mater. Eng.*, 300 , 70-79, **2015**.

[76] B. A. Rozenberg, K. Dusek (Ed.), "Kinetics, thermodinamics and mechanism of reations of epoxy oligomers with amines," in *Epoxy resins and composites II - Advances in polymer science*, vol. 75, Berlin, Germany: Springer, **1986**.

[77] Institute of Chemistry University of Tartu, Estonia, [Online]. Available: http://lisa.chem.ut.ee/IR_spectra.

[78] R. Auvergne, S. Caillol, G. David, B. Boutevin, J. P. Pascault, "Biobased Thermosetting Epoxy: present and future," *Chem. Rev.*, 114, 1082-1115, **2014**.

[79] O. Faruk, M. Sain, Biofibre Reinforcement in Composite Materials, Sawtson; UK: Woodhead Publishing, **2015**.

[80] D. Fox, N. Kaufman, J. Woodcock, C. Davis, J. Gilman, J. Shields, "Epoxy Composites Using Wood Pulp Components as Filler," in *Composites from Renewable and Sustainable Materials*, London, UK: IntechOpen, **2016**, 200-215.

[81] R. J. Ross, Wood Handbook - Wood as an Engineering Materials, Madison: United States Department of Agriculture Forest Service, **1999**.

[82] A. K. Bledzki, J. Gassan, "Composites reinforced with cellulose based fibres," *Prog. Polym. Sci.*, 24, 221–274, **1999**.

[83] G. L. Li, H. Mohwald, D. G. Shchukinab, "Precipitation polymerization for fabrication of complex core–shell hybrid particles and hollow structures," *Chem. Soc. Rev.*, 42, 3628 - 3646, **2013**.

[84] Q. Tian, D. Yua, "Preparation and properties of polymer microspheres filled epoxy composite films by UV-curable polymerization," *Mater. Des.*, 107, 221–229, **2016**.

[85] L. J. Borthakur, T. Jana, S. Dolui, "Preparation of core–shell latex particles by emulsion co-polymerization of styrene and butyl acrylate, and evaluation of their pigment properties in emulsion paints," *J. Coat. Technol. Res.*, 7, 6, 765–772, **2010**.

[86] X. Yang, L. Chen, B. Han, X. Yang, H. Duan, "Preparation of magnetite and tumor dual-targeting hollow polymer microspheres with pH-sensitivity for anticancer drug-carriers," *Polymer*, 51, 2533–2539, **2010**.

[87] S. Miao, C. Zhang, Z. Liu, B. Han, Y. Xie, S. Ding, Z. Yang, "Highly Efficient Nanocatalysts Supported on Hollow Polymer Nanospheres: Synthesis, Characterization, and Applications," *J. Phys. Chem. C.*, 112, 774–780, **2008**.

[88] X. Xu, S. A. Asher, "Synthesis and Utilization of Monodisperse Hollow Polymeric Particles in Photonic Crystals," *J. Am. Chem. Soc.*, 126, 7940-7945, **2004**.

[89] R. Payne, "The dynamic properties of carbon black-loaded natural rubber vulcanizates. Part I," *J. Appl. Polym. Sci.,* 6, 57-63, **1962**.

[90] R. Payne, "The dynamic properties of carbon black loaded natural rubber vulcanizates. Part II.," *J. Appl. Polym. Sci.,* 6, 368–372, **1962**.

[91] S. K. Srivastava, Y. K. Mishra, "Nanocarbon reinforced rubber nanocomposites: detailed insights about mechanical, dynamical mechanical properties, Payne, and Mullin effects," *Nanomaterials,* 8, 945, **2018**.

[92] T. McNally, P. Potschke, Polymer Carbon Nanotube Composites: Preparation, Properties and Applications, Sawston, UK: Woodhead Publishing, **2011**.

[93] C. C. Peng, A. Gopfert, M. Drechsler, V. Abetz, "Smart silica-rubber nanocomposites in virtue of hydrogen bonding interactions," *Polym. Adv. Technol.,* 16, 770-782, **2005**.

[94] R. Yang, Y. Song, Q. Zheng, "Payne effect of silica-filled styrene-butadiene rubber," *Polymer.,* 116, 304-313, **2016**.

[95] M. I. Aranguren, E. Mora, J. V. DeGroot, C. W. Macoscko, "Effect of reinforcing fillers on the rheology of polymer melts," *J. Rheol.,* 36, 1165-1182, **1992**.

[96] C. Gauthier, E. Reynaud, R. Vassoille, L. Ladouce-Stelandre, "Analysis of the non-linear viscoelastic behaviour of silica filled styrene butadiene rubber," *Polymer.,* 45, 2761-2771, **2004**.

[97] J. Ramier, C. Gauthier, L. Chazeau, L. Stelandre, L. Guy, "Payne effect in silica-filled styrene–butadiene rubber: Influence of surface treatment," *J. Polym. Sci. Pol. Phys.,* 45, 286, **2007**.

[98] R. Hentschke , "The Payne effect revised," *Express. Polym. Lett.,* 11, 4, 278-292, **2017**.

[99] G. D. Shay, J. V. Koleske (Ed.), "Thickeners and rheology modifiers," in *Paint and coating testing manual*, West Conshohocken, Pensylvania, USA:ASTM, **2012**, 341-372.

[100] H. H. Murray, "Applied clay mineralogy today and tomorrow," *Clay Miner.,* 34, 39-49, **1999**.

[101] S. A. Garea, H. Iovu, "New epoxy coating systems which contain multipurpose additives based on organophilic montmorillonite," *Prog. Org. Coat.,* 56, 319-326, **2006**.

[102] S. Ismadji, D. Shen Tong, F. Edi Soetaredjo, "Bentonite hydrochar composite for removal of ammonium from Koi fish tank," *Appl. Clay. Sci.,* 119, 146–154, **2016**.

[103] H. Murray, "Structure and composition if the clay minerals and their physical and chemical properties," in *Applied Clay Mineralogy*, Vol. 2, New York, USA: Elsevier, **2007**, 7-32.

[104] W. S. Mardis, "Organoclay Rheological Additives: Past, Present and Future," *J. Am. Oil. Chem. Soc.,* 61, 382-387, **1984**.

[105] A. A. Cuadri, M. García-Morales, F. J. Navarro, P. Partal, "Isocyanate-functionalized castor oil as a novel bitumen modifier," *Chem. Eng. Sci.,* 97, 320–327, **2013**.

[106] E. Hablot, D. Zheng, M. Bouquey, L. Avérous, "Polyurethanes Based on Castor Oil: Kinetics, Chemical, Mechanical and Thermal Properties," *Macromol. Mater. Eng.,* 293, 922–929, **2008**.